CELL AND DEVELOPMENTAL BIOLOGY

FORKHEAD TRANSCRIPTION FACTOR REGULATES PROSTATE-SPECIFIC GENE EXPRESSION AND PROSTATIC MORPHOGENESIS: A FUNCTIONAL INTERACTION WITH ANDROGEN SIGNALING

NAN GAO

Dissertation under the direction of Professor Robert J Matusik

Comparative genome analysis implied that a progressively more elaborate regulation of gene expression rather than invention of new genes is responsible for the organismal complexity, and that a constrained organization of metazoan enhancers is essential for the precise patterns of gene expression during development. This project was focused on studying of the transcriptional regulatory complex that directs tissue-specific gene expression and organ development in the prostate.

Genetic manipulation of the rat probasin (Pbsn) gene promoter in transgenic mice uncovered a ~150 base pair core DNA fragment, which confers prostate-selectivity to the expression of this gene. Among a cluster of DNA sequence-specific transcription factors directly binding to this region, there are two cell-type limited proteins: the androgen receptor, a nuclear receptor, and Foxa1, a forkhead protein. Reporter assays indicated the forkhead response elements are crucial for AR-mediated transcriptional regulation. *In vitro* and *in vivo* binding assays established that the two proteins can bind adjacent DNA sequence concomitantly while the binding is not interdependent. A physical interaction

occurs between Foxa1 and AR when the ligand for AR is present. This interaction is mediated through the forkhead domain and the AR DNA binding domain. Alignment of the forkhead and the androgen response elements resulted in the identification of a shared cis-regulatory code that is present in a variety of prostate-specific enhancers across species.

The impact of Foxa1 loss-of-function and haploinsufficiency on mouse prostatic organogenesis was analyzed. Foxa1-/- prostates showed drastic morphologic alteration including a disorganized epithelial pattern resembling primitive epithelial cords, and an expansion in the mesenchymal smooth muscle layer. Cell type and ultrastructural studies demonstrated that Foxa1-/- epithelium is predominantly arrested as immature basal cells, consistent with a failure of luminal determination. Foxa1-/- basal cells actively express Sonic hedgehog (Shh), Ptc1 and Foxa2, proteins that are normally elevated during embryonic ductal budding in the UGS. Alteration of these signals correlates with the expansion of precursor cells and the modified epithelial-stromal pattern in Foxa1-/- prostates. In contrast, expression of the Nkx3.1 homeobox protein is absent in these Foxa1-/- cells. In addition a haploinsufficient phenotype was observed in heterozygous dorsal prostates showing a similar ductal morphologic defect. A novel Foxa1 target gene was identified. Upon examination of its promoter, critical forkhead response elements were identified to be immediately flanked by androgen response elements. We propose that Foxa1 regulates genes involved in prostatic ductal morphogenesis, and promotes epithelial cell maturation through balancing the effects of Shh, Foxa2, and Nkx3.1.

FORKHEAD TRANSCRIPTION FACTOR REGULATES PROSTATE-SPECIFIC GENE EXPRESSION AND PROSTATIC MORPHOGENESIS: A FUNCTIONAL INTERACTION WITH ANDROGEN SIGNALING

By

Nan Gao

Dissertation

Submitted to the Faculty of the

Graduate School of Vanderbilt University

in partial fulfillment of the requirements

for the degree of

DOCTOR OF PHILOSOPHY

in

Cell and Developmental Biology

December, 2004

Nashville, Tennessee

Approved:

Professor Robert J. Matusik

Professor Stephen R. Hann,

Professor Marie-Claire Orgebin-Crist,

Professor Michael H. Melner

Professor Stephen J. Brandt

ACKNOWLEDGEMENTS

I wish to acknowledge and thank all those who have given me their support, encouragement and assistance in helping me to complete my Ph.D. degree. In particular, thanks to Dr. Robert J. Matusik, my advisor and mentor, whose continuous support, belief and patience to me has made my dream become true. I would like to extend my heartfelt gratitude and appreciation to Dr. Susan Kasper and Dr. Simon W Hayward for giving me numerous precious advices on my project during these years; to Mr. Tom Case and Mr. Manik Paul for their constant technical assistance; to Dr. Jiangfeng Zhang for his suggestion on my project; and to all the other members in Matusik lab, Kasper lab and Hayward lab for their generous ideas, discussions and always friendships.

In addition, I am truly grateful to my committee members, Dr. Stephen R. Hann, Dr. Marie-Claire Orgebin-Crist, Dr. Michael H. Melner and Dr. Stephen J. Brandt, for helping me to design the project and finish the thesis.

Finally, I want to thank my family and friends, whose emotional and mental support and confidence in my abilities gave me the courage to reach and attain this goal.

TABLE OF CONTENTS

LIST OF TABLES

LIST OF FIGURES

ABBREVIATIONS

AF-1	activation function 1
AF-2	activation function 2
AP	anterior prostate
AP-1	activator protein 1
AR	androgen receptor
ARBS	androgen receptor binding site
ARE	androgen response element
ARR	androgen response region
BLE	bladder epithelium
BMP	bone morphogenetic protein
bp	base pair
ChIP	chromatin immunoprecipitation
Ck	cytokeratin
DBD	DNA-binding domain
DD	ductus deferens
DHT	dihydrotestosterone
DLP	dorsolateral prostate
E	embryonic day
EB	ethidium bromide
EGF	epidermal growth factor
EGFR	epidermal growth factor receptor
EMSA	electrophoretic mobility shift assay

ER	estrogen receptor
FGF	fibroblast growth factor
FGFR	fibroblast growth factor receptor
FH	forkhead
Foxa1	forkhead box a1
Foxa2	forkhead box a2
Foxa3	forkhead box a3
GR	glucocorticoid receptor
GST	glutathione-*S*-transferase
Hh	hedgehog
HMG	high mobility group
HNF-3	hepatocyte nuclear factor-3
hPAP	human prostatic acid phosphatase
IGF	insulin-like growth factor
IMS	Imaging Mass Spectrometry
IP	immunoprecipitation
JAK	Janus kinase
LBD	ligand binding domain
MALDI	matrix assisted laser desorption ionization
MAPK	mitogen-activated protein kinase
mPSA	mutant PSA
MS	mass spectrometry
NF1	nuclear factor 1

NFκB	nuclear factor κB
NTD	N-terminal domain
2xmR2	two copies of mutant R2
nt	nucleotide
Oct1	octamer transcription factor 1
P	postnatal day
PAP	prostatic acid phosphatase
PAS	periodic acid Schiff
Pbsn	probasin
PDEF	prostate derived ets factor
PMSF	phenylmethylsulfonic fluoride
PrE	prostate epithelium
PSA	prostate-specific antigen
PSA-EP	PSA-enhancer/promoter
Ptc1	patched1
rPAP	rat PAP
Sbp	spermine binding protein
SDS	sodium dodecyl sulfate
Shh	sonic hedgehog
SMA	smooth muscle α-actin
Smad	sma- and mad-related protein 3
SRY	sex-determining region Y
STAT	signal tansducer and activator of transcription

SV	seminal vesicle
TBP	TATA binding protein
Tfm	testicular feminized
Tgf	transforming growth factor
TOF	time-of-flight
TNT	transcription and translation
TS	tissue specific
TTR	transthyretin
UGE	urogenital sinus epithelium
UGM	urogenital sinus mesenchyme
UGS	urogenital sinus
UR	urethra
VP	ventral prostate
Wnt	wingless

CHAPTER I

GENERAL INTRODUCTION

The prostate is a male accessory sex gland that is important for normal reproduction of the species. Diseases occurring in this gland remain a major health problem in the expanding population of elder men in the world. The lack of an effective way to prevent or treat prostatic disease is largely due to an incomplete understanding of the molecular events that underlie normal prostate cell growth and gene regulation. It is now largely believed that normal organ development is dependent on a concerted organization and communication of various cell types, while the individual cell type is specified through a regulated interaction of diverse signaling pathways that activate unique subsets of genes, and make the cells become functionally specialized. Disruption of precisely controlled cellular processes or genetic pathways could affect organ development or function, leading to phenotypically abnormal organs having wrong identity, leading to disease, or loss of function. Like many insights that are being made in other organs, major progress in the prostate research field is greatly attributed to the studies involving *in vitro* tissue culture or transgenic animal models. Here, I will summarize some critical findings in this area and introduce some current knowledge about the prostate in terms of developmental biology, endocrinology, cell and molecular biology.

Prostatic Development and Hormone Regulation

Male accessory sex organs include the prostate, bulbourethral gland, seminal vesicle, ductus deferens and the epididymis, all of which have served as ideal models for studying androgen-regulated cell growth and gene function (Cunha et al., 1987). However the prostate has been studied extensively since it is one of the most frequently disease-affected organs. Prostate cancer and benign prostatic hyperplasia are two major diseases in the prostate. Both diseases feature an abnormally high rate of cell proliferation, which results in an enlargement of the gland and/or disruption of the ductal-acinar structure. Until now, it is not clear why bulbourethral gland, seminal vesicle and epididymis have a substantially low incidence of disease compared to the prostate (Cunha et al., 1987).

The prostate gland is an exocrine gland that can only be found in mammals. It is composed of highly branched ductal networks that produce major components of the seminal fluids. The prostate is located immediately below the bladder and closely associated with the urethra, therefore the prostatic secretions can be discharged from the prostatic ducts into the urethra by muscular contractions (Fig. 1-1). Many proteins produced by the prostate may be fundamentally important for sperm movement and liquification, which may assist in normal reproductive activity in male adult animals (Cunha et al., 1987).

A. Prostatic Induction and Morphogenesis

The prostate is derived from the embryonic urogenital sinus (UGS), a subdivision of the cloaca, which belongs to the endodermal hindgut. The UGS is a midline structure which is composed of an endodermally derived epithelial layer and a surrounding

mesodermally derived mesenchymal layer (Marker et al., 2003). In both male and female mice, the UGS, located just caudal to the neck of the developing bladder, can be first observed at embryonic day 13 (E13) (Staack et al., 2003). There is no morphologic difference between male and female UGS until E17.5, during which the prostatic induction occurs due to an increased level of serum androgens produced by the fetal testes. At E17.5 in the mouse (E18-E19 in the rat), the first sign of prostatic morphogenesis is observed as the urogenital sinus epithelium (UGE) invades into the surrounding urogenital sinus mesenchyme (UGM), forming the earliest prostatic buds (Marker et al., 2003). In the following a few days [E17.5-postnatal day 7 (P7)], the outgrowth of these prostatic buds gives rise to a number of solid epithelial cords in a precise spatial pattern which eventually establishes different lobe subdivisions of the prostate (Sugimura et al., 1986a). In the mouse, the ventral prostate (VP) lobes are derived from up to 3 main ducts that are emerged from each ventral side of the UGS; the dorsolateral prostate (DLP) lobes are derived from around 25 main ducts from each dorsolateral side of the UGS; and the anterior prostate (AP) lobes are derived from 2 large buds, from each side of the UGS, which eventually grow into the mesenchyme of the seminal vesicles. Most of these main ducts are not branched at birth (Sugimura et al., 1986a).

Neonatally, as these main ducts continue to elongate into the surrounding mesenchyme as a result of intense proliferative activity at their tip, they start to send out side-branches. This process is called ductal branching morphogenesis, which takes place in the first 1-2 weeks after birth (Fig. 1-2). The patterns of branching morphogenesis are distinctive for each prostate lobe, and the results of branching morphogenesis are the

generation of three distinct bilaterally symmetrical prostatic lobes: AP, DLP and VP (Sugimura et al., 1986a). During branching morphogenesis, ductal canalization is initiated in the solid epithelial cords from the urethral terminus toward the distal ductal tips. Concomitantly with all these changes in ductal morphology, prostate epithelial and stromal cell differentiation occurs (Marker et al., 2003) (Fig. 1-2).

The prostate branching morphogenesis is almost completely finished around P14 in the mouse. At puberty (around P20), the prostate wet weight increases significantly due to an increased protein and DNA synthesis that are stimulated by the surging serum androgen levels. Due to lobe-specific differences in the patterns of branching morphogenesis, the final shape of each lobe is distinct. Furthermore, the different lobes have distinct histologic features. AP shows extensive epithelial cell infolding. DLP shows less extensive epithelial cell infolding and VP shows minimal epithelial cell infolding (Marker et al., 2003).

B. Prostate Epithelial and Mesenchymal Cell Differentiation

As prostate branching morphogenesis proceeds, prostatic cells differentiate simultaneously in the first 1-3 weeks after birth. The epithelial cells within the embryonic UGE or the early developing epithelial cords are immature epithelial cells, which are characterized by coexpression of a number of basal cytokeratins (Ck) such as Ck5, Ck14, and luminal Ck8, Ck18, and other markers such as basal nuclear protein p63 (Wang et al., 2001). As the solid epithelial cords branch and canalize, these epithelial cells differentiate and reorganize into two distinct cell populations: the basal epithelial cells and the luminal epithelial cells. Each of these two cell populations can be identified according to their distinct cell distribution, morphology, and specific markers. Basal epithelial cells are

localized along the basement membrane, forming a discontinuous layer and expressing Ck5, Ck14 and p63. Luminal cells are tall columnar cells, lining the lumen and expressing Ck8 and Ck18 (Hayward et al., 1996a). In mature prostate gland, columnar luminal cells exhibit basally located rough endoplasmic reticulum, supranuclear Golgi complexes and apical vesicles that contain dense secretory materials, all of which are typical features of secretory function (Sahlen et al., 2002). At sexual maturity, the luminal cells undergo functional differentiation and produce prostate-specific secretory proteins, which demonstrate a lobe specific manner. For example, the prostate spermine binding protein (Sbp) is a VP enriched protein (Chang et al., 1987), while a range of dorsolateral proteins are the major secretory proteins in DLP (Donjacour et al., 1990). As the prostatic epithelium differentiates, the immature prostatic mesenchymal cells differentiate into a layer of smooth muscle that surrounds the prostatic ducts (Hayward et al., 1996b).

Thus, the adult prostate glands contain three major cell types, luminal secretory cells, basal epithelial cells and stromal smooth muscle cells. In addition to these cell types, there are a few less common cell populations present in the epithelium and the stroma. The neuroendocrine cells are present as a very rare cell population in both developing and adult prostate ducts (Garabedian et al., 1998). Although it is widely accepted that luminal and basal cells are derived from the common epithelial precursor of the cloaca (Wang et al., 2001), the origin of the neuroendocrine cell is unclear. One study suggested that neuroendocrine cells are derived from neural crest and migrate into the UGE through the UGM during early prostate development (Aumuller et al., 1999); while another hypothesis holds that the neuroendocrine cells share a common progenitor with secretory

cells (Xue et al., 1998a; Xue et al., 1998b). The neuroendocrine cells can be identified as expressing specific markers such as the chromogranin A, serotonin, synaptophysin and neurophysin (Xue et al., 1997; Abrahamsson, 1999; Rodriguez et al., 2003). Recent research also suggested that in the prostate there is another very small population of cells which have the potential for regeneration. These cells are proposed to be stem cells and are located in the basal epithelial compartment (Xin et al., 2003; Collins et al., 2001). In the mouse, a very rare basal cell population has been shown to express a marker gene profile which is characteristic of immature/undifferentiated transient or intermediate cells (Wang et al., 2001). Although no prostate stem cell has yet been isolated, these studies collectively suggested that the prostate stem cells are present and concentrated in embryonic UGE but are sparse in mature glands, and they preferentially expresses Ck5, Ck14, p63 and high levels of α2β1-integrin (Collins et al., 2001; Wang et al., 2001).

In addition to the smooth muscle cells, the prostate stromal layer also contains several less common cell types including the fibroblastic, lymphatic and vascular cells (Cunha et al., 1987).

C. Steroid Hormones Regulate Prostatic Development

Androgens have been shown to play a central role in organogenesis of the male reproductive tract (Thomson, 2001). The development of the prostate and other male internal accessory sexual structures is dependent on circulating androgens. The research performed by Jost and colleagues more than half century ago demonstrated that testicular factors are required for the formation of the male reproductive organs (Jost A, 1953). They showed that the development of the reproductive tract was independent of the genetic mechanism of sex determination but under the regulation of hormones. In their

experiments, administration of androgens to embryos *in utero* resulted in the development of male accessory sex organs such as the prostate in females. *In vitro* organ culture experiments confirmed that androgens are able to induce prostatic budding in embryonic female reproductive tracts (Price D., 1965; Cunha, 1973; Lasnitzki and Mizuno, 1977; Takeda et al., 1986). On the other side, ablation or surgical removal of fetal testes during the ambisexual period of sex differentiation inhibited the development of male sex glands including the prostate (Cunha et al., 1987). Likewise, administration of estrogens or antiandrogens blocked the development of the prostate and other male accessory sex glands (Neumann et al., 1970a; Neumann et al., 1970b; Steinbeck et al., 1970; Elger et al., 1974).

These observations demonstrated that androgens are critical in inducing prostatic organogenesis. Moreover, during postnatal period, prostatic development is also dependent on androgens. Castration of neonatal mice inhibited the continued growth and development of the prostate, while castration of adult mice induced a striking reduction in prostatic size (80-85%) and DNA content (Berry and Isaacs, 1984; Sugimura et al., 1986b; Donjacour and Cunha, 1988). On the other hand, administration of testosterone to immature male animals accelerated the prostatic development and maturation (Cunha et al., 1987). These observations suggested that androgens are required for the development, morphogenesis and maintenance of the prostate.

Androgen production by the developing fetal testes initiates before prostatic induction and continues throughout the entire periods of prostatic morphogenesis (Pointis et al., 1980). Testosterone is the primary androgen that is produced by the fetal testes, while dihydrotestosterone (DHT) is the active intracellular androgen responsible for

prostatic growth (Cunha et al., 1987). DHT is produced within the UGS by enzymatic reduction of testosterone by 5α-reductase (Lasnitzki et al., 1974; Wilson and Lasnitzki, 1971).

Androgens act via the androgen receptor (AR), a member of the nuclear hormone receptor superfamily. AR is an important signal transducer which mediates the effect of the extracellular androgens and activates androgen-responsive target gene in the cellular nuclear. In the embryonic prostate, the expression of stromal AR coincides with prostatic budding while the expression of epithelial cell AR initiates at the end of the first postnatal week when the solid prostatic ducts begin to canalize (Shannon and Cunha, 1983). Males who lack AR or contain a defective AR do not develop male secondary sex organs even though their testes produce sufficient amount of androgens (Wilson et al., 1981; Griffin and Wilson, 1984). This syndrome, called testicular feminisation (Tfm), has been described in human, mouse and rat (Cunha et al., 1987).

In addition to androgens, the prostate growth is also significantly affected by the stimulation of estrogens. Exposure of male fetuses to estrogen compounds at extremely low environmental levels caused an enlargement of the prostate (Nagel et al., 1999; vom Saal et al., 1997). However, developmental exposure of males to high levels estrogen compounds reduced the prostatic growth and induced altered glandular morphology (Prins et al., 2001; Prins, 1997; Prins, 1992). Estrogen receptors have also been detected in both epithelial and stromal compartments (Bruner-Lorand et al., 1984). A direct effect of estrogen is to induce squamous metaplasia which is mediated through estrogen receptors in both epithelium and stroma (Triche and Harkin, 1971; Mawhinney and Neubauer, 1979). An indirect mechanism of estrogen is to act via the hypothalamus and

pituitary by suppressing the secretion of gonadotropins which reduce testicular androgen production (Shearer et al., 1973). However, mice with inactivating mutation in estrogen receptor α or β or both have normal prostatic development (Jarred et al., 2002; Dupont et al., 2000). These data suggest that prostatic development is sensitive to the overall endocrine environment, including the estrogen levels.

Epithelial-Mesenchymal Interactions

The interactions between epithelial and mesenchymal cells are essential for directing the organogenesis of the prostate and almost all other organs. The differentiation and morphogenesis of either epithelium or stroma will not happen if the epithelium or stroma is grown separately. During prostatic induction, AR is first expressed in mesenchyme but is absent in epithelium. Epithelium starts to express AR at a relatively late stage during ductal canalization (Cunha et al., 1987). Androgen signalling in the mesenchyme has been shown to be both necessary and sufficient for prostatic organogenesis (Cunha and Lung, 1978; Cunha et al., 1980a; Cunha et al., 1981; Lasnitzki and Mizuno, 1980). These observations led to the hypothesis that androgens regulate prostatic epithelial development through eliciting the activity of paracrine factors produced by the mesenchyme.

When prostatic organogenesis is initiated in the embryonic stage, prostatic epithelium buds into the great mass of surrounding urogenital sinus mesenchyme, and these small embryonic rudiments eventually generates a complete adult organ. This is an observation not unique to the prostate, since other organs such as the mammalian salivary, mammary glands, lung, seminal vesicle and bulbourethral also undergo a similar early

stage of organogenesis during which the epithelial component is a tiny bulbous or tubular rudiment surrounded by a vast mass of mesenchyme (Lung and Cunha, 1981; Cunha, 1972; Alescio and Cassini, 1962; Kratochwil, 1969; Sakakura et al., 1976). During prostatic development, the epithelial ducts elongate and branch within the mesenchyme, and the mesenchymal mass becomes progressively organized into the smooth muscle sheaths and connective tissues that wrap the epithelial ducts. Thus, during prostatic development, the rodent prostate transforms from a predominantly mesenchymal to a predominantly epithelial organ.

The *in vivo* interactions between UGE and UGM were modeled in a series of classical tissue recombination experiments, which were pioneered by Cunha and colleagues. Their comprehensive research demonstrated that UGM can act both as a permissive and an instructive inductor. Permissive inductions are those in which mesenchyme permits the epithelium to adopt its normal developmental program, while instructive inductions are those in which mesenchyme induces and specifies the epithelium to adopt a new developmental fate. An example of permissive induction is the interaction between UGM and seminal vesicle epithelium. Recombinants derived from UGM plus seminal vesicle epithelium differentiate into seminal vesicle, since seminal vesicle epithelium is derived from the mesodermally derived Wolffian duct, whose developmental repertoire has been stably committed to the formation of epididimis, ductus deferens and seminal vesicle, but not the prostate (Cunha et al., 1987). In contrast, in instructive inductions, the epithelium retains the ability to respond to a heterologous inductor. For example, UGM can elicit prostatic development in epithelium of UGS derivatives such as urethra, bladder, and vagina (Cunha et al., 1987). Extensive

observations from these tissue recombination analysis demonstrated that these epithelial ducts can be induced by UGM to give rise to prostate histology and ultrastructure, as well as to express androgen-dependent prostate-specific proteins. And most strikingly, in the presence of androgens, the female UGS can be induced to give rise to prostate (Cunha et al., 1987). However, the responsiveness to prostatic induction is not shared by the endodermal compartments that are out of the UGS. For example, the esophagus, a foregut endoderm derivative, cannot be induced by UGM to form prostate (Cunha et al., 1987). These data demonstrated that the embryonic derivation from hindgut endoderm is a prerequisite for epithelial cell responsiveness to inductive UGM.

In fact, the differential response of epithelium to distinct inductive mesenchymes is not unique to UGS organs. Studies in other animal models have shown that endodermal domains are usually patterned by interactions with overlying mesodermal tissue (Szuts et al., 1998). Classic tissue transplant studies using chick embryos showed that the cardiogenic mesoderm, which is transiently apposed to the prospective hepatic endoderm, provides a signal that is crucial for inducing liver progenitors in the endoderm (Zaret, 2002). In mice, during tissue specification, signals from the cardiogenic mesoderm initiate the liver gene program in proximal endoderm and suppress the pancreatic program (Deutsch et al., 2001). Ventral endoderm cells sufficiently distal to the cardiogenic mesoderm escape the latter inhibitory effect and initiate the pancreatic gene program. Ventral foregut explants, when exposed to cardiogenic mesoderm, initiate liver gene expression, otherwise they initiate pancreatic gene expression in the absence of such inductor (Deutsch et al., 2001).

Tissue recombination experiments have demonstrated that in addition to the paracrine signaling from mesenchymal cells to epithelial cells, epithelium can also pattern or permit the development of smooth muscle cells in the stroma (Cunha et al., 1996). Rat UGM has been recombined with either mouse or human prostate epithelium. Grafts of UGM paired with mouse epithelium formed a thin smooth muscle layer identical with the mouse stromal architecture; while grafts of UGM paired with human epithelium formed a thick smooth muscle layer identical to the human stromal architecture (Hayward et al., 1998). These experiments suggested that prostatic epithelium is able to pattern and induce the surrounding smooth muscle cells by producing instructive paracrine signals. Similarly, such reciprocal signaling is also supported in other modeling system for non-prostatic organs. For example, at an early developmental stage of the embryonic chick, the hepatic endoderm is also important to induce the cardiogenic mesoderm in a reciprocal manner (Schultheiss et al., 1995; Sugi and Lough, 1995; Gannon and Bader, 1995). Thus, such reciprocal signaling seems a common and crucial mechanism for coordinating the organ development in the embryo.

At present, several mesenchymal paracrine regulators have been described such as FGF7, FGF10 and IGF1 (Baker et al., 1996; Ruan et al., 1999; Sugimura et al., 1996; Thomson and Cunha, 1999). Recently, growing evidence indicated that a few crucial and well-conserved signaling pathways may play key roles in regulating prostatic epithelial-mesenchymal interactions.

Conserved Signaling Pathways in Regulating Prostatic Development

Embryonic organ induction is one of the general principles that has to be determined in order to further study the organ development. One of the first demonstrations showing that cells can communicate with adjacent cells was the observation of two-headed salamanders in a tissue transplantation experiment (Pires-daSilva and Sommer, 2003). The transplanted tissue was able to induce the fate of the neighbor cells in the host embryo, suggesting that cells might talk with each other through some kind of signals. In the past two decades, extensive research in embryonic and developmental biology has demonstrated a strikingly simplified principle in the generation of the organism complexity. That is, despite the huge number of cell types and patterns found in the diverse animals, only a few conserved signaling pathways are required to generate them (Pires-daSilva and Sommer, 2003). Surprisingly, although after a million years of evolution, signaling pathways have evolved into complex networks, recent studies revealed that most cell-cell interactions during embryonic development involve Hedgehog (Hh) (Ingham and McMahon, 2001), Wingless (Wnt) (Cadigan and Nusse, 1997), Notch (Mumm and Kopan, 2000), transforming growth factor-β (Tgf-β) (Massague and Chen, 2000), receptor tyrosine kinase (Schlessinger, 2000) and nuclear hormone pathways (McKenna and O'Malley, 2002). It is now thought that the organ specificity is controlled by the intensity of these signals, the cross-modulation and interaction within different signaling cascades, and the competence or originality of the cells that are receiving these signals (Zaret, 2002). Recently it has been suggested that molecules that are involved in these pathways also play crucial roles in various developmental aspects of the prostate (Marker et al., 2003).

A. Hedgehog Signaling – Prostatic Ductal Morphogenesis

Members of the Hh family were isolated in the early 1990s (Lee et al., 1992; Mohler and Vani, 1992; Tabata et al., 1992). Since then, they have been recognized as key regulators of many crucial processes during embryonic development. Now Hedgehog signaling is thought to be pivotal in controlling the growth, patterning and morphogenesis of almost every organ in the bodies of vertebrates (Ingham and McMahon, 2001). Depending on different contexts, Hedgehog signals can act as either morphogens inducing distinct cell fates within its target field, or mitogens regulating cell proliferation (Ingham and McMahon, 2001).

The Sonic hedgehog (Shh) gene is the vertebrate homolog of the *Drosophila* gene *hedgehog* (Echelard et al., 1993b). Both *hedgehog* and Shh encode secreted glycopeptides that bind to a membrane-bound receptor, Patched (Ptc), and activate a cascade event of intracellular signal transduction, which finally leads to transcriptional activation or repression of specific genes (Marigo and Tabin, 1996; Stone et al., 1996; Fuse et al., 1999). In *Drosophila*, Ci is the transcriptional regulator that functions as an activator while the protein is intact, and acts as a suppressor while the protein is cleaved (Aza-Blanc et al., 1997). Although both forms are present in Hedgehog-responsive cells, Hedgehog signaling strongly inhibits the cleavage event thus promoting transcriptional activity (Motzny and Holmgren, 1995; Wang and Holmgren, 1999). Gli1, Gli2 and Gli3 proteins are vertebrate homologs of Ci with a highly conserved zinc finger DNA-binding domain (Walterhouse et al., 1999; Matise and Joyner, 1999). Although three Gli proteins may have overlapping or redundant functions, Gli1 is a clear transcriptional activator (Sasaki et al., 1997; Yoon et al., 1998). Interestingly, the receptor Ptc itself is a

downstream target of Shh signaling, and functions to attenuate Shh activity (Ingham, 1991; Capdevila and Guerrero, 1994; Gailani et al., 1996; Dahmane et al., 1997).

In the urogenital tract, Podlasek *et al*. first showed that Shh is expressed in the UGE in an androgen-dependent manner, and the temporal expression of Shh coincides with the formation of the main prostatic ducts and the following ductal morphogenesis (Podlasek et al., 1999a). Examination of the spatial expression in UGS suggested that the most abundant expression level was in the lumen of the UGS as well as in the adjacent proximal duct areas. During prostatic budding, focused expression of Shh was observed in the nascent prostatic epithelial buds as well as in the growing ductal tips (Lamm et al., 2002; Freestone et al., 2003). Expression of Ptc1, Gli1 and Gli2 is localized primarily to mesenchyme surrounding the newly developed prostatic buds, while Gli3 is expressed throughout UGM in a diffused pattern (Lamm et al., 2002; Berman et al., 2004). Expression of Ptc1 and Gli1 is highly dependent on the Shh signaling, since treatment of UGM with Shh peptide upregulated expression of both genes in cultured tissue or in intact organ (Lamm et al., 2002). Blockage of Shh signaling with a neutralizing antibody, or with the chemical inhibitor cyclopamine, in organ culture experiments, inhibited the Shh signaling and abrogated the growth and ductal morphogenesis in transplanted tissues (Podlasek et al., 1999a; Lamm et al., 2002). This inhibitory effect is mediated through the inhibition of Gli protein expression (Lamm et al., 2002).

In vitro organ culture as well as renal capsule rescue of Shh mutant UGS suggested that Shh is not required for prostatic induction (Berman et al., 2004; Freestone et al., 2003). However, the developed Shh-null prostates demonstrated aberrant branching morphogenesis as well as cytodifferentiation, confirming the role of Shh signaling in

prostatic ductal morphogenesis (Berman et al., 2004; Freestone et al., 2003). In addition, *in vitro* treatment of postnatal VP with recombinant Shh caused a decrease in the number of ductal tips as well as an expansion in mesenchyme (Freestone et al., 2003). The negative effect of Shh signaling on ductal branching was supported by another report which further suggested that this is an indirect effect through the surrounding stromal cells, since Shh treatment caused upregulated expression of activin A and transforming growth factor-β1, both of which have been shown to inhibit epithelial cell branching (Wang et al., 2003). Collectively, these studies indicate that Shh signaling plays a role in early prostatic branching morphogenesis and epithelial/stromal pattern formation, but not in prostatic induction.

B. Wnt Signaling – A Crosstalk with AR Pathway

Wnt proteins are another family of secreted glycoproteins that are developmentally important. Wnt provides crucial signals for embryonic induction, generation of cell polarity, and the specification of cell lineages (Cadigan and Nusse, 1997). Mutations in several components of Wnt signaling have been implicated in the genesis of various human cancers (van Es et al., 2003). Wnt-1 in the mouse is the first Wnt member, while others share significant sequence homology to Wnt-1 (Nusse and Varmus, 1982; van Ooyen and Nusse, 1984). All Wnt proteins encode secreted glycoproteins, just as Hedgehog proteins (Nusse, 2003). In *Drosophila*, Wnt proteins act on its receptor Frizzled, which is a cell-surface transmembrane protein with an amino-terminus positioned outside of the cell (Bhanot et al., 1996; Rocheleau et al., 1997a). Frizzled, upon ligand binding, activates Disheveled, which is a cytoplasmic G-protein regulator (Klingensmith et al., 1994; Theisen et al., 1994). Activated Disheveled in turn

inhibits zw3 (or vertebrate counterpart GSk-3) kinase (Dominguez et al., 1995; He et al., 1995), which directly binds to and phosphorylates β-catenin, destabilizing the latter by promoting its entry into the ubiquitin-proteasome degradation pathway (Aberle et al., 1997). β-catenin is the essential mediator of Wnt signaling. Mutations in β-catenin resulted in phenotypes similar to that observed in Wnt inactivation (Heasman et al., 1994; Wieschaus and Riggleman, 1987), while increased levels of β-catenin in cells caused activation of Wnt signaling (Schneider et al., 1996; Larabell et al., 1997). Wnt signals positively regulate β-catenin post-transcriptionally, leading to the accumulation of cytoplasmic and nuclear β-catenin (Larabell et al., 1997; Riggleman et al., 1990). Nuclear-accumulated β-catenin can bind to HMG box transcription factors, Tcf-LEF-1 proteins, which by themselves are weak transcriptional activators. Complexes between Tcf and β-catenin act as potent transcriptional activators (Molenaar et al., 1996; Korinek et al., 1997; Morin et al., 1997). Thus β-catenin is a key component in classical Wnt pathways since it provides a link between Wnt signaling and transcriptional regulation. Furthermore, β-catenin also binds to E-cadherin and links cell adhesion complexes to the cytoskeleton (McCrea et al., 1991).

In the normal prostate epithelium, nuclear translocation of β-catenin was found to occur concomitantly with androgen-induced regrowth of the prostate (Chesire et al., 2002). Remarkably, β-catenin can interact with AR but not with other steroid hormone receptors such as estrogen receptor-α, progesterone receptor-β, or glucocorticoid receptor (Yang et al., 2002). This interaction requires the ligand binding domain and the amino-terminus of AR, and the first six armadillo repeats of β-catenin. Through this specific interaction, β-catenin promotes AR activity in a ligand-dependent manner in prostate

cancer cells (Yang et al., 2002). Consistently, upregulation of E-cadherin in prostate cancer cells leads to redistribution of the cytoplasmic β-catenin to the cell membrane and reduction of AR-mediated transcription (Yang et al., 2002). More evidence suggested that AR can promote nuclear translocation of β-catenin in prostate cancer cell lines (Mulholland et al., 2002). By performing a time course cell fractionation, AR has been shown to be capable of shuttling β-catenin into the nucleus when exposed to exogenous androgen. In this experiment, cells exposed to androgen demonstrated nuclear co-localization of AR and β-catenin (Mulholland et al., 2002). Furthermore, β-catenin has been shown to indirectly bind Pbsn promoter in an AR-dependent manner (Mulholland et al., 2002). These results supported β-catenin as a co-activator for AR, at the same time established a novel mechanism of nuclear accumulation of β-catenin by AR-mediated import. A recent study reported that in addition to an interaction with β-catenin, AR can also interact with T cell factor 4, the transcriptional mediator of Wnt signaling, through AR DNA binding domain (Amir et al., 2003). Tcf4 was found to coimmunoprecipitate with β-catenin and AR (Amir et al., 2003; Mulholland et al., 2003). Collectively, these data provided important insight into the intracellular cross talk between Wnt signaling and AR pathway in normal and prostate cancer cells. The direct AR-Tcf4 interaction, in conjunction with AR-β-catenin and Tcf4-β-catenin interactions, provides a mechanism for cooperative and selective gene regulation by AR nuclear hormone receptor pathway and Wnt/β-catenin/Tcf pathway that may contribute significantly to normal and neoplastic prostate growth (Amir et al., 2003). Moreover, β-catenin nuclear activation is thought to be correlated with abnormal cell growth in the prostate (Bierie et al., 2003; Cheshire and Isaacs, 2003).

C. Notch Signaling – A Correlation with Prostatic Progenitor Cell

Notch genes encode large Type I transmembrane receptors that have been conserved during evolution (Schweisguth, 2004). Notch receptors are activated by Type I transmembrane DSL ligands, known as Delta, Serrate and Lag2, to receive short-range signals between immediate adjacent cells (Mumm and Kopan, 2000). Ligand binding to Notch receptor induces a proteolytic cascade which results in release of the Notch intracellular domain (Schweisguth, 2004). Notch intracellular domain binds to multiple transcription repressors (CBF1, Su and Lag) and converts them into transcription activators (Lai, 2004). Activated Notch signaling eventually leads to the up-regulation of immediate downstream targets (Lai, 2004).

In the prostate, *in situ* hybridization showed Notch1 was selectively expressed in the epithelial cell but not in the stromal cell compartment of developing mouse prostates (Shou et al., 2001). Using quantitative RT-PCR and Notch1-GFP transgenic mice, Shou *et al*. demonstrated that strong Notch1 expression coincides with the prostatic branching morphogenesis with peak levels around P3-P10, while its expression is significantly downregulated in adult prostates (Shou et al., 2001). Interestingly, Notch1-expressing cells appeared to correlate with prostatic basal epithelial cells during development (Wang et al., 2004). Consistent with this finding, Notch1 expression following castration and hormone replacement is tightly associated with basal marker-expressing cells (Wang et al., 2004). Although Notch1 was found to be upregulated in prostate cancer cell lines as well as prostate cancer mouse models (Shou et al., 2001; Greenberg et al., 1995), activation of Notch signaling by transfecting cells with a constitutive active form of Notch1 inhibited the proliferation of prostate cancer cells (Shou et al., 2001).

Since the temporal and spatial expression pattern of Notch1 in the prostate highly suggested a correlation of Notch1 with prostatic progenitor cells, Wang *et al*. generated a transgenic mouse line in which Notch1-expressing cells can be ablated in an inducible manner (Wang et al., 2004). In both organ culture of early postnatal prostates and prostatic regeneration after castration, ablation of Notch-expressing cells inhibited the branching morphogenesis, growth and differentiation in early postnatal prostates, as well as affected the regrowth of post-castration prostates with androgen replacement (Wang et al., 2004). These data provided preliminary evidence showing that Notch1-expressing cells define the progenitor cells in the prostatic epithelium, and that they are indispensable for normal development as well as regrowth of the prostate.

D. Tgf-β Signaling – Epithelial-Stromal Communication

A distinct and attractive feature of the transforming growth factor-β (Tgf-β) superfamily is that this signaling pathway employs a large group of agonists but a very simplified intracellular signaling engine (Massague and Chen, 2000). Among the Tgf-β ligands, the bone morphogenetic proteins (BMPs) form the largest subgroup within the Tgf-β family and include various BMP factors and growth and differentiation factors. The BMPs have been well-documented for their remarkable roles as instructive signals in embyogenesis and maintenance of bone and other tissue in the adult (Balemans and Van Hul, 2002). The various forms of Tgf-β and Activin are structurally different from the BMPs and are well known for their roles in late stages of embryogenesis and the mature organism (Massague and Chen, 2000). The Tgf-βs have dual biological roles: they are crucial inhibitors of epithelial cell growth, immune and hematopoietic function; on the

other hand, they serve as strong promoters for the growth of connective tissues (Massague and Chen, 2000).

Although Tgf-β signaling pathways employ a huge group of ligands and elicit very diverse physiological responses, the core of the signaling machinery is surprisingly simple across all the species of vertebrates, insects and nematodes. The basic signaling machinery is composed of type I and type II receptors, both of which are receptor serine/threonine protein kinases, as well as a family of receptor substrates, the Smad proteins, which move into the nucleus (Massague and Chen, 2000). Typically, the ligand binds and assembles the receptor complex, in which the type II receptor phosphorylates a "GS" region in type I receptor, resulting in the activation of the receptor I kinase. This kinase in turn phosphorylates Smad proteins, the only direct substrates mediating Tgf-β signaling to date, and Smads assemble multisubunit protein complexes that regulate the transcription of target genes (Massague, 1998). In vertebrates, the type I receptors for Tgf-β, Activin and Nodal, recognize Smad2 and Smad3, while the receptors for BMPs and growth and differentiation factors recognize Smad1, Smad5 and Smad8 (Massague and Chen, 2000). Receptor-mediated phosphorylation of these related Smads (R-Smads) allows the association of R-Smads with co-Smads (Smad4 and 4β in vertebrates), as well as the subsequent nuclear accumulation of the complexes (Howell et al., 1999). Although the selection of Smad by a given Tgf-β receptor provides the first level of target gene specificity, a given Smad can elicit different cellular responses depending on the cell types. The selectivity of target genes by activated Smad complexes is largely controlled by the DNA-binding cofactors, with which Smads form complexes (Massague and Wotton, 2000). A number of such Smad-binding partners have been identified including

p300/CBP, AP-1, AR etc (Derynck et al., 1998). Although Smads by themselves have DNA binding capacity with low affinity, such binding is not selective for gene activation (Shi et al., 1998). Hence the associated DNA-binding cofactors must provide a tight and highly specific recognition of DNA elements (Massague and Chen, 2000)

a) BMPs in the Prostate

The expression of BMP2, BMP3, BMP4, BMP6 and BMP7 has been reported in either normal prostate or prostate cancer cells (Harris et al., 1994), with BMP6 and BMP7 implicated in potentially mediating osteoblastic metastases in prostate cancer (Bentley et al., 1992), while BMP2 is frequently lost during prostate cancer progression (Horvath et al., 2004). An essential role played by BMP in normal prostate development was demonstrated by a functional study of BMP4 (Lamm et al., 2001). The BMP4 gene was observed to be highly expressed in the male UGS from E14 through birth, a period marked by the formation of main prostatic ducts and initiation of ductal morphogenesis (Lamm et al., 2001). Thts expression was significantly decreased around P5-P10, and reduced to an even lower level in adult prostate. *In situ* hybridization revealed that BMP4 message is initially localized to a broad and uniform domain of the E15 male UGS. As prostatic main buds appeared, expression of BMP4 remained highly concentrated around the newly formed ducts. Postnatal expression of BMP4 at P1-P10 is most abundant in the mesenchyme immediately surrounding the epithelial buds. This expression is significantly downregulated in adult prostates (Lamm et al., 2001). Throughout the entire developmental stages, no expression was detected in the epithelium. BMP4 signal is mediated by its receptor BMPR. Expression of BMP4, BMPR-IA and BMPR-IB were detected in both UGM and UGE (Lamm et al., 2001).

In an *in vitro* organ culture system, treatment of UGS with exogenous BMP4 inhibited epithelial cell proliferation and exhibited a dose-dependent suppression of ductal budding in these tissues. Consistent with this finding, adult BMP4 haploinsufficient mice exhibited an increase in the number of duct tips in both VP and AP (Lamm et al., 2001). Taken together, these observations indicated that BMP4 is a UGM factor that negatively regulates prostate ductal budding and branching morphogenesis.

b) Tgf-β in the Prostate

In the normal prostate, Tgf-β1 is expressed in smooth muscle cells, which are closely adjacent to the epithelial compartment, while Tgf-β receptors are predominantly expressed in epithelial cells (Timme et al., 1994; Itoh et al., 1998). This pattern of distribution of ligand and receptor indicated a paracrine mode of action. The action of Tgf-β on the normal prostate is centrally focused at the interaction between the smooth muscle cells and epithelial cells (Lee et al., 1999). Tgf-β produced in prostatic smooth muscle cells acts as both a potent inhibitor of prostatic epithelial cells and a promoter of epithelial apoptosis (Sutkowski et al., 1992; Story et al., 1993; Ilio et al., 1995). In normal prostate glands, multiple layers of smooth muscle cells in the proximal region induce extensive apoptosis in the epithelium; however, in the distal region, extensive epithlial cell proliferation is observed concomitantly with a very thin and discontinuous smooth muscle cell layer (Lee et al., 1999). A recent study demonstrated that a layer of smooth muscle, which differentiates between the ventral mesenchymal pad and the urethral epithelium in E20.5 female mice but not in males, negatively regulates the prostatic induction (Thomson et al., 2002). These observations support the concept that smooth

muscle cells play a negative growth-regulatory role in epithelial cells through the production of Tgf-β1. However, other studies have reported that low concentrations of Tgf-β1 can increase the proliferation of prostatic cells, suggesting that Tgf-β1 may play a differential role in the regulation of prostatic cells (Zhou et al., 2003; Robson et al., 1999) (Collins et al., 1996). Furthermore, a recent organ culture study demonstrated that Tgf-β1 stimulates cellular proliferation at the periphery of the organs while inhibiting cellular proliferation in the center of the organs (Tomlinson et al., 2004).

In androgen-ablated prostate, Tgf-β signaling has also been proposed to be one of the most important pathways activated during castration-induced regression. Tgf-β expression increases following castration and reaches a peak at post-castration day eight. Expression of Tgf-β receptors also increases simultaneously. Such an increase in Tgf-β signaling is correlated with an elevated apoptotic status in epithelial cells during androgen deprivation. A newly formed layer of smooth muscle cells surrounding the distal prostatic ducts was observed, and these smooth muscle cells express Tgf-β1. At the same time, stromal cells surrounding the proximal prostatic ducts show reduced expression of both smooth muscle a-actin and Tgf-β1. This reduced Tgf-β1 expression in the proximal region is consistent with the observation that epithelial cells are viable in this region during castration-induced prostatic regression (Lee et al., 1999).

Although prostatic stromal cells are also responsive to Tgf-β1, the action of Tgf-β1 on stromal cells is different from the action on epithelial cells. It has been shown that a continuous exposure of prostatic stromal cells to Tgf-β1 resulted in an aggregation of smooth muscle cells, a condition in which the fibroblastic lineage is converted into muscular lineage (Peehl and Sellers, 1997). Also, examination of the three dimensional

distribution of smooth muscle in prostatic organs after treatment with Tgf-β1 showed that the smooth muscle distribution was affected by Tgf-β1, causing well-defined smooth muscle adjacent to epithelial ducts (Tomlinson et al., 2004), The action of Tgf-β1 on stromal cell differentiation may play an important role during the development of benign prostatic hyperplasia. A recent study has further highlighted the essential role of stromal Tgf-β1 action in prostate cancer progression, by showing that ablation of Tgf-β1 signaling in prostatic stromal cells leads to prostatic neoplasia (Bhowmick et al., 2004). Overall, these results demonstrated that Tgf-βs can have diverse activities in the prostate,

c) Smads Link Tgf-β Pathway to AR

Androgen promotes cell growth and inhibits cell apoptosis through AR, while the Tgf-β pathway controls prostate cell proliferation, differentiation, and apoptosis. By using transient transfection systems, Hayes *et al*. first demonstrated the molecular mechanism by which Tgf-β inhibits AR-mediated transcriptional activation (Hayes SA et al., 2001). They showed that the Tgf-β signaling downstream mediator, Smad3 can specifically repress the androgen-responsive activation of the MMTV and the prostate specific antigen (PSA) gene promoters, both of which are natural androgen-regulated promoters. This inhibitory effect is transmitted through Tgf-β signaling and can be regulated by other Smad proteins (Hayes SA et al., 2001). Importantly, Smad3 directly interacts with AR via its MH2 domain and the transactivation domain of AR. The repressive effect of Smad3 is solely mediated through the MH2 domain (Hayes SA et al., 2001). These results provided the first insight into the mechanism by which Tgf-β regulates the androgen-signaling pathway in normal prostate and cancer cells.

A second study demonstrated a mutual regulation between androgen and Tgf-β signaling pathways (Chipuk et al., 2002). Androgens negatively regulate the expression of Tgf-β ligands and receptors. In addition androgen inhibits the activation of Smad through the direct interaction between ligand-bound AR and Smad3. This interaction is specific for Smad3 but not other Smad proteins. AR ligand binding domain directly blocks the binding of Smad3 to Smad-binding element, resulting in suppression in Smad3 transactivation (Chipuk et al., 2002). Collectively, these data illustrate from a different view that ligand-activated AR inhibits Tgf-β transcriptional responses.

Along these lines, Kang *et al*. further demonstrated that Smad4 can interact with the DNA-binding and ligand-binding domains of AR, when Smad3 is present (Kang et al., 2002). Surprisingly, addition of Smad3 enhanced AR transactivation in the prostate cancer PC3 and LNCaP cells, while addition of both Smad3 and Smad4 repressed AR transactivation in various androgen responsive promoters, including the PSA genes (Kang et al., 2002). However, in a Smad4-null cell line, the influence of Smad3 on AR transactivation is differentially dependent on the specific androgen responsive promoters. The effect of Smad3/Smad4 on AR transactivation was further proposed to involve acetylation events (Kang et al., 2002). Taken together, these results suggest that the cross-modulation between androgen and Tgf-β signaling is at least in part mediated by the interactions between AR, Smad3, and Smad4, and such a mutual regulatory mechanism may play a balancing role facilitating normal prostate development. Disregulation of either pathway may result in abnormal cell growth and unexpected gene activation or inactivation, which are associated with cancer progression.

E. Receptor Tyrosine Kinase Pathways

Receptor tyrosine kinase is a large family of cell surface receptors that contain intrinsic protein tyrosine kinase activity. These receptors catalyze the transfer of the gamma phosphate of ATP to the tyrosine of target proteins. Receptor tyrosine kinase signaling pathways play an important role in the control of many fundamental cellular processes including cell cycle, survival, proliferation, differentiation and metabolism (Schlessinger, 2000).

All receptor tyrosine kinases contain an extracellular ligand binding domain that is usually glycosylated. This ligand binding domain is connected with a cytoplasmic domain by a transmembrane helix. The cytoplasmic domain has a conserved protein tyrosine kinase core and supplementary regulatory sequences which are subjected to phosphorylation and regulation by heterologous protein kinases (Hunter, 2000; Hubbard et al., 1998). All known receptor tyrosine kinases (e.g. EGF receptor, FGF receptor, IGF receptor) are monomers on the cell membrane, except the insulin receptor which is a heterodimer. Ligand binding induces receptor dimerization, resulting in the autophosphorylation of their cytoplasmic domains (Lemmon et al., 1994; Jiang and Hunter, 1999). Although all receptor tyrosine kinases are activated by dimerization, different ligands employ different mechanisms for inducing the active state of the receptors. Structural studies of the catalytic core of several receptor tyrosine kinases, as well as the biochemical studies of receptor phosphorylation and activation suggest that receptor oligomerization can increase the local concentration of the protein tyrosine kinase, leading to efficient transphosphorylation of tyrosine residues (Schlessinger, 2000).

In addition to its role in controlling protein kinase activity, autophosphorylation of receptor tyrosine kinases is essential for the recruitment of a variety of signaling proteins, since most tyrosine autophosphorylation sites function as binding sites for various signaling proteins or docking proteins, which contain Src homology 2 or phosphotyrosine binding domains. Docking proteins contain specific domains such as binding domains that are responsible for complex formation with cell surface receptors, hence functioning as platforms for the recruitment of signaling proteins in response to receptor stimulation. For example, upon FGF stimulation, most of the activated signaling proteins are recruited via docking proteins but not by their direct binding to FGF receptor. A total number of activated signaling proteins is the sum of those recruited by receptor itself and those recruited by docking proteins that are phosphorylated by the same receptor (Schlessinger, 2000). The diverse downstream effector proteins involve a variety of signaling pathways including Ras/MAP, JNK, and PI-3 pathways (Schlessinger, 2000). These pathways regulate the activity of transcriptional factors by phosphorylation and by other mechanisms, leading to an overall physical or pathological response to the activation of the specific receptor.

a) EGF Signaling – Prostate Cell Proliferation

The epidermal growth factor receptor (EGFR) was the first identified receptor tyrosine kinase. Many mechanisms for activation and recruitment of intracellular signaling pathways after growth factor stimulation were discovered through the studies of EGF signaling. The EGFR family has four members: EGFR (ErbB1), ErbB2, ErbB3, and ErbB4. EGFR has numerous ligands including EGF, Tgf-α, HB-EGF. Activating

mutations and overexpression of this receptor family were found in a variety of cancers and other diseases (Schlessinger, 2000).

In normal prostate, EGF is produced in stromal cells, while EGFR is primarily expressed in basal epithelial cells (Sherwood and Lee, 1995). Expression of EGF was observed to be elevated in prostate cancer cells. In contrast, Tgf-α is prominently expressed in prostate cancer cells but not in normal prostate (Byrne et al., 1996). EGF and Tgf-α function as strong promoters for cell proliferation in both stroma and epithelium (Culig et al., 1996). Blocking antibody against EGFR inhibited prostate cell proliferation and downregulated MAP kinase signaling pathway (Prewett et al., 1996). It has been shown that castration of adult mice reduced the production of EGF in prostate, and androgen restoration also restored the EGF levels (Hiramatsu et al., 1988). Since androgen regulates the growth of the stromal cells from which EGF is produced, this androgen-dependent effect on EGF expression may be due to an indirect mechanism. On the other hand, EGF signaling also increases coactivation of the AR in prostate cells, suggesting a mutual regulatory mechanism (Gregory et al., 2004).

In prostate cancer, EGF and Tgf-α stimulate cancer cell proliferation. High levels of Tgf-α expression has been observed in high-grade prostate cancers (Sherwood and Lee, 1995). Overexpression of Tgf-α in transgenic mice causes prostatic hyperplasia, suggesting that activation of EGFR signaling plays a key role in prostate cancer progression (Wong et al., 1998). Several studies also suggested that EGF signaling as least in part account for the progression of androgen-independent prostate cancer (Djakiew, 2000).

b) FGF Signaling – Paracrine Regulator for Prostatic Organogenesis

The fibroblast growth factor (FGF) family contains at least 23 related growth factors; while there are four known receptors (FGFR1, FGFR2, FGFR3 and FGFR4) mediating FGF signals (Naski and Ornitz, 1998). FGFs activate FGF receptors (FGFR) with the cooperation of the accessory molecule heparin sulfate proteoglycan (Yayon et al., 1991), which is essential for stabilizing FGF-FGFR complex. The dual ligand-dependent activation of FGFR provides a mechanism for localized activation of FGFR and cell proliferation or differentiation (Spivak-Kroizman et al., 1994). The heparin is synthesized in limited areas in extracellular matrix and provides a scaffold where FGFR-expressing cells migrate toward and hence survive, proliferate and differentiate.

FGFs are key regulators of early organogenesis and play important roles in the development of almost every organ in the body. For example, FGF signaling is essential for limb induction and maintenance (Ohuchi et al., 1997; Xu et al., 1998), as well as for lung branching morphogenesis (Bellusci et al., 1997b; Park et al., 1998). In the prostate, two well characterized FGFs are FGF7 and FGF10. FGF7 is also called keratinocyte growth factor. Both FGF7 and FGF10 play important roles in prostate growth (Sugimura et al., 1996) (Thomson and Cunha, 1999; Donjacour et al., 2003).

FGF7 is expressed in prostate mesenchymal cells and acts as a paracrine regulator on the growth of epithelial cells, since the receptor for FGF7 is expressed in epithelial cells. It has been shown that FGF7 regulates the growth of the VP (Sugimura et al., 1996) and seminal vesicle (Alarid et al., 1994). Similar to the effects of EGF and Tgf-α, FGF7 is also mitogenic to epithelial cells, since treatment of VP and seminal vesicle with FGF7 stimulated tissue growth in organ culture system; while addition of FGF7 antibody

partially blocked organ growth (Sugimura et al., 1996). Consistent with this biological role, FGF7 mRNA is abundant during the active development of VP and seminal vesicle *in vivo* (Thomson et al., 1997). However, unexpectedly, transgenic mice with targeted gene deletion in FGF7 did not show a phenotype in the male reproductive organ including the prostate (Guo et al., 1996), suggesting that FGFs may work in a redundant manner and other FGFs may compensate for the loss of FGF7 in the prostate.

FGF7 has long been suggested as an androgen-regulated mesenchymal paracrine factor (Peehl and Rubin, 1995). Although *in vitro* cultured prostatic stromal cells responded to androgens by upregulating FGF7 (Yan et al., 1992), *in vivo* studies showed an opposite result that FGF7 mRNA was decreased rather than increased upon androgen treatment (Nishi et al., 1996; Thomson et al., 1997). Also, FGF7 mRNA was observed to be inversely proportional to androgen activity in an *in vitro* organ culture system (Thomson et al., 1997). These results indicated that FGF7 is not directly regulated by androgen *in vivo*. This was further supported by studies of the protein distribution of FGF7 in the prostate, where the distribution of FGF7 is not affected by androgen manipulation (Nemeth et al., 1998).

Since FGF10 shares a very high sequence homology with FGF7, it has been hypothesized as another candidate for paracrine regulator which may play key roles in mesenchymal-to-epithelial cell signaling. FGF10 mRNA was highly expressed in VP and seminal vesicle (Thomson and Cunha, 1999), and it was also found in tissues that do not belong to male reproductive organs such as the lung and skin. However, the tissue distribution of FGF10 is much more tissue restrictive as compared with the distribution of FGF7, which is widely expressed (Thomson and Cunha, 1999).

In the prostate, FGF10 is expressed during the earliest stages of prostatic development. The highest FGF10 mRNA levels were found to be in the time window during which prenatal and neonatal prostatic organogenesis occurs. In adult prostate tissues, FGF10 levels were significantly decreased to a very low or even undetectable level. Spatially, FGF10 mRNA was only detected in a small population of mesenchymal cells in both VP and seminal vesicle by *in situ* hybridization. In neonatal prostate, FGF10 mRNA was found to be in the mesenchymal cells of peri-urethral area as well as around the growing tips of prostatic buds; while in later stages, FGF10 mRNA was found in mesenchyme surrounding epithelial buds which undergo branching morphogenesis (Thomson and Cunha, 1999).

Addition of FGF10 to *in vitro* cultured prostate organ stimulated the development of prostatic rudiments. Recombinant FGF10 also can stimulate the growth of prostate epithelial cells but not stromal cells, suggesting a mitogenic effect as EGF, Tgf-α and FGF7 (Thomson and Cunha, 1999). However, FGF10 does not appear to be acting synergistically with androgen on protatic growth. Similar to FGF7, in an *in vitro* cell culture study, prostatic fibroblasts produced more FGF10 in response to androgen (Lu et al., 1999), while *in vivo* examination of FGF10 levels suggested an opposite correlation of FGF10 and androgen stimulation (Thomson and Cunha, 1999). Organ culture experiments also did not support the idea that FGF10 is regulated by androgen (Thomson and Cunha, 1999). Moreover, the growth stimulating effect of FGF10 could not be completely inhibited by anti-androgens, further suggesting that FGF10 action was independent of the androgen signaling pathway (Thomson and Cunha, 1999). These data

supported FGF10 as a paracrine regulator that functions directly to regulate prostatic growth.

Recently, the male reproductive tracts of FGF10 knockout mice were analyzed. Interestingly, although the testis of FGF10 knockout mice produces sufficient androgens, most of the male secondary sex organs, including the prostate and the seminal vesicle, were absent (Donjacour et al., 2003). Addition of FGF10 to *in vitro* cultured FGF10 knockout UGS partially reversed the phenotype by inducing prostatic budding and differentiation in the presence of androgens (Donjacour et al., 2003). These *in vivo* functional studies demonstrated that FGF-10 is the first identified mesenchymal factor required for prostatic organogenesis.

AR Protein Biology and Transcriptional Regulation

AR is the mediator of the biological action of androgens. AR belongs to the nuclear receptor superfamily. Androgen-bound AR translocates from cytoplasm to the nucleus and acts as a transcription factor to regulate gene expression. AR-regulated genes participate in a variety of biological and physiological activities including two most important functions: the differentiation of male reproductive organs and the maintenance of spermatogenesis (Gelmann, 2002). AR regulates gene transcription through recognition and binding to the specific androgen response element (ARE) within the promoter or enhancer sequences of its target genes. AR transcriptional activity is frequently influenced by numerous co-activators or co-repressors that affect different aspects of AR functionality, encompassing ligand binding and DNA binding. The fascinating and complicated AR biology stems largely from these AR coregulators which

modulate AR activity either by direct or indirect modification of histones or by recruitment of basal transcription machinery (Heinlein and Chang, 2002). Abnormal AR biology due to aberrant coregulator activity contributes to the progression of androgen/AR-related diseases, including prostate cancer (Suzuki et al., 2003). Although AR shares many similarities with other nuclear receptor family members (e.g. ER, GR), in terms of structure and biology, it displays distinct features including functional interaction with coregulators (Heinlein and Chang, 2002).

A. The Protein Structure of AR

Nuclear receptor members function as ligand-inducible transcription factors, which can be divided into three types. Type 1 receptors typically form ligand-induced homodimer and bind to inverted repeat DNA cis-elements. AR, estrogen receptor (ER), progesterone receptor, glucocorticoid receptor (GR) and mineralocorticoid receptor belong to type 1 receptor. The type 2 receptors frequently form heterodimer with retinoic acid receptors and bind to direct repeat DNA *cis*-elements. Vitamin D3 receptor, peroxisome proliferator-activated receptor, thyroid hormone receptor and all-trans-retinoic acid receptor belong to type 2 receptor. Type 3 receptors are orphan receptors whose ligands are unknown (Heinlein and Chang, 2002).

The protein structure of AR can be divided into four functional domains: the NH_2-terminal domain (NTD), DNA binding domain (DBD), hinge region, and ligand-binding domain (LBD). Both NTD and LBD contain transactivation function individually. The transcriptional activation function of NTD is contained in a region called AF-1, which functions in a ligand-independent manner (Jenster et al., 1995), while the transactivation

activity in LBD is located in AF-2, which functions in a ligand-dependent manner (Danielian et al., 1992; He et al., 1999).

There are two functional regions in the NTD: a polyglutamine repeat and the AF-1 transactivation region. The polyglutamine repeat is required for full receptor activity and interacts with different coregulators (Simental et al., 1991; Jenster et al., 1991); while the AF-1 contains a WXXLF motif, which has been shown to serve as an interface for protein interaction with AR LBD (He et al., 2000). Interaction between NTD and LBD can be faciliatated by a variety of coregulators, and this interaction has been shown to be important for stabilizing the ligand-bound status of the receptor (Ikonen et al., 1997)

As with other members of nuclear receptor family, AR DBD consists of two zinc fingers that recognize a specific DNA consensus sequence, GGTACAnnnTGTTCT. AR always binds as a dimer to classical AREs, as well as to various complex DNA response elements (Kasper et al., 1994; Verrijdt et al., 1999; Zhou et al., 1997; Claessens et al., 2001). Some proteins modulate AR transcriptional activity by affecting the binding capacity of AR to its *cis*-elements. For example, receptor accessory factor binds AR NTD and enhances AR DNA binding (Kupfer et al., 1993), while calreticulin prevents AR DNA binding by interacting with AR DBD (Dedhar et al., 1994). Most recently, the 3D crystal structure of AR DBD bound to a naturally occurring selective AREs has been solved. The study revealed an unexpected head-to-head arrangement of the two monomers rather than a head-to-tail arrangement seen in nuclear receptors bound to the response elements with similar geometry (Shaffer et al., 2004). Compared with GR, the AR DBD dimerization interface contains additional interactions that stabilize the dimer and increase the affinity for nonconsensus response elements (Shaffer et al., 2004). These

results provided a definitive answer to the mechanism which underlies the selective binding of AR to its specific response elements. Although AR is normally thought to function as a homodimer, it can also form heterodimers with other nuclear receptor members such as GR and ERα (Panet-Raymond et al., 2000; Chen et al., 1997).

The hinge region of AR links the DBD and LBD, and contains a ligand-dependent nuclear localization signal, which may interact with nuclear trafficking protein importin (Jenster et al., 1993; Zhou et al., 1994).

AR LBD forms a ligand-binding pocket with 11-13 alpha-helices. By comparing the receptor structure in ligand absent status and in ligand-bound status, crystallographic studies demonstrated that ligand binding induces a conformational change in LBD, in which helix 12 and the AF-2 domain folds across the ligand-binding pocket (Williams and Sigler, 1998; Brzozowski et al., 1997). In addition to binding ligand, LBD also mediates AR interaction with heat shock proteins (Fang et al., 1996), as well as the interaction with AR NTD. The interaction between the AR NTD and LBD creates a coregulator interaction interface that is different from that of ER (Heinlein and Chang, 2002). This observation supported the functional analysis of full-length receptors which suggested distinct differences between AR and ER. However, until now, no 3D structure has yet been determined for any full-length nuclear receptor.

B. AR-Mediated Transcriptional Activation through the Basal Machinary

Transcriptional activation of genes by AR requires the final recruitment of RNA polymerase II onto the target genes' promoter. The recruitment of RNA polymerase II is initiated with the binding of TATA Binding Protein (TBP) near the transcriptional initiation site and mediated through the assembly of general transcription factors. TBP is

part of a complex called transcription factor IID (TFIID). The binding of TBP at TATA element causes bending in DNA and brings TATA upstream elements close to the general transcription machinery, leading to important interactions between general transcription factors and AR-coregulator complex. After TBP binding, TFIIB binds directly to TBP and recruits the TFIIF-polymerase II complex, which in turn recruits the ATPase/kinase, TFIIE, and the helicase, TFIIH, then transcription is initiated (Heinlein and Chang, 2002).

AR has been shown to be directly or indirectly interacting with various general transcription factors. For example, AR NTD has been shown to directly recruit TFIIF (McEwan and Gustafsson, 1997), and bind TFIIH (Lee et al., 2000). Also, it has been demonstrated that AR interacts with some of the transcription elongation factor (Lee et al., 2001). These data suggest that AR may regulate transcriptional activity by interacting with TFIIF and TFIIH, as well as by facilitating the recruitment of elongation factors to androgen-regulated promoters. In addition, AR also indirectly influences transcription through coregulators which have an effect on basal transcription machinery. For example, ligand-dependent transactivation of AR by ARA160 is through the modification of the DNA binding capacity of TBP (Hsiao and Chang, 1999).

C. AR Coregulators Modulate the Receptor Activity

AR coregulators are generally considered as proteins that can interact with AR but do not possess DNA binding activity. Based on their different functional mechanisms, AR coregulators are subdivided into two categories. Type I coregulators function primarily with the AR at the target gene's promoter to facilitate DNA occupancy, chromatin remodeling, or the recruitment of general transcription factors that are

associated with the RNA polymerase II. Type II coregulators function primarily to modulate the appropriate protein conformation of AR, facilitate the interaction between AR NTD and LBD, or influence AR protein stability and subcellular distribution AR. The overall effect of type II coregulators on AR can result in a changed transcriptional activity (Heinlein and Chang, 2002).

Several important type I coregulators include CBP/p300, SRC-1, and SWI/SNF. Both CBP/p300 and SRC-1 have histone acetyltransferase activity and interact with the basal transcriptional machinery (Ogryzko et al., 1996; Spencer et al., 1997). CBP has been found to interact with a number of AR coactivators (Chakravarti et al., 1996). These proteins and CBP may therefore bridge AR function to the basal transcriptional machinery. SRC-1 was isolated by a yeast two-hybrid screen as a steroid receptor coactivator and has been shown to be able to promote the ligand-dependent transcription of a number of steroid receptors including AR (Onate et al., 1995; Spencer et al., 1997). The mechanism of SRC-1 action may be through the recruitment of additional coregulators including CBP (Yao et al., 1996), and through the interactions with TBP and TFIIB (Takeshita et al., 1996). In addition, CBP/p300 and SRC-1 have both been demonstrated to have histone acetyltransferase activities, which are associated with reduced nucleosome-nucleosome contacts and active genes (Spencer et al., 1997; Ogryzko et al., 1996).

SWI/SNF complex have been shown to interact with ER and GR (Ichinose et al., 1997; Yoshinaga et al., 1992). It is thought that the recruitment of the SWI/SNF complex to the nuclear receptor is facilitated by other coactivators (Heinlein and Chang, 2002). SWI/SNF complex contains a DNA-dependent ATPase and modifies the conformation of

nucleosome in an ATP dependent manner, resulting in a decreased histone-DNA association and an increased gene transcriptional activity (Workman and Kingston, 1998).

Several important type II coregulators include ARA70 and the f-actin binding protein filamin. Wild type ARA70 is localized to the cytoplasm, while ARA70 N-terminal truncate protein can translocate with ligand-bound AR into nucleus and function as a strong transcriptional co-activator. ARA70 has also been shown to interact with other AR coactivors and may therefore act as a molecular platform for the transcriptional activity (Yeh and Chang, 1996). Mutation of filamin has been shown to prevent AR nuclear translocation even in the presence of androgen, suggesting that filamin facilitates the cytoplasmic to nuclear translocation of the ligand-bound receptor (Ozanne et al., 2000).

D. Cross-Modulation between AR and Other Signaling Pathways

In addition to the basal transcriptional machinery and the various coregulators, AR has also been shown to interact with other DNA-binding transcription factors. These AR-interacting proteins could be important mediators or effectors of a number of intracellular signaling transduction pathways. The transcriptional activity of AR has been found to be frequently influenced by a mechanism called cross-modulation, in which androgen signaling interplays with different signal cascades induced by either growth factors or cytokines (Heinlein and Chang, 2002). AP-1 and NFκB are two of the best characterized AR-interacting transcription factors which play key roles in affecting AR transcriptional activity (Sato et al., 1997; Palvimo et al., 1996). In addition, AR interacts with STAT3 and Smad3, both of which are signal transduction mediators (Matsuda et al., 2001; Chipuk et al., 2002). AR can also interact with tissue specific transcription factors

such as SRY and Prostate Derived Ets Factor (PDEF) (Yuan et al., 2001; Oettgen et al., 2000).

a) AP-1 and AR Interaction

The proto-oncoprotein c-Jun heterodimerizes with c-Fos to form the transcription factor AP-1. AP-1 regulates transcription through binding to a consensus AP-1 cis-DNA sequence. In a search for interacting partners, AR was found to inhibit the protein DNA interaction between c-Jun and AP-1 site; however AR itself cannot interact with AP-1 DNA element. This mechanism was proposed for AR transcriptional inhibition of neurotrophin receptor promoter (Kallio et al., 1995).

Bubulya *et al*. reported an indirect mechanism by which c-Jun can stimulate transcription via AR. In this process, c-Jun was found to support AR-mediated transactivation in the absence of its interaction with c-Fos or with AP-1 DNA element (Bubulya et al., 1996). They further showed that this positive effect of c-Jun on AR transactivation is dose-dependent and maybe through a direct interaction with AR DNA binding domain/hinge region. However, c-Jun loses its ability of enhancing AR-mediated transactivation when heterodimerized with c-Fos (Bubulya et al., 1996). Thus c-Jun was proposed as a mediator for AR-induced transactivation.

However, in another experiment, the transcription of androgen-regulated PSA gene was measured when the AP-1 level in LNCaP cells was elevated by either 12-O-tetradecanoylphorbol 13-acetate treatment or c-Jun expression vector transfection (Sato et al., 1997). It was found that androgen-induced PSA gene expression was inhibited by tetradecanoylphorbol 13-acetate without altering nuclear levels of AR protein. Transient overexpression of c-Jun and c-Fos also inhibited androgen-induced PSA promoter

activity. These observations were proposed to be related with the disruption of AR interaction with ARE, which was demonstrated in electrophoretic mobility shift assays (EMSA). Such repression was also found to be mutual, since AR-glutathione S-transferase (GST) proteins inhibited the formation of c-Jun/AP-1 complexes. Co-immunoprecipitation experiments suggested such mutual repression of DNA binding is due to a direct interaction between AR and c-Jun, while the degree of repression may be controlled by the ratio of AR to c-Jun (Sato et al., 1997). Using a series of mutant proteins, the interaction domains were tracked to the DBD and LBD of AR and the leucine zipper region of c-Jun (Sato et al., 1997). However, by using mutated AR proteins and transcription assays, Lobaccaro *et al*. demonstrated that several segments of the AR, including the first 188 amino acids of the NTD and the intact LBD of AR are necessary to obtain a full transrepression with the AP-1 pathway, while mutations within the DBD of AR highly impair this cross talk (Lobaccaro et al., 1999).

Fronsdal *et al*. proposed an alternative mechanism, which may explain the mutual regulation of AR and AP-1. In this experiment, ectopically expressed CBP can largely relieve AP-1-mediated repression of AR activity. CBP can physically interact with both NTD and LBD of AR. These results suggested that the transcriptional interference between AR and AP-1 could be a result of competition for limiting amounts of CBP in the cell (Fronsdal et al., 1998).

b) **NFκB and AR Interaction**

Cross-modulation between AR and NFκB/Rel proteins is another well-documented model in which distinct signaling pathways affect each other to provide opportunities for cell- or tissue-specific responses (Palvimo et al., 1996). Using various

androgen-regulated and NFκB-regulated reporter genes in transient transfection assays, RelA (p65), a major NFκB member, repressed AR-mediated transactivation in a dose-dependent manner. However NFκB1 (p50), another major member of the NFκB family, did not affect the transactivation. This transcriptional interference between RelA and AR is mutual since cotransfected AR also inhibited RelA-mediated transactivation. A weak protein-protein interaction was detected between AR and RelA; however this interaction did not affect the DNA-binding activities of either protein (Palvimo et al., 1996).

As mentioned above, CBP is capable of relieving AP-1 mediated transrepression of AR activity. A similar mechanism applies to NFκB (Aarnisalo et al., 1998). Exogenously transfected CBP was also capable of diminishing the mutual transcriptional repression between AR and RelA (Aarnisalo et al., 1998). These observations implied that transcriptional interference between AR and AP-1 or NFκB is mediated, at least partially, through competition for intracellular CBP protein. CBP may serve as an integrator or modulator between AR and other signaling pathways.

c) STAT3 and AR Interaction

Signal Transducer and Activator of Transcription 3 (STAT3), combined with upstream Janus Kinase (JAK) and downstream Mitogen-Activated Protein Kinase (MAPK), is important mediator of cytokine signaling such as the Interleukin 6 (IL-6). IL-6 is also able to induce AR-mediated gene activation in prostate cancer, and this activation requires activated STAT3, which associates with AR in an androgen-independent but IL-6-dependent manner (Chen et al., 2000). Inhibition of STAT3 results in inhibition of AR-mediated gene activation in response to IL-6. These findings revealed the importance of activated STAT3 in prostate cancer progression (Lou et al., 2000).

Matsuda *et al*. provided evidence for a direct physical interaction between AR and STAT3 (Matsuda et al., 2001). They found that IL-6-induced activation of STAT3 was augmented in the presence of dihydrotestosterone (DHT). Reciprocally, phosphorylation of STAT3 in response to IL-6 allows STAT3 to interact with AR and enhanced AR transcription (Matsuda et al., 2001). These data suggested a model of cross-stimulation between two pathways. Later, by using immunoprecipitation and transactivation studies in LNCaP cells, Ueda *et al*. showed a direct interaction between amino acids 234-558 of the AR NTD and STAT3, following IL-6 treatment (Ueda et al., 2002).

However, in another study, IL-6 was found to inhibit DHT-mediated expression of PSA gene (Jia et al., 2004). In this study, IL-6 prevented the promoter recruitment an AR coactivator, p300, resulting a partially inhibited histone H3 acetylation at the same element. Interestingly, the inhibitory effect by IL-6 was partially abrogated by knocking down STAT3, suggesting that this inhibition is mediated through STAT3 (Jia et al., 2004). These results argue that the resulting effects of the crosstalk between these two pathways may be dependent on specific cellular context.

d) Smad3 and AR Interaction

As introduced earlier, Tgf-β-induced phosphorylation of Smad3 also results in interaction between Smad3 and AR (Kang et al., ; Hayes SA et al., 2001; Chipuk et al., 2002). The overall effect of AR and Smad3 interaction is cell type-dependent, possibly due to the differential availability of other AR and/or Smad3 interacting proteins. For example, in prostate cancer cells DU145 and PC3, Smad3 enhances AR transcriptional activity, while in CV-1 cells, Smad3 inhibited AR transcriptional activity (Kang et al., 2002).

e) **SRY and AR Interaction**

The Sex-determining Region on the Y chromosome (SRY) encodes a testis-expressed protein essential for male sex determination. Coexpression of AR and SRY caused a significant repression in AR transcriptional activity on a number of androgen-responsive genes, including the human PSA gene (Yuan et al., 2001). Although no SRY-promoter interaction was identified in this study, mammalian two-hybrid experiments demonstrated an AR-SRY interaction, which is mediated through the AR DBD. *In vitro* binding experiments confirmed this interaction as direct protein-protein interaction, and further mapped the AR-interacting domain to the SRY high mobility group box DNA binding domain (Yuan et al., 2001). *In vivo* stable SRY expression inhibited the endogenous PSA gene in LNCaP cells. These findings regarding AR-SRY interaction suggested a combinatory regulation role of AR and SRY in determining normal male reproductive organ development and function.

f) **Ets Factor and AR Interaction**

The Ets transcription factor family comprises more than 20 members that are involved in normal development and oncogenesis. Ets factors have conserved DBD of around 85 amino acids, named the ETS domain. Schneikert *et al*. first demonstrated that AR negatively regulates matrix metalloproteinase-1 expression not through AP-1 but rather through a family of Ets factors (Schneikert et al., 1996). This negative regulation is AR-specific and requires AR NTD but not the DNA binding activity of AR (Schneikert et al., 1996). However, in a GST pull-down assay, AR interacts physically with a representative Ets factor, ERM, and this interaction was not mediated through AR NTD but through AR DBD-LBD (Schneikert et al., 1996). This result indicated that the

interaction of AR with ERM may allow the apposition of the two proteins to enable AR NTD to interfere with ERM transcriptional activity. These results identified a novel regulatory pathway in which steroid hormone receptor such as AR negatively regulates the expression of matrix metalloproteinases through interacting with Ets factors.

In addition, AR negatively regulates the expression of maspin gene, a tumor suppressor frequently lost in prostate cancer cells. Ets positively regulates maspin gene (Zhang et al., 1997). During the progression of cells from normal to cancer status, loss of maspin expression is a result from both the absence of positive regulation by the Ets element and the presence of negative regulation by AR. This observation provided a balancing mechanism between AR and Ets transcriptional regulation (Zhang et al., 1997).

Recently, Oettgen *et al*. isolated a novel, prostate epithelium-specific Ets transcription factor, named PDEF (Oettgen et al., 2000). Reporter assay demonstrated that PDEF acts as an androgen-independent transcriptional activator on the PSA promoter. PDEF also directly interacts with the AR DBD and enhances androgen-mediated activation of the PSA promoter (Oettgen et al., 2000). It is interesting that Nkx3.1, a prostate specific homeobox protein, interacts with PDEF and attenuates PDEF-mediated transactivation of PSA promoter (Chen et al., 2002b). These data depicted a multiprotein nuclear complex involving several cell-type specific proteins (AR, PDEF and Nkx3.1) that participate in transcriptional regulation in prostate cells. Although PDEF was identified as a prostate-enriched transcription factor, follow-up studies showed it is also overexpressed in human breast cancer cells (Feldman et al., 2003).

The Transcriptional Synergy

Transcriptional regulation of gene expression involves a synergistic effect from the basal transcriptional machinery, proximal sequence-specific activators, cofactors, long-range enhancer-promoter interactions, chromatin remodeling complexes, as well as the signal transduction cascades. Transcriptional synergy has long been proposed as an important mechanism to achieve organism diversity, in addition to two other mechanisms: alternative splicing and DNA rearrangement (Levine and Tjian, 2003). Whole-genome sequence assemblies have been available for seven different animals, including nematode worms, fruitflies, mosquitoes, sea squirts, pufferfish, mice and humans. Computer-assisted comparative genome analyses indicated that increases in gene number, during animal evolution, cannot account for the increased morphological and behavioural complexity. Instead, the organism complexity arises from a progressively more elaborate regulation of gene expression (Levine and Tjian, 2003).

Levine *et al*. has recently pointed out the following: 1) vertebrate genomes have only about twice the number of genes that invertebrate genomes have, and the increase is primarily due to the duplication of existing genes rather than the invention of new ones; 2) the simple nematode worm, *Caenorhabditis elegans*, contains around 20,000 genes but does not have the complex cell types and tissues seen in the fruitfly *Drosophila*, which contains less than 14,000 genes; most strikingly, the human genome contains only around 30,000 protein-coding genes (Levine and Tjian, 2003). They proposed that a greater elaboration of *cis*-regulatory DNA sequences, and an increased complexity in the multiprotein transcription complexes, could be two pervasive mechanisms that lead to the observed correlation between gene number and physiological/behavioral complexity

(Levine and Tjian, 2003). Thus, genome analysis provided definitive evidence for the progressively complicated transcriptional synergy.

In a complex eukaryote in particular, an organism differentially transcribes 30,000-50,000 genes in precise spatial and temporal patterns to maintain cell specificity as well as to respond dynamically to its environment. The generally accepted concept is that cell accomplishes this by employing combinatorily subsets of basal transcription factors, ubiquitous DNA binding factors or cofactors, signal-responsive or tissue-specific activators or coactivators. A small grouping of these factors could lead to an exponentially larger number of regulatory decisions (Brivanlou and Darnell, Jr., 2002).

For instance, Carey pointed out earlier that a given RNA polymerase II enhancer responds to various signal cascades by organizing a unique array of activators in a tightly clustered fashion which produces great opportunities for their interaction with the DNA and the basal machinery. On the other hand, a given RNA polymerase II transcriptional machinery is also designed to respond in a synergistic fashion to multiple activators (Carey, 1998).

The basis for the transcriptional synergy stems from the highly sophisticated *cis*-regulatory DNA seen in higher and complex eukaryotes. However, the rapidly expanding cofactor and chromatin remodelling complexes might be critical for the integration of such complex *cis*-regulatory information. For example, different enhancers recognize different cofactor complexes, while distinct core promoters interact with various TFIID complexes. The overall diversification comes from the mixing and matching of these complexes, resulting in a huge variety of gene expression patterns (Levine and Tjian, 2003).

The nuclear receptor is a special class of transcription factors. Transcriptional synergy applies to the action of members of this family. Combinatorial control of gene expression by nuclear receptors was well exemplified by their differential recruitment of functionally diverse coregulator complexes as well as their differential interaction with various pathways (Fig. 1-3). Indeed, the functional flexibility seen in nuclear receptors is largely due to this principle of cooperativity (McKenna and O'Malley, 2002).

Probasin (Pbsn): A Gene Ideal for Studying Prostate-Specific Gene Regulation

The rat Probasin gene encodes a prostate basic protein, which is expressed as a prostate epithelium-specific and androgen-regulated gene (Kasper and Matusik, 2000). The expression of Pbsn was first described in the rat prostate, where the Pbsn protein was localized to the nuclei of luminal epithelial cells as well as in the luminal secretions (Matuo et al., 1985). Although all the rat prostate lobes express Pbsn, the expression level is highest in LP, followed by DP, AP and VP. Analysis of the Pbsn cDNA revealed a signal peptide that may account for the secretory nature of this protein. Amino acid sequence analysis of Pbsn indicated that this protein belongs to the lipocalin family (Spence et al., 1989). The tertiary protein structure of Pbsn suggested it may function as a ligand carrier protein (Kasper and Matusik, 2000).

Pbsn expression is tightly limited to the prostate epithelium; hence it is one of the best markers for prostatic differentiated response. The high prostate specificity of the Pbsn promoter has been confirmed in various *in vitro* and *in vivo* studies, and has been applied to numerous gene targeting and gene therapy studies (Greenberg et al., 1994; Yan et al., 1997; Kasper et al., 1998; Zhang ZF et al., 2000; Greenberg et al., 1995; Barrios et

al., 1996; Green et al., 1998). The proximal Pbsn promoter encompassing the element of −426/+28 bp has been shown to target a reporter gene specifically in prostate cell lines, with very low levels of reporter gene expression observed in the non-prostate cell lines (Yan et al., 1997). *In vivo*, either a 12-kb large Pbsn promoter or a 500 bp small promoter have been successfully used to target reporter genes or oncogenes into the transgenic mouse prostate (Kasper et al., 1998; Greenberg et al., 1995).

The Pbsn gene is androgen-regulated. Expression of the Pbsn gene is initiated around the third postnatal week, during which the serum androgen levels increase. Castration of adult animals led to a drastic reduction in Pbsn mRNA to nearly undetectable levels, while androgen replacement restored Pbsn expression (Kasper and Matusik, 2000).

DNase I protection assays identified two AREs located in the proximal Pbsn promoter (Rennie et al., 1993). The first ARE at -236/-223 bp was named as androgen receptor binding site-1 (ARBS-1). The second ARE at -140/-117 bp was named as ARBS-2. *In vitro* binding assay determined that ARBS-2 is a strong ARE with higher affinity to AR than ARBS-1. However, both sites are occupied even when AR is at very low levels, and both sites are required for the full androgen-responsive promoter activity. Mutation of either ARE significantly reduced androgen inductivity >95% of Pbsn promoter, further suggesting that two ARE function in a cooperative fashion (Rennie et al., 1993). Thus, the region (-244/-96 bp) that encompasses the two ARBSs and is required for full androgen-induction of Pbsn expression was designated as androgen responsive region (ARR) (Kasper et al., 1999). Later, improved dimethyl sulfate (DMS) methylation protection assays revealed two additional AR binding sites (G1 and G2) with

atypical half-site sequences located at (−209/−196 bp) and (−107/−93 bp) (Reid et al., 2001). Reid *et al*. further illustrated that ARBS-1 and ARBS-2 belongs to class-1 ARE which displays conventional guanine contacts; G1 and G2 belong to class-2 ARE which shows atypical sequence features. The binding of AR to class-2 ARE can dramatically alter the allosteric interactions between the receptor and adjacent DNA, stabilizing AR binding to adjacent class-1 sites and resulting in synergistic transcriptional activity and increased hormone sensitivity (Reid et al., 2001).

Recently, by testing a series of truncated Pbsn promoter fragments, Zhang *et al* identified two more nonconventional ARBSs, named ARBS-3 and ARBS-4, within -705/-426 bp of Pbsn (Zhang ZF et al., 2004a). Functional analysis of these individual ARE supported use of the Pbsn promoter as a model, in which six ARBSs function in a cooperative manner for maximum androgen-regulated prostate-specific gene transcription (Zhang ZF et al., 2004a).

An artificial Pbsn promoter ARR_2PB, which contains an extra copy of ARR (-244/-96 bp) fused in front of the -286/+28 bp proximal promoter, targeted high levels of reporter genes into both prostate cell lines and transgenic mouse prostate. Interestingly, this artificial Pbsn promoter has striking similarity in the organization of the AREs as the natural Pbsn promoter. This version of Pbsn construct has been widely used by many research groups for *in vitro* or *in vivo* prostatic targeting (Zhang ZF et al., 2004b). Further analysis using transgenic mice delimited the prostate specific control region to ARR, a 147 bp DNA fragment, which contains sufficient cis-regulatory information for directing prostate expression (Zhang ZF et al., 2004b).

Hypothesis

Androgen signaling is essential but not sufficient for prostate-specific gene (e.g. Pbsn, PSA) expression, since AR is expressed in other tissues (e.g. seminal vesicle, muscle, mammary gland), and AREs are also contained in non-prostatic gene promoters. When the Pbsn promoter sequences between the two ABRSs were replaced with a random DNA element with the same size, all promoter activity was abolished although AR still bound to ARBSs. This observation suggested that non-AR transcription factors play crucial roles in Pbsn gene regulation (Kasper et al., 1999). Thus, additional *cis*-regulatory information as well as other key signaling pathways is required to direct this prostatic differentiated function. Five key *cis*-acting elements were identified within -286/+28 bp using linker scan mutagenesis and reporter assays in cell culture. Two of these elements, named as tissue specific-1 (TS-1) and tissue specific-2 (TS-2), when mutated, reduced promoter bioactivity only in prostatic cell lines but not in non-prostatic cell lines. In contrast, the other three elements, when mutated, reduced bioactivity in all the cell lines (Zhang *et al* unpublished). TS-1 and TS-2 are tightly adjacent to an individual ARBS site and the core region of each is almost identical. In transgenic mice, mutation of TS1 reduced expression of a linked reporter gene, but the expression was still prostate specific; mutation of TS2 abolished all reporter activity in all transgenic lines (Zhang ZF et al., 2004b). The hypothesis is that the transcription factors bound to these key *cis*-acting elements are essential for prostatic differentiated response, and therefore may be relevant for prostatic organogenesis; a cluster of nuclear proteins bound within this region involves prostate-specific regulation via transcriptional synergy by responding to various signaling pathways and integrating diverse cellular information.

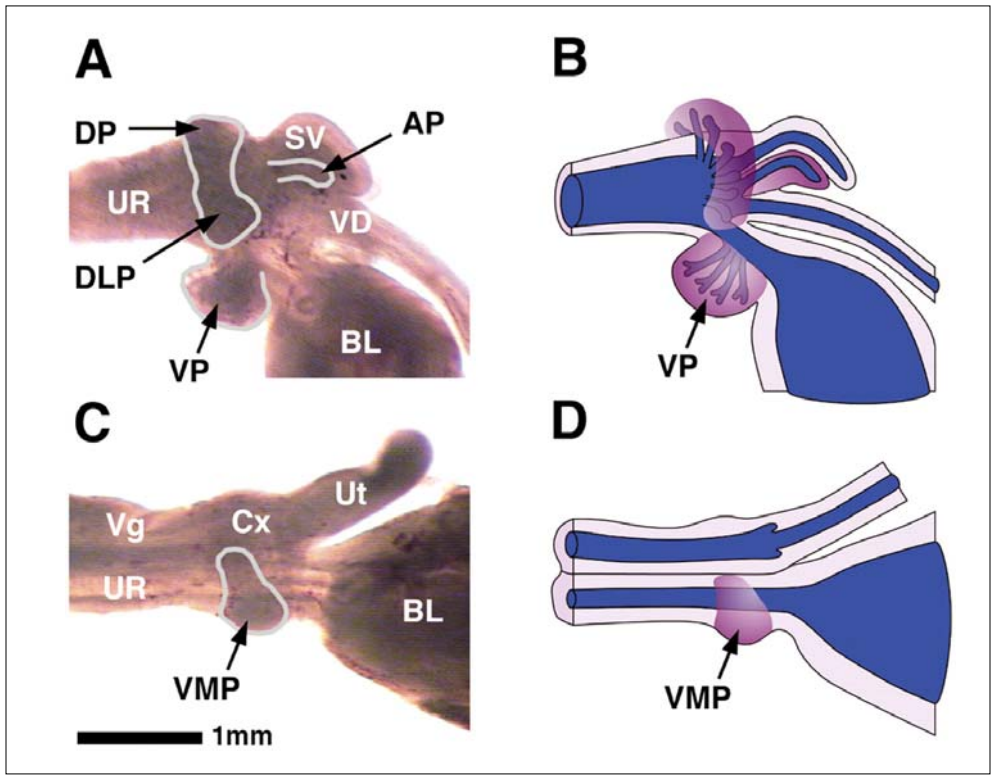

Figure 1-1. Perinatal urethra and associated reproductive organs. (A) P0 male rat urogenital tract: DP, dorsal prostate; DLP, dorsolateral prostate; AP, anterior prostate; VP, ventral prostate; UR, urethra; VD, vas deferens; BL, bladder. (B) Diagram of A. (C) P0 female urogenital tract: VMP, ventral mesenchymal pad; Vg, vagina; Cx, cervix; Ut, uterus. (D) Diagram of C. Scale bar: 1 mm. Adapted from (Thomson et al., 2002)

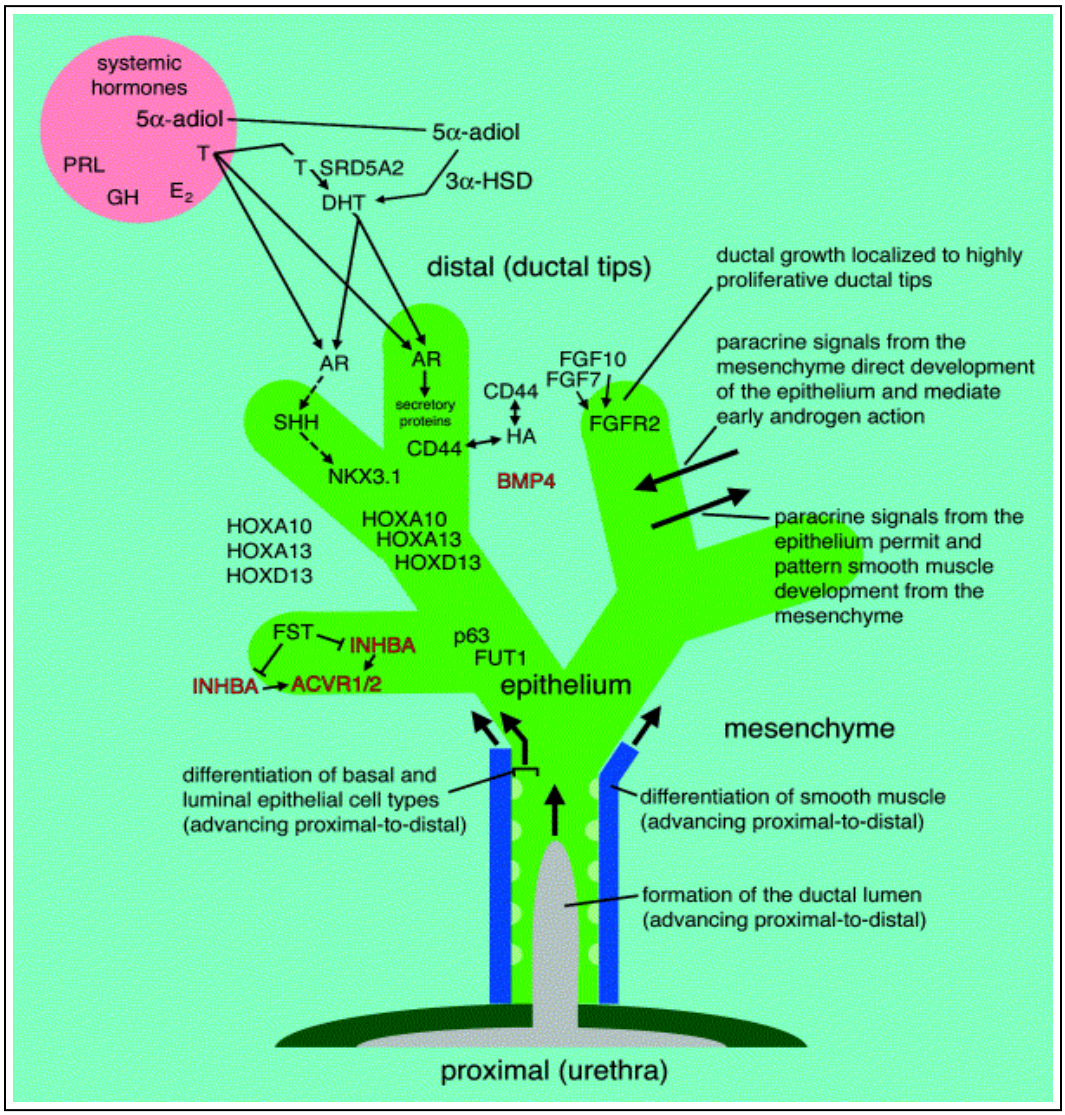

Figure 1-2. Molecular aspects of prostatic branching morphogenesis. The diagram shows that reciprocal signaling between prostatic epithelium and mesenchyme is essential for the development and morphogenesis of the gland. Ductal canalization occurs from proximal to distal in the solid epithelial cords. This process is accompanied by epithelial and mesenchymal cell differentiation. This complex genetic network involves androgen signaling pathway, Shh signaling and mesenchymal paracrine signaling molecules such as the FGFs and the BMPs. Adapted from (Marker et al., 2003).

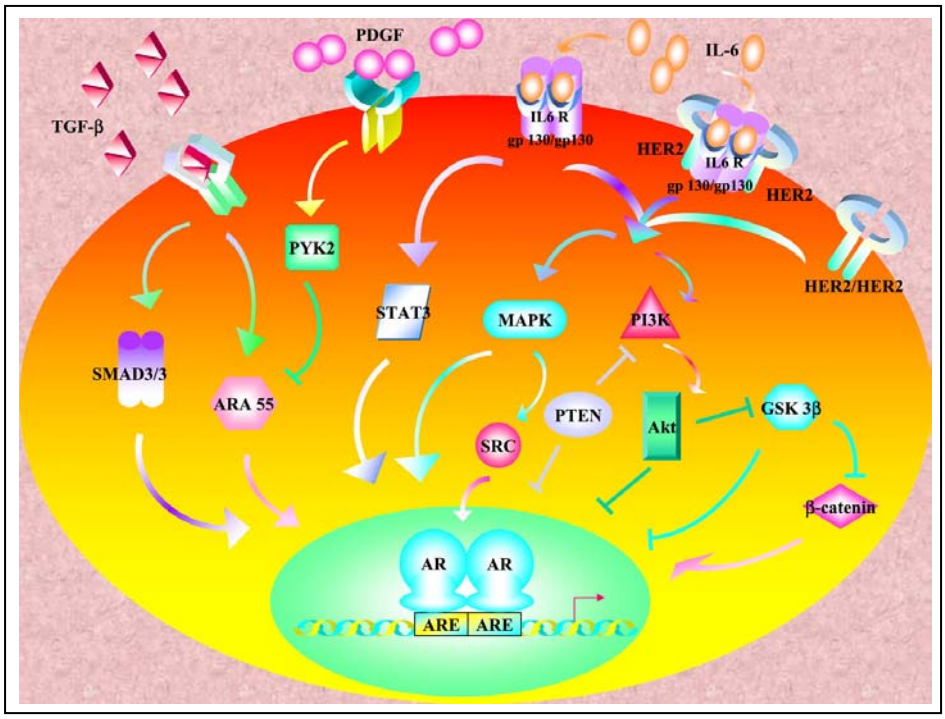

Figure 1-3. Cross talk of androgen-AR signaling with various signal transduction pathways. The combinatorial control of gene expression by AR and coregulators involve interactions among diverse signaling cues (Tgf-β/Smad3, Wnt/β-catenin, STAT3 and MAPK) at different molecular levels. The overall effect may lead to a dynamic and context-dependent expression of specific genes (see text for details). Diagram is adapted from (Heinlein and Chang, 2002).

CHAPTER II

MATERIALS AND METHEDS

Reporter Plasmids and Expression Vectors

A. Luciferase Reporter Plasmids

ARR_2PBLuc reporter (where ARR is the androgen response region) contains an additional androgen response region (-244 to -96 bp) fused upstream of the -286/+28bp Pbsn promoter to enhance the androgen response (Zhang ZF et al., 2000).

A 621-bp fragment of PSA minimal promoter (-610 to +11 *nt*) was amplified by PCR and cloned at the *SmaI* and *XhoI* sites of pGL3-basic luciferase vector (Promega), then an 823-bp upstream enhancer fragment (-4758 to -3935 bp) containing the -4.1/-3.9 kb PSA core enhancer region was obtained by PCR and inserted upstream of the PSA promoter at *SacI* and *SmaI* sites, resulting in PSA-EPLuc reporter construct (EP stands for enhancer/promoter).

For promoter mutagenesis studies, three mutant Pbsn promoter fragments and two mutant PSA enhancer fragments were generated using PCR-based site-directed mutagenesis. All mutant and wild type fragments were cloned into pGL3-basic vector. The primers used for PCR are listed in Table 2-1.

B. Expression Vectors

Mammalian HNF-3α expression vector pRB-HNF-3α (Jackson et al., 1993) was kindly provided by Dr. Kenneth S. Zaret (Fox Chase Cancer Center, Philadelphia, PA). Full-length wild type HNF-3α cDNA and eight cDNAs encoding differently truncated

HNF-3α fragments were PCR amplified and directionally cloned into pcDNA3.1D/V5/His-TOPO expression vector (Invitrogen, K4900) in frame with the carboxy-terminal V5 epitope and 6×His tag. The resulting expression vectors are pHNF-3α-WT_{1-466}, pHNF-3α-$\Delta NT_{141-466}$, pHNF-3α-$FH_{141-294}$, pHNF-3α-ΔCT_{1-294}, pHNF-3α-$\Delta 23_{1-385}$, pHNF-3α-$\Delta 3_{1-420}$, pHNF-3α-NT_{1-180}, pHNF-3α-$CT_{295-466}$, and pHNF-3α-DN_{59-345}. The pcDNA3.1D/V5/His/lacZ is an expression control vector included in the pcDNA3.1 Directional TOPO Expression Kit.

The rat AR expression vector (Zhang ZF et al., 2000), GST-$AR_{NT/DBD}$, GST-AR_{DBD} and GST-$AR_{DBD/LBD}$ vectors (Snoek et al., 1996) have been described previously. GST-AR_{NT} was amplified by PCR and cloned into pRC/CMV (Invitrogen) as a *BamHI* fragment and subcloned into the *BamH1* site of pGEX-3X vector (Pharmacia) in frame with the GST fusion. GST-AR_{LBD} was cloned using pCMV/AR6 as the template (Snoek et al., 1996), and the PCR product was digested with *BamHI* and cloned into the *BamHI* site of pGEX-3X vector. All reporter and expression constructs were confirmed by sequencing.

For synthesis of specific Foxa1 and Foxa2 in situ probes, specific fragments for *Foxa1* (270bp) and *Foxa2* (200bp) were RT-PCR amplified, using primer sets: *Foxa1*-f, GGCCTGGGCTCTATGAACTC and *Foxa1*-r, GCCGTTCATGGAGGTGAC; *Foxa2*-f, CCCATTCCAGCGCTTCTC and *Foxa2*-r, GTAATGGTGCTCGGGCTTC. PCR fragments were cloned into pCR2.1-TOPO vector (Invitrogen).

Cell Culture and Transfection Assays

The human prostate carcinoma cell lines DU145, LNCaP and PC-3; the human cervical adenocarcinoma cell line Hela; the human hepatocellular carcinoma cell line HepG2 were obtained from American Type Culture Collection (Manassas, VA). All cell lines were cultured as recommended by American Type Culture Collection, except for PC-3 cells which were maintained in RPMI medium, 10% FBS and 250 nM dexamethasone. The AR-Hela cells expressing stably integrated flag-tagged full-length AR were acquired from Dr. Michael Carey (UCLA School of Medicine, Los Angeles, CA) (Huang et al., 1999).

Transient transfection assays were performed using lipofectin reagent (4μl/well) for LNCaP cells and lipofectamine 2000 for other cell lines. The pRL-CMV containing the *Renilla* luciferase reportor gene (Promega, Madison, WI) was used to optimize transfection efficiencies for each cell line. Optimal volumes of liposome and transfection durations were obtained and used to get highest transfection efficiencies. Briefly, cells were seeded at an initial density of 8-10 $\times$ 10^4 /well in 24-well plates one day before transfection. The following morning, cells were transfected with plasmid DNA and lipofectin or lipofectamine 2000 in Opti-MEM I Reduced Serum Medium (Gibco, 31985). In transfection experiments where AR expression was required, 0.2 μg of rat AR expression vector was transfected for each well. The total amount of plasmid DNA was normalized to 0.8-1 μg /well by the addition of pVZ-1 plasmid. In addition, all samples received 12.5 *ng* /well of pRL-CMV reporter plasmid. After 4-6 h of transfection, the medium was replaced by Minimum Essential Medium (Gibco, 11090) with 5% Charcoal/Dextran Treated Fetal Bovine Serum (HyClone, Logan, Utah) in the presence

or absence of 10^{-8} M of R1881 or DHT. Cells were harvested and lysed with 80-µl passive lysis buffers after 24 h of incubation.

Luciferase Reporter Assay

The luciferase activity was determined using the dual luciferase reporter assay system (Promega, E1960) and LUMIstar (BMG lab Technologies, INC., Durham, NC). Background activity of the cell lysate with no DNA transfecton was subtracted from the activities obtained from experimental group. All values were normalized by *Renilla* activity to correct for the transfection efficiency. Results are presented as relative luciferase activities. Each experiment was at least repeated three separate times in triplicate. In promoter mutagenesis experiments, mean normalized values from samples showing the highest inhibition of promoter activity were compared with those from samples transfected with the wild type promoter by using Student's paired *t* test.

Nuclear Extract Preparation

A minimum of 10^9 cells was used for a single nuclear extraction experiment. Cell pellet volume (CPV) was measured, and pellet was washed with 5×CPV volume of cold PBS, and centrifuged for 5 min at 2000 rpm (HS-4 rotor) at 4 C. Cells were resuspended in 2×CPV volume of Buffer A [10mM HEPES (pH 7.9), 1.5mM MgCl2, 10mM NaCl, 1mM DTT, Protease Inhibitor]. Cells were broken with 10 strokes using pestle "A" (loose), spin 15 min at 3000 rpm (HB-6 rotor). Supernant was decanted and spun 20 min at 25,000 g (HB-6 rotor at 12,500 rpm). Pellets were resuspended with Buffer C [20mM HEPES (pH 7.9), 1.5mM MgCl2, 420mM NaCl, 25% (v/v) glycerol, 0.2mM EDTA,

1mM PMSF, 1mM DTT, Protease Inhibitor) in 2×CPV volume/10^9 cell. Nuclei was broken with 10 strokes using pestle B (tight), and mixed end-over-end on a rotator for 30 min at 4 C. Spin 30 min at 25,000 g. Supernatant was then collected. Dialysis tube (6,000-8,000D, cut-off) was heated in H2O until boiling. Supernatant was dialyzed in 50 volume of Buffer D [20mM HEPES (pH 7.9), 100mM NaCl, 20% (v/v) glycerol, 0.2mM EDTA , 1mM PMSF, 1mM DTT, Protease Inhibitor] for 2 hours per change of buffer, with total of 3 changes. After last dialysis, samples were spun for 25,000 g for 15 min. Supernatant, the nuclear extract, was stored at -80 C. Pellets were discarded.

Electrophoretic Mobility Shift Assays (EMSA)

Nuclear extract for PC-3 cells was prepared as described above. Nuclear extract for LNCaP cells was purchased from Geneka Biotechnology Inc., Montreal, Canada. Recombinant wild type and truncated HNF-3α proteins were synthesized in vitro using the TnT T7 Quick Coupled Transcription/Translation System, (Promega, L1170). GST-AR fusion proteins were purified as described previously (Snoek et al., 1996). All nuclear extracts and purified proteins were stored in buffers containing 1× concentration of Complete protease inhibitor cocktail (Roche Molecular Biochemicals). All oligonucleotides for EMSA were synthesized by Integrated DNA Technologies, Inc., Coralville, IA. After annealing the sense and antisense strands, the double-stranded DNA probes were end-labeled with T4 polynucleotide kinase (New England Biolab), [γ-32P] ATP and purified with a 15% Polyacrylamide Gel Electrophoresis (PAGE), eluted with elution buffer [10mM Tris.HCl (pH 7.5), 1mM EDTA (pH 8.0), 50mM NaCl, 0.3M

NaAc, 0.5% SDS], and sequentially washed with >3 volumes of 95% ethanol and 500 ul 100% ethanol. Probes were dissolved in nuclease-free water and stored in -20 C

A typical binding reaction involved a 10-min preincubation with 10 μg of nuclear extract, 1 μg of the non-specific competitor poly (dI-dC) and buffer D (20 mM Hepes-NaOH, pH 7.9; 100 mM NaCl; 0.2 mM EDTA; 1.5 mM $MgCl_2$; 1 mM dithiothreitol; 20% glycerol; and 1 mM PMSF), followed by a 15 min incubation with 200,000 cpm of radiolabeled probe on ice in a total volume of 20 μl.

In oligonucleotide competitions, 200-600 fold molar excess of cold, double-stranded oligonucleotide was added to the preincubation mix. In experiments where *in vitro* synthesized HNF-3α proteins were used, 1-5 μl out of 50 μl products from the TnT reaction system were added to the preincubation mix.

In supershift analyses, antibodies were added after the binding reaction and incubated for an additional 20 min on ice prior to electrophoresis. All supershift antibodies were purchased from Santa Cruz Biotechnology, Inc. (AR, C-19: sc-815X; AR, N-20: sc-816X; HNF-3α, C-20: sc-6553X; HNF-3β, M-20: sc-6554X; HNF3-γ, N-19: sc-5361X; p-c-Jun: sc-822X; c-Fos: sc-447X; NF-1, H-300: sc-5567X; Oct-1: sc-8024X). The concentration of antibody in each EMSA reaction was 0.2 *μg/μl*.

Complexes were resolved by electrophoresis for 2.5-h at 160 V on a 5% native polyacrylamide gel, which was later fixed in fixation buffer (10% methanol, 10% acetic acid) for 20 min, dried for 3.5-h, and processed for autoradiography.

SDS-PAGE Fractionation of Nuclear Extract Proteins for EMSA

Thirty μg of LNCaP nuclear extract was combined with appropriate volume of 4×NuPAGE LDS sample buffer and denatured by incubating at 65 C for 10 min. Denatured samples were run on a 10% NuPAGE gel along with molecular marker. Proteins were transferred to PVDF membrane (Invitrogen) in a transfer buffer without methanol. Membrane lane with nuclear extract protein was cut into 2-3 mm slices and the migration distance of molecular marker was recorded for migration curve calculation. Each slice of membrane was placed into a 1.5 mL tube with 50 μL 1×EMSA binding buffer containing 1% Triton and 0.1 mg/mL BSA (final concentrations). Binding reaction was performed in tubes on a shaker at 4 C for 4 hr with shaking. Samples were stored at -70 C for future usage. Use 10-20 μL of each of the eluted protein fractions for EMSA assay.

Southwestern Analysis

An oligonucleotide containing two tandem copies of wild type –124/-109bp (2×R2: 5'-ACCTATTTGTATACTAACCTATTTGTATACTAGATGACA-3'), and another oligonucleotide containing two mutant sites (2×mR2: 5'-ACCTAGAAGTATACTAACCTAGAAGTATACTAGATGACA-3') were radiolabeled by extension of an annealed 10-bp primer, 5'-TGTCATCTAG-3'. (Underscored letters represent the nucleotide replacements in the wild type TATTTGTAT motif.) The primed oligonucleotide probes were radiolabeled with the Klenow fragment of *Escherichia coli* DNA polymerase, dNTPs, [α-32P] dATP, and [α-32P] dTTP. An oligonucleotide containing two copies of consensus androgen receptor binding site (see Table 2-1) was

radiolabeled in the same condition and used for a positive control. Nuclear extracts (30 μg) of PC-3 and LNCaP cells were heated at 70 °C for 10 min in 1 × LDS loading buffer (Invitrogen), resolved on 4% stacking, 12% resolving SDS-polyacrylamide gel, and eletrophoretically transferred to nitrocellulose membranes (Bio-Rad). Membranes were soaked in PBS for 15 min, blocked for 4 hr at room temperature with buffer A (20 mM Hepes-NaOH, pH 7.8, 50 mM NaCl, 12.5 mg/ml skim milk, 2.5 mg/ml bovine serum albumin, 200 μg /ml native salmon sperm DNA, 5 μg /ml poly dI-dC, and 50 ng/ml single stranded DNA), and incubated overnight at room temperature in 2.5 ml of buffer A plus ≥ 10^7 cpm of radiolabeled probe. Membranes were washed three times for 15 min each at room temperature in a washing buffer containing 20 mM Hepes-NaOH, 50 mM NaCl, 1 mg/ml of skim milk, and 0.025% Nonidet P-40. Membranes were dried completely in air at room temperature, prior to autoradiography.

Chromatin Immunoprecipitation (ChIP)

The procedure and PCR primers used in ChIP assay have been reported previously (Shang et al., 2002). LNCaP cells were initially grown in RPMI-medium 1640 with 5% Charcoal/Dextran Treated Fetal Bovine Serum (HyClone, Logan, Utah). After 3 days of cultivation, cells were either treated with 10^{-8} M DHT or allowed to grow in the androgen-depleted medium. After 48 h of treatment, cells were washed with PBS and cross-linked with 1% formaldehyde at 37°C for 10 min. Cells were scraped into conical tube, pelleted for 4 min at 2000 rpm at 4°C, resuspended in SDS lysis buffer (1% SDS, 10mM EDTA, 50mM Tris-HCl, pH 8.1, 1 × proteinase inhibitor cocktail) for 200 μl per 10^6 cells, and sonicated with 4-5 sets of 10-second pulses at an 80% maximum power

(Fisher Sonic Dismembrator, Model 50). After centrifugation for 10 min, supernatants were collected and diluted 1:10 in chip dilution buffer (0.01% SDS, 1.1% Triton X-100, 1.2 mM EDTA, 16.7 mM Tris-HCl, pH 8.1, 167 mM NaCl), followed by pre-clearing for 30 min with 3 µg of sonicated salmon sperm DNA with protein A agarose (80 µl. of 50% slurry in 10 mM Tris-HCl, 1 mM EDTA). Immunoprecipitation was performed overnight at 4°C with specific antibodies. Protein A agarose (60 µl) with salmon sperm DNA was added for 1 h with rotation to collect the complex. Beads were sequentially washed for 5 min each with low salt wash buffer (0.1% SDS, 1% Triton X-100, 2 mM EDTA, 20 mM Tris-HCl, 150 mM NaCl), high salt wash buffer (0.1% SDS, 1% Triton X-100, 2 mM EDTA, 20 mM Tris-HCl, 500 mM NaCl), LiCl wash buffer (0.25 M LiCl, 1% NP40, 1% deoxycholate, 1 mM EDTA, 10 mM Tris-HCl) and twice with TE buffer (10 mM Tris-HCl, 1 mM EDTA). Complex was eluted twice with 250 µl of elution buffer (1% SDS, 0.1 M $NaHCO_3$) and eluates were pooled. The formaldehyde crosslinking was reversed by adding 20 µl 5 M NaCl and incubating for 6-8 h at 65°C. Eluates were incubated for another 1 h at 45°C with 2 µl of 10 mg/ml Proteinase K. DNA was extracted by using QIAquick Spin Column (Qiagen) and 3-5 µl of DNA extraction was used in PCR amplification.

Western Blot Analysis

Cell pellets and freshly dissected mouse tissues were collected, sonicated and centrifuged in cold RIPA buffer (1×PBS, pH 7.4, 1% Nonidet P-40, 0.5% Sodium deoxycholate, 0.1% SDS, 1 mM PMSF and 1 × concentration of complete protease inhibitor cocktail). Following the transfer to polyvinylidene fluoride (PVDF) membrane

(Invitrogen), membranes were blocked in Tris-buffered saline containing 0.1% Tween-20 (TBS-T) and 5% skim milk, and incubated with primary antibody (1:1000 dilution: anti-HNF-3α, anti-HNF-3β, anti-HNF-3γ, anti-AR, anti-PSA and anti-flag) for 1 hr with shaking at room temperature. Anti-flag M2 monoclonal antibody was purchased from Sigma (F3165). In cases where anti-V5-HRP antibody (Invitrogen, R96125) was used to detect the recombinant V5-tagged HNF-3α proteins, a dilution of 1:5000 was used according to the protocol by manufacturer. The signal was visualized by enhanced chemiluminescence (ECL) assay (Amersham Pharmacia Biotech).

Co-Immunoprecipitation (Co-IP) Analysis

DHT-treated or untreated LNCaP cells ($0.5\text{-}1\times10^7$) were washed 3 times with cold PBS and lysed with 1 ml of non-denaturing lysis buffer (50 mM Tris, 150 mM NaCl, 10 mM EDTA, 0.02% NaN_3, 50 mM NaF, 1 mM Na_3VO_4, 1% NP-40, 1 mM PMSF, 0.5 mM DTT and 1× concentration of complete protease inhibitor cocktail). Following sonication and centrifugation, 1 mg of total cell lysate for each reaction was incubated at 4 °C for 3 hr with 20 μl (dry volume) protein G-Sepharose beads (Amersham), which were conjugated with 1 μg experimental antibody or mock antibody. Bovine serum albumin (1 mg) was added to quench the non-specific binding. Immunoprecipitations were performed in the presence of ethidium bromide (0-100 μg/ml as indicated in the results) to disrupt DNA-protein interaction (Lai and Herr, 1992). Beads were washed four times with lysis buffer and once with PBS for 5 min each with rotation, which was followed by Western blot. The anti-AR (441) mouse monoclonal IgG (Santa Cruz, sc-

7305) was used for immunoprecipitate AR, and the anti-HNF-3α (C-20) goat polyclonal IgG (Santa Cruz, sc-6553) was used to immunoprecipitate HNF-3α.

For Co-IP experiments in AR-Hela cells, cells were maintained in medium with DHT and transfected with V5-tagged HNF-3α or LacZ expression vectors. Anti-Flag M2 affinity gel (Sigma) was used to immunoprecipitate the flag-tagged AR, according to the protocol provided in the Flag Tagged Protein Immunoprecipitation Kit (Sigma, FLAGIPT-1). Complexes were washed with buffers and procedures described for LNCaP cells. Western blot was performed with anti-V5 HRP-conjugated antibody.

In Vitro **Transcription and Translation (TnT) of HNF-3α and Mutant Proteins**

Wild type HNF-3α and a series of truncated mutant HNF-3α expression vectors, with a T7 promoter, were transcribed and translated *in vitro* using the TnT T7 Quick Coupled Transcription/Translation System (Promega, L1170). A standard reaction involved a 90-min incubation at 30°C with 40 µl of TnT Quick Master, 2 µl of cold 2 mM methionine, and 2 µg of plasmid DNA in a final volume of 50 µl. A LacZ expression vector was translated using the same conditions as a control. *In vitro* translated recombinant HNF-3α and LacZ proteins were labeled with a C-terminal V5-epitope and were used immediately for *in vitro* binding reactions, or for EMSA.

Purification of GST-AR Fusion Proteins

GST-AR fusion proteins were purified as described previously (Snoek et al., 1996). Five mLs of overnight cultures of pGEX-3X-AR plasmids in LB/ampicillin were added into 200 mLs LB/ampicillin in the next morning. Cultures were grown at 37°C

until OD600=0.6 (approximately 2 hrs), then protein expression was induced with 0.1mM IPTG (20uL of 1M IPTG stock). Bacteria (JM109) were allowed to grow at 30°C with shaking for 2 hrs. Cultures were centrifuged at 8000 rpm for 10 min at 4°C. Cell were resuspended in 2mL Lysis buffer (PBS, protease inhibitors, 100 ug/mL lysozyme) and transfered to 15mL falcon tube. Cells were placed on ice for 30 min, and sonicated at maximum setting for 10 seconds then placed on ice for 10 seconds. Sonication was repeated for 5-6 times until solution turns clear. Solutions were aliquoted into 1.5mL tubes and centrifuged at 13,000rpm for 30 min at 4°C to pellet out the cellular debris. Supernatants were combined from each tube in a 15mL falcon tube that has preswelled glutathione-agarose beads. Incubation was performed with end-over-end rotation for 1hr at 4°C, and then tubes were centrifuged at 2000rpm for 15 seconds at 4°C. Beads were washed with ice cold PBS (with 1× protease inhibitor) for 4 times. Beads were then resuspended in 10mL PBS with protease inhibitors and stored at 4°C for 2 weeks.

To elute the GST-proteins, beads were centrifuged at 2000rpm for 15sec at 4°C and supernatants were removed. One mL of elution buffer (20mM HEPES, pH7.6, 150mM KCl, 5mM $MgCl_2$, 1mM EDTA, 0.05% NP-40, protease inhibitor, 0.046g glutathione) was added and incubation was performed at room temperature with rotation for 15 min. Elute was collected after centrifugation at 2000 rpm for 15 seconds (fraction #1). Elution was repeated for 2 times and fractions #2 and #3 were collected. After determination of protein concentration, proteins were resolved run a SDS-PAGE followed by Commassie Blue staining to check protein quality.

To pre-swell the glutathione-agarose beads (Sigma #G-4501), 0.08g beads were measured out for each GST fusion protein. 14mL of ice cold PBS was added to the beads

and swelling was performed for at least 1 hr on ice. Beads were centrifuged at 2000rpm for 15 seconds and washed with PBS. Supernatant was removed before adding the GST-protein lysate.

GST-Pull Down Assays

For GST-pull down assays, 50 µl swelled glutathione agarose beads (Sigma G-4510) were incubated with 20 µg GST or GST-AR fusion proteins for each reaction. GST-bound beads were equilibrated with PBS-T binding buffer (1×PBS, pH 7.4, 1% Tween-20, and protease inhibitors) and incubated for 2 h at 4°C with 5-10 µl products from the TnT reactions. Complexes were washed four times with 1.5 ml of cold binding buffer, heated for 10 min at 70°C in 1×LDS loading buffer, and separated by SDS-PAGE. Then, V5-HRP antibody was used in a standard Western blot to detect proteins that interact with AR *in vitro*.

Transgenic Mice, Genotyping and Renal Capsule Organ Rescue

Foxa1 loss-of-function mutant mice were generated as previously described, and the mice were obtained from Dr. Markus Stoffel lab in Rockfeller University (Shih et al., 1999). Newborn pups were sacrificed after birth. The entire prostatic rudiments with partial bladder, urethra and both seminal vesicles from 55 male mice were grafted underneath of the renal capsules of adult male nude mouse hosts. Meanwhile, PCR genotyping of the remained carcass was performed using primers specific for wild type allele: F, 5'-GGCCTGAGTCCCGGTGCTGTG-3' and R, 5'-AGGCGGCTTGGCGTGAGGGTAG-3' (product size 250-bp); for mutant (3αa-Lacz)

allele: F, 5'-ATGACCACGAGCGGCAACATG-3' and R, 5'-GGTTACGTTGGTGTAGATGGG-3' (product size 350-bp). PCR conditions were: 1) 94°C 5min, 2) 94°C 30sec, 65°C 30sec, 72°C 30sec for 35cycles, 3) 72°C 10min.

Prostate tissues were recovered from host kidneys after 4, 8 and 12 weeks, and genotypes were re-confirmed by using PCR, Foxa1 immunohistochemistry or β-galactosidase staining.

Tissue Recombination

In tissue recombination experiments, E18 rat UGM was used as embryonic inductive mesenchyme and prepared as described (Cunha and Donjacour, 1987). Bladder epithelial (BLE) tissue fragments were separated from bladder stroma with the treatment of 20mM EDTA for ~30 min at 37°C (Cunha and Donjacour, 1987), pooled by genotype and recombined with rUGM. The bladder epithelial cells were separated from a total of 89 newborn mice. The resulting recombinants (BLE+rUGM) were grafted underneath the renal capsules of male nude mice in triplicates for each time points (4 weeks and 12 weeks)

For tissue recombination using prostate epithelium (PrE), recombinants (PrE+rUGM) were grafted into adult male nude mouse hosts for 2, 4, or 12 weeks. For each time point, recombinants were grafted in triplicate for individual genotypes.

Histology Analysis

Hematoxylin and Eosin (H&E) staining was performed on 10% formalin-fixed paraffin-embedded 5 um sections as following: 1) Histoclear 5 min, 2) Histoclear 5 min,

3) 100% ethanol 3 min, 4) 95% ethanol 3 min 5) 95% ethanol 3 min, 6) 75% ethanol 10 dips, 7) 70% ethanol 10 dips, 8) 50% ethanol 10 dips, 9) washing in running distilled water, 10) Hematoxylin 5 min, 11) washing in running distilled water, 12) 1% acid alcohol 2-3 dips, 13) washing in running distilled water, 14) 0.3% ammonia water 10 dips, 15) wash in running distilled water, 16) 70% ethanol 10 dips, 17) Eosin 2 min, 18) 70% ethanol 20 dips, 19) 70% ethanol 20 dips, 20) 95% ethanol 10 dips, 21) 95% ethanol 10 dips, 22) 100% ethanol 20 dips, 23) 100% ethanol 20 dips, 24) Histoclear 20 dips, 25)Histoclear 20 dips, 26) Histoclear 20 dips, 27) mount.

For PAS staining, paraffin-embedded sections were deparaffinized, oxidized in periodic acid solution for 5 min, rinsed in H_2O, and placed in Schiff's reagent for 15 min. Sections were then rinsed in running water for 10 min and counterstained with hematoxylin.

β-Galactosidase Staining

Fresh tissues were prefixed for 6 hr in 2% paraformaldehyde, 0.2% glutaraldehyde in PBS at 4°C, and embedded in OCT. Frozen sections were cut and immersed in the same paraformaldehyde/glutaraldehyde solution for 10 min at 4°C, then rinsed in water for 1 min. After one more rinse with PBS, β-galactosidase staining solution (Roche) was applied to sections and incubated at 37°C for 1-6 hr. Reactions were stopped, before non-specific staining was detected in wild type prostate tissues, with 2 times of rinse in deionized water.

Electron Microscopy

Upon dissection, fresh prostate tissues with different genotypes were fixed in 2% glutaraldehyde in 0.1M cacodylate buffer at 4°C overnight. The specimens were dehydrated in alcohol and polymerized. 1μm sections were cut and stained with toluidine blue. Seventy nanometer sections were then cut on a Leica Ultracut UCT ultramicrotome and ultrastructural analysis was performed on Phillips CM-12 Transmission Electron Microscope equipped with AMT digital camera system.

Immunohischemical and Immunofluorescent Analysis

Urogenital sinus and individual prostatic lobes were dissected and fixed in 10% buffered formalin for 24 hr, processed and embedded in paraffin. Immunohistochemical and immunofluorescent staining was performed on 5 mm-thick sections, which were deparaffinized, rehydrated through a graded alcohol series, and washed in H2O for 5 min. Tissue sections were placed in antigen retrieval solution (Vector Laboratories, Burlingame) and antigen retrieval was performed by microwaving the sections for 20 min at boiling on 30% power in a 900 W microwave oven. Slides were cooled for 1 hr at room temperature in the antigen retrieval solution and then washed twice for 5 min in PBS, pH 7.4.

For immunohistochemistry, all incubations were carried out at room temperature unless otherwise stated. Endogenous peroxidase activity was blocked with DAKO1 Peroxidase Blocking Reagent (DAKO Corp., Carpinteria) for 15 min and sections were washed in PBS for 5 min. Immunohistochemistry was performed using the Vectastain1Elite ABC peroxidase kit (Vector Laboratories) according to the

manufacturer's protocol. Briefly, non-specific antibody binding was minimized by incubating sections for 20 min in diluted normal blocking serum. Sections were incubated overnight at 48°C in a humidified chamber with specific primary antibodies, diluted in PBS. Following overnight incubation, the slides were washed in PBS for 5 min. Sections were then incubated for 30 min with biotinylated secondary antibody solution diluted in PBS, followed by Vectastain Elite ABC Reagent diluted in PBS for 30 min. Between incubations, sections were washed for 5 min in PBS. Visualization of immunoreactivity was achieved by incubating sections in either DAKO Liquid DAB Substrate-Chromogen System (DAKO Corp.) for 2–4 min or the DAB peroxidase substrate kit (Vector Laboratories) for 10 min. The sections were washed in double distilled H_2O, counterstained with hematoxylin, dehydrated, and coverslipped.

Primary antibodies used in immunohistochemistry at the indicated concentrations were AR (rabbit, 1:1000; Santa Cruz, sc-816), CK5 (rabbit, 1:500; Covance Research Products, PRB-160P), CK14 [mouse, LL001, 1:10 (Wang et al., 2001); gift from Dr. E. Birgitte Lane, University of Dundee], CK8 [mouse, LE41, 1:10 (Wang et al., 2001); gift from Dr. E. Birgitte Lane], CK-Pan (rabbit, 1:1000; DAKO, Z0622), alpha-actin (mouse, 1:1500; Sigma, 1A4), gamma-actin [mouse, B4, 1:10000 (Lessard, 1988); gift from Dr. James L Lessard], Foxa1 (goat, 1:1000; Santa Cruz, sc-6553), Foxa2 (goat, 1:1000; Santa Cruz, sc-9187), Nkx3.1 [rabbit, 1:3000 (Kim et al., 2002); gift from Dr. Cory Abate-Shen] and Probasin [rabbit, 1:1500 (Kasper and Matusik, 2000)]

For immunofluorescence, all incubations were carried out at room temperature unless otherwise stated. Tissue sections were blocked with PBS containing 2% normal donkey serum (Vector Laboratories) and 2% BSA (Sigma, St. Louis) for 1 hr, and

incubated overnight at 4°C with primary antibodies diluted in PBS with 2% BSA and 2% donkey serum. After washing for 30 min in PBS, sections were incubated for 1 hr with fluorescent conjugated anti-goat, anti-rabbit and anti-mouse secondary antibodies, diluted in PBS with 2% BSA and 2% donkey serum. Sections were washed for 30 min in PBS and visualized by conventional fluorescent microscopy.

Primary antibodies used in immunofluorescence at the indicated concentrations were AR (rabbit, 1:200), CK14 (mouse, 1:5), CK8 (mouse, 1:10), E-Cadherin (mouse, 1:200; BD Transduction Laboratories), β-Catenin (mouse, 1:100; BD transduction laboratories), p63 (rabbit, 1:200; Santa Cruz, sc-8343), Sonic Hedgehog (rabbit, 1:100; Santa Cruz, sc-9024), Patch1 (goat, 1:100; Santa Cruz, sc-6149) and Ki67 (Rat, 1:15; DakoCytomation, M7249). Secondary antibodies were anti-mouse IgG TRITC (1:100; Sigma, T2402), anti-mouse IgG (Fab specific) TRITC (1:100; Sigma, T6528), anti-mouse (1:200; Molecular probes, A21203), anti-goat (1:200; Molecular probes, A11055), anti-rabbit IgG (1:200; Molecular probes, A21206, A21207) and anti-rat IgG TRITC (1: 100; Sigma, T4280). In some experiments, DAPI staining was performed by using VECTASHIELD Mounting Medium (Vector, H-1200).

***In Situ* Hybridization**

A. Preparation of Tissues for In Situ Hybridization

Freshly dissected pelvic organs were immediately placed into 5 volumes of cold RNAlater for at least 1 hr. Various lobes were dissected in the presence of RNAlater. After dissection, tissues were fixed in 4% paraformaldehyde in DEPC-treated PBS for 1 hr at 4°C. 4% paraformaldehyde was made by heating 50mL of PBS in a 65°C water bath

and then adding 2g of paraformaldehyde, and cooling to 4°C on ice. After process the specimens, 4 um sections were cut and mounted onto slides and air dried overnight.

B. Synthesis of RiboProbes

Specific gene fragments for Foxa1 and Foxa2 were amplified by PCR from mouse liver cDNA, then cloned into pCR2.1-TOPO vector and transformed into TOP10 cells. Sense or anti-sense orientations were identified by sequencing. Correct clones for each sense and anti-sense probes were amplified by minipreps (Qiagen). To prepare a template for production of "run off" transcripts derived from the insert sequence only, plasmids containing the required cDNAs were linearised with BamHI. One uL of undigested and digested plasmid DNA were electrophoresed on a 0.8% agarose gel to ensure the plasmid has been completely linearized. Entire digested sampleand 1 uL of undigested sample was electrophoresed and on a 1% low melt preparative grade agarose gel, and linearized plasmid was excised. DNA was purified by using Gel Extraction Kit (Qiagen), and eluted in 30uL of elution buffer.

The Digoxigenin (DIG) RNA labeling reaction is composed of 1 ug linearized DNA, 2uL DIG RNA Labeling Mix, 10×concentration, 2uL 10×transcription buffer, 2uL T7 RNA polymerase (20U/uL), 1uL of RNase inhibitor (20units/uL) in a 20uL reaction system [Roche #1175025, DIG RNA Labeling Kit (SP6/T7)]. Reaction was mixed and incubated in 37°C for 2 hrs. 2 uL RNase-free DNase I (10u/uL) was added to remove template DNA by incubating for 15 min at 37°C. Reaction was stopped by adding 2 uL 0.2M EDTA solution, pH8.

After labeling reaction, probes were transfered to 0.5mL tubes and 2.5 uL (0.1 volume) of 4M LiCl and 75uL (2.5 volume) 100% ethanol (-80°C) were added to the

standard reaction. Solution was mixed and stored at -70°C for 30 min or 2 hr at -20°C, followed by centrifugation at 13,000g at 4°C for 15 min. Pellet was carefully washed with 50 uL cold 70% ethanol (-20°C) and centrifuged at 13,000g for 5 min at 4°C and air-dried. Pellet was dissolved in 50uL sterile water with 1uL of RNase inhibitor and store at -70°C.

To determine the labeling efficiency, serial dilutions of DIG labeled transcripts were prepared in sterile water. One uL of each dilution was spotted onto Hybond-N+ membrane, air-dried and cross-linked with UV. Membrane was equilibrated in Buffer 1 (Tris 100mM, NaCl 150mM, pH 7.5) for 1 min, and incubated in Buffer 2 [Buffer 1 with 0.5% blocking reagent (Roche #1096176)] for 30 min at room temperature, followed by incubation of 30 min with anti-DIG alkaline phosphatase (AP)-conjugated antibody (Roche # 1093274) diluted 1:5000 in buffer 2. Membrane was then washed in Buffer 1 for 10 min, 2 times, equilibrated in Buffer 3 (Tris 100mM, NaCl 100mM, $MgCl_2$ 50mM, pH9.5) for 2 min, and then incubated in Buffer 3 with 45uL NBT and 35uL BCIP per 10mL, in dark at room temperature. Staining reaction was stopped with water and the membrane was air dried. Samples were semi-quantitated by comparing signals with standard DIG labeled control RNA of known concentration.

To determine the DIG RNA transcript quality, 2ug of each sample were heated at 65 C for 10 min, stored on ice for 5 min, and dissolved on 2% agarose gel.

C. Hybridization

Tissue sections were deparaffinized and hydrated through xylenes and ethanol series with gradient concentration (Xylene 1×10 min, 1×3 min, 100% ethanol 2×3 min, 95% ethanol 2×3 min, 75% ethanol 1×3 min, 50% ethanol 1×3 min, DEPC-treated water

1×3 min, DEPC-treated PBS 1×3 min). Sections were postfixed for 10 min in 4% paraformaldehyde in DEPC-treated PBS (with 5 drops of 5M NaOH) followed by washing for 2×15 min in PBS with 0.1% active DEPC. After equilibration for 15 min in 5×SSC, DEPC-treated, hybridization was performed immediately. Hybridization box was prepared and saturated with 5×SSC, 50% formamide solution. Prehybridization was performed for 2 hrs at 58°C in 5×SSC, 50% formamide solution, 40ug/mL salmon sperm DNA. Probes were denatured for 5 min at 80°C and added into the hybridization mixture (400 ng/mL of DIG-labeled probe, 5×SSC, 50% formamide, 40ug/mL salmon sperm DNA). Hybridization was performed for 4-40 hr at 58°C, and covered by rectangular cover slip.

Sections were washed for 30 min in 2×SSC at room temperature, followed by 1 hr wash in 2×SSC at 65°C and 1 hr wash in 0.1×SSC at 65°C. Sections were equilibrated for 5 min in Buffer 1 at room temperature, followed by 2 hrs of incubation with anti-DIG antibody, AP-conjugated, diluted 1:5000 in Buffer 2 at room temperature. Sections were then washed with Buffer 1 twice for 15 min each, equilibrated for 5 min in Buffer 3, and stained in Buffer 3 with 45uL NBT and 35uL BCIP per 10mL of Buffer 3, in the dark. Reaction was stopped with TE buffer (Tris 10mM, EDTA 1mM, pH 8.0) for 10 min. Non-specific background was removed with 95% ethanol for ~1 hr and rinsed in water for 15 min to dissolve and remove potential crystals due to TE buffer. Slides were air-dried and mounted with aqueous mounting solution (Biomeda #M01).

RNA Isolation and RT-PCR

Upon dissection, fresh tissues were immediately placed in 5 volumes of RNAlaterTM (Ambion, Austin). The prostates were dissected in RNAlaterTM, incubated at 4°C overnight and then stored at -20°C. Total RNA was extracted from pooled prostate tissues using the QiagenTM RNeasy extraction kit (Qiagen, Valencia) and treated with RNase-Free DNase (Qiagen). Two micrograms of total RNA was reverse transcribed using Superscript-IITM reverse transcriptase (Invitrogen) according to the manufacturer's instructions. PCR was performed to produce gene specific fragments for *Sbp* (277bp), *probasin* (243bp), and *Foxa2* (200bp). The PCR primers are: *Sbp*-f, CCCAGAATGTCCTGGGGAATG; *Sbp*-r, CCACACGCCCCTTGTTTGTAG; *probasin*-f, TGCACAGTATGAAGGGAGCA; *probasin*-r, TTGATCTTGCTTGGACAGTTG; *Foxa2*-f, CCCATTCCAGCGCTTCTC; *Foxa2*-r, GTAATGGTGCTCGGGCTTC.

Matrix Assisted Laser Desorption Ionization Time-of-flight (MALDI-TOF) Mass Spectrometry (MS)

The prostate tissues were dissected and then snap-frozen in liquid nitrogen. Using a cryostat, 10 μm tissue sections were cut and mounted onto a conductive glass MALDI plate. Three to four sections were obtained per specimen. For histological information and to identify regions of interest for profiling, sections were stained with MALDI-compatible cresyl violet as described previously (Chaurand et al., 2004). Areas of interest were then spotted with approximately 150nL of saturated sinapinic acid as matrix prepared in acetonitrile/H_2O/TFA (50/50/0.1) by volume and allowed to dry. Each section was then analyzed by MALDI-TOF MS in the linear mode using an Applied

Biosystems Voyager DE-STR mass spectrometer (Framingham, MA) in Mass Spectrometry Core Lab in Vanderbilt University. Acquired spectra were baseline subtracted and normalized by a costumer program. Spectra from each prostate sample were then averaged before comparison.

Table 2-1. Oligonucleotides used in CHAPTER II			
Name	Sequence	Purpose	Restriction Site Added
TTRs	5'-TGACTAAGTCAATAATCAGAATCAG-3'	EMSA, Competition	
PB-127/-102	5'-AGAACCTATTTGTATACTAGATGACA-3'	EMSA	
PB-257/-232	5'-CAGTTAAGAAAATATGATAGCATCTT-3'	EMSA	
ARBS2/R2	5'-GCCTAGTAAAGTACTCCAAGAACCTATTTGTATACTAGA-3'	EMSA	
ARBS2/R2-M1	5'-GCCTAGTAAAGTACTCCAAGAACCTA**gaa**GTATACTAGA-3'	EMSA	
ARBS2/R2-M2	5'-GCCTAGTAAAGTACTCCAAGAACCTATTTG**atg**ACTAGA-3'	EMSA	
ARBS1/R1	5'- CAGTTAAGAAAATATGATAGCATCTTGTTCTTAGTCTTTTT-3'	EMSA	
ARBS1/R1-M3	5'- CAGTTAA**ct**AAAT**ta**GA**at**GCATCTTGTTCTTAGTCTTTTT-3'	EMSA	
PB-127/-102-M1-F	5'-AGAACCTA**gaa**GTATACTAGATGACA-3'	EMSA, Mutagenesis	
PB-127/-102-M1-R	5'-TGTCATCTAGTATAC**ttc**TAGGTTCT-3'	EMSA, Mutagenesis	
PB-127/-102-M2-F	5'-AGAACCTATTTG**atg**ACTAGATGACA-3'	EMSA, Mutagenesis	
PB-127/-102-M2-R	5'-TGTCATCTAGT**cat**CAAATAGGTTCT-3'	EMSA, Mutagenesis	
PB-257/-232M-F	5'- CAGTTAA**ct**AAAT**ta**GA**at**GCATCTT-3'	Mutagenesis	
PB-257/-232M-R	5'-AAGATGC**at**TC**ta**ATTT**ag**TTAACTG-3'	Mutagenesis	
2×R2	5'-ACCTATTTGTATACTAACCTATTTGTATACTAGATGACA-3'	Southwestern	
2×mR2	5'-ACCTA**gaa**GTATACTAACCTA**gaa**GTATACTAGATGACA-3'	Southwestern	
PB-Primer	5'-TGTCATCTAG-3'	Southwestern	
2×AR-consensus	5'-GTCTGGTACAGGGTGTTCTTTTTGGTACAGGGTGTTCTTTTTG	Southwestern	
AR-Primer	5'-CAAAAAGAAC-3'	Southwestern	
PSA1	5'-CCTACTCTGGAGGAACATATTGTATTGATTGTCCTTGACAGTAAACAAATCTGTT-3'	EMSA	
PSA2	5'-GGATGCCTGCTTTACAAACATCCTTGAAAC-3'	EMSA	
mPSA1	5'-CCTACTCTGGAGGAACATATTGTATTGATTGTCCTTGACAGTA**c**ACA**c**ATCTGTT-3'	EMSA	
mPSA2	5'-GGATGCCTGCT**c**T**c**CA**c**ACATCCTTGAAAC-3'	EMSA	
hPAP	5'-TTCTTTTGTTTGTTTTTTGTTGTTGTTTGTTTGTTTTGCTG-3'	EMSA	
rPAP1	5'-TGGTTTTGTTTTCTTTTTAATGTTTGTTAT-3'	EMSA	
rPAP2	5'-GCCAATCTCTTGATTAAATAGGCACTTCCC-3'	EMSA	
rPAP3	5'-TCTTGACAGAACAGGAAGCCGAGAGTGAGC-3'	EMSA	
PBPC1-1	5'-ATTGACTGAATGTTTATTTAATTTCTCCTT-3'	EMSA	
PBPC1-2	5'-GAATTAGCAAATAATTTCTCTTATAAAAAT-3'	EMSA	
PSA-P-F	5'-CCCGGGTTGGATTTTGAAATGCTA-3'	PSA-EPLuc	*SmaI*
PSA-P-R	5'-CTCGAGAAGCTTGGGGCTGG-3'	PSA-EPLuc	*XhoI*
PSA-E-F	5'-GAGCTCCTGCAGAGAAATTA-3'	PSA-EPLuc	*SacI*
PSA-E-R	5'-CCCGGGCCATGGTTCTGTCA-3'	PSA-EPLuc	*SmaI*
mPSA1-F	5'-TGACAGTA**c**ACA**c**ATCTGTTGTAAG-3'	Mutagenesis	
mPSA2-F	5'-TGCT**c**T**c**CA**c**ACATCCTTGAAACAA-3'	Mutagenesis	
WT (1-466)-F	5'-CACCGAATTCATGTTAGGGACTGTGAAGAT-3'	WT construct	*EcoRI*
WT (1-466)-R	5'-AGCTCGAGCGGAAGTATTTAGCACGGGTCT-3'	WT construct	*XhoI*
NT (1-180)-R	5'-AGCTCGAGCGGTGATGAGCGAGATGTAGGA-3'	NT construct	*XhoI*
FH (141-294)-F	5'-CACCGAATTCATGGCGTACGCTCCGTCCAA-3'	FH construct	*EcoRI*
FH (141-294)-R	5'-AGCTCGAGCTGAGGGGTCTTTGCGGTTTTC-3'	FH construct	*XhoI*
CT (295-466)-F	5'-CACCGAATTCATGGGCCCGGTTAACCCCAGTGC-3'	CT construct	*EcoRI*
Δ23 (1-385)-R	5'-AGCTCGAGCGGCCCCTTTCAGGTGCAGCTG-3'	Δ23 construct	*XhoI*
Δ3 (1-420)-R	5'-AGCTCGAGCGTACTGCAGTGCCTGCTGATA-3'	Δ3 construct	*XhoI*
DN (59-345)-F	5'-CACCGAATTCATGACCCCGGCTTCCTTCAA-3'	DN construct	*EcoRI*
DN (59-345)-R	5'-AGCTCGAGCCAACTCCGAACCGCCCCCTGT-3'	DN construct	*XhoI*
AR-LBD-F	5-TCCGGATCCAAGGCTATGAATGTCAACCT-3'	GST-AR-LBD	*BamHI*
AR-LBD-R	5'-TCCGGATCCTCACTGTGTGTGGAAATAGAT-3'	GST-AR-LBD	*BamHI*
AR-NT-F	5'-TTTGGATCCCCATGGAGGTGCAGTTAGGGCTG-3'	GST-AR-NTD	*BamHI*
AR-NT-R	5'-TTTGGATCCTCACATGTCCCCATAAGGTCCGGA-3'	GST-AR-NTD	*BamHI*
For EMSA probes, only the sense strand sequences are shown here. *Underscored* sequences represent the binding sites for HNF-3 or AR. Sequences in *bold lowercase* characters are nucleotide replacements in mutagenesis study.			

CHAPTER III

ANDROGEN RECEPTOR-FOXA1 (HNF-3*α*) *CIS*-REGULATORY ELEMENTS ARE INVOLVED IN THE REGULATION OF PROSTATE DIFFERENTIATED FUNCTION

Introduction

The prostate is a male accessory sex organ that is found exclusively in mammals. This organ produces various components found in the semen. Androgens are required to initiate prostatic development, to establish prostatic morphogenesis, and to begin secretory activities. In the mouse, the developing fetal testis begins to produce androgens at embryonic day 12.5-13 (E12.5–13) with peak production at E17-18, during which the earliest signs of prostatic formation are observed (Pointis et al., 1979; Pointis et al., 1980). Ablation or surgical removal of fetal testes during the ambisexual period inhibits the development of prostate and other male internal sex organs (Cunha et al., 1987). Androgens act directly through AR to elicit their effects (Gelmann, 2002). Testicular feminized (Tfm) mice, which express a non-functional AR, never develop a prostate, even though their testes produce adequate amounts of testosterone (Cunha et al., 1987; Quigley et al., 1995). In addition, prostatic epithelial cells that do not express functional AR, also do not express characteristic secretory markers (Donjacour and Cunha, 1993). These observations demonstrated the essential requirement of androgens and AR for prostate development and function. Interestingly, tissue recombination experiments showed that the urogenital epithelium (UGE) from Tfm mice develops normal prostate gland histology when combined with wild type urogenital mesenchyme (UGM), although these UGE contains a defective AR (Cunha and Chung, 1981). Also, it has been observed

that the induction of prostatic epithelial buds occurs prior to AR expression in wild type prostatic epithelial cells (Takeda et al., 1985; Cooke et al., 1991; Hayward et al., 1996a). These results argue that the epithelial AR is not required for prostatic determination, although it is essential for the production of androgen dependent secretory proteins at later stages (Donjacour and Cunha, 1993).

Extensive tissue recombination studies have proven that mesenchymal-epithelial interactions play a key role in directing prostate development (Cunha et al., 1992; Cunha et al., 1987). Epithelial cells from other urogenital sinus derivatives (bladder, urethra and vagina) can be instructively induced by UGM to give rise to prostatic tissue (Cunha et al., 1987; Cunha, 1975; Cunha et al., 1980b; Neubauer et al., 1983; Cunha et al., 1983). Similar results have been obtained using human bladder epithelial cells (Aboseif et al., 1999). The ductal-acinar structures that form in such experiments histologically resemble prostatic epithelium and produce prostate specific antigen (PSA) (Aboseif et al., 1999). Nevertheless, the response of epithelia to inductive mesenchyme is limited by the developmental repertoire of the germ layer origin of the epithelium (Hayward, 2002). For example, mesodermally derived seminal vesicle epithelium responds to either urogenital sinus or seminal vesicle mesenchyme by generating seminal vesicle. In contrast, the endodermally derived epithelia of the prostate, bladder or urethra respond to the same inductive mesenchyme by generating prostatic tissue. Therefore, it is apparent that the cell developmental program is determined by both epithelial and mesenchymal factors. Although androgens and mesenchymal factors are critical to prostatic development, epithelial factors that directly participate in this process are still unknown.

Forkhead Box A (Foxa) transcription factors, Foxa1, Foxa2 and Foxa3, (formerly known as HNF-3α, HNF-3β and HNF-3γ) are a group of endoderm-related developmental factors that belong to the forkhead transcription factor family (Kaestner et al., 2000; Zaret, 1999; Kaufmann and Knochel, 1996). In mouse, Foxa2 (HNF-3β) is first expressed in the endoderm progenitor during gastrulation (E6.5), immediately followed by the expression of Foxa1 (HNF-3α) (before organogenesis, E7-8) and Foxa3 (HNF-3γ) (Sasaki and Hogan, 1993; Zaret, 1999). The targeted null mutation of Foxa2 gene results in embryonic lethality due to a lack of endodermal progenitors (Weinstein et al., 1994), while homozygous mutation of Foxa1 gene leads to perinatal death due to pancreatic defects (Kaestner et al., 1999). All three Foxa (HNF-3) genes are restrictively expressed in the endoderm-derived organs in the adult and are involved in endodermal differentiation (Zaret, 1999). *In vivo* footprinting using mouse embryo liver cells showed that Foxa factors, among a few earliest transcription factors, bind to the enhancer of liver-specific albumin gene before this gene is activated (Zaret, 1999; Cirillo et al., 2002). This binding of Foxa is believed to provide developmental competence to the target gene, which becomes activated during hepatic induction when additional liver-enriched transcription factors are recruited (Zaret, 1999; Jackson et al., 1993; Zaret, 2002). Although Foxa proteins were first discovered in liver (Lai et al., 1990), the highest Foxa1 mRNA level was detected in the prostate gland by comparison of 16 human tissues (Peterson et al., 1997). A novel expression pattern of Foxa1 in the epithelium of the bladder, urethra and prostate has also been reported (Peterson et al., 1997; Kopachik et al., 1998). However, in the urogenital system, target genes that are regulated by Foxa1 have not been identified. The role of Foxa1 in the urogenital system remains to be defined.

In the adult prostate, fully differentiated luminal epithelial cells secrete androgen-dependent prostate-specific proteins, such as Pbsn in the rat and PSA in the human. Activation of these characteristic genes in epithelium signifies that prostatic differentiation has occurred. The transcription factors that regulate these genes may also be involved in the process of prostate development. Therefore, a better understanding of the transcriptional regulation of these prostate specific genes is likely to provide insight into the organ development. In the present study, characterization of the Pbsn promoter has led to the identification of the binding of a cluster of ubiquitous transcription factors, and two forkhead response elements, which are immediately adjacent to functional AR binding sites. A similar organization of the AREs adjacent to forkhead response elements was observed in the PSA gene enhancer and the prostatic acid phosphatase (PAP) gene promoter/enhancer, suggesting that a common functional mechanism is involved. DNA mutation studies showed that these Foxa sites are essential for maximal androgen-induction of both Pbsn and PSA gene. Chromatin immunoprecipitation assay confirmed that Foxa1 occupies the PSA enhancer *in vivo*. In addition, we detected a direct protein/protein interaction between Foxa1 and AR. These data suggest that an endodermal transcription factor Foxa1 and a steroid receptor AR may coordinately participate in the assembly of a nucleoprotein complex, which directs the prostatic differentiated function. The regulatory mechanism between Foxa1 and AR may also apply to the transcriptional control of other prostatic epithelial cell specific genes.

Results

A. Octamer-binding transcription factor 1 (Oct1), Nuclear factor 1 (NF1) and c-jun Bind Pbsn Proximal promoter

The rat Pbsn is a prostate-specific and androgen-regulated gene, which has been extensively characterized (Rennie et al., 1993; Greenberg et al., 1994; Kasper et al., 1994; Yan et al., 1997; Kasper et al., 1999; Kasper et al., 1998; Zhang ZF et al., 2000; Masumori et al., 2001; Kasper and Matusik, 2000). It has been shown that a 12 kb fragment of the Pbsn 5'-flanking sequence, a –426/+28 base-pair (bp) fragment as well as an artificial Pbsn promoter ARR2PB, which contains an extra copy of –244/-96 bp fused in front of the –286/+28bp region, is able to specifically target genes to transgenic mouse prostate (Greenberg et al., 1994; Yan et al., 1997; Zhang ZF et al., 2000). Therefore, the minimal fragment that confers prostate specificity was mapped to the 315 bp region (–286/+28) (Zhang ZF et al., 2000), which contains two functional AR binding sites (ARBS-1 at –236/–223 and ARBS-2 at –140/-117) (Rennie et al., 1993). Based on the hypothesis that additional key cis-acting elements remain to be uncovered, an extensive linker scan mutation analysis was performed by Zhang *et al*. Thirty one mutant Pbsn promoter fragments were generated by sequential replacing every ten base pair of Pbsn -286/+28 sequence with a random ten base pair DNA sequence (Fig. 3-1).

Luciferase reporter assay in cell culture experiments identified five key cis-elements, mutation of which significantly affected Pbsn promoter activity (Zhang ZF et al., 2004b). Transcription factor data base search predicted a POU domain transcription factor Oct1 binding site, a NF1 binding site and a AP-1 binding site within three of these essential DNA elements. Mutation of these three cis-acting elements individually resulted in a reduction of promoter activity in all tested cell lines. In contrast, mutation of the

other two elements, named TS-1 and TS-2, led to a decrease in promoter activity only in prostatic cell lines, but not in non-prostatic cell lines (Zhang ZF et al., 2004b).

Using LNCaP nuclear extract, EMSA was performed to confirm the binding of these transcription factors to Pbsn promoter. Both competition and antibody supershift assays were performed for each of these elements. Fig. 3-2A shows that the complexes formed with Pbsn -226/-187 bp can be competed by an increasing amount of cold Oct1 consensus binding sites (lane 3-5), and it was true reversely (lane 9-11). In addition, antibody to Oct1 produced a supershifted band in Pbsn bound complexes (lane 6). Lane 12 shows a positive control for this supershift assay. These data indicated Oct1 binds directly to Pbsn -226/-187 bp.

Similar experiments were performed for the putative NF1 binding site at Pbsn -96/-67 bp. Fig. 3-2B shows that using LNCaP nuclear extract, a specific complex was formed with Pbsn -96/-67 bp (lane 2). The formation of this complex was impaired by mutating the putative NF1 element (lane 3). Also this complex can be competed off by an increasing amount of cold Pbsn -96/-67 bp oligonucleotide (lane 4-5) or NF1 consensus binding sites (lane 6-7), but cannot be competed by control oligonucleotides (lane 8-11), suggesting binding specificity. In addition, supershift assay demonstrated a reduction in the binding of this complex to Pbsn -96/-67 bp when a NF1 antibody was added to the reaction (Fig. 3-2C, lane 3). Control antibodies had no effect (lane 5-7). Consensus NF1 binding site was also radiolabeled and included in the supershift experiment as a positive control (lane 9). To rule out the possibility that the NF1 antibody may have artificial effect on the EMSA binding patterns, a negative control using radiolabeled consensus Oct1 binding site was included in the same experiment, and the same antibody had no

effect on the binding pattern of Oct1 probes (lane 12), suggesting the "immunoelimination" seen in Pbsn -96/-67 bp and NF1 consensus site are specific and not artificial effects. These data strongly indicated NF 1 binds to Pbsn -96/67 bp directly.

Similarly, a strong complex was formed at Pbsn -116/-87 bp when LNCaP nuclear extract was incubated with the radiolabeled probe (Fig. 3-2D, lane 2). Mutation of the putative AP-1 binding element led to a reduction in the complex formation (lane 3). Interestingly, this complex can be apparently competed off by an increasing amount of cold -116/-87 bp (lane 4-5), cold AP-1 consensus sites (lane 6-7) and cold C/EBPβ consensus sites (lane 8-9), but not by a control sequence (lane 10-11). The mutation and competition assays suggested the specificity of this complex bound at Pbsn -116/-87 bp. Supershift assay (Fig. 3-2E) demonstrated that antibodies to c-jun (lane 3) and C/EBPβ (lane 6), but not to c-fos (lane 4) or other control antibodies (lane 5), produced supershifted bands for the Pbsn -116/-87 complexes, supporting the finding that both c-jun and C/EBPβ are involved in the complex formation at Pbsn -116/-87 bp. Furthermore, the same c-jun antibody cannot elicit supershift in the complexes formed with a mutant Pbsn -116/87 bp probe, which contains a disrupted AP-1 binding element (lane 12).

Collectively, these data unambiguously demonstrated that at least four ubiquitous transcription factors participate in the assembly of the multiprotein complex on Pbsn promoter. These ubiquitous sequence-specific DNA-binding proteins, together with tissue restricted proteins (forkhead protein and AR) discussed later, may create the first level of transcriptional control that responds to various intracellular signaling pathways.

B. Molecular Weight Mapping of Tissue-Specific Binding Proteins

In contrast to these ubiquitous transcription factor binding sites, two tissue specific elements, TS-1 and TS-2, are more important due to several functional features: i) both TS-1 and TS-2 are tightly adjacent to a functional ARBS site and the core region of each is almost identical; ii) in transgenic mice, mutation of TS1 reduced expression of reporter gene, but the expression was still prostatic specific, while mutation of TS2 abolished all reporter activity in all transgenic lines (Zhang ZF et al., 2004b). In EMSA using LNCaP nuclear extract, the binding patterns of TS-1 and TS-2 are almost identical, and both oligonucleotides can compete with each other for the binding of target proteins, suggesting that similar, if not identical, factors bind these elements (Zhang ZF et al., 2004b).

In addition to transcription factor database search, which generated multiple hits, two strategies were used to try to map the molecular mass of the proteins that are directly bound with TS-1 and TS-2. Initially, LNCaP nuclear extract was fractionated with SDS-PAGE according to standard molecular weight markers. Fractionated nuclear proteins were used to test the binding with TS-1 and TS-2 in EMSA (Materials and Methods). Active fractions containing the binding activity were identified. Fig. 3-3A is an EMSA demonstrating the binding activities of 9 fractions of LNCaP nuclear extract with TS-1 (lane 11-20) or TS-2 (lane 1-10) probes. Notably, TS-1 and TS-2 showed a similar binding pattern. Using molecular weight markers and corresponding migration distances, a standard curve was generated (Fig. 3-3B), and the active binding fractions were calculated to be corresponding to molecular weight of 35-44 kDa, 45-52 kDa, 53-70 kDa

and 90-115 kDa. TS-2 showed higher affinity to both 35-44 kDa and 53-70 kDa fractions (Fig. 3-3A, lane 6 and 8) compared with TS-1 (lane 16 and 18).

Southwestern blotting was performed as a more precise mapping assay for the molecular weight. Two strong TS2-binding activities were detected at around 52 kDa and 46 kDa, the details of which will be discussed. Importantly, these molecular mapping experiments, combined with database search, directly facilitated the identification of the binding of Foxa1.

C. Two Foxa (HNF-3) Binding Sites Are Identified on the Pbsn Promoter

In order to identify putative transcription factor binding sites in TS-1 and TS-2, two web-based search engines TESS (www.cbil.upenn.edu/tess) and TFSEARCH (www.cbrc.jp/research/db/TFSEARCH.html) were employed. The search was restricted to a maximum of 20% mismatch within an element length of 6 nucleotides or greater. Either a 9-nt sequence (-252/-244bp) located in R1 or a 9-nt sequence (-121/-113bp) located in R2 highly matched with the Foxa consensus binding sequence (5'-TRTTTRYTY-3') (Kaufmann and Knochel, 1996) (Fig. 3-4A). R1 and R2 are corresponding to the TS-1 and TS-2 element respectively. The first 7-nt 5'-T(A/G)TT(T/G)(G/A)(T/C)-3', extracted from various known Foxa-regulated gene promoters (Kaufmann and Knochel, 1996), perfectly matched with the TATTTGT motif in R2 (Fig. 3-4A). Fig. 3-4B shows an EMSA using nuclear extract prepared from LNCaP human prostate cancer cells, which express Foxa1 (Fig. 3-4C). TTRs is a strong Foxa binding unit on the liver transthyretin (TTR) gene promoter and was originally used to affinity-purify Foxa proteins (Lai et al., 1991; Lai et al., 1990; Costa et al., 1989). Strong complexes were formed when this TTR consensus Foxa binding site was used

(Fig. 3-4B, lane 2), and these complexes were reduced with addition of antibodies against Foxa1 or Foxa2 (lanes 3 and 4). RT-PCR using primers specific for Foxa2 failed to detect the expression of Foxa2 in LNCaP cells (data not shown), indicating the effect caused by Foxa2 (M20) antibody may due to the cross-reactivity of this antibody since Foxa1 and Foxa2 have highly homologous C-terminals. Four complexes, designated as a, b, c and d, were formed with radiolabeled Pbsn-127/-102, which overlaps R2 (Fig. 3-4B, lane7). Three complexes, designated as A, B and C, were formed with Pbsn-257/-232, which overlaps R1 (Fig. 3-4B, lane 20). Foxa1 antibody distinctly abolished the binding of two R2 complexes (lane 8, b and c) and R1 complex B (lane 21), while mock antibodies had no visible effect (lanes 10-16, and 23). A 200-fold molar excess of cold TTRs oligonucleotide completely competed off the complexes b and c (lane 17), indicating binding specificity. An increasing competitor (400 to 600-fold) further affected complex a (lanes 18 and 19), suggesting that a higher-order Foxa1 complex might be contained in complex a. Since complex "a" was not affected by Foxa1 antibody (lane 8), it indicates that this complex may have higher stability and the epitope in this complex may not be accessible to Foxa1 antibody. Western blot in Fig. 3-4C shows that Foxa1 protein was strongly detected in LNCaP and PC3, but weakly detected in DU145 cells in comparison with the positive control HepG2 cells, and the negative control Hela or Cos-1 cells.

Since ARBS-2 is tightly close to the Foxa1 motif in R2, it is necessary to determine: 1) whether Foxa1 still binds R2 when ARBS-2 site is occupied by AR, 2) whether the Foxa1/R2 interaction is dependent on adjacent AR binding. To address these questions in vitro, we used a radiolabeled probe (Table 2-1, ARBS2/R2) containing both ARBS-2 and R2. Fig. 3-4D shows that, among the multiple complexes formed with

LNCaP nuclear extract, two complexes were specifically reduced or removed by Foxa1 antibody (lane 1 vs. 2), while both complexes were disrupted by mutating the HNF-3 motif in ARBS2/R2 string (lane 3 vs. 7 and Table 2-1, ARBS2/R2-M1). Competition assay, using 100, 200 and 500-fold molar excess of cold ARBS-2 site (lane 3 vs. 4-6), showed that several complexes (indicated as asterisks) were sensitive to the competitor while none of the Foxa1 complexes were competed off. These results demonstrated in vitro that Foxa1/R2 binding can occur concomitantly with AR/ARBS-2 interaction, but Foxa1 binding is independent of AR/ARBS-2 interaction.

In Fig. 3-4E, Southwestern blot was used to determine the relative molecular sizes of R2-interacting proteins. LNCaP and PC-3 cell nuclear extracts were resolved on SDS-polyacrylamide gel and transferred to nitrocellulose membranes. The blots were probed with ^{32}P-labeled oligonucleotides containing two tandem copies of wild type R2 (2×R2). For both LNCaP and PC-3 cells, two proteins with molecular weight around 52-kD and 46-kD were detected (lanes 1 and 3). Similar blots probed with 2×mR2 (containing two copies of mutant R2, see Table 2-1 for sequence) showed that the binding of both proteins were distinctly reduced in LNCaP cells or completely blocked in PC-3 cells (lanes 2 and 4), indicating that the binding is sequence-specific. A radiolabeled oligonucleotide containing 2 tandem copies of AR consensus binding site (Table 2-1), serving as a positive control, was hybridized specifically to a 110-kD protein (the size of human AR), but not the low molecular weight proteins (lane 5). A parallel western blot using Foxa1 antibody showed a specific band around 52-kD (lanes 6 and 7), suggesting that the 52-kD protein detected by Southwestern was Foxa1. The 46-kD protein detected in both LNCaP and PC3 might be an Foxa1 minor degradation product, which escaped

antibody detection but still retained DNA binding activity. However, the presence of a higher-order protein complex on R2 (complex "a" in Fig. 3-4B, lane 7) suggests that additional DNA-binding protein on R2 may exist.

D. *In Vitro* Synthesized Foxa1 Binds Pbsn Promoter

Since crude nuclear extracts were used in EMSA and Southwestern experiments, it was necessary to confirm the results with Foxa1 synthesized by *in vitro* transcription/translation (TNT). Fig. 3-5A shows that synthesized Foxa1 specifically bound to the radiolabeled R2 in EMSA (lane 3), in contrast to the TNT blank control (lane 2), which only formed a non-specific band. Three Foxa1 mutants deleted in N-terminal (ΔN), C-terminal (ΔC) or both terminal regions (FH) still showed binding activities (lanes 4-6), since all mutants still contain the forkhead (FH) DNA binding domain. The binding of Foxa1 was completely removed by an antibody against the Foxa1 C-terminal (Fig. 3-5B, lane 2 vs. 3). The same antibody could not eliminate the complex formed by the mutant Foxa1 deleted in C-terminal (lane 5 vs. 6). In addition, a mutant probe (mPbsn-127/-102 bp) containing a mutated Foxa1 motif also affected the specific binding (lane 2 vs. 4). Similar results were observed when using R1 (Pbsn-257/-232 bp) sequence. As shown in Fig. 3-5C, Foxa1/R1 interaction is relative weaker in contrast to Foxa1/R2 (Fig. 3-5C, lane 2 vs. 4), since R1 has 1-bp mismatch with Foxa cognate binding site while R2 is a perfect match. The presence of multiple Foxa sites with different affinities has been proposed to be relevant for transcriptional modulation (Gaudet and Mango, 2002). These *in vitro* binding experiments confirmed the identification of two forkhead response elements immediately adjacent to the ARBSs in Pbsn proximal promoter.

E. Foxa1 is Expressed in Normal Prostate Epithelium

Two previous studies have reported the mRNA expression profile of Foxa in the mouse and rat prostates by using in situ hybridization and Northern blot (Kopachik et al., 1998; Peterson et al., 1997). We examined the Foxa protein expression pattern in the human and mouse prostate by immunohistochemical and Western blot analyses. In Fig. 3-6, immunohistochemistry showed a clear nuclear staining of Foxa1 in both mouse (panels A and B) and human (panels C and D) prostate luminal epithelial cells. Foxa2 and Foxa3 were not detected (data not shown). Consistently, Western blot showed that Foxa1 is expressed in all mouse prostate lobes, with highest level of expression in ventral prostate (VP) (panel E). This pattern is consistent with the previous study showing that Foxa1 mRNA level in VP is 14 times more abundant than in liver (Peterson et al., 1997). Results from RT-PCR using primers specific for Foxa1, Foxa2 or Foxa3 are consistent with immunohistochemistry and Western blot (data not shown). The absence of Foxa2 expression in adult mature prostate has been reported before (Kopachik et al., 1998) and this is different from the expression patterns in other organs where Foxa1 and Foxa2 are often co-expressed (Lai et al., 1991).

F. Foxa1 Binding Sites are Essential for Maximum Androgenic Induction

The mechanism of Foxa1 transcriptional regulation, in some part, involves nucleosome disruption (Cirillo et al., 1998; Cirillo et al., 2002). Although transiently transfected DNA cannot assemble the same higher-order chromatin structure as genomic DNA, certain levels of nucleosome-mediated regulation can be observed on transiently introduced DNA (Smith and Hager, 1997; Crowe et al., 1999). Studies using transient transfection have demonstrated that Foxa1 relieves nucleosome-mediated transcriptional

repression of a liver specific α-Fetoprotein gene (Crowe et al., 1999). In order to examine the biological role of the two Foxa1 binding motifs, we compared the activities of mutant Pbsn promoters with wild type promoter in transfection assay. PCR based site-directed mutagenesis was used to generate point mutations in Foxa1 binding sites (R1 and R2). As seen in Fig. 3-7A, three mutant promoters were generated. Two of them, M1 and M2, contain mutant forkhead motif in R2. The third one, M3, contains mutant forkhead motif in R1. EMSA in Fig. 3-7B demonstrated that M1 completely abolished Foxa1 complexes a, b and c. M2 slightly affected complexes b and c, but distinctly removed complex a. Addition of Foxa1 antibody further removed complex b and c, indicating that M2 affects the formation of a higher-order complex, which was competed by the Foxa consensus sequence (Fig. 3-4B, lanes 18 and 19). All mutant as well as a wild type Pbsn reporter constructs were transfected into LNCaP cells and luciferase activities were compared. Experiments were repeated at least six times. Fig. 3-7C is a representative experiment showing that the maximal androgen-induction of Pbsn promoter activity was significantly affected in either mutant R1 or mutant R2. In contrast to R1 motif, R2 may have a greater biological relevance since both M1 and M2 mutations almost completely ablated Pbsn activity ($P<0.001$). The significant decrease in M2 activity suggests that the complex a (Fig. 3-7B), which is in a higher-order, is biologically important. The reduction in M3 activity is consistent with a previous study (Patrikainen et al., 1999) conducted by another group, who demonstrated a significant loss in Pbsn activity by deleting a region overlapping with R1. Similar results were obtained when these transfection experiments were performed in PC3 cells (data not shown). In addition, EMSA in Fig. 3-7D demonstrated in vitro that a purified GST-AR-DBD fusion protein bound to these mutant

ARBS-1/R1 or ARBS-2/R2 strings (Table 2-1 for sequences) with similar intensity as to the wild type sequence, indicating that these mutations generated in forkhead motifs do not directly abrogate the AR/ARBS interaction. Thus, the activity loss in Pbsn promoter (Fig. 3-7C) is not directly due to the loss of AR/ARBS binding. However, such mutations may destabilize the formation of a complete nucleoprotein complex in these regions, and this will be further discussed in this paper. These data strongly suggested that two forkhead motifs are required for the maximal androgenic induction in Pbsn gene.

G. Dominant Negative Mutant Foxa1 Inhibits Pbsn Activity

Both the N- and C-terminal regions of Foxa proteins have been suggested to have transactivation activities (Pani et al., 1992; Qian and Costa, 1995). Recent studies using in vitro nucleosome assembly showed that the transcriptional modulation by Foxa1 is mediated through its C-terminal region (Cirillo et al., 2002). We generated two recombinant Foxa1 mutants (ΔN141-466, ΔC1-294) with deletions in either N- or C-terminal region. These mutants as well as a wild type Foxa1 expression vector (0.2 μg/well) was co-transfected into LNCaP cells with the ARR2PB-Luc reporter construct. Luciferase activities were measured and compared. As shown in Fig. 3-8A, over-expression of wild type Foxa1 did not significantly increase the androgen-induction of Pbsn activity, indicating that the endogenous Foxa1 level is sufficient for the maximal promoter response. In contrast to wild type and ΔN141-466 proteins, over-expressing ΔC1-294 significantly inhibited the total Pbsn activity (Fig. 3-8A, $P<0.01$), and this inhibition displayed a dose-responsive manner (Fig. 3-8B). In contrast, transfection of same amount of ΔC1-294 cannot significantly inhibit the activity of the mutant Pbsn promoter (Fig. 3-8C), which contains a non-functional Foxa site (M1 in Fig. 3-8C).

Western blot showed that transient expression of these Foxa1 proteins in LNCaP cells did not result in a detectable change in the endogenous AR protein level (Fig. 3-8D), suggesting that the reduction in Pbsn promoter activity was not due to a reduced AR level. These results strongly indicated a dominant negative mechanism for ΔC1-294, and further supported the regulatory role of Foxa1 C-terminal region in transcriptional modulation.

H. Identification of Two Functional Foxa1 Binding Sites in PSA Core Enhancer

The results obtained for rat Pbsn gene prompted the determination of whether Foxa1 is also required for the regulation of human PSA gene. It has been reported that the core enhancer region (–4.2/-3.8 kb) of PSA gene, but not the proximal promoter, is essential and sufficient for androgen regulation and prostate-specificity (Schuur ER et al., 1996; Cleutjens et al., 1997; Farmer et al., 2001; Pang et al., 1997). Six ARE are located in this region (Huang et al., 1999). Among these AREs, ARE III (at –4154/-4132bp) shows the highest AR-affinity and biological activity, since mutations in ARE III significantly abolished PSA enhancer activity (Huang et al., 1999). Interestingly, we identified two strong Foxa binding motifs in this enhancer region (Fig. 3-9A). The first site, designated as PSA1, is located at -4122/-4109 bp, immediately downstream of the ARE III. The second site, PSA2, is located at –4028/-4005 bp, between ARE IIIA and ARE IIIB (Fig. 3-9A). *In vitro* synthesized Foxa1 bound to both elements (Fig. 3-9B, lane 2 vs. 3 and 3-9E, lane 3 vs. 4). Similar to the results for Pbsn, mutant Foxa1 proteins (ΔN, ΔC and FH) containing the FH domain also showed binding activity (Fig. 3-9B lanes 4-6). In addition, the binding of Foxa1 was supershifted by Foxa1 antibody (lane 3

vs. 7). Therefore, both elements were confirmed to be authentic Foxa1 site by these in vitro experiments.

Since PSA1 is closely adjacent to ARE III, it was intriguing to ask whether Foxa1 and AR can bind to the DNA concomitantly. Thus, an oligonucleotide (Table 2-1) containing both ARE III and PSA1 was radiolabeled and incubated with constant amount of a purified GST-AR-DBD fusion protein. A specific AR-DBD/DNA complex was formed (Fig. 3-9C, lane 4). As increasing amount of Foxa1 proteins were added to the reaction, a specific Foxa1/DNA complex as well as a slow-migrating band (AR/Foxa1/DNA ternary complex) became stronger (lanes 5-8). Addition of Foxa1 antibody disrupted the complex (lane 9). Similarly, in EMSA using LNCaP nuclear extract, Foxa1 antibody disrupted a strong complex that formed with this oligonucleotide (Table 2-1, PSA1) containing both Foxa1 and AR binding sites (Fig. 3-9D, lane 2 vs. 3). These data indicate that AR and Foxa1 can bind to respective DNA binding sites concomitantly. Thus, the binding of one protein does not negatively affect the adjacent binding of another protein. However, the dislocation of Foxa1 from target binding site (Fig. 3-9C, lane 9) may destabilize a higher-order protein complex associated with this entire regulatory region, which may include AR.

A similar mutation assay was performed to determine the biologic relevance of these Foxa1 motifs in PSA enhancer. Fig. 3-10A shows two mutant PSA reporter constructs, mPSA1-EP and mPSA2-EP, which were generated by PCR and transfected into LNCaP cells. Luciferase activities were measured and compared with wild type construct. Fig. 3-10B shows that point mutations that abolish Foxa1 binding in either PSA1 (Fig. 3-10C, lane 2) or PSA2 (lane 4) significantly affected the maximal androgen-

induced PSA activities (Fig. 3-10B, $P<0.01$). A reduction of 95% activity in PSA enhancer has been reported previously by deleting the region corresponding to PSA1 (Farmer et al., 2001). Similarly, the direct interaction between AR and ARE III remained intact when mutant oligonucleotide (Table 2-1, mPSA1), containing both ARE III and mutant Foxa motif, was used in EMSA (Fig. 3-10D), indicating that the loss of PSA activity is not directly due to the loss of AR/ARE III binding. These results suggest that both Foxa1 motifs are essential for maximal PSA induction by androgen.

I. Foxa1 Binds PSA Enhancer *In Vivo*

Since LNCaP cells express endogenous PSA gene, chromatin immunoprecipitation (ChIP) was performed to investigate the *in vivo* association of Foxa1 with PSA enhancer. Fig. 3-11A is a schematic diagram of PSA regulatory region. Five previously described DNA fragments (Shang et al., 2002) corresponding to the distal region, ARE III, middle region, ARE II and ARE I were tested in the experiment. The ARE III region (-4170/-3978 bp) is a 192-bp fragment that covers both Foxa1 motifs we identified in this study (Fig. 3-11A). To determine the occupancy of Foxa1 on active versus inactive PSA chromatin status, LNCaP cells were initially grown in RPMI-medium 1640 supplemented with 5% charcoal/dextran treated fetal bovine serum. After 3 days of cultivation, cells were either treated with 10^{-8} M DHT or retained in androgen-depleted medium. Soluble chromatin was prepared after formaldehyde treatment of cells (Fig. 3-11C). Specific antibodies against Foxa1 or AR were used to immunoprecipitate antigen-bound genomic DNA fragments. The DNAs were amplified by PCR using specific primers (Shang et al., 2002) spanning the tested regions. After 48 h of DHT treatment, PSA expression was induced as compared to the undetectable level in

untreated cells (Fig. 3-11B). In contrast, the expression levels of Foxa1 protein were almost identical in androgen-treated and untreated cells. In agreement with previous study (Shang et al., 2002), DHT induced the recruitment of AR onto multiple AREs, but not control regions (Fig. 3-11D). In contrast to AR, Foxa1 constantly occupies the ARE III region independently of DHT treatment (Fig. 3-11D). These ChIP assays demonstrated the in vivo association of Foxa1 with PSA enhancer, and also indicated that the occupancy of Foxa1 alone does not result in the transactivation of PSA gene.

J. Foxa1 Binds Other Prostate-Specific Enhancers

Foxa1 binding sites were further identified in other prostate specific gene regulatory regions. As shown in Fig. 3-12A, the proximal promoter of the rat prostatic acid phosphatase gene (rPAP) contains a Foxa1 binding sequence at –113/-103 bp. This sequence as well as an upstream ARE is well conserved in its human homologue hPAP gene promoter (Virkkunen et al., 1994). In the hPAP upstream enhancer (-1258/-779 bp), a G/T rich region (-1183/-1151 bp) contains two Foxa1 binding sites with a putative ARE in the middle. This region also exists in rPAP enhancer (Fig. 3-12A), except that only one Foxa1 binding site was found. Importantly, the hPAP enhancer (-1258/-779 bp) is related with the cell-specific expression of hPAP gene (Patrikainen et al., 1999). In addition, two Foxa1 motifs (at -184/-173 bp and -141/126 bp, Fig. 3-12A) were found in the rat prostatic steroid binding protein C1 (PBP C1) gene promoter (Claessens et al., 1989). All these Foxa1 sites were experimentally confirmed by EMSA. The sequences used in EMSA were shown in Table 2-1. Fig. 3-12B is a schematic diagram showing a striking similarity in the organization of binding motifs for Foxa1 and AR in these highly prostate-specific genes, suggesting a common functional mechanism may apply.

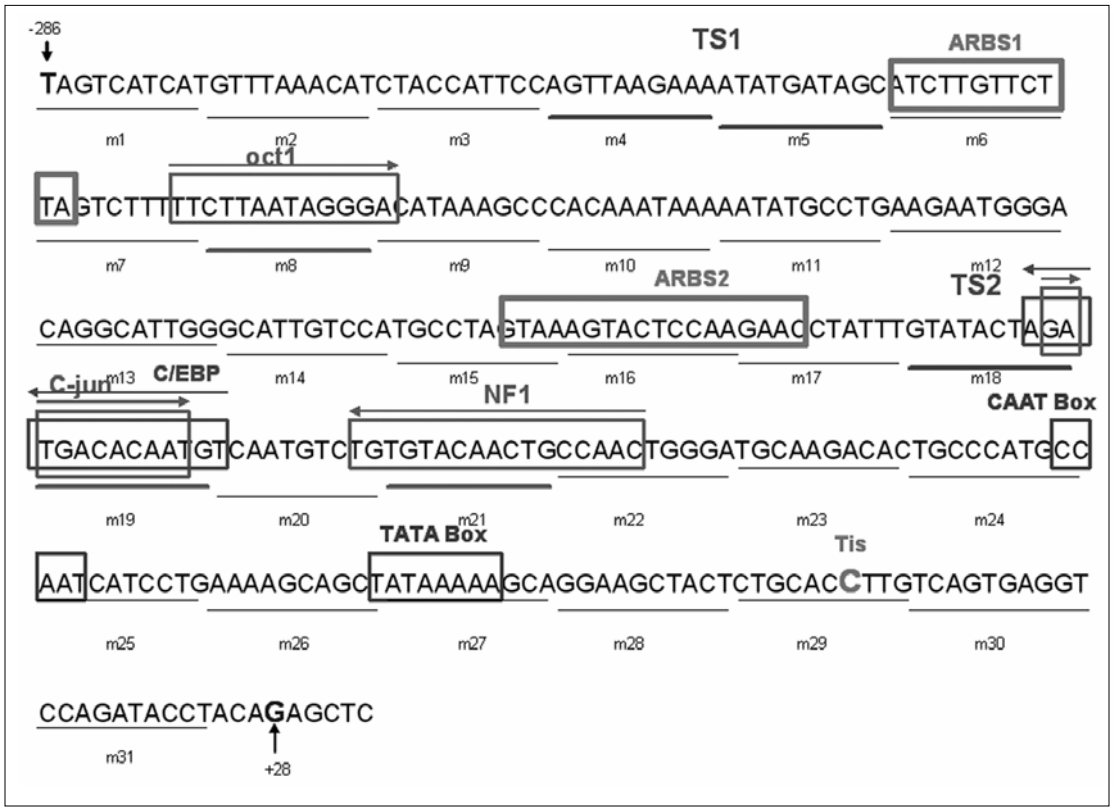

Figure 3-1. Key cis-regulatory elements in the prostate tissue-specific Pbsn promoter -286/+28 bp. Linker scan mutagenesis mapped five important cis-regulatory elements in addition to ARBS1 and ARBS2. Among these elements, there are potential binding sites for ubiquitous transcription factor Oct1, c-jun, C/EBP and NF1. In addition two tissue specific elements, namely TS1 and TS2, were revealed to be just immediately flanking the individual androgen response elements.

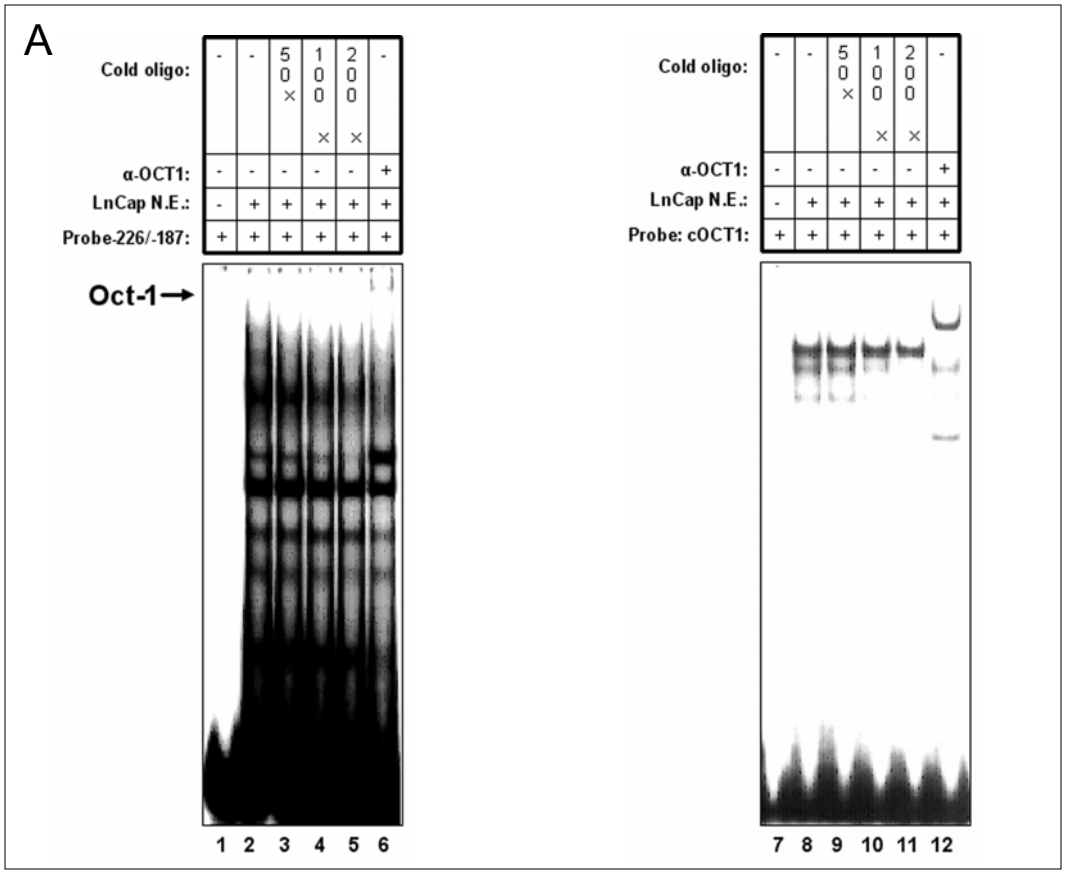

Figure 3-2. Ubiquitous transcription factors bind Pbsn -286/+28 bp. (A) Oct1 binds to Pbsn promoter. EMSA shows LNCaP nuclear extracts (N.E.) bind to radiolabeled Pbsn -226/-187 bp (lane 2), as compared to lane 1 where no nuclear extract was added. The binding was competed by 50×, 100× and 200× amount of cold Oct1 consensus oligonucleotides (lanes 3-5). Lane 5, binding was also supershifted by an antibody to Oct1. Competition assay was performed reversely by using Pbsn -226/-187 bp to compete the binding of Oct1 consensus probe (lanes 7-11). Lane 12, supershift assay shows Oct1 antibody supershifted the complex formed by LNCaP N.E. and Oct1 consensus probe. (B) NF1 binds to Pbsn promoter. EMSA shows LNCaP N.E. bind to radiolabeled Pbsn -96/-67 bp (lane 2). The binding intensity was reduced when a mutant Pbsn -96/-67 bp probe was used (lane 3). The complex was also competed off by cold Pbsn -96/-67 bp (lane 4-5) or by consensus NF1 binding site (lane 6-7). The binding was not competed by control oligonucleotides (lane 8-11). (C) The complex formed on Pbsn -96/-67 bp was eliminated by NF1 antibody (lane 3 vs. 2), but not reduced by control antibodies (lane 4-6). The complex formed on consensus NF1 binding site was also reduced (or supershifted) by NF1 antibody (lane 9 vs 8), but not an Oct1 antibody (lane 10). Same NF1 antibody has no effect on the complex formed with a control Oct1 binding site (lane 12 vs. 11), while Oct1 antibody produced a supershift (lane 13). (D) AP1 and C/EBP bind to Pbsn. The complexes formed by LNCaP and Pbsn -116/-87 bp (lane 2) were reduced by using a mutant -116/-87 bp probe (lane 3). The binding was also competed off by cold -116/-87 bp oligonucleotides (lane 4-5), AP1 consensus (lane 6-7) and C/EBP consensus (lane 8--9) binding sites, but not by a control oligonucleotide (lane 10-11).

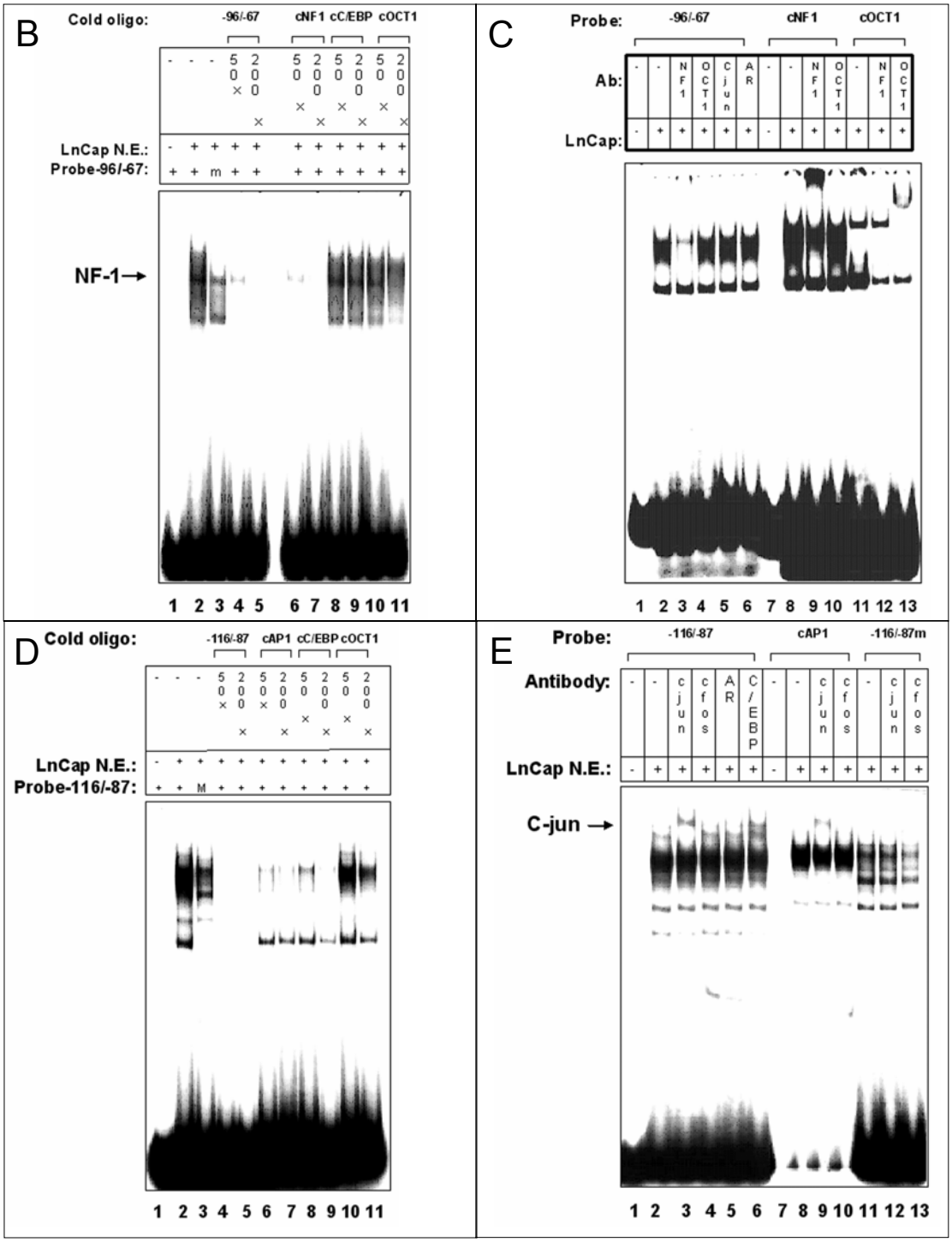

Figure 3-2 (continued). (E) EMSA shows that c-jun antibody (lane 3) and C/EBP antibody (lane 6) supershifted the complex formed by LNCaP and radiolabeled Pbsn -116/-87 bp (lane 2). Other control antibodies (lane 4-5), including c-fos antibody (lane 4), had no effect. C-jun antibody also supershifted the complex formed on the consensus AP1 binding site (lane 9 vs 8). Same antibody had no effect on the complex formed on a mutant Pbsn -116/-87 probe.

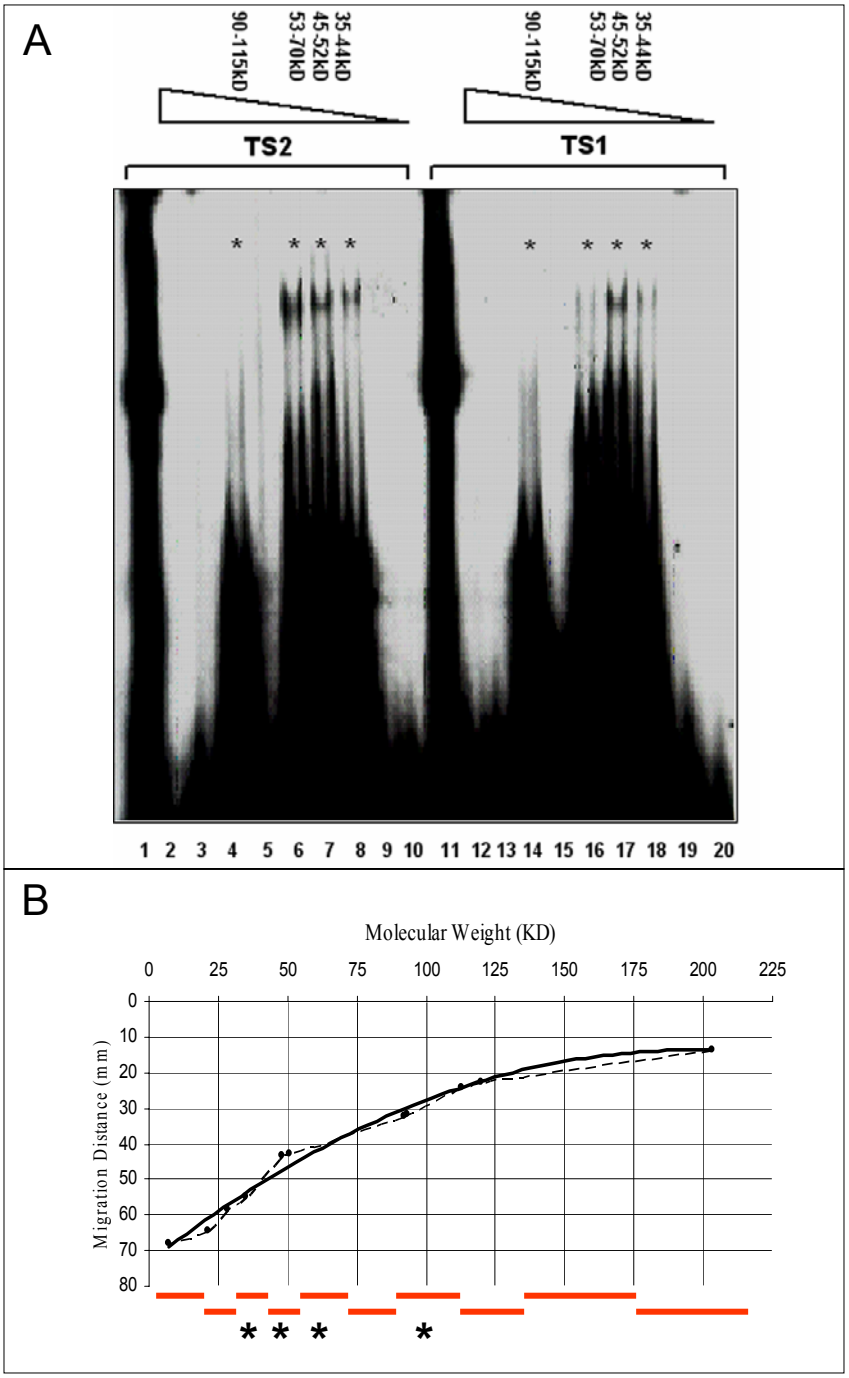

Figure 3-3. SDS-PAGE fractionation of LNCaP nuclear extracts and molecular mapping of TS1-, TS2-interacting proteins. (A) LNCaP N.E. were fractionated into 9 factions according to molecular weight. DNA binding activities to TS1 (lane 11-20) or TS2 (lane 1-10) were tested by EMSA, which revealed a similar binding pattern. Lane 1 and 11 are controls using total LNCaP N.E. (B) Binding activities for both TS1 and TS2 were calculated to be at 35-44 kDa, 45-52 kDa, 53-70 kDa and 90-115 kDa, based on the migration-molecular weight curve.

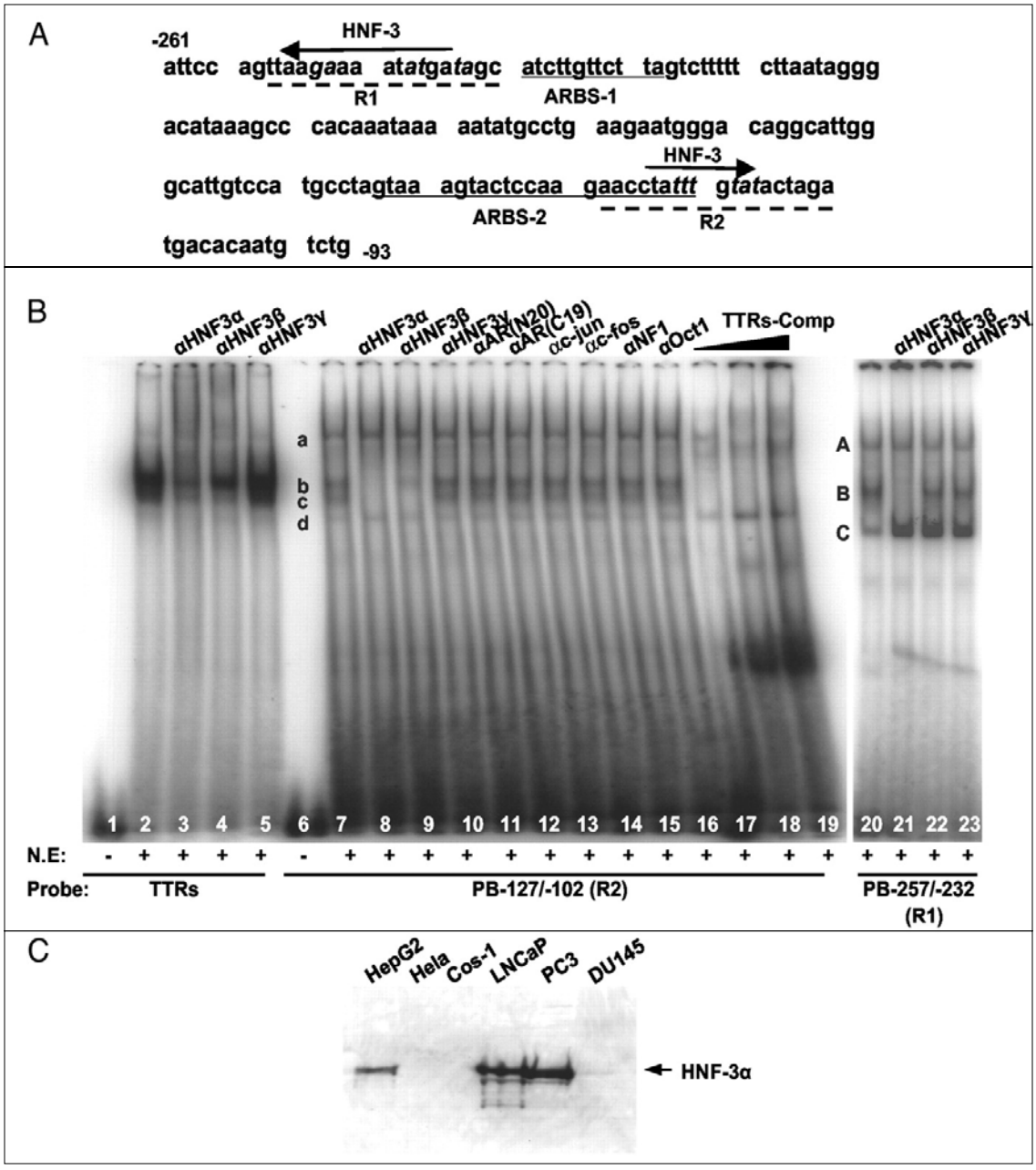

Figure 3-4. Identification of Foxa (HNF-3) motifs in Pbsn promoter (A) Location of Foxa motifs. Mutation study revealed two key *cis*-acting elements R1 and R2 (dashed lines). Each contains a potential Foxa binding motif (bold arrows). The direction of the arrow indicates the sense or the antisense strand that matched the consensus sequence. Two adjacent ARBSs (ARBS-1 and ARBS-2) are underlined. Sequences in italic indicate the nucleotide replacements in mutation assays. (B) LNCaP nuclear extracts were incubated with radiolabeled TTRs (consensus Foxa binding sequence), Pbsn -127/-102, or Pbsn -257/-232 probes. Strong complexes formed with TTRs (lane 2). Foxa1 or Foxa2 antibody reduced the corresponding band (lanes 3 and 4). Four complexes, a, b, c and d, were formed with R2 (lane 7). Complexes b and c were specifically removed by Foxa1 or Foxa2 antibody (lanes 8 and 9), but not other mock antibodies (lanes 10–16).

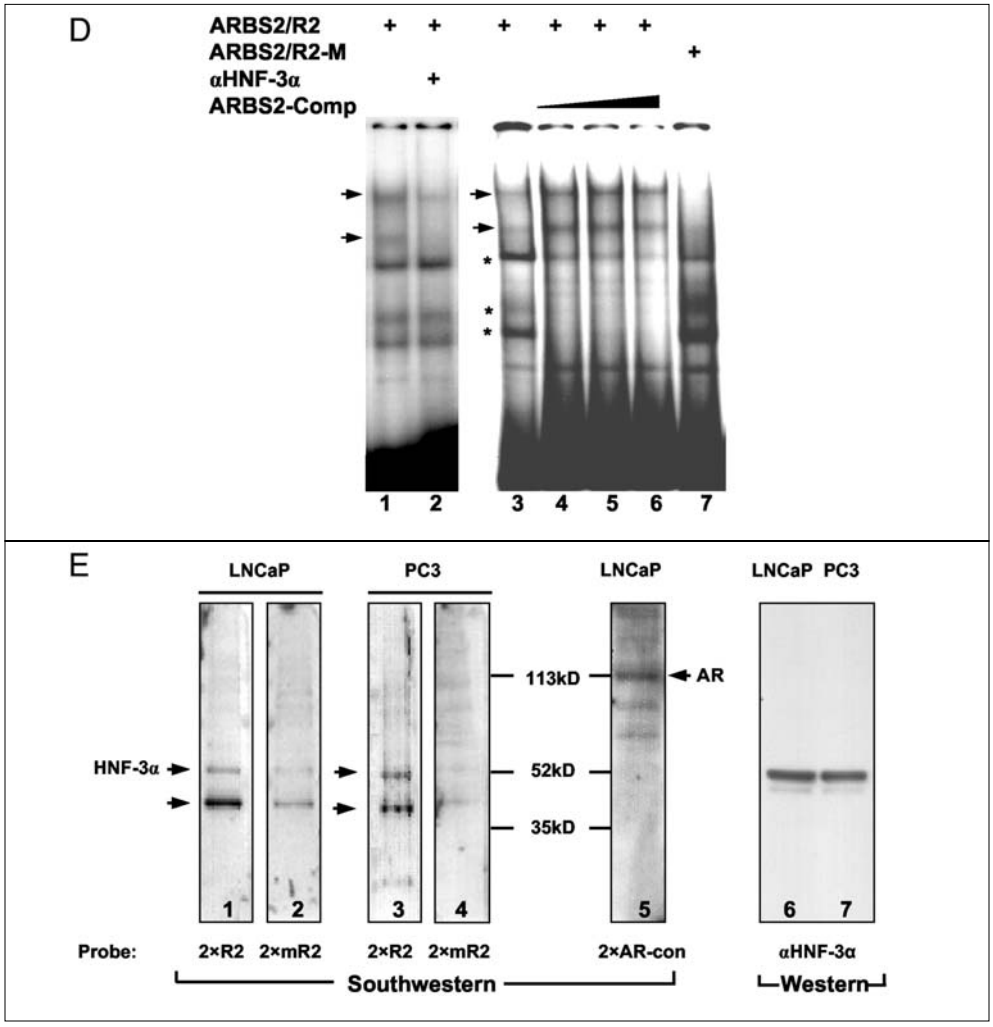

Figure 3-4 (continued). Molar excess (200-fold) of cold TTRs oligonucleotides completely competed off complexes b and c (lane 17), whereas 400- and 600-fold molar excess of TTRs also affected complex a (lanes 18 and 19). Three complexes, A, B, and C, were formed with R1 (lane 18). Complex B was specifically eliminated by Foxa1 (HNF-3α) antibody (lane 19). (C) Western blot. Whole-cell lysates (20 μg) from HepG2, Hela, Cos-1, LNCaP, PC3, and DU145 cells were resolved on SDS-PAGE and probed with Foxa1 antibody. (D) A radiolabled oligonucleotide (ARBS2/R2, Table 2-1) containing both ARBS-2 and R2 was used in EMSA with 10 μg LNCaP nuclear extract. With the presence of an ARBS, two Foxa1 complexes (arrows) still formed with R2, because both complexes were reduced or removed by Foxa1 antibody (lane 1 vs. 2), or eliminated by mutating the Foxa1 motif in ARBS2/R2-M (lane 7, Table 2-1). Both complexes were not affected by 100-, 200-, and 500-fold molar excess of cold ARBS-2 site (lanes 4–6), whereas several other complexes (asterisk) were sensitive to the competition. (E) Southwestern bloting. Nuclear extracts from LNCaP and PC-3 cells were separated on SDS-PAGE, transblotted to nitrocellulose membranes, and probed with radiolabeled 2xR2 (lanes 1 and 3), 2xmR2 (lanes 2 and 4) or 2xAR-con probes (lane 5). A Western blot using Foxa antibody was performed as a parallel control. Arrows indicate migration of proteins bound to the respective probes or antibody.

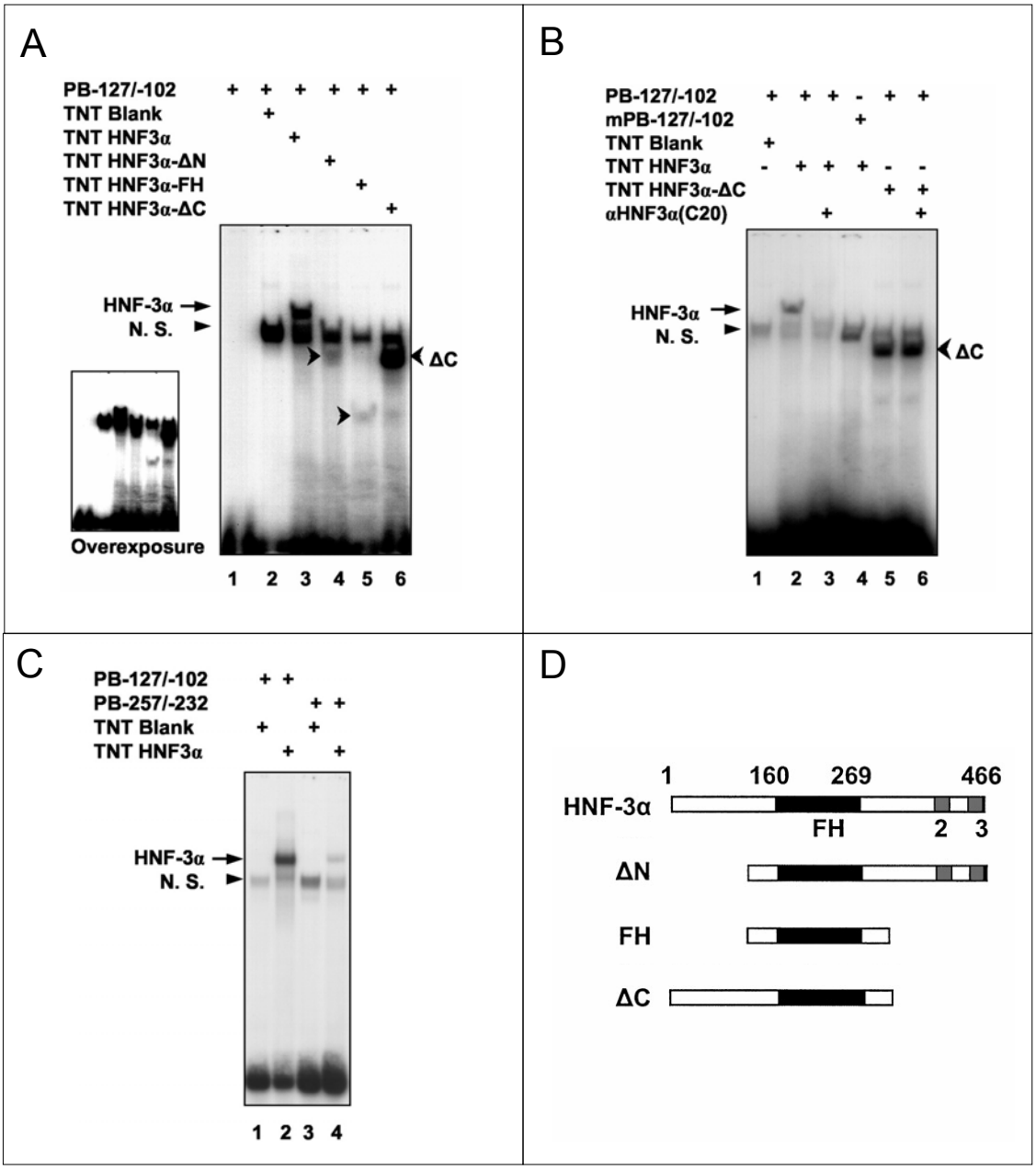

Figure 3-5. ***In vitro*** **synthesized Foxa1 (HNF-3α) binds Pbsn promoter.** (A) Wild-type Foxa1 and three truncated proteins (ΔN, FH, and ΔC shown in panel D) were synthesized by in vitro TNT, and incubated with radiolabeled PB-127/-102 probe. In contrast to a nonspecific band (arrowhead) formed with the TNT blank control (lane 2), wild- type Foxa1 and Foxa1ΔC formed a strong complex (lanes 3 and 6), whereas ΔN and FH (arrowhead) showed weak binding ability (lanes 4 and 5, overexposure). (B) The binding of Foxa1 with Pbsn -127/-102 was eliminated by an antibody raised against the Foxa1 C terminus (lane 3 vs. 2). The same antibody did not affect the complex formed by Foxa1Δ C, which has a deletion in the C terminus (lane 6 vs. 5). The Foxa1 binding was also affected by mutating the TRTTTGY motif (lane 4 vs. 2). (C) Weaker binding affinity was observed when Pbsn -257/-232 was used as a probe (lane 4 vs. 2).

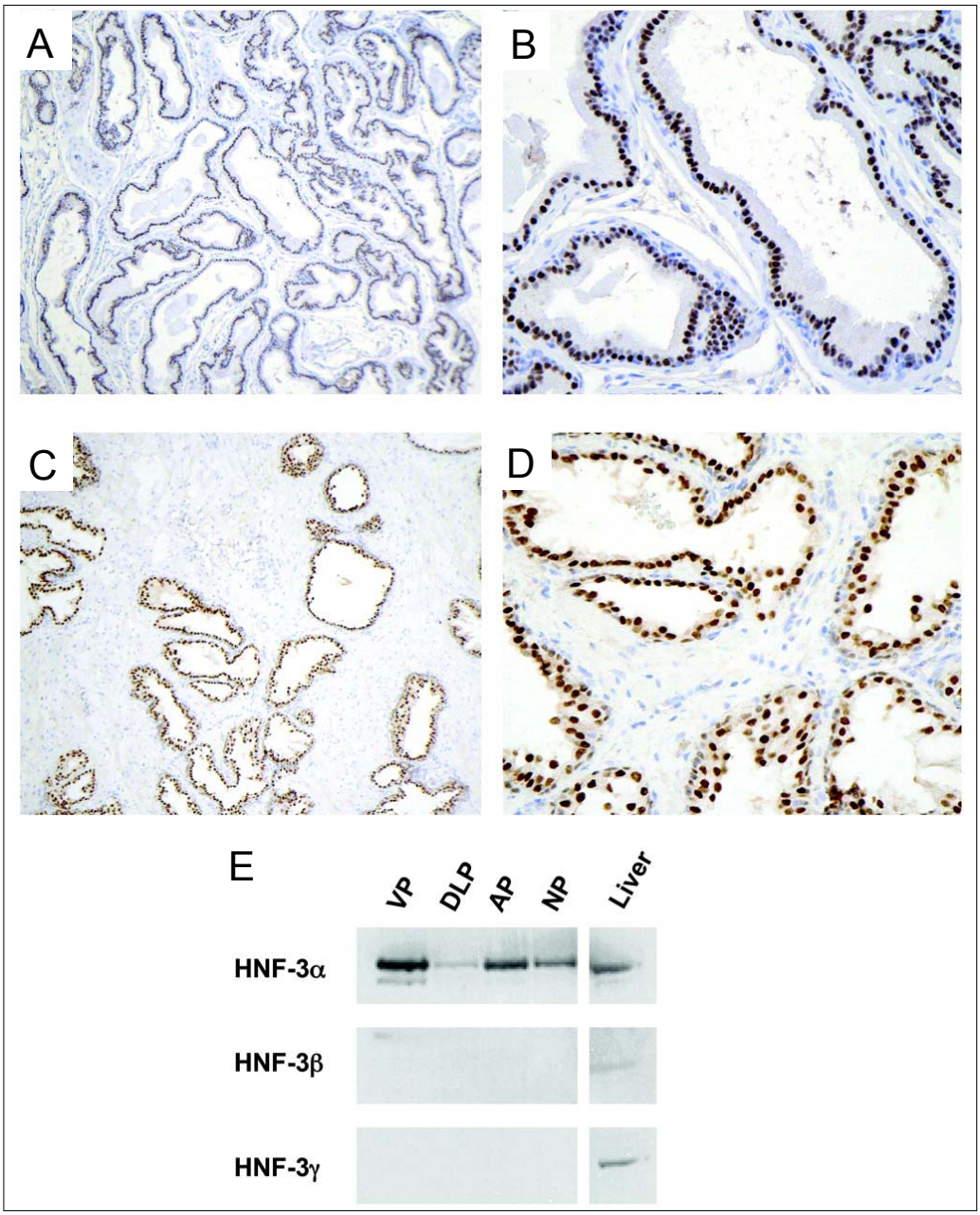

Figure 3-6. Prostate epithelium expresses Foxa1 (HNF-3α). (A–D) Immunohistochemistry for Foxa1. Nuclear staining of Foxa1 protein was restrictively detected in both mouse (A and B) and human prostate epithelium (C and D). (E) Western blot. Fresh mouse prostate tissue lysates from different lobes (VP, ventral prostate; DLP, dorsal-lateral prostate; AP, anterior prostate; NP, whole normal prostate) were separated by SDS-PAGE and detected with antibodies for Foxa1, Foxa2 (HNF-3β), and Foxa3 (HNF-3γ).

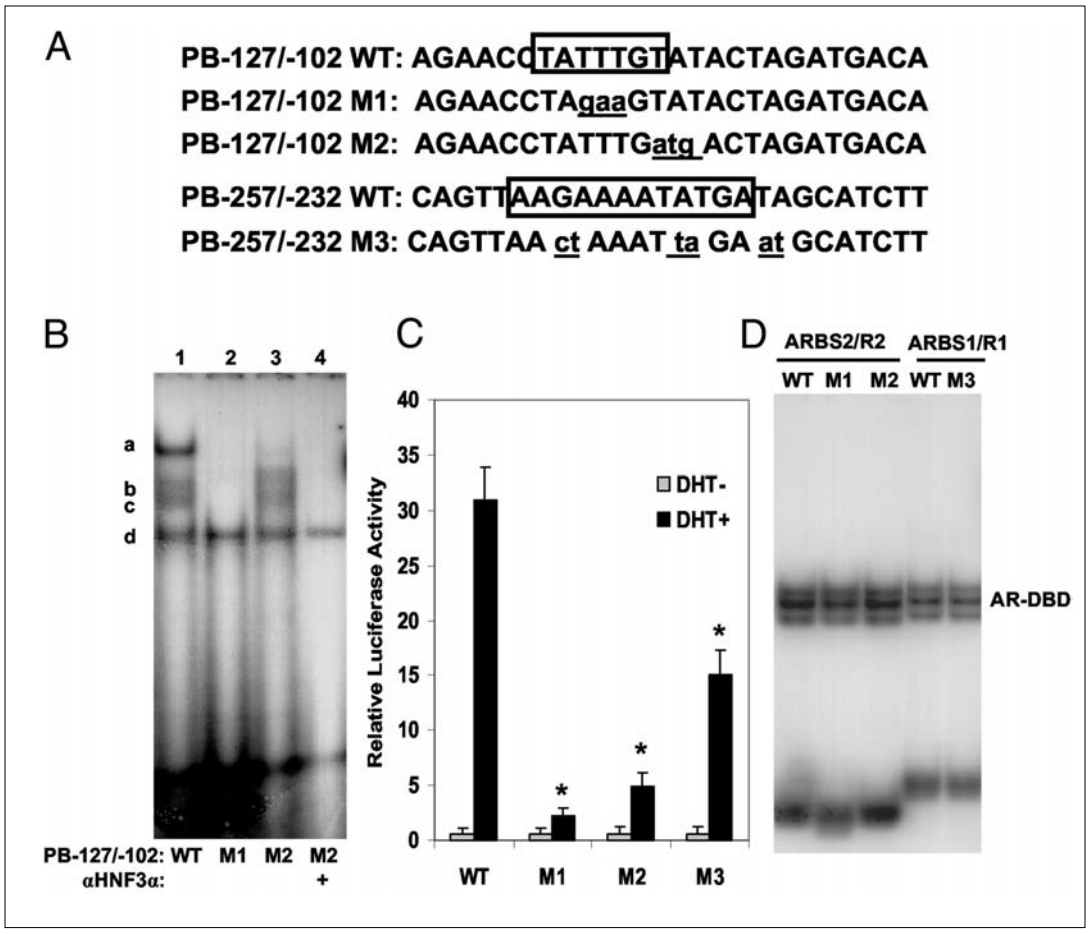

Figure 3-7. Foxa1 (HNF-3α) motifs are essential for maximum androgenic induction of Pbsn. (A) Wild-type PB promoter sequences containing boxed Foxa1 motifs were mutated (underlined lowercase characters) as indicated in M1–M3. (B) EMSA was conducted using 10 μg LNCaP cell extracts incubated with either wild-type PB-127/-102 or mutant R2 probes (lanes 1–3). M1 disrupted the binding of three complexes (lane 2, a, b, and c), whereas only the higher-order complex "a" was eliminated by M2 (lane 3). Addition of Foxa1 antibody further removed complexes b and c (lane 4). (C) LNCaP cells were transiently transfected with luciferase reporter constructs (0.2 μg/well) containing either wild-type or mutant (M1–M3) PB promoters. Each well also received 0.0125 μg of Renilla vector. Cells were treated with or without 10^{-8} M DHT for 24 h before harvest. Background activities of cell lysates with no DNA transfection were subtracted from the data obtained in the experimental group, before the normalization with Renilla activities. Results are presented as relative luciferase activity. Data shown here is a representative from at least six independent experiments in triplicate. Error bars indicate SD values. Asterisk indicates where $P < 0.01$ as compared with the androgen-induced activity in wild-type (WT) reporter. (D) Probes (ARBS2/R2-M1, -M2, and ARBS1/R1-M3, Table 2-1) containing mutant Foxa1 motifs were used in EMSA to determine their interactions with a purified GST-AR-DBD protein.

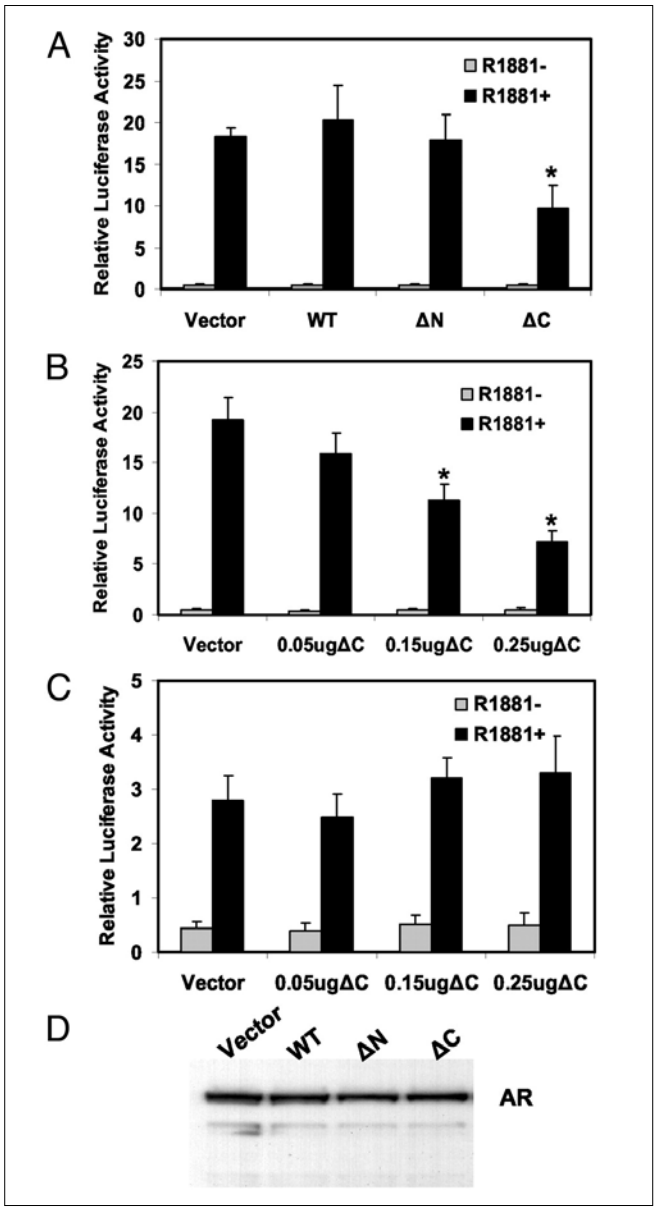

Figure 3-8. Dominant negative Foxa1 (HNF-3α) inhibits Pbsn promoter activity. (A) An empty vector as well as expression vectors corresponding to wild-type Foxa1, $\Delta N_{141\text{-}466}$, or $\Delta C_{1\text{-}294}$ (0.2 μg per well) were cotransfected with a Pbsn luciferase reporter into LNCaP cells. Cells were treated with or without 10^{-8} M R1881 for 24 h followed by luciferase assays. (B) Different amounts of $\Delta C_{1\text{-}294}$ (0.05 μg, 0.15 μg, or 0.25 μg per well) were cotransfected into LNCaP cells with Pbsn reporter. Luciferase activities were determined after 24 h incubation in the presence or absence of androgen. (C) In contrast to panel B, $\Delta C_{1\text{-}294}$ (0.05 μg, 0.15 μg, or 0.25 μg per well) was cotransfected into LNCaP cells with a mutant Pbsn reporter (M1, in Fig. 3-7A). *Error bars* indicate SD values. *Asterisk* indicates $P < 0.01$ in comparison with androgen-induced activities in control wells, which were transfected with empty vector. (D) No significant change in AR protein level was detected by Western blot in cells transiently transfected with wild-type Foxa1, $\Delta N_{141\text{-}466}$, or $\Delta C_{1\text{-}294}$.

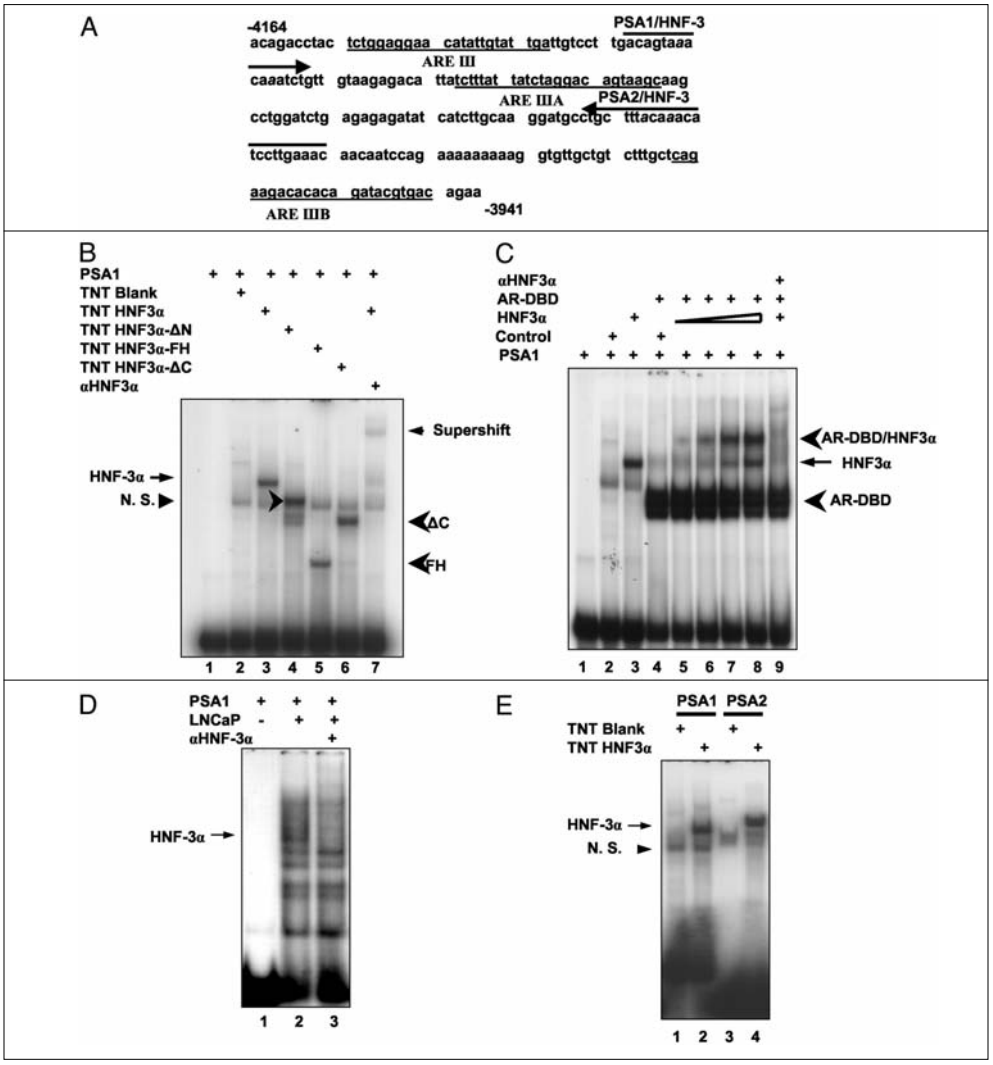

Figure 3-9. Identification of Foxa1 (HNF-3α) Binding Motifs in PSA Enhancer. (A) Two Foxa1 binding sequences (bold arrow) were identified in the PSA core enhancer (-4.2/-3.9 kb) region. The first element (-4122/-4109), designated as PSA1, is adjacent to ARE III (underlined). The second one (-4028/-4005), designated as PSA2, is located in the middle of ARE IIIA and ARE IIIB (underlined). (B) EMSA. In vitro synthesized wild-type Foxa1 and mutant proteins (ΔN, FH, and ΔC) were able to bind PSA1 (lanes 3–6) as compared with the TNT blank control (lane 2). The Foxa1 binding was supershifted by the Foxa1 antibody (lane 3 vs. 7). (C) Concomitant DNA binding of AR and Foxa1. Radiolabeled oligonucleotide containing both ARE III and PSA1 was incubated with a constant amount (0.1 μg) of a purified GST AR-DBD protein. A slow migrating ternary complex (AR/Foxa1/DNA) (lanes 5–8) was formed as addition of increasing amounts (1, 2, 3, and 4 μl) of in vitro synthesized Foxa1, in contrast to Foxa1 alone (lane 3) or AR alone (lane 4), indicating that Foxa1 and AR can occupy DNA concomitantly. The ternary complex was disrupted by addition of Foxa1 antibody (lane 9). (D) EMSA using LNCaP nuclear extract shows the formation of Foxa1/PSA1 complexes (lane 2), which were disrupted by Foxa1 antibody (lane 3). The probe PSA1 (see Table 2-1 for sequence) contains binding sites for both AR and Foxa1. (E) In vitro synthesized wild-type Foxa1 also interacts with PSA2 (lane 4).

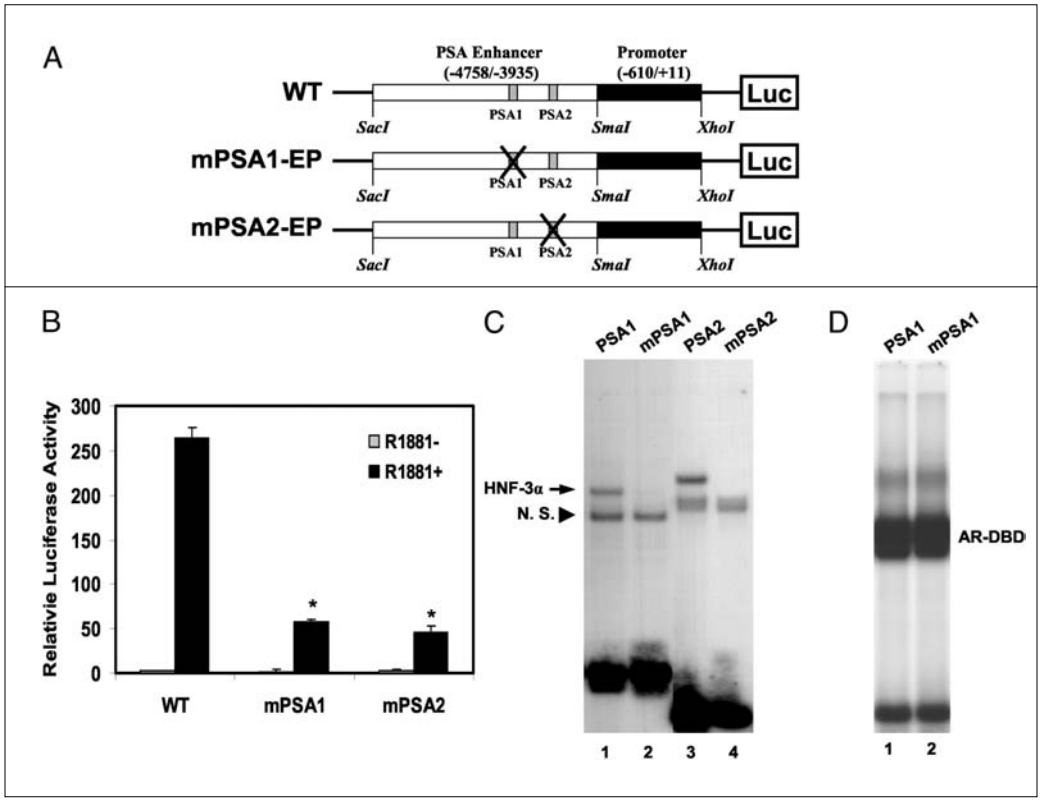

Figure 3-10. Mutations in forkhead motifs inhibited maximal androgen induction of PSA. (A) Two mutant PSA reporters (mPSA1-EP and mPSA2-EP) were generated by introducing point mutations to Foxa1 (HNF-3α) motifs in PSA1 and PSA2, individually. (B) LNCaP cells were transiently transfected with wild-type and mutant PSA-EP luciferase constructs. Luciferase activities were determined after 24 h incubation in the presence or absence of 10^{-8} M R1881. Three independent experiments were performed in triplicate. Background activity of untransfected cell lysate was subtracted from the results before normalization with *Renilla* activities. *Error bars* indicate SD values. *Asterisk* indicates where $P < 0.01$ in comparison with the androgen-induced activity in wild-type reporter. (C) Oligonucleotides containing mutant Foxa1 sites (mPSA1 and mPSA2, Table 2-1) was used in EMSA to determine the Foxa1 binding. (D) An oligonucleotide (mPSA1, Table 2-1 for sequence) containing both ARE III and a mutant Foxa1 motif shows similar binding intensity with a purified GST AR-DBD protein in EMSA.

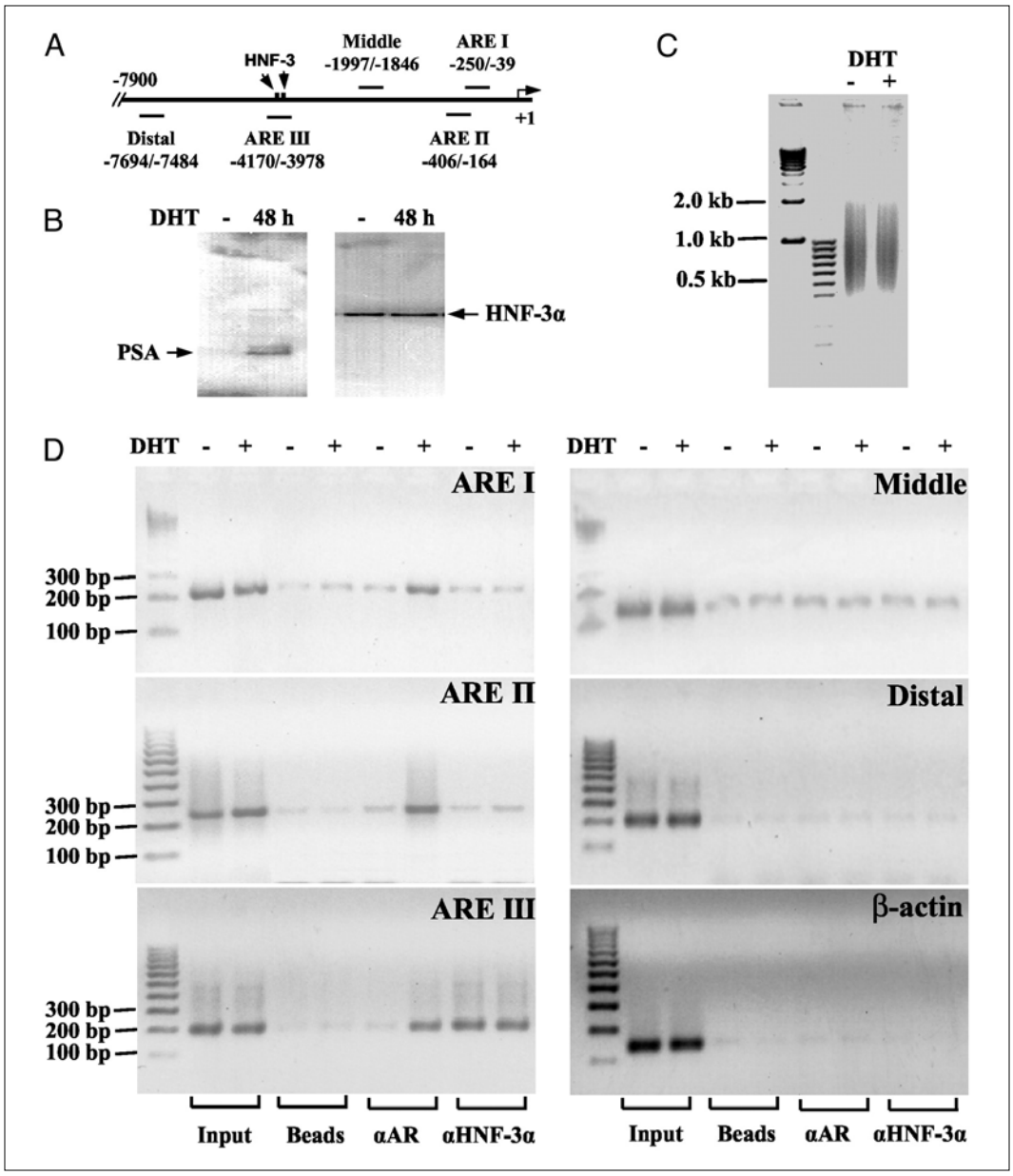

Figure 3-11. Foxa1 (HNF-3α) binds PSA Enhancer *in vivo*. (A) Schematic diagram of PSA gene 5'-upstream region. Six DNA fragments corresponding to the distal, ARE III, middle, ARE II, and ARE regions were amplified in ChIP assays using primers described previously. (B) LNCaP cells were initially grown in RPMI 1640 with 5% charcoal/dextran-treated fetal bovine serum for 3 d. Cells were then incubated for another 48 h with or without 10^{-8} M DHT treatment. Western blot was performed to determine the expression levels of PSA and Foxa1. (C) Formaldehyde-cross-linked chromatins were sheared by sonication into an average size of 0.5–1.0 kb. (D) After an overnight IP with AR or Foxa1 antibodies, formaldehyde cross-linking was reversed, and DNA fragments were extracted, followed by PCR amplification (Materials and Methods).

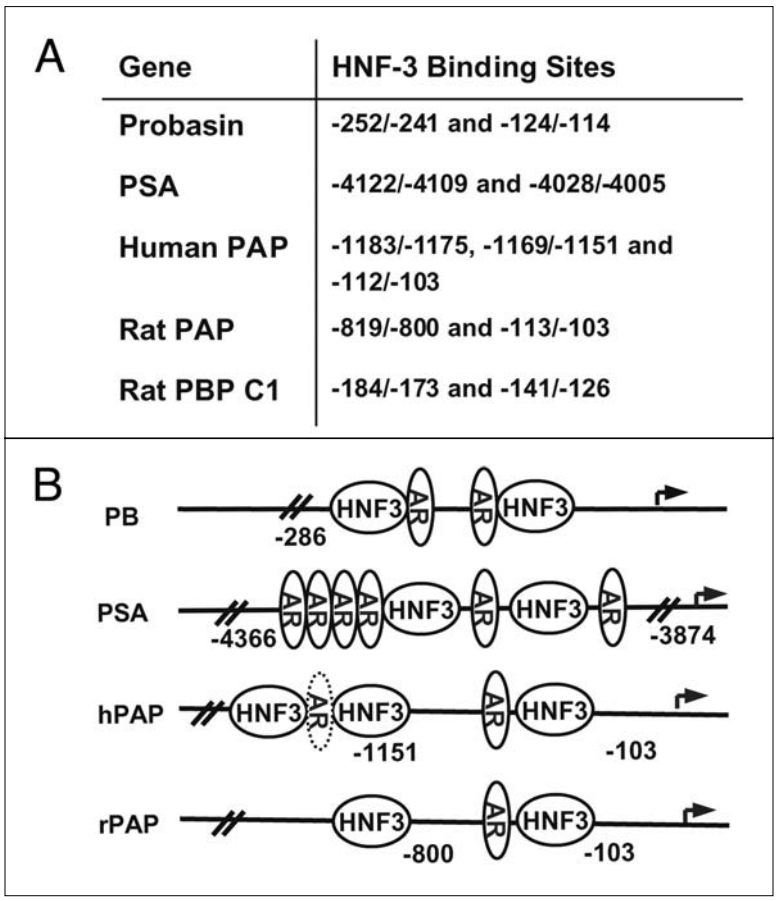

Figure 3-12. Similar organization of forkhead and androgen response elements in prostate-specific gene enhancers. (A) A summary of Foxa1 (HNF-3α) binding motifs identified in prostate-specific enhancers. (B) Schematic diagram showing remarkable similarity in the organization of AR and Foxa1 binding motifs in different prostate-specific gene regulatory regions.

CHAPTER IV

FOXA1 (HNF-3α) PHYSICALLY INTERACTS WITH ANDROGEN RECEPTOR

Introduction

Steroid receptors play a pivotal role in transcriptional control of numerous genes. In addition to acting via specific steroid response DNA elements, steroid receptors interact with many co-regulators as well as other DNA-binding transcription factors (Heinlein and Chang, 2002).

The cross-modulations between androgen and other pivotal signaling pathways through the direct interaction between AR and several sequence-specific transcription factors have been well-documented. Some of these AR-interacting proteins are essential mediators of other crucial intracellular signaling pathways. The overall effects of such cross-modulation from growth factors or cytokine signaling may result in altered transcriptional activity of AR, providing opportunities for tissue-specific or environment-responsive gene expression.

AP-1 and NFκB are two of the best characterized AR-interacting transcription factors which play key roles in affecting AR transcriptional activity. In addition, AR has also been found to be directly interacting with STAT3 and Smad3, both of which are signal transduction mediators. In addition, AR can also interact with tissue specific transcription factors such as the testis-specific factor SRY, and the prostate-enriched ets factor PDEF and the T cell factor 4 (Amir et al., 2003).

It has been reported that GR-mediated activation of multiple liver-specific genes requires Foxa2 (HNF-3β) (Espinas et al., 1995; Stafford et al., 2001; Wang et al., 1999; O'Brien et al., 1995; Wang et al., 1996; Christoffels et al., 1998). Recent studies showed that ER interacts with three forkhead transcription factors, FKHR, FKHRL1 and AFX (Schuur et al., 2001; Zhao et al., 2001). AR is a member of the steroid receptor family and shares many similarities with GR and ER in terms of structure and mechanism of function. The observation of close proximity of AR and Foxa1 (HNF-3α) binding sites in various gene promoters prompted us to examine if these two proteins can interact with each other.

Results

A. Foxa1 Precipitates with AR

Co-Immunoprecipitation (Co-IP) was performed in an AR-Hela cell line (Huang et al., 1999), in which a flag-tagged full-length AR was stably integrated. Since Hela cells do not express Foxa1 (Fig. 3-4C), we transfected a Foxa1 mammalian expression vector (pcDNA3.1D/V5-Foxa1) and a control LacZ expression vector (pcDNA3.1D/V5-LacZ) into these cells. Western blot using anti-V5 confirmed the expression of V5-tagged LacZ and Foxa1 proteins in transfected cells (Fig. 4-1A, lanes 3, 4 vs. 1, 2). Cells were grown in medium with 10-8 M DHT. All cell lysates were immunoprecipitated with anti-flag M2 affinity gel in the presence of ethidium bromide (EB, 0-100 μg/ml), which was used to disrupt DNA/protein interactions (Lai and Herr, 1992). The gel was washed prior to Western blot analysis. As seen in Fig. 4-1B, flag-AR was detected in all AR-Hela precipitates (lanes 6-10) in contrast to normal Hela precipitate (lane 5). Only Foxa1 (lane

14-16) but not LacZ (lane 13) was detected in the AR-Hela precipitates, indicating that flag-AR specifically immunoprecipitates with Foxa1. Importantly, this interaction was resistant to the presence of EB (lanes 15 and 16), ruling out the possibility that it was mediated through DNA.

B. Endogenous Foxa1 Physically Interacts with AR

Since the IP experiment in AR-Hela cells was performed in a condition where both Foxa1 and AR are overexpressed, the observation may not reflect a physical situation. Since LNCaP cells expressed both proteins, Co-IP was performed in LNCaP cells to examine this interaction in a physical circumstance where AR and Foxa1 proteins are expressed at endogenous levels. LNCaP cells were either grown in androgen-depleted medium for at least 3 days or grown in the presence of 10^{-8} M DHT. Cell lysates (1 mg per IP reaction) were immunoprecipitated with anti-AR-conjugated protein G-sepharose beads in the presence of EB. Similar IP were performed using Foxa1 antibody instead of anti-AR. Each reaction was performed in the presence of 1% NP-40 and 1 mg BSA to quench the non-specific binding. Fig. 4-1B unambiguously demonstrated a physical interaction of AR and Foxa1 in DHT-treated cells in contrast to androgen-depleted condition. This interaction was resistant to the presence of EB at a concentration of 100 μg/ml, demonstrating a direct protein/protein interaction (Fig. 4-1B). These IP experiments strongly suggested that AR and Foxa1 are involved in the assembly of a multi-nucleoprotein complex.

C. Responsible Domains for AR/Foxa1 Interaction

In vitro GST pull-down assay was performed to confirm the AR/Foxa1 interaction as well as to determine the interacting regions. A full-length Foxa1 protein labeled with a

C-terminal V5 epitope was synthesized *in vitro*. Five GST-AR fusion proteins containing different AR subdomains (Fig. 4-2A) were purified as described before (Snoek et al., 1996). Fig. 4-2B is a GST pull down experiment showing that the AR DBD/hinge region (524-649 amino acids) alone is sufficient to mediate the interaction with Foxa1. Experiments were repeated at least five times.

In the experiments, the ARNT/DBD showed a weaker interaction with Foxa1 as compared with ARDBD/Hinge or ARDBD/LBD (Fig. 4-2B), suggesting AR N-terminal might have a negative effect on the interaction. Although the biological relevance of this effect is currently unknown, this effect was obviously not due to the lower activity of ARNT/DBD protein, since it bound to ARBS-1 sequence (on Pbsn promoter) with a similar extent as ARDBD/Hinge or ARDBD/LBD on a molar basis (Fig. 4-2C).

In Fig. 4-2A and D, *in vitro* synthesized Foxa1 fragments were used to map the AR-interacting region(s) in Foxa1 protein. Most interestingly, the forkhead domain (amino acids 141-294) alone was sufficient to mediate a strong interaction with AR (Fig. 4-2D, lanes 13, 22 and 31), whereas the N- or C- terminal domain alone did not bind with AR. Fig. 4-2E demonstrates that the interaction between ARDBD/Hinge and Foxa1 forkhead domain was insensitive to the presence of EB (0-150 μg/ml), supporting a direct protein/protein interaction.

The ligand effect on this interaction was also examined (data not shown) and the results suggested that, under these *in vitro* conditions, the interaction between ARDBD/LBD and Foxa1 could occur without ligand. This was not surprising since in vitro purified GST-ARDBD/LBD fragment may not act identically as in vivo wild type AR, in terms of protein folding. Although these *in vitro* binding experiments cannot

exactly reflect the physical conditions, they identified responsible regions for AR/Foxa1 interaction.

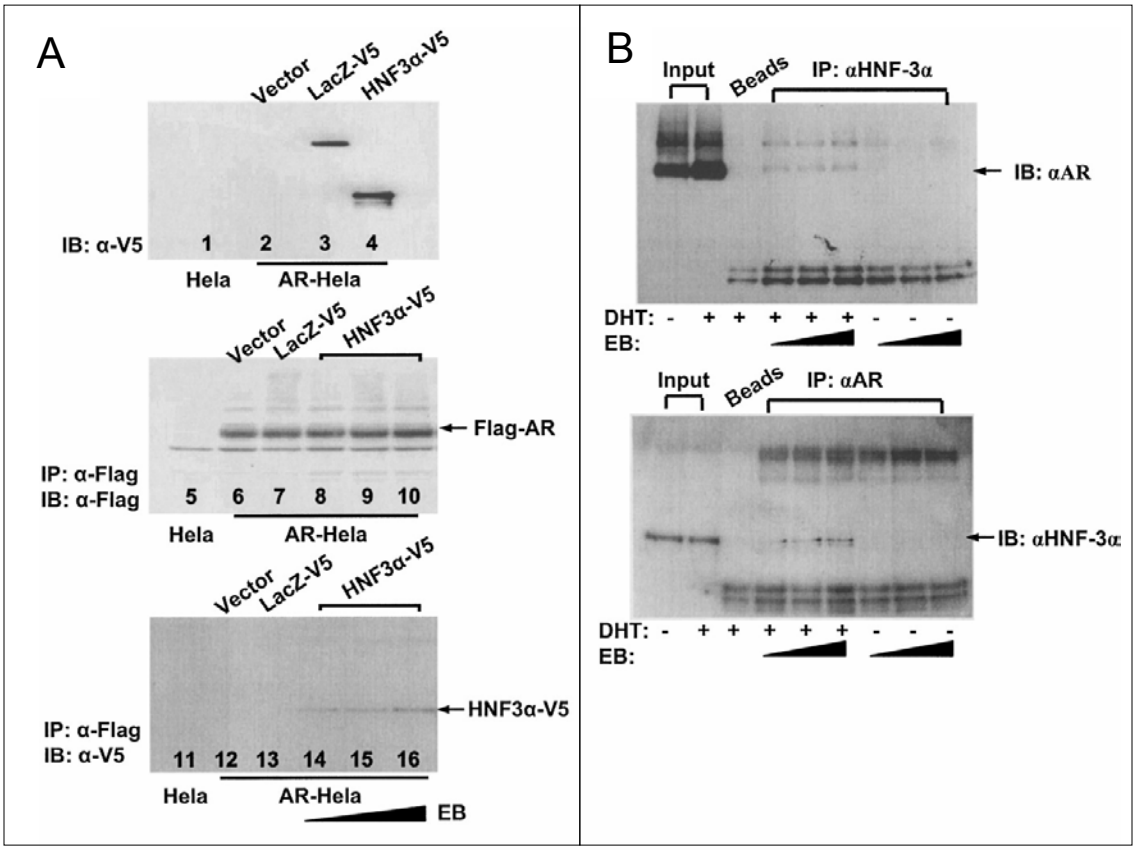

Figure 4-1. Foxa1 (HNF-3α) co-immunoprecipitates with AR. (A) AR-Hela cells, with stably integrated flag-AR, were transfected with an Foxa1 expression vector (pcDNA3.1D/V5-Foxa1) and a control LacZ expression vector (pcDNA3.1D/V5-LacZ). Western blot using anti-V5 antibody detected the V5-labeled LacZ (lane 3) and Foxa1 (lane 4) proteins in transfected cells, but not in nontransfected cells (lanes 1 and 2). All cell lysates were immunoprecipitated by an anti-flag M2 affinity gel in the presence of EB. The gel was washed before Western blot analysis. Anti-flag detected flag-AR in all AR-Hela cell precipitates but not in normal Hela cells (lanes 5 vs. 6–10). Anti-V5 detected Foxa1 (lanes 14–16) but not LacZ (lane 13) in AR-Hela precipitates. The AR/Foxa1 interaction was not affected in the presence of 25 μg/ml (lane 15) and 100 μg/ml (lane 16) EB. (B) LNCaP cell lysates (1 mg per IP) from DHT-treated or untreated cells were immunoprecipitated with Foxa1 or AR antibody in the presence of EB (0–100 μg/ml) as indicated. Western blot was performed using individual antibodies as indicated.

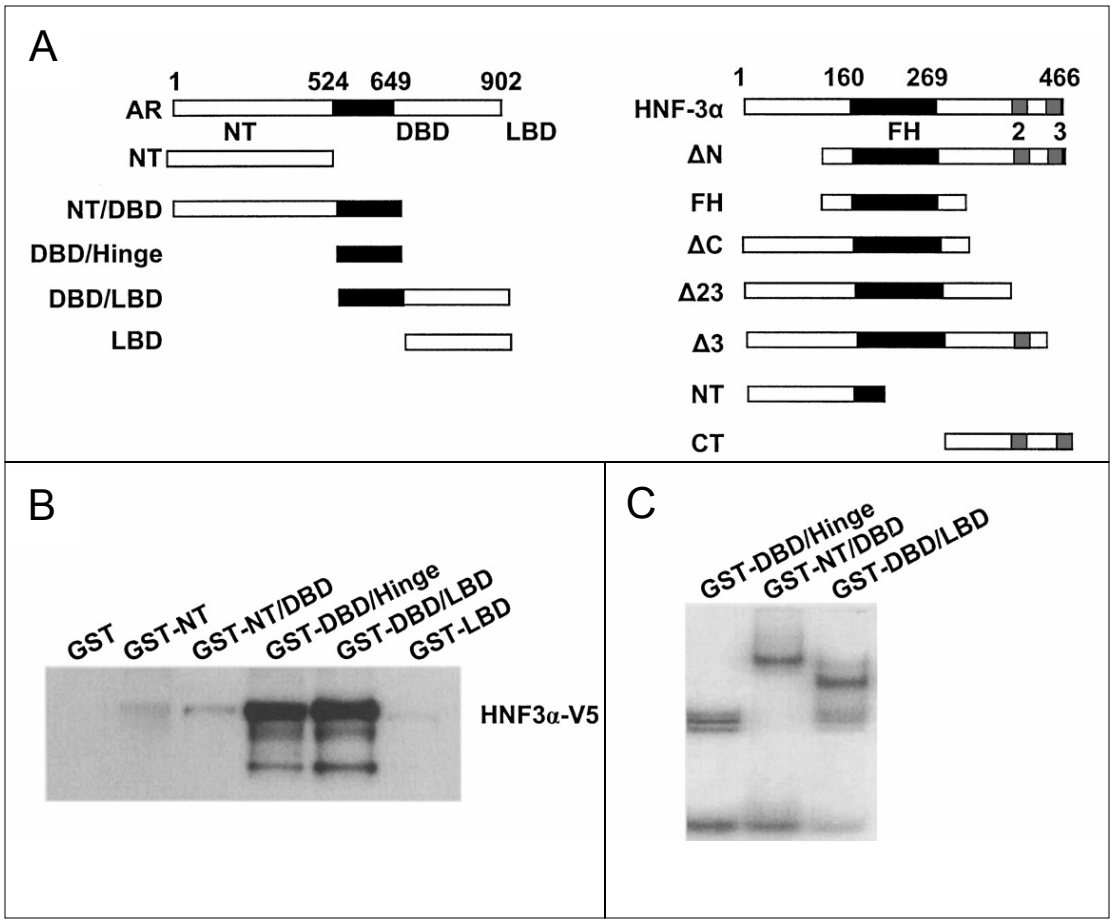

Figure 4-2. Mapping interaction domains by GST pull-down. (A) A schematic diagram showing a series of AR and Foxa1 (HNF-3α) subdomains used in in vitro GST pull-down assays. The AR DBD/hinge region and the Foxa1 FH domain are highlighted in black. Two conserved Foxa1 C-terminal domains designated as region 2 and 3 are in striped boxes. (B) Five purified GST-AR fusion proteins (20 μg for each) were bound to glutathione agarose beads, followed by incubation with V5-labled Foxa1 protein synthesized in vitro. Western blot was performed to determine the Foxa1-interacting domain in AR. (C) The GST AR fusion proteins DBD/Hinge (50 ng), NT/DBD (250 ng), and DBD/LBD (150 ng) were used in EMSA to determine their DNA binding activities with ARBS-1 on a molar basis. (D) The expression of eight V5-labeled Foxa1 subdomains as well as a LacZ protein was confirmed in Western blot (lanes 1–9). These proteins were in vitro synthesized and incubated with the GST-bound AR NT/DBD, DBD/Hinge, and DBD/LBD to determine the AR-interacting region in Foxa1. (E) The interaction of AR-DBD/Hinge and Foxa1 FH domain was resistant to the presence of 25–150 μg/ml of EB. LBD, Ligand-binding domain; NT, N-terminal domain.

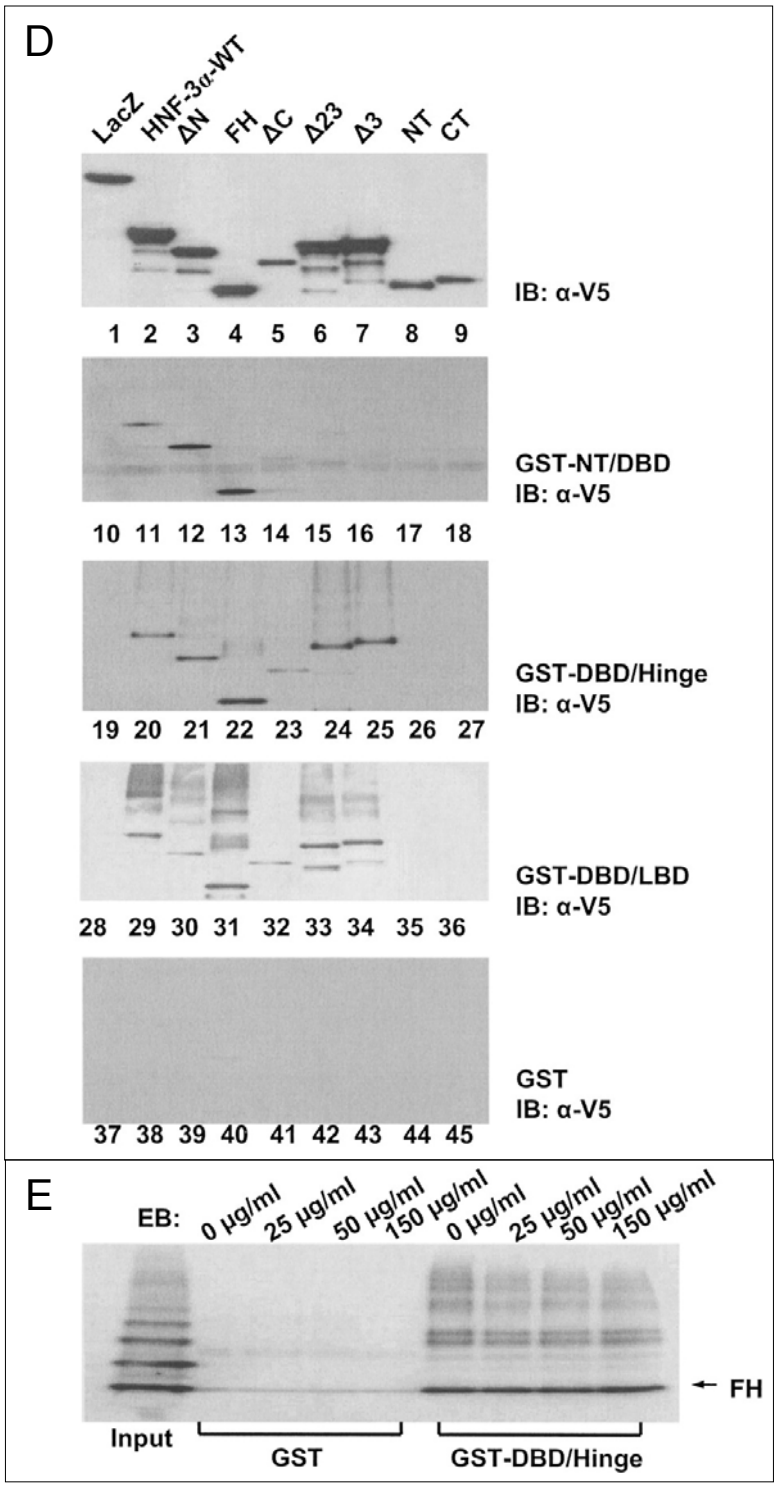

Figure 4-2 (continued).

CHAPTER V

FOXA1 IS ESSENTIAL FOR REGULATED PROSTATIC DUCTAL MORPHOGENESIS AND EPITHELIAL CELL MATURATION

Introduction

The impetus for studying the development of the prostate gland stems from the increasing incidence of diseases that affect it. The prostate is an exocrine gland composed of extensively branched ductal networks which develop from the embryonic urogenital sinus (UGS), a derivative of the hindgut (Cunha et al., 1987). In mice, at around embryonic day 18 (E18), the endoderm-derived urogenital sinus epithelium (UGE) invades into the surrounding urogenital sinus mesenchyme (UGM), forming the earliest prostatic epithelial buds. This initial morphological event is dependent on systemic androgens produced by the fetal testis (Cunha et al., 1987). The subsequent outgrowth of prostatic buds gives rise to a number of solid epithelial cords, in which immature progenitor cells co-express numerous cytokeratins (Ck), Ck5, Ck8, Ck14, Ck18, and other markers such as p63 (Wang et al., 2001). Prostate branching morphogenesis and cytodifferentiation occur postnatally (1-3 week) (Sugimura et al., 1986a). As the ducts branch and canalize, epithelial cells differentiate into two distinct cell populations, the luminal and basal cells, each expressing a subset of characteristic markers (Ck8 and Ck18 for luminal cells, Ck5, Ck14 and p63 for basal cells) (Wang et al., 2001; Hayward et al., 1996a). Prior to puberty, the serum levels of androgens rise and the luminal cells begin to produce secretory proteins characteristic of the different prostatic lobes: the anterior prostate (AP), the ventral prostate (VP) and the dorsolateral prostate (DLP). By sexual

maturation (6 weeks), secretions increase substantially as the serum androgen levels peak (Cunha et al., 1987).

Regulated interactions among key signaling pathways are prerequisite for organ development (Chuang and McMahon, 2003). Spontaneous and engineered gene inactivation in the mouse, combined with organ culture and tissue recombination, have highlighted the essential roles of androgenic signaling and epithelial-stromal interactions in directing prostatic development (Marker et al., 2003; Abate-Shen and Shen, 2000). In the absence of androgens or of androgen receptor (AR), the prostate does not develop (Bardin et al., 1973; Cunha et al., 1987). Tissue recombination experiments using Tfm mice provide direct evidence that the stromally-located AR is essential for eliciting many aspects of prostatic epithelial differentiation (Donjacour and Cunha, 1993). Thus, under normal conditions, the growth and differentiation of prostatic epithelium is controlled through androgen-regulated paracrine signaling from the mesenchyme (Cunha et al., 1987). Conversely, reciprocal paracrine signaling from the epithelium also patterns stromal cell differentiation (Cunha et al., 1996). Recently, emerging evidence suggested that the epithelial-mesenchymal interaction during early prostatic morphogenesis involves several conserved families of molecules, including the Sonic hedgehog (Shh) (Podlasek et al., 1999a; Lamm et al., 2002; Wang et al., 2003; Freestone et al., 2003; Berman et al., 2004), the Wnt (Yang et al., 2002), the Bone Morphogenetic Protein (Lamm et al., 2001), the Fibroblast Growth Factors (Thomson and Cunha, 1999; Donjacour et al., 2003), the Notch-Delta membrane molecule (Wang et al., 2004; Shou et al., 2001), and the Nkx3.1 homeobox protein (Bhatia-Gaur et al., 1999; Schneider et al., 2000; Tanaka et al., 2000).

The mechanism by which androgen and diverse signaling pathways are integrated during prostatic organogenesis is still under active investigation. For example, Shh signaling regulates prostatic ductal morphogenesis, while testosterone treatment of *in vitro* cultured mouse embryonic urogenital sinus (UGS) upregulated Shh activity (Podlasek et al., 1999a). However, androgen treatment of rat prostate at a postnatal stage did not affect Shh or Ptc1 expression while the addition of recombinant Shh to in vitro cultured prostates caused an expansion in the mesenchyme (Freestone et al., 2003). Treatment of the embryonic UGS with a neutralizing antibody (Podlasek et al., 1999a) or cyclopamine, a chemical blocker of Shh signaling, abrogated prostatic ductal budding (Lamm et al., 2002). Further, abnormal activation of Shh has been reported in various pathologic conditions including prostate cancer (Fan et al., 2004).

Signaling interactions could occur through different levels. In prostatic epithelial cells, β-catenin is a key transcriptional effector of Wnt signaling which mediates the interaction with androgen signaling by directly interacting with the ligand binding domain of AR and enhancing gene transcription (Yang et al., 2002). T cell factor 4, the downstream nuclear effector of Wnt/β-catenin signaling, also directly binds to the AR DNA binding domain and represses androgen signaling (Amir et al., 2003). Further evidence indicates that Wnt/β-catenin is required for endoderm formation (Logan et al., 1999; Imai et al., 2000; Rocheleau et al., 1997b; Stainier, 2002).. More recently, β-catenin was shown to interact with Sox17 to upregulate endodermal genes, including two forkhead proteins, Foxa1 and Foxa2 (Sinner et al., 2004).

Forkhead transcription factors play crucial roles in the development of various organs (Carlsson and Mahlapuu, 2002). The vertebrate endoderm expresses Foxa1, Foxa2,

and Foxa3, which are involved in the formation of the epithelial gut tube (Zaret, 1999; Zaret, 2002). A role for this class of genes in differentiation of the gut is a feature conserved in metazoan development: the Drosophila ortholog of Foxa, forkhead, is essential for the morphogenesis of the anterior digestive tract (Weigel and Jackle, 1990; Weigel et al., 1989); pha-4, the Foxa relative in C. elegans, specifies the cells of the pharynx (Gaudet and Mango, 2002; Kalb et al., 1998; Horner et al., 1998).

The mouse prostatic epithelium is derived from the embryonic hindgut endoderm and expresses Foxa1 and Foxa2 (Peterson et al., 1997; Kopachik et al., 1998; Mirosevich et al., 2004). Foxa1 is expressed during development and throughout differentiation, while Foxa2 is expressed only in the early prostatic ductal budding (Mirosevich et al., 2004). I have shown that Foxa1 functionally interacts with AR to enhance the transcription of multiple prostate-specific genes associated with secretory epithelial differentiation (Gao et al., 2003). However, the *in vivo* role of Foxa1 in earlier stages of prostatic development has not been established.

Several lines of evidence suggest that the expression of some mammalian forkhead genes is dependent on the Shh signaling pathway. Examples include Foxa2 in the floorplate of the neural tube (Chiang et al., 1996; Hynes et al., 1997), and the pharyngeal endoderm (Yamagishi et al., 2003), Foxc2 and Foxd2 in the presomitic mesoderm (Furumoto et al., 1999; Wu et al., 1998), and Foxf1 in lung and foregut mesenchyme (Mahlapuu et al., 2001). Studies suggested that the time course of Shh expression in normal prostate coincides with the formation of the main prostatic ducts, and the expression is down-regulated at the conclusion of prostate ductal development

(Podlasek et al., 1999a). However, a detailed cell-specific distribution and correlation of these key signaling molecules within developing UGS is currently unknown.

Transgenic mice with targeted gene inactivation have provided tremendous insights into the mechanisms that underlie organ development. Some genetically engineered mice, however, die at embryonic stages prior to prostatic development; hence functional assessments of such genes were prevented. Until now, only a few transcription factors have been reported to participate in prostatic development at the molecular level. *Nkx3.1* homeobox gene loss-of-function mutant mice are viable, and display reduced prostate ductal branching as well as progressive epithelial hyperplasia (Bhatia-Gaur et al., 1999; Schneider et al., 2000; Tanaka et al., 2000). Similarly, mice carrying single or compound mutations in a series of *Hox* genes (*Hoxa13*, *Hoxb13* and *Hoxd13*) have impaired prostate branching morphogenesis (Podlasek et al., 1999b; Warot et al., 1997; Economides and Capecchi, 2003). In contrast, a basal epithelial nuclear protein, p63, is thought to be critical for prostatic induction, since *p63*-deficient mice do not form prostatic buds and die at birth (Signoretti et al., 2000). Because p63 is not expressed in mesenchymal cells, the absence of prostatic induction must not be directly caused by mesenchymal signaling, but rather by defects in the UGE progenitor cells. Although these data provided important insights into some aspects of prostate development; they cannot fully explain the molecular mechanisms that control prostatic specification and differentiation.

In the mouse, *Foxa1* is first expressed in the definitive endoderm at the late primitive streak stage (E7-8) and later in endoderm-derived tissues (Sasaki and Hogan, 1993). *Foxa1* homozygous mutant mice die perinatally due to impaired glucose

homeostasis (Kaestner et al., 1999; Shih et al., 1999). Prior to the expression of *Foxa1*, *Foxa2* is expressed in the early primitive streak (E6.5), and later in the definitive endoderm, the notochord and the floor plate of the neural tube (Sasaki and Hogan, 1993). In contrast to Foxa1 deletion, homozygous inactivation of *Foxa2* results in a more severe phenotype which includes defective foregut morphogenesis and absence of the notochord (Weinstein et al., 1994).

Since Foxa1 interacts with AR to control genes associated with differentiation (Gao et al., 2003) and since Foxa2 expression correlated with early prostatic budding (Mirosevich et al., 2004), I hypothesized that Foxa1 and Foxa2 play essential but distinct roles in prostatic organogenesis. Here the impact of Foxa1 loss-of-function and haploinsufficiency on the development of mouse prostate was evaluated through two *in vivo* model systems: organ rescue and tissue recombination. Our findings established that Foxa1 regulates prostatic ductal morphogenesis, and controls epithelial cell organization, proliferation, and maturation. Altered epithelial-stromal patterning found in Foxa1-/- prostates is due at least in part to the hyperactivity of Shh and Foxa2, and the loss of Nkx3.1 signaling molecules in Foxa1-/- epithelial cells. Thus, through the identification of a cis-regulatory code, Foxa1 was revealed to be crucial for the prostatic organogenesis.

Results

A. Distribution of Foxa1, Foxa2, Shh, Ptc1, β-catenin and AR in embryonic UGS

Embryonic UGS is a simple tubular structure containing a multilayered endoderm-derived epithelium and a surrounding undifferentiated mesenchyme. Prostatic morphogenesis is initiated at embryonic day 17-18 (E17-18) in the mouse, with the

epithelium budding into the surrounding urogenital sinus mesenchyme (UGM) (Cunha et al., 1987). Fig. 5-1A shows an E18 mouse UGS. The entire urogenital sinus epithelium (UGE) is immunopositive for Foxa1. As expected, no positive staining was observed in UGM. The same section was stained for cytokeratin 14 (Ck14), a marker for basal epithelial cells (Fig. 5-1B). Both Ck14-positive and Ck14-negative epithelial cells express Foxa1 at similar levels (Fig. 5-1C). At the same time, prostatic sections from a six week old mouse were stained for Foxa1. Strong nuclear staining was observed in the mature glands (Fig. 5-1D), indicating that Foxa1 expression is elevated and maintained in all postnatal prostate epithelium.

Foxa2 immunoreactivity in E18 UGS was highest in the peripheral layers of basal epithelial cells immediately adjacent to the surrounding mesenchymal cells (Fig. 5-1E). Epithelial cells localized proximal to the urethral lumen were either unstained or weakly stained for Foxa2 (Fig. 5-1E). Dual staining revealed that Shh was co-expressed with Foxa2 (Fig. 5-1F, G) in the basal precursor cells which subsequently give rise to the nascent prostatic buds. This observation is consistent with the ability of Shh to induce Foxa2 expression (Sasaki et al., 1997).

To determine how Shh signal is transduced in embryonic UGS, we checked the expression of Patched1 (Ptc1), which is a transmembrane receptor for Shh and is a direct downstream target for Shh signaling. Fig. 5-1 H-J shows a double immunofluorescent staining for Shh and Ptc1 in an E21 mouse UGS. Expression of Shh was continuously detected in the UGE with strongest activity observed in the peripheral basal epithelial cell layer and in the newly formed prostatic epithelial buds (white arrow in Fig. 5-1I). Ptc1 and Shh were co-expressed in these cells (Fig. 5-1H and J). In addition to the UGE

compartment, Ptc1 was also detected in a mesenchymal cell population close, but not immediately adjacent to the UGE (Fig. 5-1H). Approximately ten-cell layers separate this stromal Ptc1-expressing cell population and the epithelial cell source of Shh. Such an arrangement is within the effective range of Shh signaling (Ingham and McMahon, 2001). Analysis of serial sections illustrated that this Ptc1-positive stromal cell population also expressed smooth muscle α-actin (SMA) (Fig. 5-1K), an early differentiation marker for smooth muscle cells and a direct mesenchymal target of Shh signaling (Weaver et al., 2003). Detection of Ptc1 in both UGE and UGM suggested that Shh can act in both a juxtacrine and a paracrine fashion in the UGS as in other organs such as the developing limb (Dillon et al., 2003).

AR is the classical mediator of androgen signaling in the UGS. AR staining in an E21 UGS demonstrated that all UGS cells, including the basal epithelium (Fig. 5-1L), were AR-positive. However, the intensity of staining was stronger in UGM as compared to UGE (Fig. 5-1K-L). Fig 5-1M shows that in E21 UGS, a proportion of the UGE co-expressed both the basal cell marker p63 and the luminal cell marker Ck8, indicating its immature status (Wang et al., 2001).

Staining was also performed to detect the localization of β-catenin, which, in cooperation with Sox 17, can promote Foxa1 and Foxa2 (Sinner et al., 2004). Staining for β-catenin detected specific membrane-localized signals in both UGE and the adjacent mesenchymal cells surrounding the epithelium (Fig. 5-1N). However, the strongest expression was seen in the p63-expressing peripheral basal epithelial cells (Fig. 5-1O-P).

Finally, using *in situ* hybridization, we show that Foxa1 continued to be expressed in the postnatal developing prostate (Fig. 5-1Q) and in adult glands (Fig. 5-1S). In

contrast, Foxa2 was strongly but transiently expressed only during prostatic induction (Fig. 5-1R), its expression decreased to undetectable levels in mature secretory glands (Fig. 5-1T).

Collectively, these data establish the temporal and spatial expression of crucial developmental proteins at the epithelial-mesenchymal interface where key signaling interactions could orchestrate prostatic organogenesis.

B. Foxa1 is essential for ductal morphogenesis

Conventional Foxa1 knockout mice have been generated using a targeting vector which deletes Foxa1 DNA-binding domain and creates an in-frame fusion with the Escherichia coli lacZ gene (Shih et al., 1999). The neonatal Foxal-/- mice die soon after birth, therefore the impact of Foxa1 loss-of-function on prostate development cannot be fully assessed. To circumvent this problem, we used two in vivo experimental strategies, renal capsule organ rescue (Wang et al., 2000b) and tissue recombination (Cunha and Donjacour, 1987).

Urogenital tracts were dissected from neonatal Foxa1 pups (n=64). Prostatic rudiments are visible in Foxa1-/- mice (n=13). Histologic analysis of postnatal day 1 (P1) prostates from control and Foxa1-/- mice did not show a detectable difference, indicating that prostatic induction occurs in Foxa1-/- mice. Viable prostate rudiments from these mice were rescued by renal capsule grafting to intact male athymic nude mice (Wang et al., 2000b). To ensure the integrity of the prostatic rudiments (asterisks in Fig. 5-2A), intact seminal vesicles, and a portion of the urethra were retained in the grafted tissue (region below the broken line in Fig. 5-2A). After 2-15 weeks, the host animals were sacrificed and prostates were removed from the graft site. Fig. 5-2B-D shows typical

examples of rescued organs developed in host renal capsule for 8 weeks. The Foxa1-/- prostates (asterisk in Fig. 5-2D) were consistently smaller and were solid while controls were enlarged and contained secretions (Fig. 5-2B, C). Rescued prostates and seminal vesicles were compared after fine dissections (lower panel in Fig. 5-2B-D). With the deletion of the Foxa1 allele, β-galactosidase expression occurs under control of the Foxa1 promoter. Staining detected the lacZ transgene expression in Foxa1+/- and Foxa1-/- prostate epithelium, but the abnormal epithelial cell organization was pronounced seen in the null (Fig. 5-2F, G).

Histological analysis of rescued prostates showed that, in contrast to controls, which developed a mature lumen lined with a monolayer of secretory luminal epithelium (Fig. 5-2I), age-matched null prostate developed solid epithelial cell cords with cribriform patterns (Fig. 5-2H). No normal-appearing lumen was observed in Foxa1-/- prostates (Fig. 5-2H). An identical phenotype was consistently observed in ventral, dorsolateral and anterior lobes of all rescued Foxa1-/- prostates (n=13).

Since AR signaling is pivotal in directing prostate development, we determined if loss of Foxa1 affects AR expression. Immunohistochemistry detected uniform nuclear AR staining in Foxa1-/- and control prostates (Fig. 5-2J-M). The results are consistent between different lobes (VP in Fig. 5-2J, K; DLP in Fig. 5-2L, M). Notably, when extending the rescue period up to 15 weeks, Foxa1-/- prostates show continuous growth of epithelial cords with no significant normal ductal canalization or luminal epithelial cell development (Fig. 5-2O) in contrast to control prostates (Fig. 5-2N).

As a complementary approach, tissue recombination experiments were performed using Foxa1+/+ and Foxa1-/- bladder epithelium from neonatal mice combined with wild

type embryonic E18 rat (r) UGM. Fig. 5-2P shows that recombinants, generated from Foxa1+/+ and Foxa1-/- epithelium, developed in the nude mouse renal capsule. The size and the wet weight of Foxa1-/- recombinants (n=15) are significantly smaller than control recombinants (n=15) even though the same number of rUGM cells were used (Fig. 5-2P-Q). Histological comparison revealed that the wild type inductive embryonic rUGM failed to elicit normal-appearing prostatic glandular morphogenesis in Foxa1-/- recombinants (Fig. 5-2R), as it did in age-matched wild type epithelium (Fig. 5-2S). Since wild type rUGM was used, the recombination experiments indicated that the abnormal growth in the null prostates is due to the loss of Foxa1 in the epithelium.

C. Foxa1 regulates epithelial-stromal patterning and epithelial cell maturation

To define this phenotype in Foxa1-/- prostates, we examined the distribution of distinct epithelial and stromal cell populations. Immunohistochemistry for the basal keratin Ck5 demonstrated that Foxa1-/- prostates contain a majority of basal epithelial cells (Fig. 5-3A). Under normal conditions in the mouse, mature prostate glands contain only a small proportion (around 10%, depending upon lobe) of basal cells as compared to luminal cells. Basal epithelial cells are normally organized into a discontinuous layer located between the luminal cells and the basement membrane (Fig. 5-3C). However, basal keratin-expressing cells become the predominant cell type in Foxa1-/- epithelium, and their location is extended into the epithelial cords (Fig. 5-3B). Staining tissue recombinants developed from Foxa1-/- (Fig. 5-3D) and control epithelium (Fig. 5-3E) revealed the same phenotype.

Since the structural alterations in the null prostates were strongly reminiscent of primitive epithelial cords, we performed double staining for p63 and Ck8, a nuclear basal

and cytoplasmic luminal cell marker, respectively. In normal prostatic development, basal and luminal markers are divided into each corresponding cell types as solid epithelial cords differentiate into distinct epithelial cell lineages (Wang et al., 2001; Hayward et al., 1996a). This is clearly illustrated in Fig. 5-3G showing that nuclear p63 (in green) and Ck8 (in red) were expressed by distinct epithelial cell populations in control samples. However, Foxa1-/- epithelium contained a large number of cells that co-expressed both markers (arrow in Fig. 5-3F). Epithelial cells with this expression profile can only be detected in undifferentiated UGE of normal embryo and in the solid epithelial cords of early developing prostate (Wang et al., 2001) (Fig. 5-1P). These results strongly suggested that Foxa1-/- epithelium is arrested at an immature precursor status and never matures even with prolonged grafting.

To better visualize cell types and morphology, dual staining was performed for AR and Ck14 on each prostatic lobe (Fig. 5-3H-M). In contrast to basal cells in Foxa1+/+ controls (Fig. 5-3I, K and M), Foxa1-/- basal cells were enlarged, expressed AR and formed a continuous layer surrounding the epithelial cords (Fig. 5-3H, J and L).

Given that loss of Foxa1 led to a failure of the prostatic epithelium to mature it seems likely that stromal patterning, which itself is dependent upon epithelial differentiation (Cunha et al., 1996), would also be abnormal (Fig. 5-3N). Immunohistochemistry for SMA revealed an extensive expansion in the smooth muscle layer surrounding the Foxa1-/- epithelial cords (Fig. 5-3N, O), suggesting mesenchymal hypercellularity. Age-matched normal prostate glands showed a very slender layer of smooth muscle surrounding the ductal epithelium (Fig. 5-3P). Interestingly, tissue recombinants composed of Foxa1-/- epithelium and wild type UGM show a similar

expansion in smooth muscle cells (Fig. 5-3Q) in contrast to control recombinants (Fig. 5-3R). These data suggest that the Foxa1-/- epithelium is capable of inducing abnormal mesenchymal proliferation and patterning, probably through altered epithelial-stromal signaling. To further determine the differentiation status of this smooth muscle layer, we examined the expression of γ-actin, which is a late marker of smooth muscle differentiation. Fig. 5-3S and T shows that smooth muscle cells in both control and null recombinants express γ-actin indicating that although altered paracrine signaling from Foxa1-/- epithelium elicited abnormal stromal patterning, nevertheless smooth muscle differentiation was complete.

Importantly, we detected a haploinsufficient phenotype from the heterozygous DLP of sexually mature mice, with abnormal ductal structure (Fig. 5-4B) and increased basal epithelial cells (Fig. 5-4D). This milder but similar histological abnormality confirmed that the grafting studies accurately reflected the natural consequences of the loss of Foxa1.

D. Foxa1 is essential for luminal cell determination

As prostatic branching morphogenesis and ductal canalization occur, immature epithelium differentiates. Under the direct stimulation of androgens, luminal cells produce prostate-specific secretory proteins such as Pbsn (Kasper and Matusik, 2000). Transmission electron microscopy provides an unbiased way to identify secretory features at the ultrastructural level (Sahlen et al., 2002). Electron microscopy analysis of luminal epithelial cells from 12-week wild type ventral prostate show tall columnar shapes (Fig. 5-5A), enlarged Golgi complexes, and numerous dense secretory materials, the prostasomes (Sahlen et al., 2002), within apical vesicles or at luminal surfaces

(arrows in Fig. 5-5C). These ultrastructural features, which signify secretory activity, are almost completely absent in age-matched Foxa1-/- epithelial cells (Fig. 5-5B, D).

We further analyzed the expression of prostate-specific luminal markers at both a protein and the mRNA level. Imaging Mass Spectrometry (IMS) employing MALDI-TOF analysis of hundreds of 50 μm spots (approximately a five cell width) on frozen tissue sections was used to obtain a representative protein profile of low molecular weight proteins. IMS has been previously used for profiling mouse prostate secretory proteins (Chaurand et al., 2001; Chaurand et al., 2004). Fig. 5-5E shows protein profiles obtained from 4-week rescued ventral prostates of Foxa1+/+, Foxa1+/- and Foxa1-/- genotypes. Peaks at mass to charge (m/z) 18441 and 24781 (denoted by arrows), consistent with the molecular weight of Pbsn (18-kDa) and prostate spermine binding protein (Sbp, 25-kDa) (Chang et al., 1987), were detected in Foxa1+/+ and Foxa1+/- prostates, but absent in Foxa1-/- prostates. Similar profiles were obtained from 12-week rescued prostates, indicating no change in secretory profiles with prolonged grafting.

Based upon these results, semi-quantitative RT-PCR was performed. Pbsn mRNA was completely undetectable while Sbp is dramatically decreased in Foxa1-/- prostates compared to controls (Fig 5-5F). We have reported the critical role for two forkhead response elements in directing Pbsn promoter activity (Gao et al., 2003). However, in this study, Sbp was identified as novel Foxa1 target. To investigate this finding we examined the Sbp promoter and identified two forkhead binding sites immediately flanked by two individual androgen response elements (Fig. 5-6A), a similar arrangement to that seen in other androgen-driven prostate-specific gene enhancers (Gao et al., 2003). These binding sites were experimentally confirmed by EMSA (Fig. 5-6B), strongly supporting the idea

that Foxa1 is essential for both the expression of a wide variety of secretory proteins in the prostate and for the differentiation of luminal cells.

E. Activation of Shh and Foxa2 in Foxa1-/- prostate leads to epithelial hyperproliferation and stromal expansion

The phenotype seen in Foxa1-/- prostates indicated altered epithelial-mesenchymal interaction. To explore this defect at a mechanistic level, we examined the potential signaling pathways that may attribute to this abnormality. Given that Shh signaling is important in prostatic ductal morphogenesis, we first examined Shh and Ptc1 expression by immunofluorescent staining of rescued Foxa1-/- prostates. Strong and focused Shh expression was detected in Foxa1-/- epithelial cell cords (Fig. 5-7A) and Shh-positive ductal epithelial buds were evident (Fig 5-7B). The same epithelial cell buds were positive for Ptc1 staining (Fig. 5-7C). Detection of epithelial Ptc1 in normal neonatal prostatic ductal tips has been reported recently (Pu et al., 2004). No focused staining for Shh and Ptc1 was observed in age-matched wild type prostates. By comparing the staining for SMA (top two arrows in Fig. 5-3N), which was performed on a serial section, we noted that the Shh-expressing epithelial cell buds (denoted by arrows in Fig. 5-7B) are surrounded by a thick smooth muscle layer. Since SMA is a mesenchymal target of Shh signaling, these data suggest that the localized Shh signal produced by Foxa1-/- epithelium may contribute to the altered epithelial-stromal interaction.

We have shown that Foxa2 is transiently expressed in UGE and nascent prostatic epithelial buds (Fig. 5-1R), and that Foxa2 expression correlates with Shh (Fig. 5-1E-G). To examine Foxa2 expression in Foxa1-/- epithelium, immunohistochemistry was performed on serial sections, and Foxa2 nuclear staining was detected in most of the

Foxa1-/- epithelial cells (Fig. 5-7D). Strong Foxa2 expression was seen in epithelial buds where Shh was present (Fig. 5-7E). Foxa2 positive cells formed numerous microlumen with cribiform patterns (denoted by arrows in Fig. 5-7F). These changes are consistent with the epithelial hyperproliferation in Foxa1-/- prostate. A continuous expansion of Foxa2-expressing cells was observed in rescued Foxa1-/- prostates with extended rescue period of 15 weeks (Fig. 5-7G). Age-matched control prostates, consistent with previous reports (Kopachik et al., 1998; Mirosevich et al., 2004), show complete negative staining for Foxa2 (Fig. 5-7H). We confirmed these observations in tissue recombination experiments. The Foxa1-/- recombinants show many tiny epithelial buds that contain Foxa2-positive cells (arrows in Fig. 5-7I and J), suggesting Foxa2 expression closely correlates with epithelial cell proliferation and budding, a role consistent with its expression pattern during embryonic UGE proliferation (Fig. 5-1E).

Nkx3.1 is a prostate-specific homeobox gene which has been reported as the earliest known marker for prostate development (Bhatia-Gaur et al., 1999). Nkx3.1-/- mice display progressive epithelial cell hyperplasia in the prostate (Bhatia-Gaur et al., 1999; Schneider et al., 2000; Tanaka et al., 2000). The hyperproliferation in Foxa1-/- epithelium is more severe than in Nkx3.1-/-mice. Thus, we examined Nkx3.1 expression in Foxa1-/- prostates. Fig. 5-7K shows Nkx3.1 staining on a section adjacent to the area in Fig 5-7B, showing Shh staining. No nuclear staining was observed in the Foxa1-/- epithelial cells that express Shh and Foxa2, while strong nuclear staining was detected in rescued control prostates (Fig. 5-7L). These data suggest that Nkx3.1 may be a downstream target of Foxa1.

The cross talk between β-catenin and the androgen pathway have been well-documented (Yang et al., 2002). Activation of β-catenin nuclear signaling has been implicated in abnormal prostate epithelial cell growth (Bierie et al., 2003; Cheshire and Isaacs, 2003). To determine whether nuclear translocation of β-catenin contributes to the epithelial cell disorganization, we examined β-catenin expression. Double immunofluorescent staining for β-catenin and p63 (Fig. 5-7M and N) did not suggest an increased nuclear level of β-catenin in the basal cells in Foxa1-/- prostate. Instead, β-catenin signals are still appropriately localized to the cell membrane in both the null and control cells (Fig. 5-7N and O).

Although Foxa1-/- epithelial cells generally showed a loss of cell polarity and organization (Fig. 5-7N vs. O), the epithelium did not develop into dysplasia or cancer even at prolonged rescue periods. Ki67 staining suggested an overall increase of proliferating cells in Foxa1-/- prostates (Fig. 5-8B), while the ratio of Ki67-positive cells to negative cells did not suggest a significant change when compared to controls (Fig. 5-8A). Foxa1-/- epithelial cells also express normal levels of adhesion molecules such as the E-cadherin (Fig. 5-8C and D). These data suggest that the abnormal morphogenesis observed in Foxa1-/- prostate results from failure of the epithelium to differentiate and the altered epithelial-mesenchymal interaction.

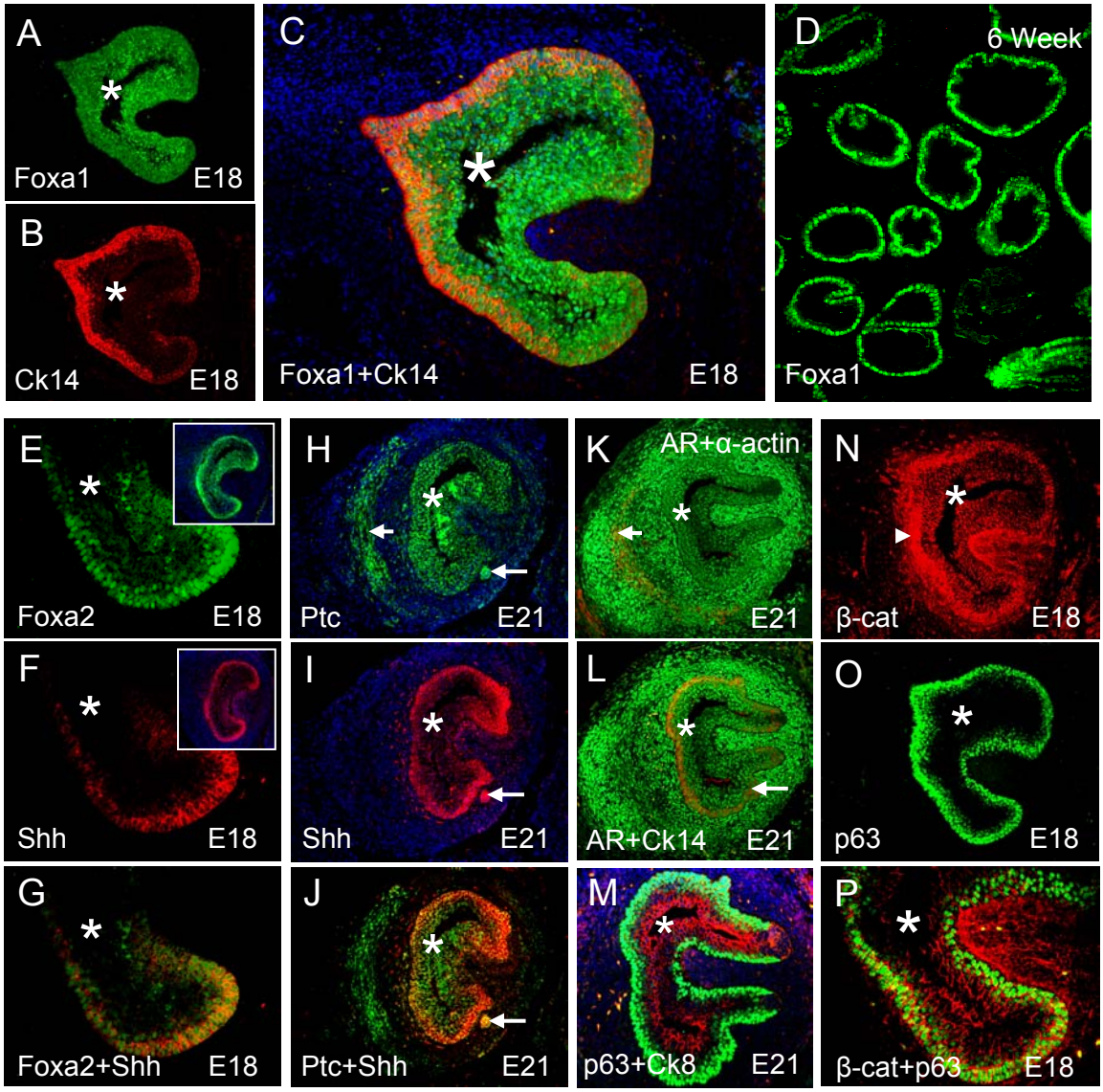

Figure 5-1. Distribution of key developmental factors in prostatic morphogenesis. (A) E18 UGS shows Foxa1 expression (green) in the entire UGE (asterisk). (B) Same section dual-stained for Ck14 (red) reveals a peripheral basal epithelial layer. (C) Triple immunofluorescence merged from A, B and DAPI nuclear counterstaining (blue). (D) Strong nuclear Foxa1 staining was detected in 6-week mature prostate. (E) E18 UGS expresses Foxa2 (nuclear signal in green) with strongest level in peripheral epithelial layer. Inset shows the entire UGS counterstained with DAPI. (F) Same section double-stained for Shh reveals a distribution pattern that overlaps with Foxa2. The Shh (red) is localized at cell-membrane. (G) Merged image from E and F. (H) In E21 UGS, Ptc1 (green) was detected in both epithelium (asterisk) and mesenchyme (short arrow). Ptc1 is also detected in nascent prostatic buds (long arrow). (I) Same E21 section shows exclusively epithelial staining for Shh (red). (J) Merged from H and I.

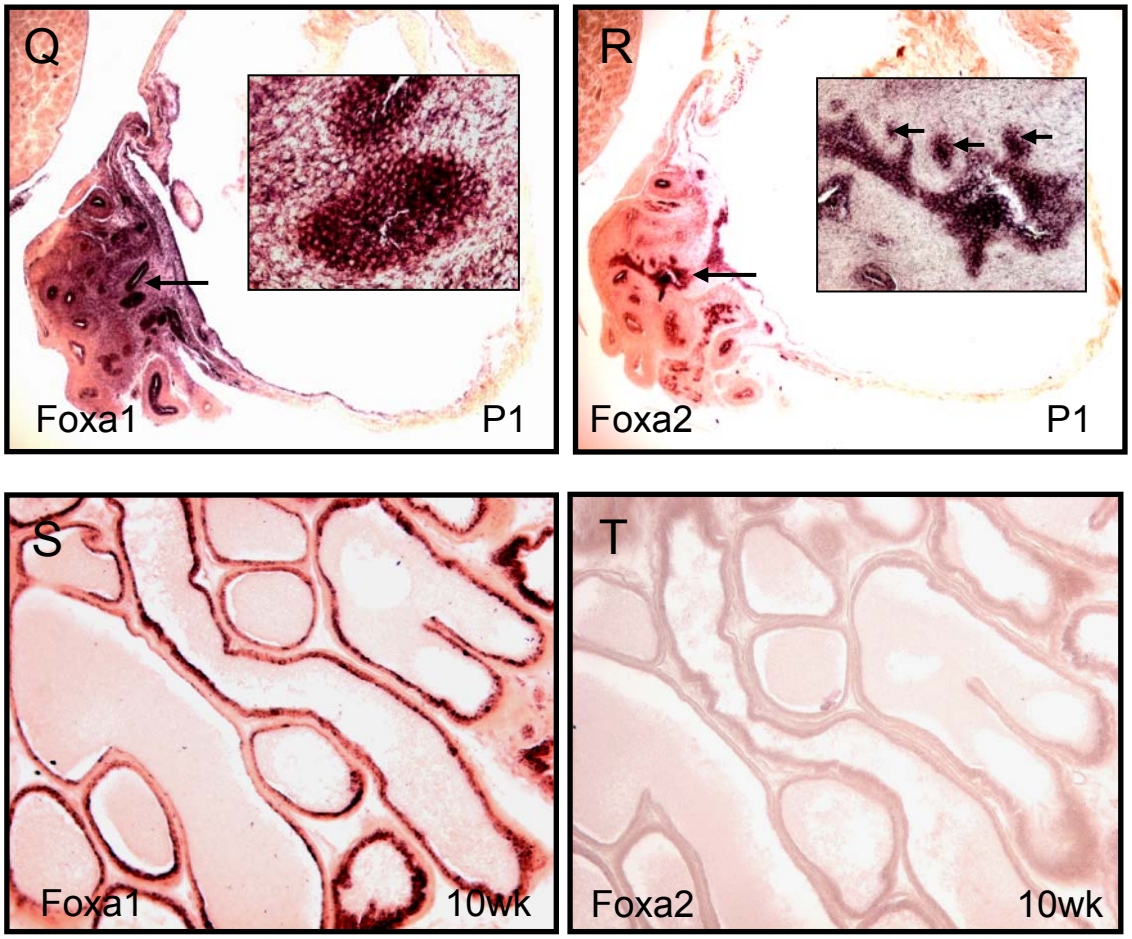

Figure 5-1 (continued). (K) E21 UGS double-stained for AR (green) and smooth muscle α-actin (SMA) (red). The SMA-expressing cells are the same cell population expressing Ptc1 (short arrow). (L) E21 UGS double-stained for AR (green) and Ck14 (red). Arrow depicts the budding epithelium. (M) E21 UGS double-stained for luminal Ck8 (red) and basal nuclear protein p63 (green). (N) E18 UGS shows β-catenin expression (red) in both epithelium and the adjacently surrounding mesenchyme, with strongest signal in the peripheral epithelium (arrowhead). (O) Same E18 section is double-stained for the basal nuclear protein p63. (P) Magnified image merged from N and O. (Q-R) In situ hybridization of Foxa1 and Foxa2 in neonatal prostatic rudiments. Inset magnifies the strongly positive epithelial buds. (S) Foxa1 is maintained in mature prostate gland. (T) In contrast, no Foxa2 transcript is detected in mature prostate gland.

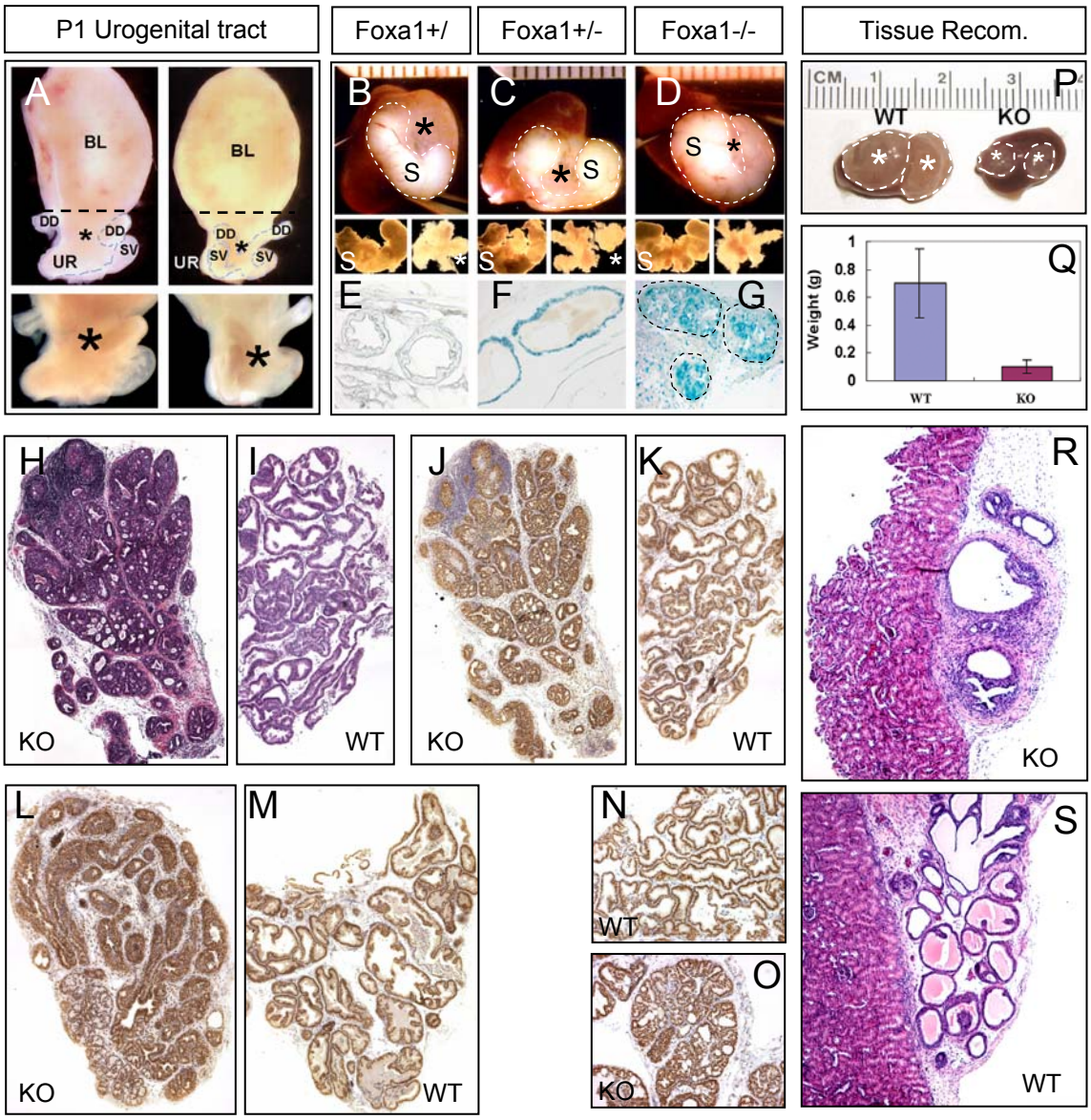

Figure 5-2. Foxa1 regulates prostatic morphogenesis. (A) Upper panels are P1 urogenital organs in lateral and dorsal views. Asterisks indicate the prostatic rudiments. Broken lines indicate where the bladder (BL) was removed. The remaining tissues (lower panels) containing prostatic rudiments and seminal vesicles (SV) were grafted into the renal capsules of nude mice. (B-D) Upper panels show rescued tissue developed in host renal capsules with indicated genotypes. Foxa1-/- prostate (asterisk) is smaller than controls. SVs are depicted with dotted lines and show no comparable difference. Lower panels show SVs and prostates after dissection. (E-G) β-galactosidase staining for rescued prostates. (H-I) Histology of age-matched Foxa1-/- and control prostates. (J-K) AR staining of Foxa1-/- and control ventral prostates. (L-M) AR Staining of Foxa1-/- and control dorsolateral prostates. (N-O) AR staining for control and Foxa1-/- prostates with extended rescue period up to 15 week. (P) Tissue recombinants derived from wild type (left) and Foxa1-/- (right) epithelium, combined with equal number of rat E18 urogenital mesenchymal cells. (Q) Foxa1-/- recombinants show significantly lower wet weight compared to controls ($P<0.01$). (R-S) Histology of age-matched Foxa1-/- and wild type tissue recombinants.

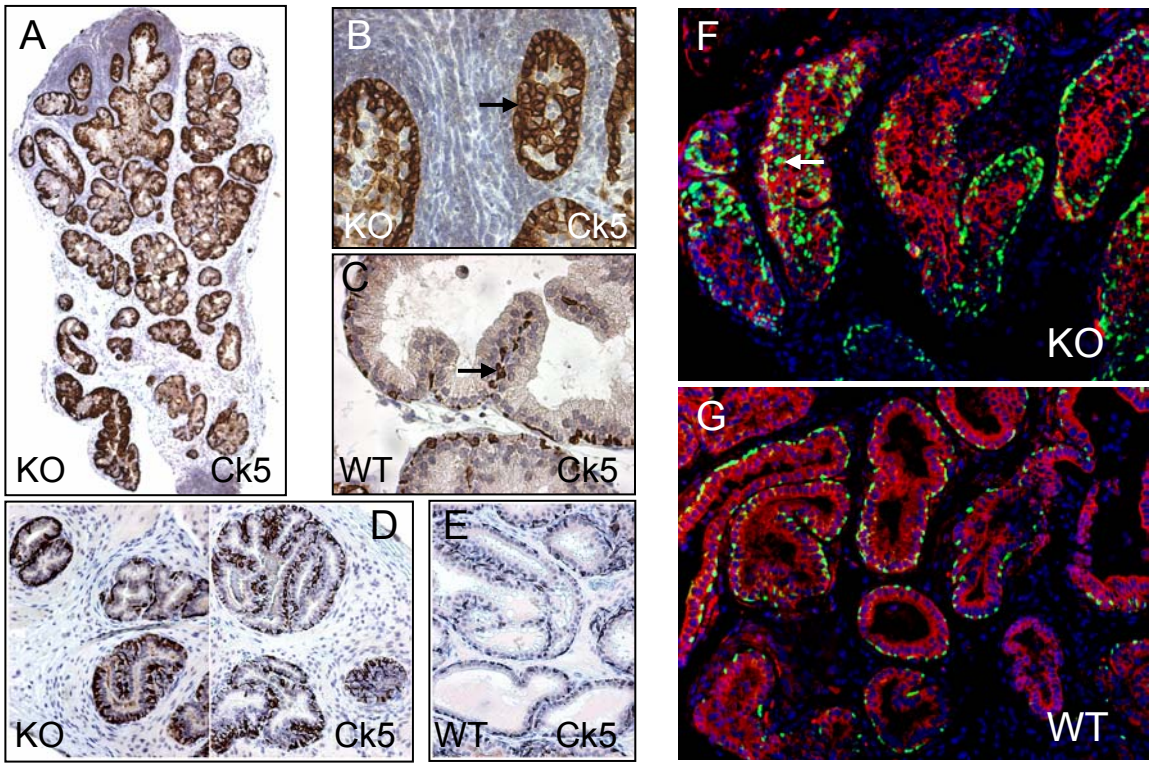

Figure 5-3. Foxa1 is critical for prostatic epithelial and stromal patterning. (A) Ck5 staining in Foxa1-/- prostate. (B) High magnification shows basal epithelial cells (arrow) within the epithelial cords. (C) Less basal cells in control prostate. (D-E) Ck5 staining for Foxa1-/- and control tissue recombinants. (F) Foxa1-/- epithelial cells co-express both p63 (green) and Ck8 (red), indicating immature differentiation status. (G) Two markers are separated into distinct cell population in wild type epithelium.

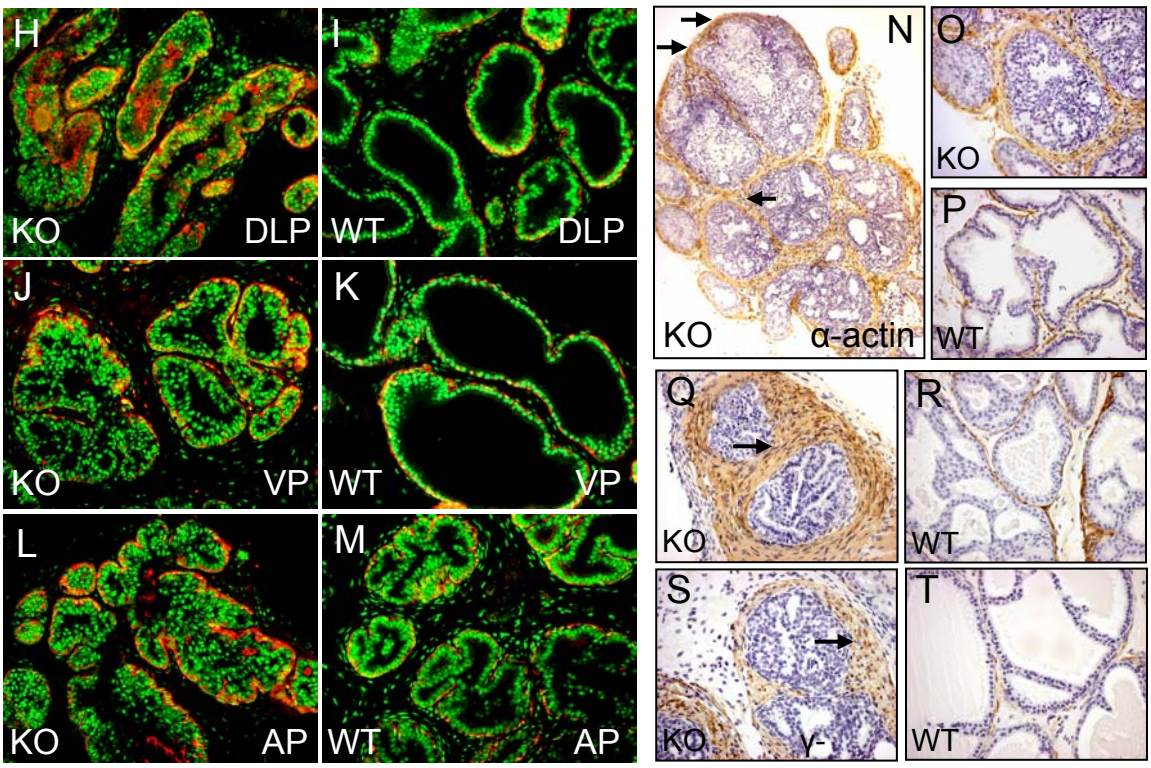

Figure 5-3 (continued). (H-M) Different lobes of rescued Foxa1-/- and Foxa1+/+ prostates were double-stained for Ck14 (red) and AR (green). (N-P) SMA staining (arrows) suggested an expended smooth muscle cells in Foxa1-/- prostate (N-O), in comparison with wild type prostates (P). (Q-R) Tissue recombinants stained for SMA. (S-T) Tissue recombinants stained for γ-actin.

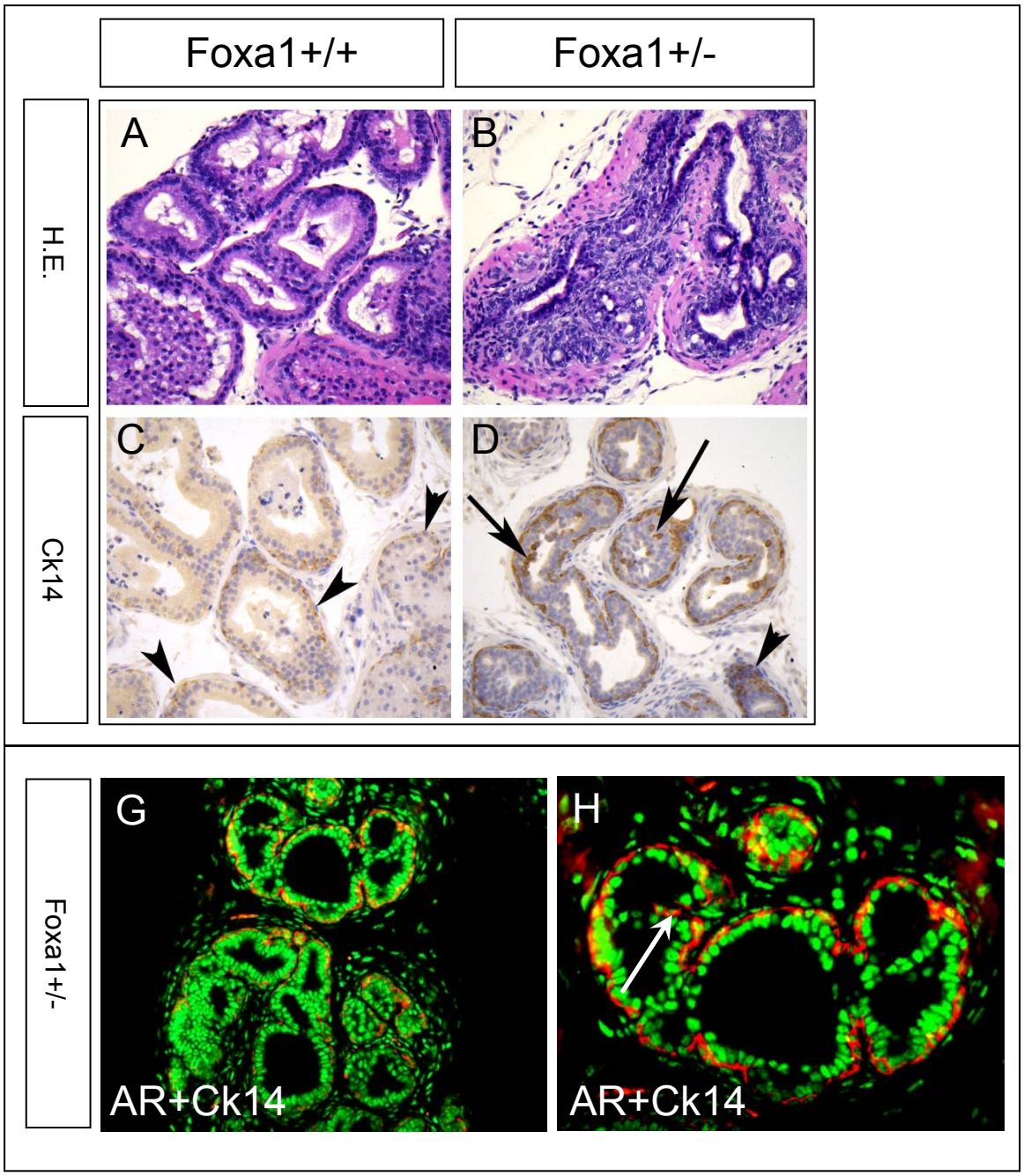

Figure 5-4. Foxa1 haploinsufficiency results in a minor phenotype in DLP. (A-D) Sexually mature dorsal prostate (H&E in Panel A,B, and basal cytokeratin 14 in Panel C,D) from wild type (Foxa1+/+) and heterozygous (Foxa1+/-). The dorsal heterozygous shows hyperproliferation and abnormal ductal development (B & D), indicating haploid insufficiency can result in a phenotype. Arrowheads point to basal cells which show hyperproliferation in the dorsal heterozygous (D) prostates. Arrows point to basal cells within the lumen. (G-H) Rescued Foxa1+/- dorsal prostate shows an increase in basal epithelial cells (arrow in H) and a mild phenotype of ductal morphogenesis (G).

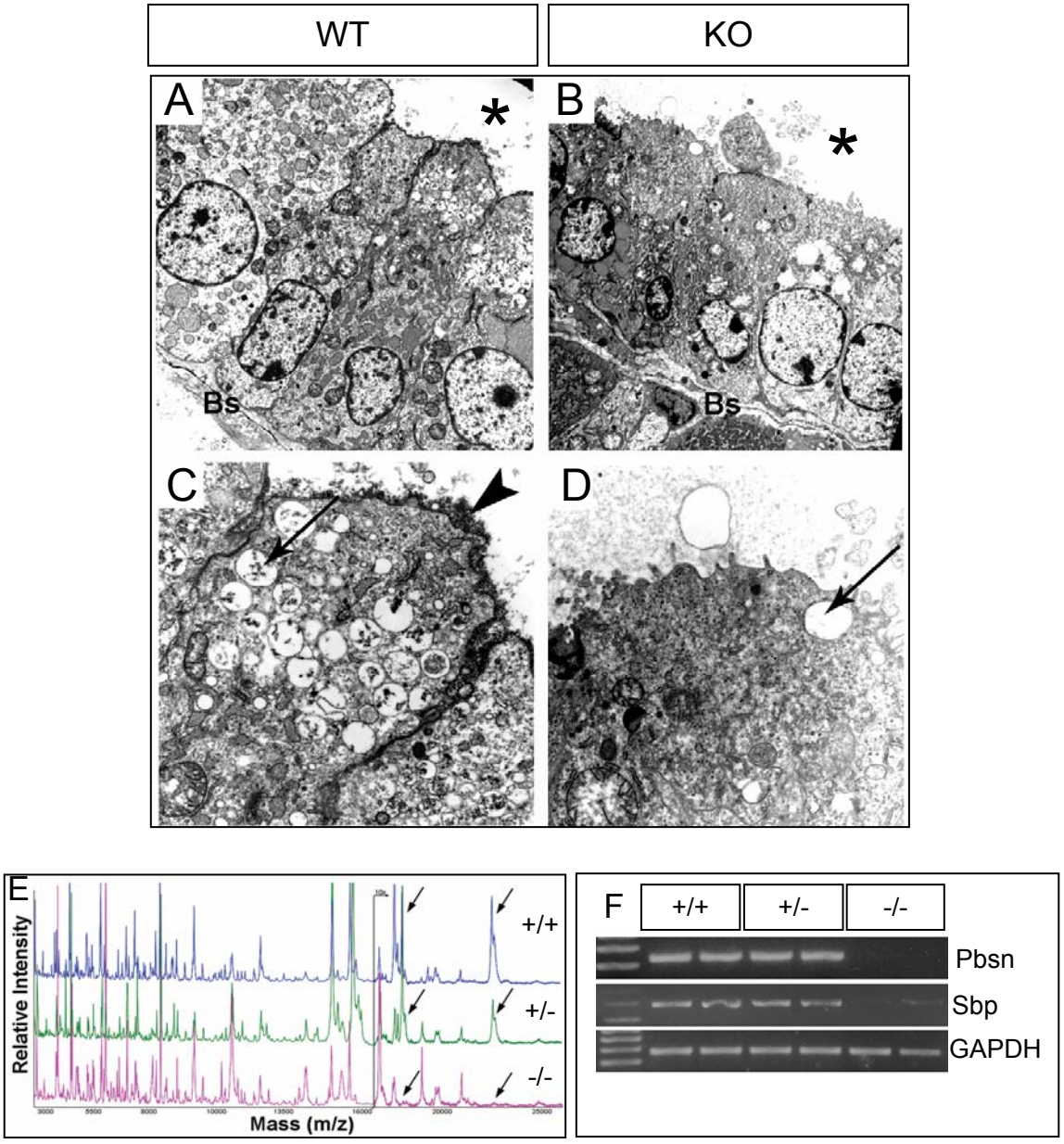

Figure 5-5. Foxa1 regulates luminal cell determination. (A-D) Ultrastructural analysis of Foxa1-/- and control prostates. Magnifications: (A,B), 7403×; (C,D), 25309×. Asterisks indicate the lumen. In wild type cells (A and C), secretory materials are seen in apical vesicles (arrow) and at luminal surface (arrowhead). No secretion is seen in Foxa1-/- cells (B and D). Bs, basement membrane. (E) MALDI-MS protein profiles of m/z range 3000-16000 obtained from rescued Foxa1+/+, +/- and -/- prostates. Continuous profiles were zoomed in at m/z range 16100-26000. Arrows denote peaks that are absent in Foxa1-/- but present in control prostates. (F) RT-PCR for Pbsn and Sbp. GAPDH serves as a loading control.

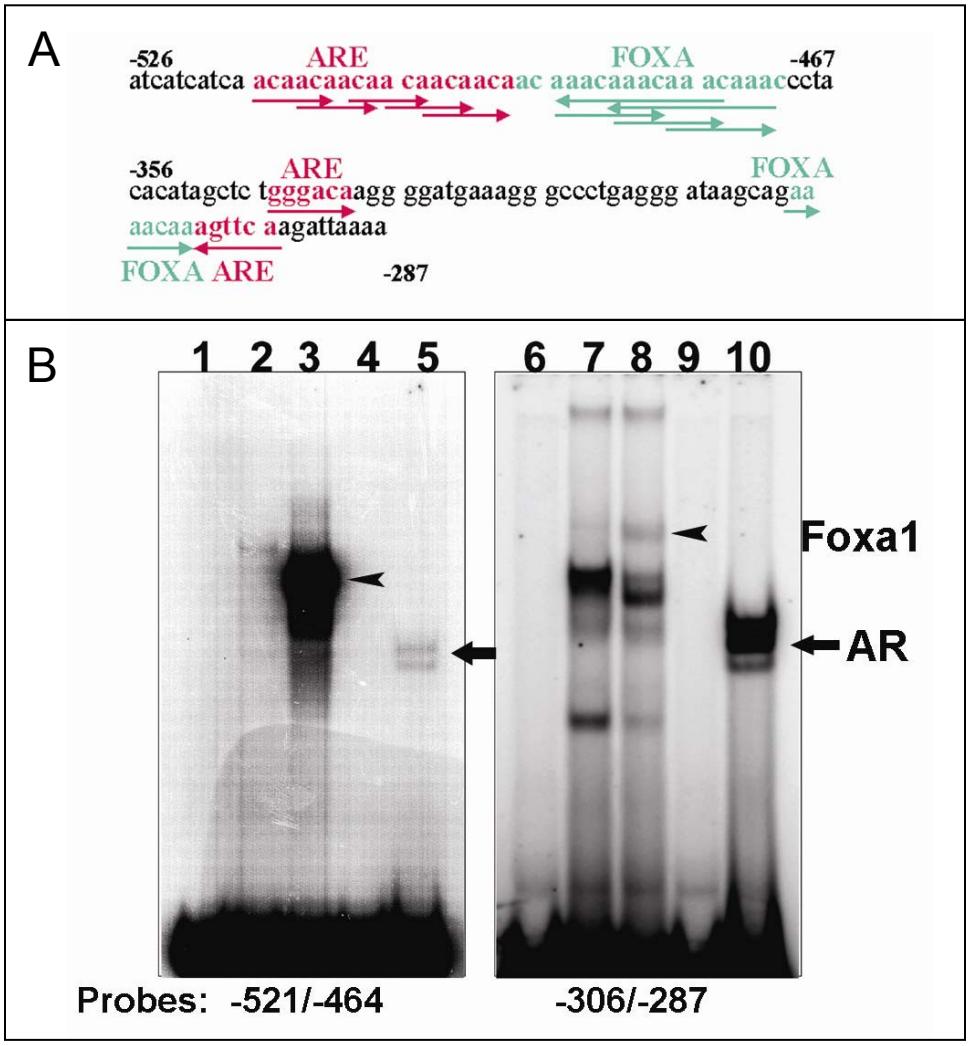

Figure 5-6. Androgen and forkhead response elements in Sbp promoter. (A) Two forkhead binding sites were found on the Sbp promoter, each immediately flanked by an ARE. (B) EMSA confirms these binding sites for Foxa1 and AR. Radiolabeled probes are indicated at bottom of each panel. Lane 1,4,6,9: probe only; lane 2,7: controls (no Foxa1 templates added to the *in vitro* transcription/translation reaction); lane 3,8: probe plus *in vitro* sythesized Foxa1; lane 5,10: probe plus recombinant AR. Arrowheads and arrows denote Foxa1/DNA and AR/DNA complexes, respectively.

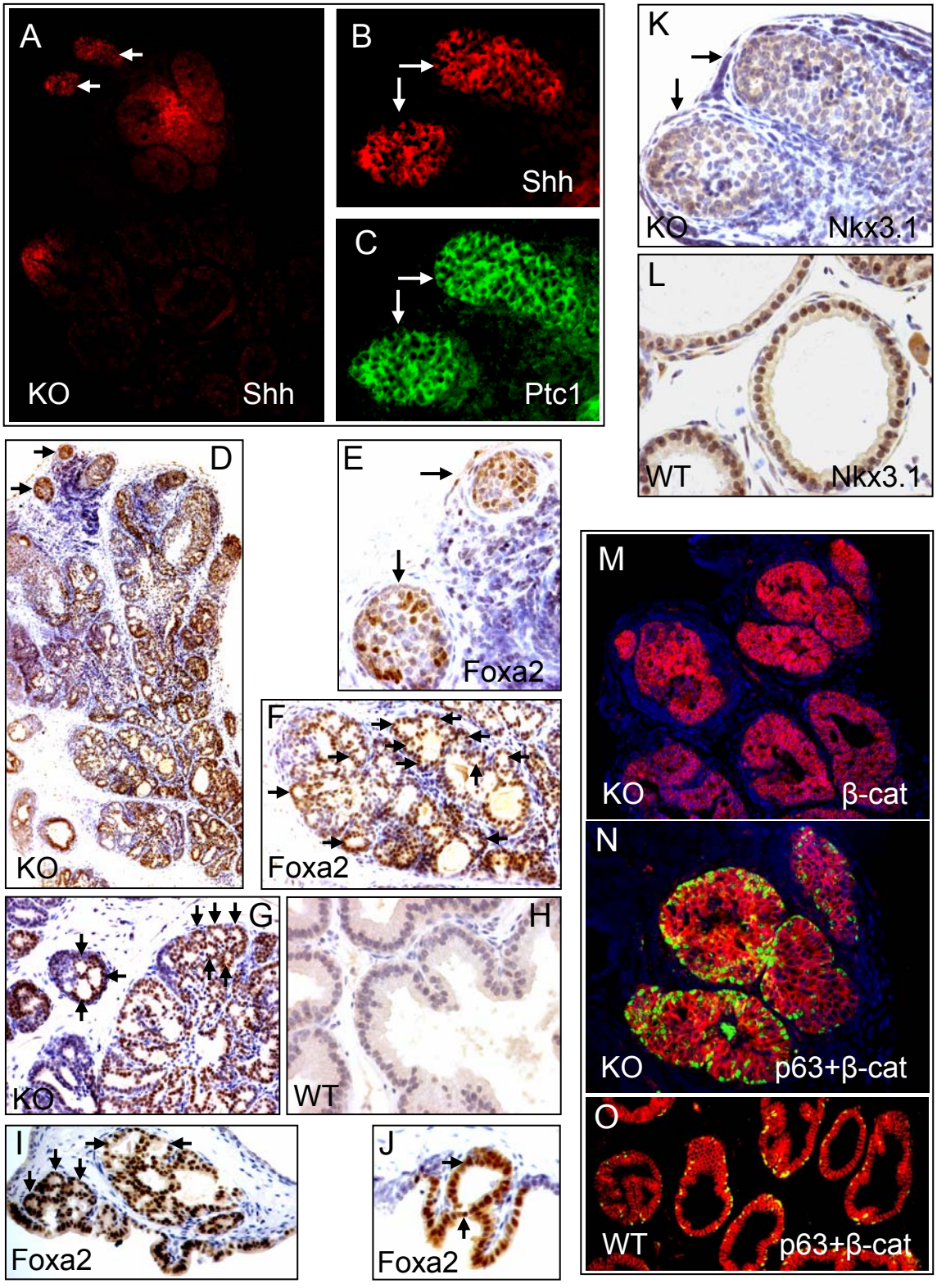
A
KO
Shh
B
Shh
C
Ptc1
K
KO
Nkx3.1
L
WT
Nkx3.1
D
KO
E
Foxa2
F
Foxa2
G
KO
H
WT
I
Foxa2
J
Foxa2
M
KO
β-cat
N
KO
p63+β-cat
O
WT
p63+β-cat

Figure 5-7. Activation of Shh and Foxa2 in Foxa1-/- prostates. (A) Strong and focused expression of Shh in Foxa1-/- prostates (arrows). (B) High magnification of two epithelial buds shows Shh activation. (C) Same section double-stained for Ptc1 shows co-expression of Ptc1 in Foxa1-/- epithelium. (D) Nuclear Foxa2 staining is detected in Foxa1-/- prostates. (E) Strong Foxa2-expression in Foxa1-/- epithelial buds (arrows). (F) Foxa2-expressing cells form numerous microlumen with cribiform pattern, indicating hyperproliferation in the epithelium (arrows). (G) Continuous expansion of Foxa2-positive cells in Foxa1-/- epithelium with extended rescue time up to 15 weeks. Arrows denote many tiny epithelial tips. (H) Foxa2 is not detected in age-matched wild type prostates. (I-J) Foxa2 staining in tissue recombinants generated from Foxa1-/- epithelium. (K-L) No nuclear staining of Nkx3.1 is detected in Foxa1-/- cells in contrast to strong nuclear immunoreactivity in control epithelium. Arrows in (K) denote the epithelial buds corresponding to the area shown in (B). (M) Foxa1-/- prostate stained for β-catenin (red) and counterstained with DAPI (blue). (N) Foxa1-/- prostate stained with β-catenin (red) and p63 (green) show that cell polarity was lost. (O) Control prostate stained with β-catenin and p63 shows polarized epithelium that forms lumen.

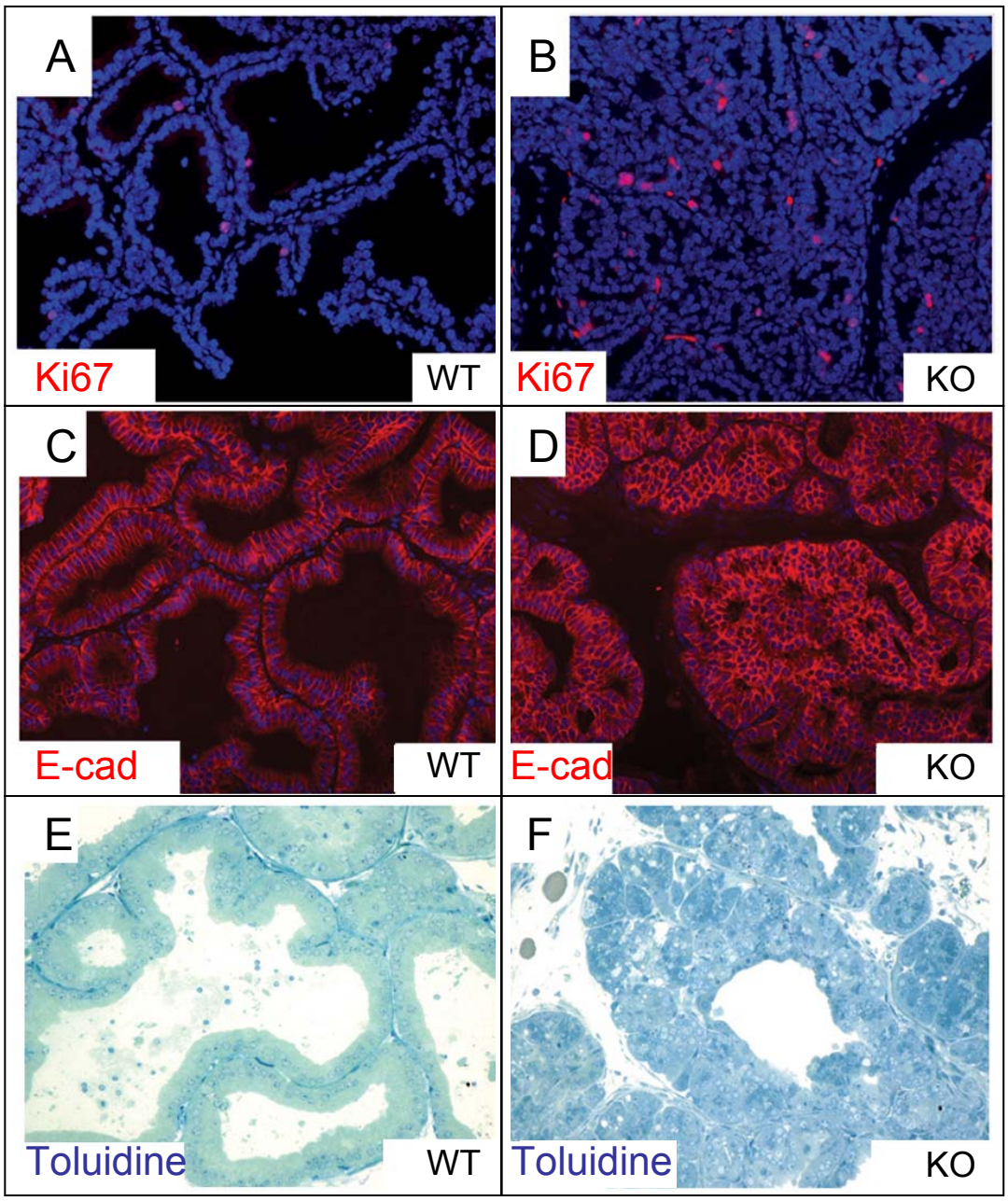

Figure 5-8. Expression of proliferation marker and adhesion molecule in Foxa1-/- prostates. (A-B) Ki67 staining did not detect an increase in the epithelial proliferation rate of null prostate. Ki67 (red); Dapi (blue). (C-D) E-Cadherin staining illustrates abnormal epithelial patterning in 12 week rescued null prostate compared to control. Nuclei were counterstained with DAPI. (E-F) 1µm thin sections from 12 week rescued control and Foxa1-null ventral prostates were stained with toluidine blue. Note that the control glands show a monolayer of luminal cells while null prostates continue to show abnormal epithelial structure.

CHAPTER VI

DISCUSSION

This study reported that an extracellular signal mediator, AR, and a tissue-restricted forkhead protein, Foxa1, coordinately participate in the prostatic gene regulation and organ development. Foxa/HNF-3 proteins are a group of transcription factors that share remarkable sequence similarity over their DNA binding domain (DBD), termed a forkhead or winged-helix domain (Weigel and Jackle, 1990; Zaret, 1999; Lai et al., 1993; Kaufmann and Knochel, 1996). The Foxa proteins are involved in the differentiation of endoderm-derived tissues. This feature has been strikingly conserved among the metazoans (Zaret, 1999). The *Drosophila* homeotic protein *fork head*, which is equivalent to Foxa, was found to be essential for the development of the terminal region including the foregut and hindgut (Weigel and Jackle, 1990); the PHA-4 protein, which is a *C. elegans* Foxa equivalent protein, is also required for the formation of terminal gut structures in the worm (Gaudet and Mango, 2002). In mammals, Foxa1, Foxa2 and Foxa3 were originally discovered as liver-enriched factors, because of their ability to bind the transthyretin (TTR) gene promoter (Lai et al., 1991; Lai et al., 1990). In early embryo development stage, Foxa proteins are believed to provide developmental competence to numerous liver specific genes through their high affinity DNA elements. This mechanism is essential for the activation of these target genes in later stages (Zaret, 1999; Zaret, 2002). The role that Foxa and some other developmental factors play in organ differentiation has been proposed as genetic potentiation (Zaret, 1999; Gualdi et al., 1996; Zaret, 2002).

We observed strong nuclear staining of Foxa1 in both human and mouse prostate epithelial cells. The prostate epithelium, like the epithelium of other urogenital sinus derivatives (bladder and urethra), is derived from the endodermal layer of the embryo. In contrast, Wolffian duct derivatives (epididymis, ductus deferens, and seminal vesicle) are derived from the mesoderm (Thomson, 2001; Hayward, 2002). Understanding the role of Foxa1 in prostate may provide an insight into the differences in epithelial cell patterning and developmental programs among prostate and Wolffian-derived organs, which are all androgen-dependent (Cunha et al., 1987; Thomson, 2001). The cell-type dependent expression of Foxa1 and other endodermal factors could easily provide an explanation why a prostatic differentiation marker such as PSA can be instructively induced in human bladder epithelial cells under proper extracellular signals (Aboseif et al., 1999), while such differentiation, under the same signals, cannot occur in a mesoderm-derived context (Cunha et al., 1987).

Using *in vitro* gel shift and mutation assays, functional Foxa1 sites were identified in both PSA and Pbsn gene regulatory regions. ChIP assay unambiguously demonstrated that Foxa1 binds to PSA enhancer *in vivo*. In our experiments, Foxa1 binding sites were further identified in other prostate specific gene promoters/enhancers. The binding site organization of forkhead and AR shows a striking similarity in these enhancers across different species, suggesting a functional relevance.

The development of a complex eukaryote requires differential expression of over 30,000 genes/proteins in precise spatial and temporal patterns (Carey, 1998). An organism uses transcriptional synergy to achieve such diversity, to maintain cell specificity, and to respond to the environment dynamically (Carey, 1998). A combinatory

use of a subgroup of general transcription factors, signal-dependent factors and cell-specific factors could lead to large number of regulatory possibilities, ensuring that every gene is precisely controlled (Brivanlou and Darnell, Jr., 2002). In the prostate, AR is a signal-dependent nuclear receptor mediating extracellular signals, whereas Foxa1 is a cell-type limited "genetic potentiator" (Zaret, 1999). A synergy between these classes of factors has been suggested in other studies (Brivanlou and Darnell, Jr., 2002), and we show Foxa1 plus AR are involved in prostatic differentiation. In an *in vitro* DNA footprinting study, a prostate-specific protein was reported to bind a DNA sequence in Pbsn promoter (Patrikainen et al., 1999). Interestingly, this region overlaps the first forkhead binding site we discovered. Similarly, a gel shift experiment disclosed several cell-specific factor-binding elements in PSA core enhancer (Schuur ER et al., 1996). Among these elements, two of them completely cover the two Foxa1 motifs, while others overlap with binding sites for GATA proteins (Perez-Stable et al., 2000), which belong to another endodermal transcription factor family (Zaret, 1999). Consistently, the first forkhead element in PSA1 enhancer, which is adjacent to ARE III, was protected by a cell-specific protein in a previous DNA footprinting study (Farmer et al., 2001). Interestingly, the Pbsn promoter (-286/+28bp), the PSA enhancer (-4.2/-3.8 kb) and the hPAP enhancer (-1278/-779bp), where Foxa1 binding sites are located, have all been implicated in prostate-specific regulation (Zhang ZF et al., 2000; Pang et al., 1997; Schuur ER et al., 1996; Zelivianski et al., 2002). These observations strongly suggest that Foxa1 and AR may coordinately participate in the transcriptional regulation of other prostate epithelial cell specific genes.

X-ray crystallographic study revealed that the structure of HNF-3 forkhead domain resembles the globular domain of linker histone H1 (Clark et al., 1993). *In vitro* nucleosome assembly experiments further showed that Foxa1 is able to open compacted chromatin by displacing linker histone H1 in an ATP-independent manner (Cirillo et al., 1998; Cirillo et al., 2002). This mechanism of Foxa1 is mediated through its high affinity DNA binding sites as well as the binding of its C-terminal to histones H3 and H4 (Cirillo et al., 2002). Transient transfection experiments were used to examine the role of Foxa1 in prostatic gene regulation. Although transiently transfected DNA does not appear to assemble the same higher-order chromatin structure observed with genomic DNA, certain aspects of nucleosome-mediated regulation can be observed on transiently expressed DNA (Smith and Hager, 1997; Crowe et al., 1999). For example, studies by Crowe *et al*., demonstrated that Foxa1 relieves nucleosome-mediated transcription repression of a liver specific gene in transient transfection experiment (Crowe et al., 1999). In our study, mutations of these Foxa1 binding motifs significantly abolished Pbsn and PSA gene activities. Overexpression of a mutant Foxa1 protein ($\Delta C_{1\text{-}294}$) suppressed Pbsn promoter activity in a dose-responsive and binding site-dependent manner. These results are consistent with the assumption that some level of nucleosome assembly occurs on the introduced plasmid. Also, these data are in agreement with previous studies showing that overproduction of mutant Foxa proteins, deleted in a similar region, suppressed multiple liver gene expressions (Vallet et al., 1995; Wang et al., 2000a).

However, AR, which binds an ARE in a ligand-dependent manner, Foxa1 occupies PSA enhancer in the absence of androgen. The DNA binding of Foxa1 seems not directly associated with PSA activation, which eventually requires the recruitment of

ligand-bound AR onto the multiple AREs. Thus, Foxa1, by itself, is not a strong transactivator. However, the occupancy of Foxa1 in the regulatory region may confer prostatic genes certain transcriptional potential, which is required for the later recruitment of additional factors as well as the activation by the rate-limiting activator, ligand-bound AR, during prostatic differentiation.

Transcriptional regulation depends not only on the interactions between DNA-binding proteins and their respective *cis*-regulatory elements but also on the interactions among these proteins and with other components of the transactivation machinery. In addition to their ability to interact with various type I or type Π co-regulators, steroid receptors also form conplexes with other DNA binding proteins, resulting in the modulation of transcriptional activity (Heinlein and Chang, 2002). In the present work, AR was found to directly interact with Foxa1, since such an interaction was resistant to the presence of the DNA intercalator, ethidium bromide (Lai and Herr, 1992).

In fact, AR has been found to interact with a number of DNA binding transcription factors including AP-1 (Sato et al., 1997), Smad3 (Kang et al., ; Kang et al., 2002), NFκB (Palvimo et al., 1996), SRY (Yuan et al., 2001), PDEF (Oettgen et al., 2000) and other steroid receptors (Heinlein and Chang, 2002). The phenomenon of the interaction of AR and these distinct transcription factors was called cross-modulation, which was illustrated by well-documented AR interactions with AP-1 and NFκB (Sato et al., 1997; Palvimo et al., 1996). Such crosstalks between different signaling pathways may increase regulatory diversity and provide opportunities for cell-specific response. For example, a testis-expressed protein, SRY, interacts with AR and plays a role in germ cell development (Yuan et al., 2001); a newly discovered prostatic epithelium-specific Ets

transcription factor PDEF directly contacts AR and activates PSA gene expression. Here, the adjacent binding of Foxa1 and a direct contact with AR may establish an efficient molecular mechanism for ligand-bound AR to rapidly target correct gene sequences. Crystallographic study of Foxa3/DNA revealed a bend of DNA of about 13° upon Foxa3 binding(Clark et al., 1993), which may provide favorable DNA conformation for adjacent factors, since chromatin-associated proteins such as high mobility group (HMG) box containing proteins have been well demonstrated for their ability to enhance DNA binding of steroid receptors by generating a sharp bend in DNA (Boonyaratanakornkit et al., 1998). A similar mechanism may apply to Foxa1 binding of DNA in the current model. It has been shown dynamically that the physical binding of GR to a glucocorticoid response element (GRE) was facilitated by the adjacent Foxa2 binding (Stafford et al., 2001). This seems true for several other liver specific genes (Wang et al., 1996; Espinas et al., 1995). In addition, Foxa proteins cooperate with estrogen receptor (ER) to activate the vitellogenin B1 gene transcription (Robyr et al., 2000). Thus, cooperation between steroid receptors and Foxa proteins may be a general mechanism for the control of various tissue specific genes.

Strong evidences suggest that Foxa1, like AP-1 (Sato et al., 1997), SRY (Yuan et al., 2001), T cell Factor 4 (Amir et al., 2003) and PDEF (Oettgen et al., 2000), is another AR-DNA binding domain (DBD)-interacting transcription factor. Even though the DBDs of steroid receptors appear to be mainly involved in DNA binding and homodimerization of receptor monomers, mounting evidence suggests that this domain also serves as an interaction interface for other proteins. Among these interacting partners are coactivators (Aarnisalo et al., 1998; Moilanen et al., 1998b; Moilanen et al., 1999; Moilanen et al.,

1998a), factors of basal transcription machinery (Schwerk et al., 1995), and other transcription factors (Sato et al., 1997; Yuan et al., 2001; Oettgen et al., 2000). Most of these interactions are biologically relevant and result in transcriptional activation or repression.

In the present work, immunoprecipitation experiments in LNCaP cells demonstrated the interaction of endogenous AR and Foxa1 occurs in the presence of androgen, suggesting the physical relevance of this interaction. *In vitro* DNA binding experiments showed that both proteins can adjacently and concomitantly bind respective *cis*-regulatory elements, which provided evidence that such AR/Foxa1 interaction does not inhibit the DNA binding of either protein, further suggesting that these interaction events are mediated through separate motifs in AR-DBD. The organized ARE and forkhead response elements in a number of different prostate-specific enhancers also suggested a fixed binding orientation (Fig. 6-1). Since winged-helix factors are asymmetric proteins, this binding site organization may facilitate the interaction between the fixed protein domains presented by each factor. A similar mechanism has been documented in a recent study, which shows that a closely linked REL and GATA binding sites are positioned in the same orientation within *Drosophila* immunity regulatory DNAs, and that this REL-GATA interaction plays a pervasive role in *Drosophila* immune response (Senger et al., 2004). The identification of AR/Foxa1 interaction may extend our understanding of the role of DBD in androgen action and provide a general insight into the regulatory mechanism between forkhead proteins and steroid receptors.

In vertebrates, the endoderm gives rise to the epithelial cell lining of the respiratory and gastrointestinal tract, as well as to the lung, the liver, the thyroid, the

pancreas, and hindgut derivatives, including the bladder and prostate (Wells and Melton, 1999; Cunha et al., 1987). Conserved molecular pathways that control endoderm development have been identified in recent studies (Abate-Shen and Shen, 2000). In addition to such generalized pathways, the prostate has its own specific regulatory mechanisms which include androgenic signaling. We propose that a regulated interaction of these conserved and specialized signaling pathways is essential for normal prostatic morphogenesis and differentiation.

Foxa1 and Foxa2 are forkhead transcription factors that participate in liver and lung formation from foregut endoderm. Overexpressing these factors in embryonic stem cells elicited expression of genes that are associated with endodermal lineage (Levinson-Dushnik and Benvenisty, 1997). We have shown that both factors are present in prostate epithelium during early prostatic morphogenesis, and have hypothesized that they play essential but distinct roles in prostate development.

The presence of early prostatic structures in neonatal Foxa1-/- mice indicates that Foxa1 is not absolutely required for initial budding process. However the buds that are formed do not follow the normal pattern of development and differentiation. Rescued Foxa1-/- prostates and tissue recombinants generated from Foxa1-/- UGE, demonstrated an epithelial hyperplasia with suppressed lumen formation, as well as abnormal stromal proliferation. These solid epithelial cell cords that appear in the null prostate form cribriform patterns, similar to those frequently seen in prostatic intraepithelial neoplasia, indicating a role for Foxa1 in ductal morphogenesis, canalization and epithelial proliferation. A number of key signaling molecules such as the Shh play crucial role in controlling prostatic ductal morphogenesis, although differential effects on embryonic

ductal budding (Podlasek et al., 1999a; Lamm et al., 2002) and on postnatal growth (Freestone et al., 2003; Wang et al., 2003) were observed. Prostatic rudiments were induced in rescued Shh-/- mouse prostates suggesting that like Foxa1, Shh is not required for prostatic bud formation (Freestone et al., 2003; Berman et al., 2004).

Shh expression and signaling is normally downregulated at the conclusion of prostatic ductal branching (Podlasek et al., 1999a). A similar temporal pattern is true for Foxa2, whose expression was shown in this study to be overlapping with Shh during prostatic induction. A temporal expression of these critical factors during prostate development is illustrated in Fig. 6-2. Shh modulates its own activity by inducing negative regulators such as Ptc1 and hedgehog-binding protein 1 (Chuang et al., 2003). Mis-activation of Shh signaling has been observed in a variety of diseases including the human prostate cancer (Fan et al., 2004). We found focused expression of both Shh and Foxa2 in Foxa1-/- prostatic epithelial cell cords. Continued expression of Shh was seen even in Foxa1-/- prostates grafted for fifteen weeks but it was not seen in the wild type controls. This continuous activation of Shh in Foxa1-/- cells could result from a defect in the negative feedback loop.

The present work is supported by previous reports that Shh signaling has important mitogenic effects on the development of various tissues including the neural tube, lung, kidney, prostate and salivary gland (Bellusci et al., 1997a; Lamm et al., 2002; Yu et al., 2002; Jaskoll et al., 2004; Thibert et al., 2003). Shh is capable of eliciting mitogenic effects on both epithelium and stroma. Overexpressing Shh in the developing lung led to increased proliferation in both mesenchymal and epithelial cells (Bellusci et al., 1997a). In the prostate, Shh stimulation induced embryonic prostatic epithelial growth

(Podlasek et al., 1999a), as well as mesenchymal expansion in postnatal prostates (Freestone et al., 2003).

Shh acts primarily through its transmembrane receptor Ptc1, a direct downstream target of Shh (Ingham and McMahon, 2001). We detected Ptc1 expression in both the epithelial and the mesenchymal cell compartments in embryonic UGS. In addition to the mesenchymal Ptc1 reported previously (Podlasek et al., 1999a; Berman et al., 2004), the detection of epithelial cell Ptc1 in embryonic prostatic buds is consistent with a recent observation made in embryonic salivary gland (Jaskoll et al., 2004). Epithelial cell Ptc1 has also been detected in neonatal prostatic ductal tips (Pu et al., 2004). We observed Ptc1 expression in Foxa1-/- prostatic epithelial cords where focused activity of Shh was detected. Collectively, our data suggest that, in addition to a paracrine mechanism, Shh signaling may also act within the prostatic epithelium in a juxtacrine manner. This provides an explanation for the constant epithelial hyperproliferation in Foxa1-/- epithelium (Fig. 6-3). A similar model picturing Shh signal transduction in the epithelium of the embryonic salivary gland has recently been proposed (Jaskoll et al., 2004).

In addition to the epithelial hyperplasia, there is a concomitant suppression of lumen formation in Foxa1-/- prostates. The genesis of the tubular structures in the prostate resembles the process in mammalian mammary gland or salivary gland, which involves cell proliferation and programmed cell death (Hogan and Kolodziej, 2002; Hogg et al., 1983). The defect observed in Foxa1-/- prostates could be due to a lack of cell death in the epithelium. Indeed, Shh has been shown to promote cell survival through binding to its receptor Ptc1, while Ptc1 acts as a proapoptotic factor in its unbound status and patterns neural tube by inducing selective cell death (Thibert et al., 2003; Guerrero

and Altaba, 2003). In the prostate, Shh signaling has also been shown to inhibit ductal canalization (Freestone et al., 2003), thus playing an opposing role to androgen, which promotes lumen formation as a part of the normal developmental process (Hayward et al., 1996a). Our data is consistent with these previous studies.

Foxa2 is fundamentally important for the formation of the mammalian node and notochord, while mis-expressed Foxa2 in the developing neural tube induces ectopic floor plate formation (Weinstein et al., 1994; Ang and Rossant, 1994). The Foxa2 enhancer contains crucial Shh-responsive element (Sasaki et al., 1997), and Shh signaling has been shown to be critical for Foxa2 expression in other organs (Yamagishi et al., 2003; Mahlapuu et al., 2001). Shh secreted from the notochord induced expression of Foxa2 in the floorplate of the neural tube; reciprocally Foxa2 maintained Shh expression in a positive feedback loop (Chiang et al., 1996; Hynes et al., 1997; Echelard et al., 1993a; Sasaki et al., 1997). Thus, the expression of Foxa2 in Foxa1-/- cells may be due to a continuous response to Shh signaling. Alternatively, Foxa1 may act as a negative regulator of Foxa2, whose gene regulatory region contains a functional forkhead binding element (Guo et al., 2002). Along these lines Foxd3 is capable of activating Foxa2 by binding to its enhancer; however, such transactivation can be abrogated by Oct-4, which binds and sequesters Foxd3 (Guo et al., 2002). We have shown an elevated nuclear Foxa1 level during normal prostatic morphogenesis and maturation. We would therefore suggest that this increased nuclear Foxa1 might act as a competitor possibly by binding the same forkhead response element in Foxa2 enhancer, thus negatively modulating its expression.

The expression of Nkx3.1 is initiated at prostatic budding, somewhat later than that of Foxa1 and Foxa2 (Bhatia-Gaur et al., 1999; Huang et al., 2004) (Fig. 6-2). The

level of Nkx3.1 expression is elevated during prostatic morphogenesis and is maintained in mature glands (Bhatia-Gaur et al., 1999), representing a reversed profile to Foxa2 expression. Both the human and mouse Nkx3.1 gene 5'-upstream regions contain forkhead binding sites (unpublished observation). Nkx3.1 nuclear expression was not detected in Foxa1-/- cells, suggesting a potential mechanism whereby Foxa1 could positively regulate Nkx3.1. Given that Nkx3.1 has been proposed as a negative transcriptional regulator (Chen et al., 2002a), we speculate that upregulation of Nkx3.1 by Foxa1 in normal prostate could serve as another mechanism for modulating early developmental molecules such as Foxa2 (Fig. 6-3).

In embryonic UGS and Foxa1-/- prostates, the cell type-specific analysis of Shh and Foxa2 expression suggested that both factors are predominantly expressed in the basal keratin-expressing cell population. The basal cells are postulated to act as the transit/amplifying population in the prostate and are widely believed to be capable of acting as luminal cell precursors (Abate-Shen and Shen, 2000). The increased number of basal cells in Foxa1-/- prostates is consistent with the activated Shh signaling, which is critical in promoting precursor cell numbers in other tissues in the body (Ruiz et al., 2002; Machold et al., 2003). Consistent with this finding, we did not detect any mature luminal epithelial cells, in Foxa1-/- prostates, in terms of ultrastructural features or the expression of differentiation markers. These data suggested that under normal developmental process, Foxa1 promotes prostatic epithelial cell maturation through functional balancing the activities of Shh and Foxa2 (Fig. 6-3).

Further, Foxa1-/- epithelium faithfully expressed AR, however the differentiated response was completely lost in the null prostates. In contrast, Tfm mice that lack a

functional AR have served as a unique model for studying the role of epithelial cell AR in prostatic differentiation. Urinary tract epithelium from Tfm mice can be instructively induced, by wild type embryonic UGM, to produce prostatic morphology (Cunha and Lung, 1978; Cunha and Chung, 1981). Although ductal/luminal structures developed in these Tfm recombinants, the luminal epithelium in those glands did not produce secretory proteins (Donjacour and Cunha, 1993). Morphologically, most of the ducts/lumena in Tfm recombinants was composed of low columnar or cuboidal luminal epithelium (Donjacour and Cunha, 1993). These observations demonstrated that epithelial cell AR is not necessary for prostatic induction but it is required for the final stage of luminal epithelial cell morphogenesis and the initiation of secretory activities (in other words, for the differentiated function of luminal cells to occur) (Donjacour and Cunha, 1993). The overall morphology of Foxa1-null prostates indicated that prostate development was defective at a stage of ductal canalization and cytodifferentiation, since the solid epithelial cords continue to grow with limited lumen formations. Epithelial cells inside the cords proliferated constantly but failed to organize into a normal luminal structure and secretory function was impaired in Foxa1-null prostates. These data suggests that although both epithelial AR and Foxa1 regulate differentiated function in prostate epithelial cells, Foxa1 plays an early role in regulating glandular morphogenesis, a process in which epithelial cell AR is not crucially involved.

In conclusion, these data collectively supported the presence of a *cis*-regulatory code composed of androgen and forkhead response elements. Through phenotypic characterization of transgenic mouse prostates and functional analysis of prostatic-

promoters, we documented the essential roles of Foxa1 in prostate development and function.

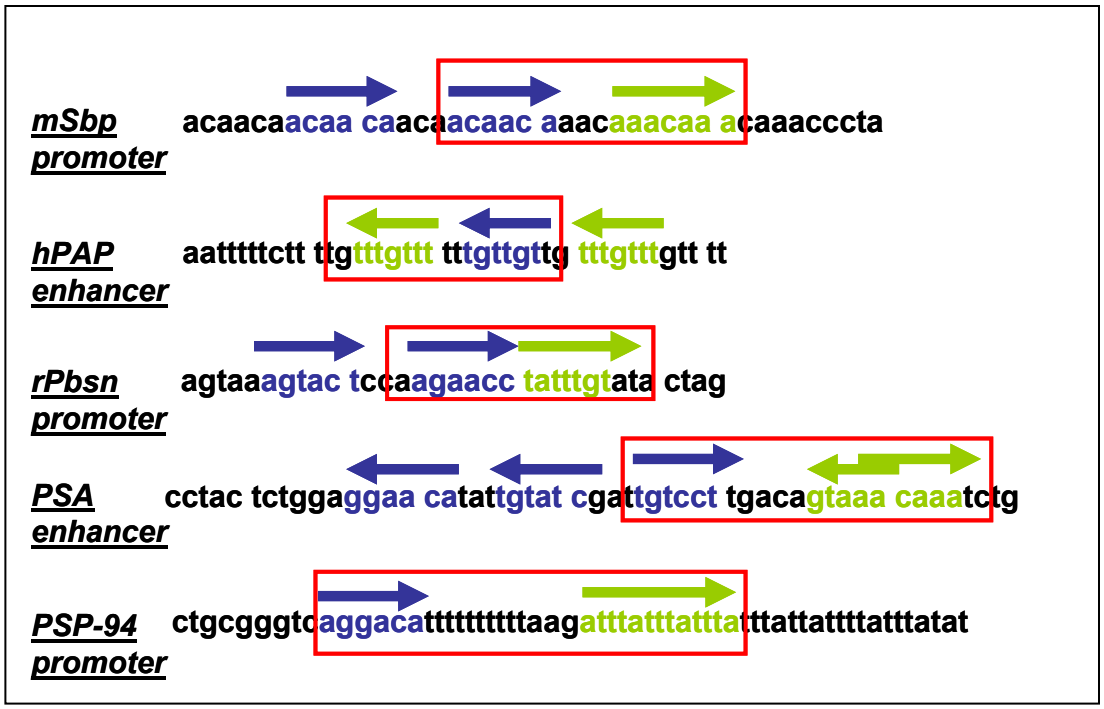

Figure 6-1. A diagram illustrates the AR-Foxa1 binding elements in various prostatic gene enhancers. Blue arrows are ARE. Green Arrows are forkhead response elements. The direction of the arrow indicates the sense or the antisense strand that matched the binding sequence. Binding sites framed by red boxes indicate a very similar binding orientation of the two proteins. Since winged-helix factors are asymmetric proteins, this binding site organization may facilitate the interaction between a fixed protein interface presented by each protein.

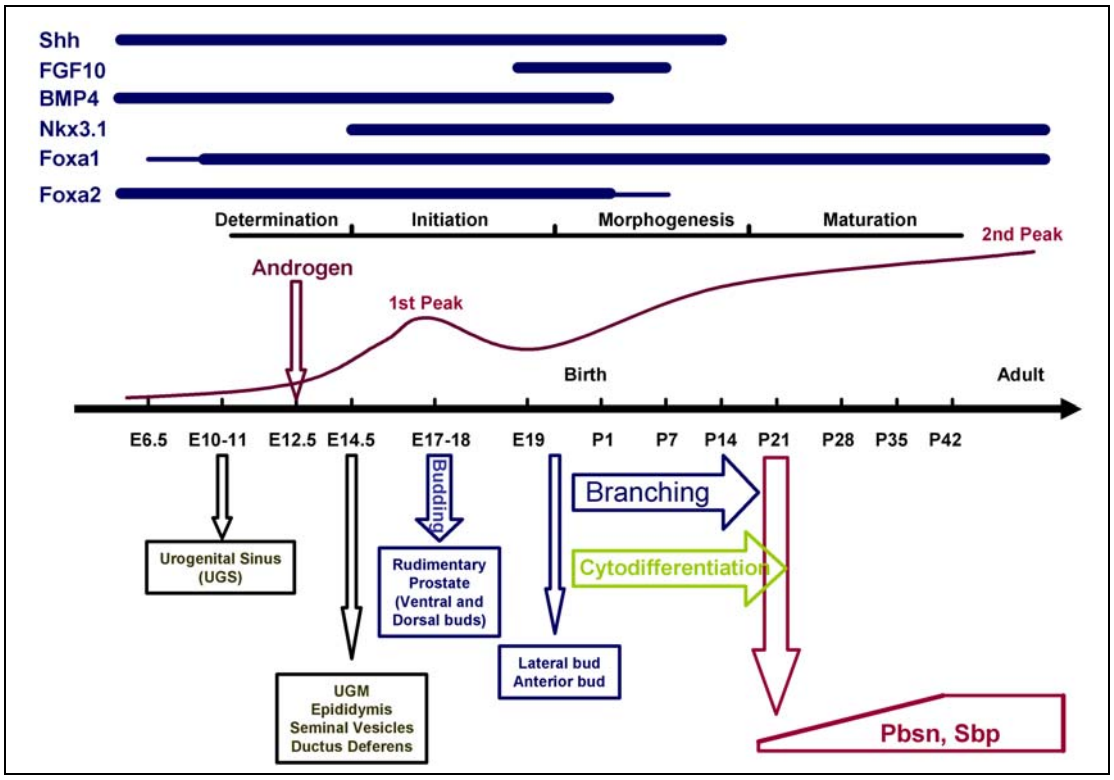

Figure 6-2. The temporal expression of key developmental factors in prostate development. Shh signaling, BMP4, FGF10, Foxa2 and androgen signaling (first peak at E17-18) are correlated with the prostatic induction and early morphogenesis. Sustained Foxa1 expression is throughout the entire developmental process, while the expression of Nkx3.1 signifies the prostatic epithelial determination. The details of the time course of prostatic morphogenesis and cytodifferentiation are described in the text.

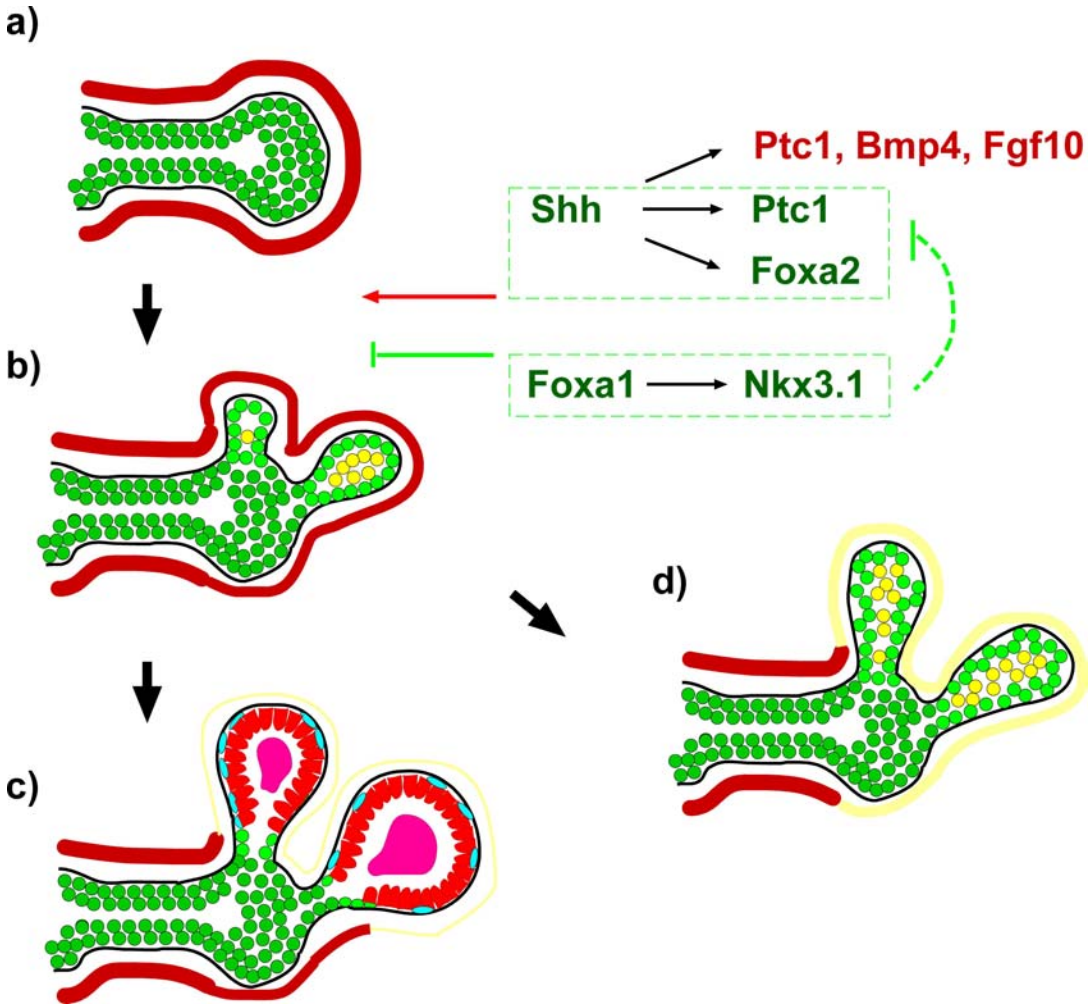

Figure 6-3. A proposed model for forkhead proteins in regulating prostatic organogenesis. (a) Embryonic UGS is composed of UGE (in green) and UGM (in red). (b) Shh produced by UGE, acts via Ptc1 receptors located in both epithelium and mesenchyme, positively regulating ductal epithelial budding and stromal proliferation. Shh signaling elicits morphogenetic effects through downstream targets including the epithelial Foxa2 and the mesenchymal Bmp4 and Fgf10 (Pu et al., 2004). In normal process, Foxa1 activates transcriptional inhibitors or differentiation modulators, such as Nkx3.1, and negatively modulates Shh and Foxa2 expression through a direct or indirect mechanism. (c) Decreased activity in Shh and Foxa2 leads to ductal canalization, while accumulated Foxa1 and Nkx3.1 induces a variety of genes associated with epithelial maturation. (d) Hyperactive Shh signaling in disease conditions or in Foxa1-/- prostates where Foxa1 or its balancing mechanism is abolished, abnormal signal induces mitogenic effects in both epithelium and stroma, leading to abnormal ductal patterning mimicking immature prostatic cords.

FUTURE DIRECTIONS

A. Identify Foxa1 downstream targets in the mouse prostate. It is important to identify the downstream effectors or signaling pathways that mediate Foxa1 function in the prostatic epithelium. Nkx3.1 is a good candidate, whose enhancer (in both human and mouse) contains a number of forkhead response elements. More targets will be identified through cDNA microarray analysis by comparing rescued Foxa1-/- prostates and rescued age-matched wild type prostates. Candidate genes will be especially interesting if they show functional links to Shh or Foxa2 signaling molecules.

B. Determine the role of Foxa2 in mouse prostate development. Foxa2 is only transiently expressed in prostatic epithelium during prostatic budding. However, Foxa1-/- prostate epithelium shows continuous Foxa2 expression. The role of Foxa2 in prostate development is important for further study. Conditional Foxa2 allele will be disrupted in the mouse prostate epithelium using a cre-lox strategy. The phenotype of Foxa2-/- prostates can then be assessed.

C. Identify the factor binding immediately next to Foxa1 on Pbsn promoter. Gel shifts and Southwester analysis indicated that there is at least one more protein directly bound to the Pbsn promoter sequence immediatedly downstream to Foxa1 binding site (-121/-115 bp). The core binding sequence of this protein covers a palindromic sequence "GTATAC", which may be a DNA target for POU domain transcription factors. Interaction between forkhead protein and POU transcription factor has been described recently (Guo et al., 2002). Binding site DNA affinity chromatography or yeast one hybrid system can be employed to identify this protein.

REFERENCES

Aarnisalo,P., Palvimo,J.J., and Janne,O.A. (1998). CREB-binding protein in androgen receptor-mediated signaling. Proc. Natl. Acad. Sci. U. S. A *95*, 2122-2127.

Abate-Shen,C. and Shen,M.M. (2000). Molecular genetics of prostate cancer. Genes Dev. *14*, 2410-2434.

Aberle,H., Bauer,A., Stappert,J., Kispert,A., and Kemler,R. (1997). beta-catenin is a target for the ubiquitin-proteasome pathway. EMBO J. *16*, 3797-3804.

Aboseif,S., El Sakka,A., Young,P., and Cunha,G. (1999). Mesenchymal reprogramming of adult human epithelial differentiation. Differentiation *65*, 113-118.

Abrahamsson,P.A. (1999). Neuroendocrine cells in tumour growth of the prostate. Endocr. Relat Cancer *6*, 503-519.

Alarid,E.T., Rubin,J.S., Young,P., Chedid,M., Ron,D., Aaronson,S.A., and Cunha,G.R. (1994). Keratinocyte growth factor functions in epithelial induction during seminal vesicle development. Proc. Natl. Acad. Sci. U. S. A. *91*, 1074-1078.

ALESCIO,T. and CASSINI,A. (1962). Induction in vitro of tracheal buds by pulmonary mesenchyme grafted on tracheal epithelium. J. Exp. Zool. *150*, 83-94.

Amir,A.L., Barua,M., McKnight,N.C., Cheng,S., Yuan,X., and Balk,S.P. (2003). A direct beta-catenin-independent interaction between androgen receptor and T cell factor 4. J. Biol. Chem. *278*, 30828-30834.

Ang,S.L. and Rossant,J. (1994). HNF-3 beta is essential for node and notochord formation in mouse development. Cell *78*, 561-574.

Aumuller,G., Leonhardt,M., Janssen,M., Konrad,L., Bjartell,A., and Abrahamsson,P.A. (1999). Neurogenic origin of human prostate endocrine cells. Urology *53*, 1041-1048.

Aza-Blanc,P., Ramirez-Weber,F.A., Laget,M.P., Schwartz,C., and Kornberg,T.B. (1997). Proteolysis that is inhibited by hedgehog targets Cubitus interruptus protein to the nucleus and converts it to a repressor. Cell *89*, 1043-1053.

Baker,J., Hardy,M.P., Zhou,J., Bondy,C., Lupu,F., Bellve,A.R., and Efstratiadis,A. (1996). Effects of an Igf1 gene null mutation on mouse reproduction. Mol. Endocrinol. *10*, 903-918.

Balemans,W. and Van Hul,W. (2002). Extracellular regulation of BMP signaling in vertebrates: a cocktail of modulators. Dev. Biol. *250*, 231-250.

Bardin,C.W., Bullock,L.P., Sherins,R.J., Mowszowicz,I., and Blackburn,W.R. (1973). Androgen metabolism and mechanism of action in male pseudohermaphroditism: a study of testicular feminization. Recent Prog. Horm. Res. *29*, 65-109.

Barrios,R., Lebovitz,R.M., Wiseman,A.L., Weisoly,D.L., Matusik,R.J., DeMayo,F., and Lieberman,M.W. (1996). RasT24 driven by a probasin promoter induces prostatic hyperplasia in transgenic mice. Transgenics *2:* 23-28.

Bellusci,S., Furuta,Y., Rush,M.G., Henderson,R., Winnier,G., and Hogan,B.L. (1997a). Involvement of Sonic hedgehog (Shh) in mouse embryonic lung growth and morphogenesis. Development *124*, 53-63.

Bellusci,S., Grindley,J., Emoto,H., Itoh,N., and Hogan,B.L. (1997b). Fibroblast growth factor 10 (FGF10) and branching morphogenesis in the embryonic mouse lung. Development *124*, 4867-4878.

Bentley,H., Hamdy,F.C., Hart,K.A., Seid,J.M., Williams,J.L., Johnstone,D., and Russell,R.G. (1992). Expression of bone morphogenetic proteins in human prostatic adenocarcinoma and benign prostatic hyperplasia. Br. J. Cancer *66*, 1159-1163.

Berman,D.M., Desai,N., Wang,X., Karhadkar,S.S., Reynon,M., Abate-Shen,C., Beachy,P.A., and Shen,M.M. (2004). Roles for Hedgehog signaling in androgen production and prostate ductal morphogenesis. Dev. Biol. *267*, 387-398.

Berry,S.J. and Isaacs,J.T. (1984). Comparative aspects of prostatic growth and androgen metabolism with aging in the dog versus the rat. Endocrinology *114*, 511-520.

Bhanot,P., Brink,M., Samos,C.H., Hsieh,J.C., Wang,Y., Macke,J.P., Andrew,D., Nathans,J., and Nusse,R. (1996). A new member of the frizzled family from Drosophila functions as a Wingless receptor. Nature *382*, 225-230.

Bhatia-Gaur,R., Donjacour,A.A., Sciavolino,P.J., Kim,M., Desai,N., Young,P., Norton,C.R., Gridley,T., Cardiff,R.D., Cunha,G.R., Abate-Shen,C., and Shen,M.M. (1999). Roles for Nkx3.1 in prostate development and cancer. Genes Dev. *13*, 966-977.

Bhowmick,N.A., Chytil,A., Plieth,D., Gorska,A.E., Dumont,N., Shappell,S., Washington,M.K., Neilson,E.G., and Moses,H.L. (2004). TGF-beta signaling in fibroblasts modulates the oncogenic potential of adjacent epithelia. Science *303*, 848-851.

Bierie,B., Nozawa,M., Renou,J.P., Shillingford,J.M., Morgan,F., Oka,T., Taketo,M.M., Cardiff,R.D., Miyoshi,K., Wagner,K.U., Robinson,G.W., and Hennighausen,L. (2003). Activation of beta-catenin in prostate epithelium induces hyperplasias and squamous transdifferentiation. Oncogene *22* , 3875-3887.

Boonyaratanakornkit,V., Melvin,V., Prendergast,P., Altmann,M., Ronfani,L., Bianchi,M.E., Taraseviciene,L., Nordeen,S.K., Allegretto,E.A., and Edwards,D.P. (1998). High-mobility group chromatin proteins 1 and 2 functionally interact with steroid

hormone receptors to enhance their DNA binding in vitro and transcriptional activity in mammalian cells. Mol. Cell Biol. *18*, 4471-4487.

Brivanlou,A.H. and Darnell,J.E., Jr. (2002). Signal transduction and the control of gene expression. Science *295*, 813-818.

Bruner-Lorand,J., Mechaber,D., Zwick,A., Hechter,O., Eychenne,B., Baulieu,E.E., and Robel,P. (1984). Characteristics of separated epithelial and stromal subfractions of prostate: I. Rat ventral prostate. Prostate *5*, 231-254.

Brzozowski,A.M., Pike,A.C., Dauter,Z., Hubbard,R.E., Bonn,T., Engstrom,O., Ohman,L., Greene,G.L., Gustafsson,J.A., and Carlquist,M. (1997). Molecular basis of agonism and antagonism in the oestrogen receptor. Nature *389*, 753-758.

Bubulya,A., Wise,S.C., Shen,X.Q., Burmeister,L.A., and Shemshedini,L. (1996). c-Jun can mediate androgen receptor-induced transactivation. J. Biol. Chem. *271*, 24583-24589.

Byrne,R.L., Leung,H., and Neal,D.E. (1996). Peptide growth factors in the prostate as mediators of stromal epithelial interaction. Br. J. Urol. *77*, 627-633.

Cadigan,K.M. and Nusse,R. (1997). Wnt signaling: a common theme in animal development. Genes Dev. *11*, 3286-3305.

Capdevila,J. and Guerrero,I. (1994). Targeted expression of the signaling molecule decapentaplegic induces pattern duplications and growth alterations in Drosophila wings. EMBO J. *13*, 4459-4468.

Carey,M. (1998). The enhanceosome and transcriptional synergy. Cell *92*, 5-8.

Carlsson,P. and Mahlapuu,M. (2002). Forkhead transcription factors: key players in development and metabolism. Dev. Biol. *250*, 1-23.

Chakravarti,D., LaMorte,V.J., Nelson,M.C., Nakajima,T., Schulman,I.G., Juguilon,H., Montminy,M., and Evans,R.M. (1996). Role of CBP/P300 in nuclear receptor signalling. Nature *383*, 99-103.

Chang,C.S., Saltzman,A.G., Hiipakka,R.A., Huang,I.Y., and Liao,S.S. (1987). Prostatic spermine-binding protein. Cloning and nucleotide sequence of cDNA, amino acid sequence, and androgenic control of mRNA level. J. Biol. Chem. *262*, 2826-2831.

Chaurand,P., DaGue,B.B., Ma,S., Kasper,S., and Caprioli,R.M. (2001). Strain-based Squence Variations and Structure Analysis of Murine Prostate Specific Spermine Binding Protein Using Mass Spectrometry. Biochemistry *40*, 9725-9733.

Chaurand,P., Schwartz,S.A., Billheimer,D., Xu,B.J., Crecelius,A., and Caprioli,R.M. (2004). Integrating histology and imaging mass spectrometry. Anal. Chem. *76*, 1145-1155.

Chen,H., Nandi,A.K., Li,X., and Bieberich,C.J. (2002b). NKX-3.1 interacts with prostate-derived Ets factor and regulates the activity of the PSA promoter. Cancer Res *62*, 338-340.

Chen,H., Nandi,A.K., Li,X., and Bieberich,C.J. (2002a). NKX-3.1 interacts with prostate-derived Ets factor and regulates the activity of the PSA promoter. Cancer Res *62*, 338-340.

Chen,S., Wang,J., Yu,G., Liu,W., and Pearce,D. (1997). Androgen and glucocorticoid receptor heterodimer formation. A possible mechanism for mutual inhibition of transcriptional activity. J. Biol. Chem. *272*, 14087-14092.

Chen,T., Wang,L.H., and Farrar,W.L. (2000). Interleukin 6 activates androgen receptor-mediated gene expression through a signal transducer and activator of transcription 3-dependent pathway in LNCaP prostate cancer cells. Cancer Res *60*, 2132-2135.

Cheshire,D.R. and Isaacs,W.B. (2003). Beta-catenin signaling in prostate cancer: an early perspective. Endocr. Relat Cancer *10*, 537-560.

Chesire,D.R., Ewing,C.M., Gage,W.R., and Isaacs,W.B. (2002). In vitro evidence for complex modes of nuclear beta-catenin signaling during prostate growth and tumorigenesis. Oncogene *21*, 2679-2694.

Chiang,C., Litingtung,Y., Lee,E., Young,K.E., Corden,J.L., Westphal,H., and Beachy,P.A. (1996). Cyclopia and defective axial patterning in mice lacking Sonic hedgehog gene function. Nature *383*, 407-413.

Chipuk,J.E., Cornelius,S.C., Pultz,N.J., Jorgensen,J.S., Bonham,M.J., Kim,S.J., and Danielpour,D. (2002). The androgen receptor represses transforming growth factor-beta signaling through interaction with Smad3. J. Biol. Chem. *277*, 1240-1248.

Christoffels,V.M., Grange,T., Kaestner,K.H., Cole,T.J., Darlington,G.J., Croniger,C.M., and Lamers,W.H. (1998). Glucocorticoid receptor, C/EBP, HNF3, and protein kinase A coordinately activate the glucocorticoid response unit of the carbamoylphosphate synthetase I gene. Mol. Cell Biol. *18*, 6305-6315.

Chuang,P.T., Kawcak,T., and McMahon,A.P. (2003). Feedback control of mammalian Hedgehog signaling by the Hedgehog-binding protein, Hip1, modulates Fgf signaling during branching morphogenesis of the lung. Genes Dev. *17*, 342-347.

Chuang,P.T. and McMahon,A.P. (2003). Branching morphogenesis of the lung: new molecular insights into an old problem. Trends Cell Biol. *13*, 86-91.

Cirillo,L.A., Lin,F.R., Cuesta,I., Friedman,D., Jarnik,M., and Zaret,K.S. (2002). Opening of compacted chromatin by early developmental transcription factors HNF3 (FoxA) and GATA-4. Mol. Cell *9*, 279-289.

Cirillo,L.A., McPherson,C.E., Bossard,P., Stevens,K., Cherian,S., Shim,E.Y., Clark,K.L., Burley,S.K., and Zaret,K.S. (1998). Binding of the winged-helix transcription factor HNF3 to a linker histone site on the nucleosome. EMBO J. *17*, 244-254.

Claessens,F., Dirckx,L., Delaey,B., Decourt,J.L., Hemschoote,K., Peeters,B., and Rombauts,W. (1989). The androgen-dependent rat prostatic binding protein: comparison of the sequences in the 5' part and upstream region of the C1 and C2 genes and analysis of their transcripts. Journal of Molecular Endocrinology *3*, 93-103.

Claessens,F., Verrijdt,G., Schoenmakers,E., Haelens,A., Peeters,B., Verhoeven,G., and Rombauts,W. (2001). Selective DNA binding by the androgen receptor as a mechanism for hormone-specific gene regulation. J. Steroid Biochem. Mol. Biol. *76*, 23-30.

Clark,K.L., Halay,E.D., Lai,E., and Burley,S.K. (1993). Co-crystal structure of the HNF-3/fork head DNA-recognition motif resembles histone H5. Nature *364*, 412-420.

Cleutjens,K.B., van der Korput,H.A., van Eekelen,C.C., van Rooij,H.C., Faber,P.W., and Trapman,J. (1997). An androgen response element in a far upstream enhancer region is essential for high, androgen-regulated activity of the prostate- specific antigen promoter. Mol. Endocrinol. *11*, 148-161.

Collins,A.T., Habib,F.K., Maitland,N.J., and Neal,D.E. (2001). Identification and isolation of human prostate epithelial stem cells based on alpha(2)beta(1)-integrin expression. J. Cell Sci. *114*, 3865-3872.

Collins,A.T., Robinson,E.J., and Neal,D.E. (1996). Benign prostatic stromal cells are regulated by basic fibroblast growth factor and transforming growth factor-beta 1. J. Endocrinol. *151*, 315-322.

Cooke,P.S., Young,P., and Cunha,G.R. (1991). Androgen receptor expression in developing male reproductive organs. Endocrinology *128*, 2867-2873.

Costa,R.H., Grayson,D.R., and Darnell,J.E., Jr. (1989). Multiple hepatocyte-enriched nuclear factors function in the regulation of transthyretin and alpha 1-antitrypsin genes. Mol. Cell Biol. *9*, 1415-1425.

Crowe,A.J., Sang,L., Li,K.K., Lee,K.C., Spear,B.T., and Barton,M.C. (1999). Hepatocyte nuclear factor 3 relieves chromatin-mediated repression of the alpha-fetoprotein gene. J. Biol. Chem. *274*, 25113-25120.

Culig,Z., Hobisch,A., Cronauer,M.V., Radmayr,C., Hittmair,A., Zhang,J., Thurnher,M., Bartsch,G., and Klocker,H. (1996). Regulation of prostatic growth and function by peptide growth factors. Prostate *28*, 392-405.

Cunha,G.R. (1972). Epithelio-mesenchymal interactions in primordial gland structures which become responsive to androgenic stimulation. Anat. Rec. *172*, 179-195.

Cunha,G.R. (1973). The role of androgens in the epithelio-mesenchymal interactions involved in prostatic morphogenesis in embryonic mice. Anat. Rec. *175*, 87-96.

Cunha,G.R. (1975). Age-dependent loss of sensitivity of female urogenital sinus to androgenic conditions as a function of the epithelia-stromal interaction in mice. Endocrinology *97*, 665-673.

Cunha,G.R., Alarid,E.T., Turner,T., Donjacour,A.A., Boutin,E.L., and Foster,B.A. (1992). Normal and abnormal development of the male urogenital tract. Role of androgens, mesenchymal-epithelial interactions, and growth factors. J. Androl. *13*, 465-475.

Cunha,G.R. and Chung,L.W. (1981). Stromal-epithelial interactions--I. Induction of prostatic phenotype in urothelium of testicular feminized (Tfm/y) mice. J. Steroid Biochem. *14*, 1317-1324.

Cunha,G.R., Chung,L.W., Shannon,J.M., and Reese,B.A. (1980a). Stromal-epithelial interactions in sex differentiation. Biol. Reprod. *22*, 19-42.

Cunha,G.R. and Donjacour,A. (1987). Mesenchymal-epithelial interactions: technical considerations. Prog. Clin. Biol. Res. *239*, 273-282.

Cunha,G.R., Donjacour,A.A., Cooke,P.S., Mee,S., Bigsby,R.M., Higgins,S.J., and Sugimura,Y. (1987). The endocrinology and developmental biology of the prostate. Endocr. Rev. *8*, 338-362.

Cunha,G.R., Fujii,H., Neubauer,B.L., Shannon,J.M., Sawyer,L., and Reese,B.A. (1983). Epithelial-mesenchymal interactions in prostatic development. I. morphological observations of prostatic induction by urogenital sinus mesenchyme in epithelium of the adult rodent urinary bladder. J. Cell Biol. *96*, 1662-1670.

Cunha,G.R., Hayward,S.W., Dahiya,R., and Foster,B.A. (1996). Smooth muscle-epithelial interactions in normal and neoplastic prostatic development. Acta Anat. (Basel) *155*, 63-72.

Cunha,G.R. and Lung,B. (1978). The possible influence of temporal factors in androgenic responsiveness of urogenital tissue recombinants from wild-type and androgen- insensitive (Tfm) mice. J. Exp. Zool. *205*, 181-193.

Cunha,G.R., Lung,B., and Reese,B. (1980b). Glandular epithelial induction by embryonic mesenchyme in adult bladder epithelium of BALB/c mice. Invest Urol. *17*, 302-304.

Cunha,G.R., Shannon,J.M., Neubauer,B.L., Sawyer,L.M., Fujii,H., Taguchi,O., and Chung,L.W. (1981). Mesenchymal-epithelial interactions in sex differentiation. Hum. Genet. *58*, 68-77.

Dahmane,N., Lee,J., Robins,P., Heller,P., and Altaba,A. (1997). Activation of the transcription factor Gli1 and the Sonic hedgehog signalling pathway in skin tumours. Nature *389*, 876-881.

Danielian,P.S., White,R., Lees,J.A., and Parker,M.G. (1992). Identification of a conserved region required for hormone dependent transcriptional activation by steroid hormone receptors. EMBO J. *11*, 1025-1033.

Dedhar,S., Rennie,P.S., Shago,M., Haegelstein,C.-Y.L., Yang,H., Filmus,J., Hawley,R.G., Bruchovsky,N., Cheng,H., Matusik,R.J., and Giguere,V. (1994). Inhibition of nuclear hormone receptor activity by calreticulin. Nature *376*, 480-483.

Derynck,R., Zhang,Y., and Feng,X.H. (1998). Smads: transcriptional activators of TGF-beta responses. Cell *95*, 737-740.

Deutsch,G., Jung,J., Zheng,M., Lora,J., and Zaret,K.S. (2001). A bipotential precursor population for pancreas and liver within the embryonic endoderm. Development *128*, 871-881.

Dillon,R., Gadgil,C., and Othmer,H.G. (2003). Short- and long-range effects of Sonic hedgehog in limb development. Proc. Natl. Acad. Sci. U. S. A *100*, 10152-10157.

Djakiew,D. (2000). Dysregulated expression of growth factors and their receptors in the development of prostate cancer. Prostate *42*, 150-160.

Dominguez,I., Itoh,K., and Sokol,S.Y. (1995). Role of glycogen synthase kinase 3 beta as a negative regulator of dorsoventral axis formation in Xenopus embryos. Proc. Natl. Acad. Sci. U. S. A *92*, 8498-8502.

Donjacour,A.A. and Cunha,G.R. (1988). The effect of androgen deprivation on branching morphogenesis in the mouse prostate. Dev. Biol. *128*, 1-14.

Donjacour,A.A. and Cunha,G.R. (1993). Assessment of prostatic protein secretion in tissue recombinants made of urogenital sinus mesenchyme and urothelium from normal or androgen-insensitive mice. Endocrinology *132*, 2342-2350.

Donjacour,A.A., Rosales,A., Higgins,S.J., and Cunha,G.R. (1990). Characterization of antibodies to androgen-dependent secretory proteins of the mouse dorsolateral prostate. Endocrinology *126*, 1343-1354.

Donjacour,A.A., Thomson,A.A., and Cunha,G.R. (2003). FGF-10 plays an essential role in the growth of the fetal prostate. Dev. Biol. *261*, 39-54.

Dupont,S., Krust,A., Gansmuller,A., Dierich,A., Chambon,P., and Mark,M. (2000). Effect of single and compound knockouts of estrogen receptors alpha (ERalpha) and beta (ERbeta) on mouse reproductive phenotypes. Development *127*, 4277-4291.

Echelard,Y., Epstein,D.J., St Jacques,B., Shen,L., Mohler,J., McMahon,J.A., and McMahon,A.P. (1993a). Sonic hedgehog, a member of a family of putative signaling molecules, is implicated in the regulation of CNS polarity. Cell *75*, 1417-1430.

Echelard,Y., Epstein,D.J., St Jacques,B., Shen,L., Mohler,J., McMahon,J.A., and McMahon,A.P. (1993b). Sonic hedgehog, a member of a family of putative signaling molecules, is implicated in the regulation of CNS polarity. Cell *75*, 1417-1430.

Economides,K.D. and Capecchi,M.R. (2003). Hoxb13 is required for normal differentiation and secretory function of the ventral prostate. Development *130*, 2061-2069.

Elger,W., Graf,K.J., Steinbeck,H., and Neumann,F. (1974). Hormonal control of sexual development. Adv. Biosci. *13*, 41-69.

Espinas,M.L., Roux,J., Pictet,R., and Grange,T. (1995). Glucocorticoids and protein kinase A coordinately modulate transcription factor recruitment at a glucocorticoid-responsive unit. Mol. Cell Biol. *15*, 5346-5354.

Fan,L., Pepicelli,C.V., Dibble,C.C., Catbagan,W., Zarycki,J.L., Laciak,R., Gipp,J., Shaw,A., Lamm,M.L., Munoz,A., Lipinski,R., Thrasher,J.B., and Bushman,W. (2004). Hedgehog signaling promotes prostate xenograft tumor growth. Endocrinology *145*, 3961-3970.

Fang,Y., Fliss,A.E., Robins,D.M., and Caplan,A.J. (1996). Hsp90 regulates androgen receptor hormone binding affinity in vivo. J. Biol. Chem. *271*, 28697-28702.

Farmer,G., Connolly,E.S., Jr., Mocco,J., and Freedman,L.P. (2001). Molecular analysis of the prostate-specific antigen upstream gene enhancer. Prostate *46*, 76-85.

Feldman,R.J., Sementchenko,V.I., Gayed,M., Fraig,M.M., and Watson,D.K. (2003). Pdef expression in human breast cancer is correlated with invasive potential and altered gene expression. Cancer Res *63*, 4626-4631.

Freestone,S.H., Marker,P., Grace,O.C., Tomlinson,D.C., Cunha,G.R., Harnden,P., and Thomson,A.A. (2003). Sonic hedgehog regulates prostatic growth and epithelial differentiation. Dev. Biol. *264*, 352-362.

Fronsdal,K., Engedal,N., Slagsvold,T., and Saatcioglu,F. (1998). CREB binding protein is a coactivator for the androgen receptor and mediates cross-talk with AP-1. J. Biol. Chem. *273*, 31853-31859.

Furumoto,T.A., Miura,N., Akasaka,T., Mizutani-Koseki,Y., Sudo,H., Fukuda,K., Maekawa,M., Yuasa,S., Fu,Y., Moriya,H., Taniguchi,M., Imai,K., Dahl,E., Balling,R., Pavlova,M., Gossler,A., and Koseki,H. (1999). Notochord-dependent expression of MFH1 and PAX1 cooperates to maintain the proliferation of sclerotome cells during the vertebral column development. Dev. Biol. *210*, 15-29.

Fuse,N., Maiti,T., Wang,B., Porter,J.A., Hall,T.M., Leahy,D.J., and Beachy,P.A. (1999). Sonic hedgehog protein signals not as a hydrolytic enzyme but as an apparent ligand for patched. Proc. Natl. Acad. Sci. U. S. A *96*, 10992-10999.

Gailani,M.R., Stahle-Backdahl,M., Leffell,D.J., Glynn,M., Zaphiropoulos,P.G., Pressman,C., Unden,A.B., Dean,M., Brash,D.E., Bale,A.E., and Toftgard,R. (1996). The role of the human homologue of Drosophila patched in sporadic basal cell carcinomas. Nat. Genet. *14*, 78-81.

Gannon,M. and Bader,D. (1995). Initiation of cardiac differentiation occurs in the absence of anterior endoderm. Development *121*, 2439-2450.

Gao,N., Zhang,J., Rao,M.A., Case,T.C., Mirosevich,J., Wang,Y., Jin,R., Gupta,A., Rennie,P.S., and Matusik,R.J. (2003). The role of hepatocyte nuclear factor-3 alpha (Forkhead Box A1) and androgen receptor in transcriptional regulation of prostatic genes. Mol. Endocrinol. *17*, 1484-1507.

Garabedian,E.M., Humphrey,P.A., and Gordon,J.I. (1998). A transgenic mouse model of metastatic prostate cancer originating from neuroendocrine cells. Proc. Natl. Acad. Sci. U. S. A *95*, 15382-15387.

Gaudet,J. and Mango,S.E. (2002). Regulation of organogenesis by the Caenorhabditis elegans FoxA protein PHA-4. Science *295*, 821-825.

Gelmann,E.P. (2002). Molecular biology of the androgen receptor. J. Clin. Oncol. *20*, 3001-3015.

Green,J.E., Greenberg,N.M., Ashendel,C.L., Barrett JC, Boone,C.W., Getzenberg,R.H., Henkin,J., Matusik,R.J., Janus,T.J., and Scher,H.I. (1998). Transgenic and Reconstitution Models of Prostate Cancer. The Prostate *36*, 59-63.

Greenberg,N.M., DeMayo,F.J., Finegold,M.J., Medina,D., Tilley,W.D., Aspinall,J.O., Cunha,G.R., Donjacour,A.A., Matusik,R.J., and Rosen,J.M. (1995). Prostate cancer in a transgenic mouse. Proc Natl Acad Sci U S A *92*, 3439-3443.

Greenberg,N.M., DeMayo,F.J., Sheppard,P.C., Barrios,R., Lebovitz,M., Finegold,M., Angelopoulou,R., Dodd,J.G., Duckworth,M.L., Rosen,J.M., and Matusik,R.J. (1994). The rat probasin gene promoter directs hormonally and developmentally regulated expression of a heterologous gene specifically to the prostate in transgenic mice. Molecular Endocrinology *8*, 230-239.

Gregory,C.W., Fei,X., Ponguta,L.A., He,B., Bill,H.M., French,F.S., and Wilson,E.M. (2004). Epidermal growth factor increases coactivation of the androgen receptor in recurrent prostate cancer. J. Biol. Chem. *279*, 7119-7130.

Griffin,J.E. and Wilson,J.D. (1984). Disorders of androgen receptor function. Ann. N. Y. Acad. Sci. *438*, 61-71.

Gualdi,R., Bossard,P., Zheng,M., Hamada,Y., Coleman,J.R., and Zaret,K.S. (1996). Hepatic specification of the gut endoderm in vitro: cell signaling and transcriptional control. Genes Dev. *10*, 1670-1682.

Guerrero,I. and Altaba,A. (2003). Development. Longing for ligand: hedgehog, patched, and cell death. Science *301*, 774-776.

Guo,L., Degenstein,L., and Fuchs,E. (1996). Keratinocyte growth factor is required for hair development but not for wound healing. Genes Dev. *10*, 165-175.

Guo,Y., Costa,R., Ramsey,H., Starnes,T., Vance,G., Robertson,K., Kelley,M., Reinbold,R., Scholer,H., and Hromas,R. (2002). The embryonic stem cell transcription factors Oct-4 and FoxD3 interact to regulate endodermal-specific promoter expression. Proc. Natl. Acad. Sci. U. S. A *99*, 3663-3667.

Harris,S.E., Harris,M.A., Mahy,P., Wozney,J., Feng,J.Q., and Mundy,G.R. (1994). Expression of bone morphogenetic protein messenger RNAs by normal rat and human prostate and prostate cancer cells. Prostate *24*, 204-211.

Hayes SA, Zarnegar M, Sharma M, Yang F, Peehl DM, ten Dijke P, and Sun Z. SMAD3 Represses Androgen Receptor-mediated Transcription. Cancer Res 61, 2112-2118. 3-1-2001.
Ref Type: Abstract

Hayward,S.W. (2002). Approaches to modeling stromal-epithelial interactions. J. Urol. *168*, 1165-1172.

Hayward,S.W., Baskin,L.S., Haughney,P.C., Cunha,A.R., Foster,B.A., Dahiya,R., Prins,G.S., and Cunha,G.R. (1996a). Epithelial development in the rat ventral prostate, anterior prostate and seminal vesicle. Acta Anat. (Basel) *155*, 81-93.

Hayward,S.W., Baskin,L.S., Haughney,P.C., Foster,B.A., Cunha,A.R., Dahiya,R., Prins,G.S., and Cunha,G.R. (1996b). Stromal development in the ventral prostate, anterior prostate and seminal vesicle of the rat. Acta Anat. (Basel) *155*, 94-103.

Hayward,S.W., Haughney,P.C., Rosen,M.A., Greulich,K.M., Weier,H.U., Dahiya,R., and Cunha,G.R. (1998). Interactions between adult human prostatic epithelium and rat urogenital sinus mesenchyme in a tissue recombination model. Differentiation *63*, 131-140.

He,B., Kemppainen,J.A., Voegel,J.J., Gronemeyer,H., and Wilson,E.M. (1999). Activation function 2 in the human androgen receptor ligand binding domain mediates interdomain communication with the NH(2)-terminal domain. J. Biol. Chem. *274*, 37219-37225.

He,B., Kemppainen,J.A., and Wilson,E.M. (2000). FXXLF and WXXLF sequences mediate the NH2-terminal interaction with the ligand binding domain of the androgen receptor. J. Biol. Chem. *275*, 22986-22994.

He,X., Saint-Jeannet,J.P., Woodgett,J.R., Varmus,H.E., and Dawid,I.B. (1995). Glycogen synthase kinase-3 and dorsoventral patterning in Xenopus embryos. Nature *374*, 617-622.

Heasman,J., Crawford,A., Goldstone,K., Garner-Hamrick,P., Gumbiner,B., McCrea,P., Kintner,C., Noro,C.Y., and Wylie,C. (1994). Overexpression of cadherins and underexpression of beta-catenin inhibit dorsal mesoderm induction in early Xenopus embryos. Cell *79*, 791-803.

Heinlein,C.A. and Chang,C. (2002). Androgen Receptor (AR) Coregulators: An Overview. Endocr. Rev. *23*, 175-200.

Hiramatsu,M., Kashimata,M., Minami,N., Sato,A., Murayama,M., and Minami,N. (1988). Androgenic regulation of epidermal growth factor in the mouse ventral prostate. Biochem. Int. *17*, 311-317.

Hogan,B.L. and Kolodziej,P.A. (2002). Organogenesis: molecular mechanisms of tubulogenesis. Nat. Rev. Genet. *3*, 513-523.

Hogg,N.A., Harrison,C.J., and Tickle,C. (1983). Lumen formation in the developing mouse mammary gland. J. Embryol. Exp. Morphol. *73*, 39-57.

Horner,M.A., Quintin,S., Domeier,M.E., Kimble,J., Labouesse,M., and Mango,S.E. (1998). pha-4, an HNF-3 homolog, specifies pharyngeal organ identity in Caenorhabditis elegans. Genes Dev. *12*, 1947-1952.

Horvath,L.G., Henshall,S.M., Kench,J.G., Turner,J.J., Golovsky,D., Brenner,P.C., O'Neill,G.F., Kooner,R., Stricker,P.D., Grygiel,J.J., and Sutherland,R.L. (2004). Loss of BMP2, Smad8, and Smad4 expression in prostate cancer progression. Prostate *59*, 234-242.

Howell,M., Itoh,F., Pierreux,C.E., Valgeirsdottir,S., Itoh,S., ten Dijke,P., and Hill,C.S. (1999). Xenopus Smad4beta is the co-Smad component of developmentally regulated transcription factor complexes responsible for induction of early mesodermal genes. Dev. Biol. *214*, 354-369.

Hsiao,P.W. and Chang,C. (1999). Isolation and characterization of ARA160 as the first androgen receptor N-terminal-associated coactivator in human prostate cells. J. Biol. Chem. *274*, 22373-22379.

Huang,L., Pu,Y., Alam,S., Birch,L., and Prins,G.S. (2004). Estrogenic regulation of signaling pathways and homeobox genes during rat prostate development. J. Androl *25*, 330-337.

Huang,W., Shostak,Y., Tarr,P., Sawyers,C., and Carey,M. (1999). Cooperative Assembly of Androgen Receptor into a Nucleoprotein Complex That Regulates the Prostate-specific Antigen Enhancer. J. Biol. Chem. *274*, 25756-25768.

Hubbard,S.R., Mohammadi,M., and Schlessinger,J. (1998). Autoregulatory mechanisms in protein-tyrosine kinases. J. Biol. Chem. *273*, 11987-11990.

Hunter,T. (2000). Signaling--2000 and beyond. Cell *100*, 113-127.

Hynes,M., Stone,D.M., Dowd,M., Pitts-Meek,S., Goddard,A., Gurney,A., and Rosenthal,A. (1997). Control of cell pattern in the neural tube by the zinc finger transcription factor and oncogene Gli-1. Neuron *19*, 15-26.

Ichinose,H., Garnier,J.M., Chambon,P., and Losson,R. (1997). Ligand-dependent interaction between the estrogen receptor and the human homologues of SWI2/SNF2. Gene *188*, 95-100.

Ikonen,T., Palvimo,J.J., and Janne,O.A. (1997). Interaction between the amino- and carboxyl-terminal regions of the rat androgen receptor modulates transcriptional activity and is influenced by nuclear receptor coactivators. J. Biol. Chem. *272*, 29821-29828.

Ilio,K.Y., Sensibar,J.A., and Lee,C. (1995). Effect of TGF-beta 1, TGF-alpha, and EGF on cell proliferation and cell death in rat ventral prostatic epithelial cells in culture. J Androl *16*, 482-490.

Imai,K., Takada,N., Satoh,N., and Satou,Y. (2000). (beta)-catenin mediates the specification of endoderm cells in ascidian embryos. Development *127*, 3009-3020.

Ingham,P.W. (1991). Segment polarity genes and cell patterning within the Drosophila body segment. Curr. Opin. Genet. Dev. *1* , 261-267.

Ingham,P.W. and McMahon,A.P. (2001). Hedgehog signaling in animal development: paradigms and principles. Genes Dev. *15*, 3059-3087.

Itoh,N., Patel,U., Cupp,A.S., and Skinner,M.K. (1998). Developmental and hormonal regulation of transforming growth factor-beta1 (TGFbeta1), -2, and -3 gene expression in isolated prostatic epithelial and stromal cells: epidermal growth factor and TGFbeta interactions. Endocrinology *139*, 1378-1388.

Jackson,D.A., Rowader,K.E., Stevens,K., Jiang,C., Milos,P., and Zaret,K.S. (1993). Modulation of liver-specific transcription by interactions between hepatocyte nuclear factor 3 and nuclear factor 1 binding DNA in close apposition. Mol. Cell Biol. *13*, 2401-2410.

Jarred,R.A., McPherson,S.J., Bianco,J.J., Couse,J.F., Korach,K.S., and Risbridger,G.P. (2002). Prostate phenotypes in estrogen-modulated transgenic mice. Trends Endocrinol. Metab *13*, 163-168.

Jaskoll,T., Leo,T., Witcher,D., Ormestad,M., Astorga,J., Bringas,P., Jr., Carlsson,P., and Melnick,M. (2004). Sonic hedgehog signaling plays an essential role during embryonic salivary gland epithelial branching morphogenesis. Dev. Dyn. *229*, 722-732.

Jenster,G., Trapman,J., and Brinkmann,A.O. (1993). Nuclear import of the human androgen receptor. Biochem. J. *293*, 761-768.

Jenster,G., van der Korput,H.A., Trapman,J., and Brinkmann,A.O. (1995). Identification of two transcription activation units in the N-terminal domain of the human androgen receptor. J. Biol. Chem. *270*, 7341-7346.

Jenster,G., van der Korput,H.A., van Vroonhoven,C., van der Kwast,T.H., Trapman,J., and Brinkmann,A.O. (1991). Domains of the human androgen receptor involved in steroid binding, transcriptional activation, and subcellular localization. Molecular Endocrinology *5*, 1396-1404.

Jia,L., Choong,C.S., Ricciardelli,C., Kim,J., Tilley,W.D., and Coetzee,G.A. (2004). Androgen receptor signaling: mechanism of interleukin-6 inhibition. Cancer Res *64*, 2619-2626.

Jiang,G. and Hunter,T. (1999). Receptor signaling: when dimerization is not enough. Curr. Biol. *9*, R568-R571.

Jost A (1953). Problems of fetal endocrinology: the gonadal and hypophyseal hormones. Recent Prog Horm Res *8*, 379.

Kaestner,K.H., Katz,J., Liu,Y., Drucker,D.J., and Schutz,G. (1999). Inactivation of the winged helix transcription factor HNF3alpha affects glucose homeostasis and islet glucagon gene expression in vivo. Genes Dev. *13*, 495-504.

Kaestner,K.H., Knochel,W., and Martinez,D.E. (2000). Unified nomenclature for the winged helix/forkhead transcription factors. Genes Dev. *14*, 142-146.

Kalb,J.M., Lau,K.K., Goszczynski,B., Fukushige,T., Moons,D., Okkema,P.G., and McGhee,J.D. (1998). pha-4 is Ce-fkh-1, a fork head/HNF-3alpha,beta,gamma homolog that functions in organogenesis of the C. elegans pharynx. Development *125*, 2171-2180.

Kallio,P.J., Poukka,H., Moilanen,A., Janne,O.A., and Palvimo,J.J. (1995). Androgen receptor-mediated transcriptional regulation in the absence of direct interaction with a specific DNA element. Mol. Endocrinol. *9*, 1017-1028.

Kang,H.Y., Huang,K.E., Chang,S.Y., Ma,W.L., Lin,W.J., and Chang,C. (2002). Differential modulation of androgen receptor-mediated transactivation by Smad3 and tumor suppressor Smad4. J. Biol. Chem. *277*, 43749-43756.

Kang,H.Y., Lin,H.K., Hu,Y.C., Yeh,S., Huang,K.E., and Chang,C. From transforming growth factor-beta signaling to androgen action: Identification of Smad3 as an androgen receptor coregulator in prostate cancer cells. Proc. Natl. Acad. Sci. U. S. A. 2001. Mar. 13. ;98. (6.):3018. -3023. *98*, 3018-3023.

Kasper,S. and Matusik,R.J. (2000). Rat probasin: structure and function of an outlier lipocalin. Biochim. Biophys. Acta *1482* , 249-258.

Kasper,S., Rennie,P.S., Bruchovsky,N., Lin,L., Cheng,H., Snoek,R., Dahlman-Wright,K., Gustafsson,J.A., Shui,R., Sheppard,P.C., and Matusik,R.J. (1999). Selective activation of

the probasin androgen responsive region by steroid hormones. Journal of Molecular Endocrinology *22*, 313-325.

Kasper,S., Rennie,P.S., Bruchovsky,N., Sheppard,P.C., Cheng,H., Lin,L., Shiu,R.P.C., Snoek,R., and Matusik,R.J. (1994). Cooperative binding of androgen receptors to two DNA sequences is required for androgen induction of the probasin gene. J. Biol. Chem. *269*, 31763-31769.

Kasper,S., Sheppard,P.C., Yan,Y., Pettigrew,N., Borowsky,A.D., Prins,G.S., Dodd,J.G., Duckworth,M.L., and Matusik,R.J. (1998). Development, Progression And Androgen-Dependence of Prostate Tumors in Transgenic: A Model For Prostate Cancer. Laboratory Investigation *78*, 319-334.

Kaufmann,E. and Knochel,W. (1996). Five years on the wings of fork head. Mech. Dev. *57*, 3-20.

Kim,M.J., Cardiff,R.D., Desai,N., Banach-Petrosky,W.A., Parsons,R., Shen,M.M., and Abate-Shen,C. (2002). Cooperativity of Nkx3.1 and Pten loss of function in a mouse model of prostate carcinogenesis. Proc. Natl. Acad. Sci. U. S. A *99*, 2884-2889.

Klingensmith,J., Nusse,R., and Perrimon,N. (1994). The Drosophila segment polarity gene dishevelled encodes a novel protein required for response to the wingless signal. Genes Dev. *8*, 118-130.

Kopachik,W., Hayward,S.W., and Cunha,G.R. (1998). Expression of hepatocyte nuclear factor-3alpha in rat prostate, seminal vesicle, and bladder. Dev. Dyn. *211*, 131-140.

Korinek,V., Barker,N., Morin,P.J., van Wichen,D., de Weger,R., Kinzler,K.W., Vogelstein,B., and Clevers,H. (1997). Constitutive transcriptional activation by a beta-catenin-Tcf complex in APC-/- colon carcinoma. Science *275*, 1784-1787.

Kratochwil,K. (1969). Organ specificity in mesenchymal induction demonstrated in the embryonic development of the mammary gland of the mouse. Dev. Biol. *20*, 46-71.

Kupfer,S.R., Marschke,K.B., Wilson,E.M., and French,F.S. (1993). Receptor accessory factor enhances specific DNA binding of androgen and glucocorticoid receptors. J. Biol. Chem. *268*, 17519-17527.

Lai,E., Clark,K.L., Burley,S.K., and Darnell,J.E., Jr. (1993). Hepatocyte nuclear factor 3/fork head or "winged helix" proteins: a family of transcription factors of diverse biologic function. Proc. Natl. Acad. Sci. U. S. A *90*, 10421-10423.

Lai,E., Prezioso,V.R., Smith,E., Litvin,O., Costa,R.H., and Darnell,J.E., Jr. (1990). HNF-3A, a hepatocyte-enriched transcription factor of novel structure is regulated transcriptionally. Genes Dev. *4*, 1427-1436.

Lai,E., Prezioso,V.R., Tao,W.F., Chen,W.S., and Darnell,J.E., Jr. (1991). Hepatocyte nuclear factor 3 alpha belongs to a gene family in mammals that is homologous to the Drosophila homeotic gene fork head. Genes Dev. *5*, 416-427.

Lai,E.C. (2004). Notch signaling: control of cell communication and cell fate. Development *131*, 965-973.

Lai,J.S. and Herr,W. (1992). Ethidium bromide provides a simple tool for identifying genuine DNA-independent protein associations. Proc. Natl. Acad. Sci. U. S. A *89*, 6958-6962.

Lamm,M.L., Catbagan,W.S., Laciak,R.J., Barnett,D.H., Hebner,C.M., Gaffield,W., Walterhouse,D., Iannaccone,P., and Bushman,W. (2002). Sonic hedgehog activates mesenchymal Gli1 expression during prostate ductal bud formation. Dev. Biol. *249*, 349-366.

Lamm,M.L., Podlasek,C.A., Barnett,D.H., Lee,J., Clemens,J.Q., Hebner,C.M., and Bushman,W. (2001). Mesenchymal factor bone morphogenetic protein 4 restricts ductal budding and branching morphogenesis in the developing prostate. Dev. Biol. *232*, 301-314.

Larabell,C.A., Torres,M., Rowning,B.A., Yost,C., Miller,J.R., Wu,M., Kimelman,D., and Moon,R.T. (1997). Establishment of the dorso-ventral axis in Xenopus embryos is presaged by early asymmetries in beta-catenin that are modulated by the Wnt signaling pathway. J. Cell Biol. *136*, 1123-1136.

Lasnitzki,I., Franklin,H.R., and Wilson,J.D. (1974). The mechanism of androgen uptake and concentration by rat ventral prostate in organ culture. J. Endocrinol. *60*, 81-90.

Lasnitzki,I. and Mizuno,T. (1977). Induction of the rat prostate gland by androgens in organ culture. J. Endocrinol. *74*, 47-55.

Lasnitzki,I. and Mizuno,T. (1980). Prostatic induction: interaction of epithelium and mesenchyme from normal wild-type mice and androgen-insensitive mice with testicular feminization. J. Endocrinol. *85*, 423-428.

Lee,C., Sintich,S.M., Mathews,E.P., Shah,A.H., Kundu,S.D., Perry,K.T., Cho,J.S., Ilio,K.Y., Cronauer,M.V., Janulis,L., and Sensibar,J.A. (1999). Transforming growth factor-beta in benign and malignant prostate. Prostate *39*, 285-290.

Lee,D.K., Duan,H.O., and Chang,C. (2000). From androgen receptor to the general transcription factor TFIIH. Identification of cdk activating kinase (CAK) as an androgen receptor NH(2)-terminal associated coactivator. J. Biol. Chem. *275*, 9308-9313.

Lee,D.K., Duan,H.O., and Chang,C. (2001). Androgen receptor interacts with the positive elongation factor P-TEFb and enhances the efficiency of transcriptional elongation. J. Biol. Chem. *276*, 9978-9984.

Lee,J.J., von Kessler,D.P., Parks,S., and Beachy,P.A. (1992). Secretion and localized transcription suggest a role in positional signaling for products of the segmentation gene hedgehog. Cell *71*, 33-50.

Lemmon,M.A., Ladbury,J.E., Mandiyan,V., Zhou,M., and Schlessinger,J. (1994). Independent binding of peptide ligands to the SH2 and SH3 domains of Grb2. J. Biol. Chem. *269*, 31653-31658.

Lessard,J.L. (1988). Two monoclonal antibodies to actin: one muscle selective and one generally reactive. Cell Motil. Cytoskeleton *10*, 349-362.

Levine,M. and Tjian,R. (2003). Transcription regulation and animal diversity. Nature *424*, 147-151.

Levinson-Dushnik,M. and Benvenisty,N. (1997). Involvement of hepatocyte nuclear factor 3 in endoderm differentiation of embryonic stem cells. Mol. Cell Biol. *17*, 3817-3822.

Lobaccaro,J.M., Poujol,N., Terouanne,B., Georget,V., Fabre,S., Lumbroso,S., and Sultan,C. (1999). Transcriptional interferences between normal or mutant androgen receptors and the activator protein 1--dissection of the androgen receptor functional domains. Endocrinology *140*, 350-357.

Logan,C.Y., Miller,J.R., Ferkowicz,M.J., and McClay,D.R. (1999). Nuclear beta-catenin is required to specify vegetal cell fates in the sea urchin embryo. Development *126*, 345-357.

Lou,W., Ni,Z., Dyer,K., Tweardy,D.J., and Gao,A.C. (2000). Interleukin-6 induces prostate cancer cell growth accompanied by activation of stat3 signaling pathway. Prostate *42*, 239-242.

Lu,W., Luo,Y., Kan,M., and McKeehan,W.L. (1999). Fibroblast growth factor-10. A second candidate stromal to epithelial cell andromedin in prostate. J. Biol. Chem. *274*, 12827-12834.

Lung,B. and Cunha,G.R. (1981). Development of seminal vesicles and coagulating glands in neonatal mice. I. The morphogenetic effects of various hormonal conditions. Anat. Rec. *199*, 73-88.

Machold,R., Hayashi,S., Rutlin,M., Muzumdar,M.D., Nery,S., Corbin,J.G., Gritli-Linde,A., Dellovade,T., Porter,J.A., Rubin,L.L., Dudek,H., McMahon,A.P., and Fishell,G. (2003). Sonic hedgehog is required for progenitor cell maintenance in telencephalic stem cell niches. Neuron *39*, 937-950.

Mahlapuu,M., Enerback,S., and Carlsson,P. (2001). Haploinsufficiency of the forkhead gene Foxf1, a target for sonic hedgehog signaling, causes lung and foregut malformations. Development *128*, 2397-2406.

Marigo,V. and Tabin,C.J. (1996). Regulation of patched by sonic hedgehog in the developing neural tube. Proc. Natl. Acad. Sci. U. S. A *93*, 9346-9351.

Marker,P.C., Donjacour,A.A., Dahiya,R., and Cunha,G.R. (2003). Hormonal, cellular, and molecular control of prostatic development. Dev. Biol. *253*, 165-174.

Massague,J. (1998). TGF-beta signal transduction. Annu. Rev. Biochem. *67*, 753-791.

Massague,J. and Chen,Y.G. (2000). Controlling TGF-beta signaling. Genes Dev. *14*, 627-644.

Massague,J. and Wotton,D. (2000). Transcriptional control by the TGF-beta/Smad signaling system. EMBO J. *19*, 1745-1754.

Masumori, N., Thomas, T. Z., Case, T., Paul, M., Kasper, S., Chaurand, P., Caprioli, R. M., Tsukamoto T, Shappell, S. B., and Matusik, R. J. A probasin-large T antigen transgenic mouse line develops prostate adeno and neuroendocrine carcinoma with metastatic potential. Cancer Res 61, 2239-2249. 2001.
Ref Type: Journal (Full)

Matise,M.P. and Joyner,A.L. (1999). Gli genes in development and cancer. Oncogene *18*, 7852-7859.

Matsuda,T., Junicho,A., Yamamoto,T., Kishi,H., Korkmaz,K., Saatcioglu,F., Fuse,H., and Muraguchi,A. (2001). Cross-talk between signal transducer and activator of transcription 3 and androgen receptor signaling in prostate carcinoma cells. Biochem. Biophys. Res Commun. *283*, 179-187.

Matuo,Y., Nishi,N., Muguruma,Y., Yoshitake,Y., Kurata,N., and Wada,F. (1985). Localization of prostatic basic protein ("probasin") in the rat prostates by use of monoclonal antibody. Biochem. Biophys. Res. Commun. *130*, 293-300.

Mawhinney,M.G. and Neubauer,B.L. (1979). Actions of estrogen in the male. Invest Urol. *16*, 409-420.

McCrea,P.D., Turck,C.W., and Gumbiner,B. (1991). A homolog of the armadillo protein in Drosophila (plakoglobin) associated with E-cadherin. Science *254*, 1359-1361.

McEwan,I.J. and Gustafsson,J. (1997). Interaction of the human androgen receptor transactivation function with the general transcription factor TFIIF. Proc. Natl. Acad. Sci. U. S. A *94*, 8485-8490.

McKenna,N.J. and O'Malley,B.W. (2002). Combinatorial control of gene expression by nuclear receptors and coregulators. Cell *108*, 465-474.

Mirosevich,J., Gao,N., and Matusik,R.J. (2004). Expression of foxa transcription factors in the developing and adult murine prostate. The Prostate *In press*.

Mohler,J. and Vani,K. (1992). Molecular organization and embryonic expression of the hedgehog gene involved in cell-cell communication in segmental patterning of Drosophila. Development *115*, 957-971.

Moilanen,A.M., Karvonen,U., Poukka,H., Janne,O.A., and Palvimo,J.J. (1998a). Activation of androgen receptor function by a novel nuclear protein kinase. Mol. Biol. Cell *9*, 2527-2543.

Moilanen,A.M., Karvonen,U., Poukka,H., Yan,W., Toppari,J., Janne,O.A., and Palvimo,J.J. (1999). A testis-specific androgen receptor coregulator that belongs to a novel family of nuclear proteins. J. Biol. Chem. *274*, 3700-3704.

Moilanen,A.M., Poukka,H., Karvonen,U., Hakli,M., Janne,O.A., and Palvimo,J.J. (1998b). Identification of a novel RING finger protein as a coregulator in steroid receptor-mediated gene transcription. Mol. Cell Biol. *18*, 5128-5139.

Molenaar,M., van de,W.M., Oosterwegel,M., Peterson-Maduro,J., Godsave,S., Korinek,V., Roose,J., Destree,O., and Clevers,H. (1996). XTcf-3 transcription factor mediates beta-catenin-induced axis formation in Xenopus embryos. Cell *86*, 391-399.

Morin,P.J., Sparks,A.B., Korinek,V., Barker,N., Clevers,H., Vogelstein,B., and Kinzler,K.W. (1997). Activation of beta-catenin-Tcf signaling in colon cancer by mutations in beta-catenin or APC. Science *275*, 1787-1790.

Motzny,C.K. and Holmgren,R. (1995). The Drosophila cubitus interruptus protein and its role in the wingless and hedgehog signal transduction pathways. Mech. Dev. *52*, 137-150.

Mulholland,D.J., Cheng,H., Reid,K., Rennie,P.S., and Nelson,C.C. (2002). The androgen receptor can promote Beta -catenin nuclear translocation independently of adenomatous polyposis coli. J. Biol. Chem. *277*, 17933-17943.

Mulholland,D.J., Read,J.T., Rennie,P.S., Cox,M.E., and Nelson,C.C. (2003). Functional localization and competition between the androgen receptor and T-cell factor for nuclear beta-catenin: a means for inhibition of the Tcf signaling axis. Oncogene *22*, 5602-5613.

Mumm,J.S. and Kopan,R. (2000). Notch signaling: from the outside in. Dev. Biol. *228*, 151-165.

Nagel,S.C., vom Saal,F.S., and Welshons,W.V. (1999). Developmental effects of estrogenic chemicals are predicted by an in vitro assay incorporating modification of cell uptake by serum. J. Steroid Biochem. Mol. Biol. *69*, 343-357.

Naski,M.C. and Ornitz,D.M. (1998). FGF signaling in skeletal development. Front Biosci. *3*, D781-D794.

Nemeth,J.A., Zelner,D.J., Lang,S., and Lee,C. (1998). Keratinocyte growth factor in the rat ventral prostate: androgen-independent expression. J. Endocrinol. *156*, 115-125.

Neubauer,B.L., Chung,L.W., McCormick,K.A., Taguchi,O., Thompson,T.C., and Cunha,G.R. (1983). Epithelial-mesenchymal interactions in prostatic development. II. Biochemical observations of prostatic induction by urogenital sinus mesenchyme in epithelium of the adult rodent urinary bladder. J. Cell Biol. *96*, 1671-1676.

Neumann,F., Berswordt-Wallrabe,R., V, Elger,W., Steinbeck,H., Hahn,J.D., and Kramer,M. (1970a). Aspects of androgen-dependent events as studied by antiandrogens. Recent Prog Horm Res *26*, 337-410.

Neumann,F., Elger,W., and Steinbeck,H. (1970b). Antiandrogens and reproductive development. Philos. Trans. R. Soc. Lond B Biol. Sci. *259*, 179-184.

Nishi,N., Oya,H., Matsumoto,K., Nakamura,T., Miyanaka,H., and Wada,F. (1996). Changes in gene expression of growth factors and their receptors during castration-induced involution and androgen-induced regrowth of rat prostates. Prostate *28*, 139-152.

Nusse,R. (2003). Wnts and Hedgehogs: lipid-modified proteins and similarities in signaling mechanisms at the cell surface. Development *130*, 5297-5305.

Nusse,R. and Varmus,H.E. (1982). Many tumors induced by the mouse mammary tumor virus contain a provirus integrated in the same region of the host genome. Cell *31*, 99-109.

O'Brien,R.M., Noisin,E.L., Suwanichkul,A., Yamasaki,T., Lucas,P.C., Wang,J.C., Powell,D.R., and Granner,D.K. (1995). Hepatic nuclear factor 3- and hormone-regulated expression of the phosphoenolpyruvate carboxykinase and insulin-like growth factor-binding protein 1 genes. Mol. Cell Biol. *15*, 1747-1758.

Oettgen,P., Finger,E., Sun,Z., Akbarali,Y., Thamrongsak,U., Boltax,J., Grall,F., Dube,A., Weiss,A., Brown,L., Quinn,G., Kas,K., Endress,G., Kunsch,C., and Libermann,T.A. (2000). PDEF, a novel prostate epithelium-specific ets transcription factor, interacts with the androgen receptor and activates prostate-specific antigen gene expression. J. Biol. Chem. *275*, 1216-1225.

Ogryzko,V.V., Schiltz,R.L., Russanova,V., Howard,B.H., and Nakatani,Y. (1996). The transcriptional coactivators p300 and CBP are histone acetyltransferases. Cell *87*, 953-959.

Ohuchi,H., Nakagawa,T., Yamamoto,A., Araga,A., Ohata,T., Ishimaru,Y., Yoshioka,H., Kuwana,T., Nohno,T., Yamasaki,M., Itoh,N., and Noji,S. (1997). The mesenchymal factor, FGF10, initiates and maintains the outgrowth of the chick limb bud through interaction with FGF8, an apical ectodermal factor. Development *124*, 2235-2244.

Onate,S.A., Tsai,S.Y., Tsai,M.J., and O'Malley,B.W. (1995). Sequence and characterization of a coactivator for the steroid hormone receptor superfamily. Science *270*, 1354-1357.

Ozanne,D.M., Brady,M.E., Cook,S., Gaughan,L., Neal,D.E., and Robson,C.N. (2000). Androgen receptor nuclear translocation is facilitated by the f-actin cross-linking protein filamin. Mol. Endocrinol. *14*, 1618-1626.

Palvimo,J., Reinikainen,P., Ikonen,T., Kallio,P., Moilanen,A., and Janne,O.A. (1996). Mutual transcription interference between RelA and androgen receptor. Journal of Biological Chemistry *271*, 24151-24156.

Panet-Raymond,V., Gottlieb,B., Beitel,L.K., Pinsky,L., and Trifiro,M.A. (2000). Interactions between androgen and estrogen receptors and the effects on their transactivational properties. Mol. Cell Endocrinol. *167*, 139-150.

Pang,S., Dannull,J., Kaboo,R., Xie,Y., Tso,C.L., Michel,K., deKernion,J.B., and Belldegrun,A.S. (1997). Identification of a positive regulatory element responsible for tissue-specific expression of prostate-specific antigen. Cancer Research. *57*, 495-499.

Pani,L., Overdier,D.G., Porcella,A., Qian,X., Lai,E., and Costa,R.H. (1992). Hepatocyte nuclear factor 3 beta contains two transcriptional activation domains, one of which is novel and conserved with the Drosophila fork head protein. Mol. Cell Biol. *12*, 3723-3732.

Park,W.Y., Miranda,B., Lebeche,D., Hashimoto,G., and Cardoso,W.V. (1998). FGF-10 is a chemotactic factor for distal epithelial buds during lung development. Dev. Biol. *201*, 125-134.

Patrikainen,L., Shan,J., Porvari,K., and Vihko,P. (1999). Identification of the deoxyribonucleic acid-binding site of a regulatory protein involved in prostate-specific and androgen receptor- dependent gene expression. Endocrinology *140*, 2063-70.

Peehl,D.M. and Rubin,J.S. (1995). Keratinocyte growth factor: an androgen-regulated mediator of stromal-epithelial interactions in the prostate. World J. Urol. *13*, 312-317.

Peehl,D.M. and Sellers,R.G. (1997). Induction of smooth muscle cell phenotype in cultured human prostatic stromal cells. Exp. Cell Res *232*, 208-215.

Perez-Stable,C.M., Pozas,A., and Roos,B.A. (2000). A role for GATA transcription factors in the androgen regulation of the prostate-specific antigen gene enhancer. Mol. Cell Endocrinol. *167*, 43-53.

Peterson,R.S., Clevidence,D.E., Ye,H., and Costa,R.H. (1997). Hepatocyte nuclear factor-3 alpha promoter regulation involves recognition by cell-specific factors, thyroid transcription factor-1, and autoactivation. Cell Growth Differ. *8*, 69-82.

Pires-daSilva,A. and Sommer,R.J. (2003). The evolution of signalling pathways in animal development. Nat. Rev. Genet. *4*, 39-49.

Podlasek,C.A., Barnett,D.H., Clemens,J.Q., Bak,P.M., and Bushman,W. (1999a). Prostate development requires Sonic hedgehog expressed by the urogenital sinus epithelium. Dev. Biol. *209*, 28-39.

Podlasek,C.A., Clemens,J.Q., and Bushman,W. (1999b). Hoxa-13 gene mutation results in abnormal seminal vesicle and prostate development. J. Urol. *161*, 1655-1661.

Pointis,G., Latreille,M.T., and Cedard,L. (1980). Gonado-pituitary relationships in the fetal mouse at various times during sexual differentiation. J. Endocrinol. *86*, 483-488.

Pointis,G., Latreille,M.T., Mignot,T.M., Janssens,Y., and Cedard,L. (1979). Regulation of testosterone synthesis in the fetal mouse testis. J. Steroid Biochem. *11*, 1609-1612.

Prewett,M., Rockwell,P., Rockwell,R.F., Giorgio,N.A., Mendelsohn,J., Scher,H.I., and Goldstein,N.I. (1996). The biologic effects of C225, a chimeric monoclonal antibody to the EGFR, on human prostate carcinoma. J. Immunother. Emphasis. Tumor Immunol. *19*, 419-427.

Price D.,O.E. (1965). The role of fetal androgens in sex differentiation in mammals. In Organogenesis. Holt, Rinehart and Winston, New York, p. 629.

Prins,G.S. (1992). Neonatal estrogen exposure induces lobe-specific alterations in adult rat prostate androgen receptor expression. Endocrinology *130*, 3703-3714.

Prins,G.S. (1997). Developmental Estrogenization of the Prostate Gland. In Prostate: Basic and Clinical Aspects, R.Naz, ed. (Boca Raton New York: CRC Press), pp. 245-263.

Prins, G. S., Birch, L., Habermann, H, Chang, W. Y., Tebeau, C., Putz, O., and Bieberich, C. J. Influence of neonatal estrogens on rat prostate development. Reproduction,.Fertility,.&.Development 13, 241-252. 2001. Ref Type: Journal (Full)

Pu,Y., Huang,L., and Prins,G.S. (2004). Sonic hedgehog-patched Gli signaling in the developing rat prostate gland: lobe-specific suppression by neonatal estrogens reduces ductal growth and branching. Dev. Biol. *in press*.

Qian,X. and Costa,R.H. (1995). Analysis of hepatocyte nuclear factor-3 beta protein domains required for transcriptional activation and nuclear targeting. Nucleic Acids Res *23*, 1184-1191.

Quigley,C.A., De Bellis,A., Marschke,K.B., el Awady,M.K., Wilson,E.M., and French,F.S. (1995). Androgen receptor defects: historical, clinical, and molecular perspectives. Endocr. Rev. *16*, 271-321.

Reid,K.J., Hendy,S.C., Saito,J., Sorensen,P., and Nelson,C.C. (2001). Two classes of androgen receptor elements mediate cooperativity through allosteric interactions. J. Biol. Chem. *276*, 2943-2952.

Rennie,P.S., Bruchovsky,N., Leco,K.J., Sheppard,P.C., McQueen,S.A., Cheng,H., Block,M.E., MacDonald,B.S., Nickel,B.E., Chang,C., Liao,S., Cattini,P.A., and Matusik,R.J. (1993). Characterization of two cis-acting elements involved in the androgen regulation of the probasin gene. Molecular Endocrinology *7*, 23-36.

Riggleman,B., Schedl,P., and Wieschaus,E. (1990). Spatial expression of the Drosophila segment polarity gene armadillo is posttranscriptionally regulated by wingless. Cell *63*, 549-560.

Robson,C.N., Gnanapragasam,V., Byrne,R.L., Collins,A.T., and Neal,D.E. (1999). Transforming growth factor-beta1 up-regulates p15, p21 and p27 and blocks cell cycling in G1 in human prostate epithelium. J. Endocrinol. *160*, 257-266.

Robyr,D., Gegonne,A., Wolffe,A.P., and Wahli,W. (2000). Determinants of vitellogenin B1 promoter architecture. HNF3 and estrogen responsive transcription within chromatin. J. Biol. Chem. *275*, 28291-28300.

Rocheleau,C.E., Downs,W.D., Lin,R., Wittmann,C., Bei,Y., Cha,Y.H., Ali,M., Priess,J.R., and Mello,C.C. (1997b). Wnt signaling and an APC-related gene specify endoderm in early C. elegans embryos. Cell *90*, 707-716.

Rocheleau,C.E., Downs,W.D., Lin,R., Wittmann,C., Bei,Y., Cha,Y.H., Ali,M., Priess,J.R., and Mello,C.C. (1997a). Wnt signaling and an APC-related gene specify endoderm in early C. elegans embryos. Cell *90*, 707-716.

Rodriguez,R., Pozuelo,J.M., Martin,R., Henriques-Gil,N., Haro,M., Arriazu,R., and Santamaria,L. (2003). Presence of neuroendocrine cells during postnatal development in rat prostate: Immunohistochemical, molecular, and quantitative study. Prostate *57*, 176-185.

Ruan,W., Powell-Braxton,L., Kopchick,J.J., and Kleinberg,D.L. (1999). Evidence that insulin-like growth factor I and growth hormone are required for prostate gland development. Endocrinology *140*, 1984-1989.

Ruiz,I.A., Palma,V., and Dahmane,N. (2002). Hedgehog-Gli signalling and the growth of the brain. Nat. Rev. Neurosci. *3*, 24-33.

Sahlen,G.E., Egevad,L., Ahlander,A., Norlen,B.J., Ronquist,G., and Nilsson,B.O. (2002). Ultrastructure of the secretion of prostasomes from benign and malignant epithelial cells in the prostate. Prostate *53*, 192-199.

Sakakura,T., Nishizuka,Y., and Dawe,C.J. (1976). Mesenchyme-dependent morphogenesis and epithelium-specific cytodifferentiation in mouse mammary gland. Science *194*, 1439-1441.

Sasaki,H. and Hogan,B.L. (1993). Differential expression of multiple fork head related genes during gastrulation and axial pattern formation in the mouse embryo. Development *118*, 47-59.

Sasaki,H., Hui,C., Nakafuku,M., and Kondoh,H. (1997). A binding site for Gli proteins is essential for HNF-3beta floor plate enhancer activity in transgenics and can respond to Shh in vitro. Development *124*, 1313-1322.

Sato,N., Sadar,M.D., Bruchovsky,N., Saatcioglu,F., Rennie,P.S., Sato,S., Lange,P.H., and Gleave,M.E. (1997). Androgenic induction of prostate-specific antigen gene is repressed by protein-protein interaction between the androgen receptor and AP-1/c- Jun in the human prostate cancer cell line LNCaP. J. Biol. Chem. *272*, 17485-17494.

Schlessinger,J. (2000). Cell signaling by receptor tyrosine kinases. Cell *103*, 211-225.

Schneider,A., Brand,T., Zweigerdt,R., and Arnold,H. (2000). Targeted disruption of the Nkx3.1 gene in mice results in morphogenetic defects of minor salivary glands: parallels to glandular duct morphogenesis in prostate. Mech. Dev. *95*, 163-174.

Schneider,S., Steinbeisser,H., Warga,R.M., and Hausen,P. (1996). Beta-catenin translocation into nuclei demarcates the dorsalizing centers in frog and fish embryos. Mech. Dev. *57*, 191-198.

Schneikert,J., Peterziel,H., Defossez,P.A., Klocker,H., Launoit,Y., and Cato,A.C. (1996). Androgen receptor-Ets protein interaction is a novel mechanism for steroid hormone-mediated down-modulation of matrix metalloproteinase expression. J. Biol. Chem. *271*, 23907-23913.

Schultheiss,T.M., Xydas,S., and Lassar,A.B. (1995). Induction of avian cardiac myogenesis by anterior endoderm. Development *121*, 4203-4214.

Schuur ER, Henderson GA, Kmetec LA, Miller JD, Lamparski HG, and Henderson DR (1996). - Prostate-specific antigen expression is regulated by an upstream enhancer. - Journal of Biological Chemistry 1996 Mar 22;271(12):7043-51 7043-7051.

Schuur,E.R., Loktev,A.V., Sharma,M., Sun,Z., Roth,R.A., and Weigel,R.J. (2001). Ligand-dependent interaction of estrogen receptor-alpha with members of the forkhead transcription factor family. J. Biol. Chem. *276*, 33554-33560.

Schweisguth,F. (2004). Notch signaling activity. Curr. Biol. *14*, R129-R138.

Schwerk,C., Klotzbucher,M., Sachs,M., Ulber,V., and Klein-Hitpass,L. (1995). Identification of a transactivation function in the progesterone receptor that interacts with the TAFII110 subunit of the TFIID complex. J. Biol. Chem. *270*, 21331-21338.

Senger,K., Armstrong,G.W., Rowell,W.J., Kwan,J.M., Markstein,M., and Levine,M. (2004). Immunity regulatory DNAs share common organizational features in Drosophila. Mol. Cell *13*, 19-32.

Shaffer,P.L., Jivan,A., Dollins,D.E., Claessens,F., and Gewirth,D.T. (2004). Structural basis of androgen receptor binding to selective androgen response elements. Proc. Natl. Acad. Sci. U. S. A *101*, 4758-4763.

Shang,Y., Myers,M., and Brown,M. (2002). Formation of the androgen receptor transcription complex. Mol. Cell *9*, 601-610.

Shannon,J.M. and Cunha,G.R. (1983). Autoradiographic localization of androgen binding in the developing mouse prostate. Prostate *4*, 367-373.

Shearer,R.J., Hendry,W.F., Sommerville,I.F., and Fergusson,J.D. (1973). Plasma testosterone: an accurate monitor of hormone treatment in prostatic cancer. Br. J. Urol. *45*, 668-677.

Sherwood,E.R. and Lee,C. (1995). Epidermal growth factor-related peptides and the epidermal growth factor receptor in normal and malignant prostate. [Review]. World J. of Urology *13*, 290-296.

Shi,Y., Wang,Y.F., Jayaraman,L., Yang,H., Massague,J., and Pavletich,N.P. (1998). Crystal structure of a Smad MH1 domain bound to DNA: insights on DNA binding in TGF-beta signaling. Cell *94*, 585-594.

Shih,D.Q., Navas,M.A., Kuwajima,S., Duncan,S.A., and Stoffel,M. (1999). Impaired glucose homeostasis and neonatal mortality in hepatocyte nuclear factor 3alpha-deficient mice. Proc. Natl. Acad. Sci. U. S. A *96*, 10152-10157.

Shou,J., Ross,S., Koeppen,H., De Sauvage,F.J., and Gao,W.Q. (2001). Dynamics of notch expression during murine prostate development and tumorigenesis. Cancer Res. *61*, 7291-7297.

Signoretti,S., Waltregny,D., Dilks,J., Isaac,B., Lin,D., Garraway,L., Yang,A., Montironi,R., McKeon,F., and Loda,M. (2000). p63 is a prostate basal cell marker and is required for prostate development. Am. J. Pathol. *157*, 1769-1775.

Simental,J.A., Sar,M., Lane,M.V., French,F.S., and Wilson,E.M. (1991). Transcriptional activation and nuclear targeting signals of the human androgen receptor. J. Biol. Chem. *266*, 510-518.

Sinner,D., Rankin,S., Lee,M., and Zorn,A.M. (2004). Sox17 and beta-catenin cooperate to regulate the transcription of endodermal genes. Development *131*, 3069-3080.

Smith,C.L. and Hager,G.L. (1997). Transcriptional regulation of mammalian genes in vivo. A tale of two templates. J. Biol. Chem. *272*, 27493-27496.

Snoek,R., Rennie,P.S., Kasper,S., Matusik,R.J., and Bruchovsky,N. (1996). Induction of cell-free, in vitro transcription by recombinant androgen receptor peptides. Journal of Steroid Biochemistry & Molecular Biology *59*, 243-250.

Spence,A.M., Sheppard,P.C., Davie,J.R., Matuo,Y., Nishi,N., McKeehan,W.L., Dodd,J.G., and Matusik,R.J. (1989). Regulation of a bifunctional mRNA results in synthesis of secreted and nuclear probasin. Proceedings of the National Academy of Sciences of the United States of America *86*, 7843-7847.

Spencer,T.E., Jenster,G., Burcin,M.M., Allis,C.D., Zhou,J., Mizzen,C.A., McKenna,N.J., Onate,S.A., Tsai,S.Y., Tsai,M.J., and O'Malley,B.W. (1997). Steroid receptor coactivator-1 is a histone acetyltransferase. Nature *389*, 194-198.

Spivak-Kroizman,T., Lemmon,M.A., Dikic,I., Ladbury,J.E., Pinchasi,D., Huang,J., Jaye,M., Crumley,G., Schlessinger,J., and Lax,I. (1994). Heparin-induced oligomerization of FGF molecules is responsible for FGF receptor dimerization, activation, and cell proliferation. Cell *79*, 1015-1024.

Staack,A., Donjacour,A.A., Brody,J., Cunha,G.R., and Carroll,P. (2003). Mouse urogenital development: a practical approach. Differentiation *71*, 402-413.

Stafford,J.M., Wilkinson,J.C., Beechem,J.M., and Granner,D.K. (2001). Accessory factors facilitate the binding of glucocorticoid receptor to the phosphoenolpyruvate carboxykinase gene promoter. J. Biol. Chem. *276*, 39885-39891.

Stainier,D.Y. (2002). A glimpse into the molecular entrails of endoderm formation. Genes Dev. *16*, 893-907.

Steinbeck,H., Neumann,F., and Elger,W. (1970). Effect of an anti-androgen on the differentiation of the internal genital organs in dogs. J. Reprod. Fertil. *23*, 223-227.

Stone,D.M., Hynes,M., Armanini,M., Swanson,T.A., Gu,Q., Johnson,R.L., Scott,M.P., Pennica,D., Goddard,A., Phillips,H., Noll,M., Hooper,J.E., de Sauvage,F., and Rosenthal,A. (1996). The tumour-suppressor gene patched encodes a candidate receptor for Sonic hedgehog. Nature *384*, 129-134.

Story,M.T., Hopp,K.A., Meier,D.A., Begun,F.P., and Lawson,R.K. (1993). Influence of transforming growth factor beta 1 and other growth factors on basic fibroblast growth factor level and proliferation of cultured human prostate-derived fibroblasts. Prostate *22*, 183-197.

Sugi,Y. and Lough,J. (1995). Activin-A and FGF-2 mimic the inductive effects of anterior endoderm on terminal cardiac myogenesis in vitro. Dev. Biol. *168*, 567-574.

Sugimura,Y., Cunha,G.R., and Donjacour,A.A. (1986a). Morphogenesis of ductal networks in the mouse prostate. Biol. Reprod. *34*, 961-971.

Sugimura,Y., Cunha,G.R., and Donjacour,A.A. (1986b). Morphological and histological study of castration-induced degeneration and androgen-induced regeneration in the mouse prostate. Biol. Reprod. *34*, 973-983.

Sugimura,Y., Foster,B.A., Hom,Y.K., Lipschutz,J.H., Rubin,J.S., Finch,P.W., Aaronson,S.A., Hayashi,N., Kawamura,J., and Cunha,G.R. (1996). Keratinocyte growth factor (KGF) can replace testosterone in the ductal branching morphogenesis of the rat ventral prostate. Int. J. Dev. Biol. *40*, 941-951.

Sutkowski,D.M., Fong,C.J., Sensibar,J.A., Rademaker,A.W., Sherwood,E.R., Kozlowski,J.M., and Lee,C. (1992). Interaction of epidermal growth factor and transforming growth factor beta in human prostatic epithelial cells in culture. Prostate *21*, 133-143.

Suzuki,H., Ueda,T., Ichikawa,T., and Ito,H. (2003). Androgen receptor involvement in the progression of prostate cancer. Endocr. Relat Cancer *10*, 209-216.

Szuts,D., Eresh,S., and Bienz,M. (1998). Functional intertwining of Dpp and EGFR signaling during Drosophila endoderm induction. Genes Dev. *12*, 2022-2035.

Tabata,T., Eaton,S., and Kornberg,T.B. (1992). The Drosophila hedgehog gene is expressed specifically in posterior compartment cells and is a target of engrailed regulation. Genes Dev. *6*, 2635-2645.

Takeda,H., Lasnitzki,I., and Mizuno,T. (1986). Analysis of prostatic bud induction by brief androgen treatment in the fetal rat urogenital sinus. J. Endocrinol. *110*, 467-470.

Takeda,H., Mizuno,T., and Lasnitzki,I. (1985). Autoradiographic studies of androgen-binding sites in the rat urogenital sinus and postnatal prostate. J. Endocrinol. *104*, 87-92.

Takeshita,A., Yen,P.M., Misiti,S., Cardona,G.R., Liu,Y., and Chin,W.W. (1996). Molecular cloning and properties of a full-length putative thyroid hormone receptor coactivator. Endocrinology *137*, 3594-3597.

Tanaka,M., Komuro,I., Inagaki,H., Jenkins,N.A., Copeland,N.G., and Izumo,S. (2000). Nkx3.1, a murine homolog of Ddrosophila bagpipe, regulates epithelial ductal branching and proliferation of the prostate and palatine glands. Dev. Dyn. *219*, 248-260.

Theisen,H., Purcell,J., Bennett,M., Kansagara,D., Syed,A., and Marsh,J.L. (1994). dishevelled is required during wingless signaling to establish both cell polarity and cell identity. Development *120*, 347-360.

Thibert,C., Teillet,M.A., Lapointe,F., Mazelin,L., Le Douarin,N.M., and Mehlen,P. (2003). Inhibition of neuroepithelial patched-induced apoptosis by sonic hedgehog. Science *301*, 843-846.

Thomson,A.A. (2001). Role of androgens and fibroblast growth factors in prostatic development. Reproduction *121*, 187-195.

Thomson,A.A. and Cunha,G.R. (1999). Prostatic growth and development are regulated by FGF10. Development *126*, 3693-3701.

Thomson,A.A., Foster,B.A., and Cunha,G.R. (1997). Analysis of growth factor and receptor mRNA levels during development of the rat seminal vesicle and prostate. Development *124*, 2431-2439.

Thomson,A.A., Timms,B.G., Barton,L., Cunha,G.R., and Grace,O.C. (2002). The role of smooth muscle in regulating prostatic induction. Development *129*, 1905-1912.

Timme,T.L., Truong,L.D., Merz,V.W., Krebs,T., Kadmon,D., Flanders,K.C., Park,S.H., and Thompson,T.C. (1994). Mesenchymal-epithelial interactions and transforming growth factor-beta expression during mouse prostate morphogenesis. Endocrinology *134*, 1039-1045.

Tomlinson,D.C., Freestone,S.H., Grace,O.C., and Thomson,A.A. (2004). Differential effects of transforming growth factor-beta1 on cellular proliferation in the developing prostate. Endocrinology *145*, 4292-4300.

Triche,T.J. and Harkin,J.C. (1971). An ultrastructural study of hormonally induced squamous metaplasia in the coagulating gland of the mouse prostate. Lab Invest *25*, 596-606.

Ueda,T., Bruchovsky,N., and Sadar,M.D. (2002). Activation of the androgen receptor N-terminal domain by interleukin-6 via MAPK and STAT3 signal transduction pathways. J. Biol. Chem. *277*, 7076-7085.

Vallet,V., Antoine,B., Chafey,P., Vandewalle,A., and Kahn,A. (1995). Overproduction of a truncated hepatocyte nuclear factor 3 protein inhibits expression of liver-specific genes in hepatoma cells. Mol. Cell Biol. *15*, 5453-5460.

van Es,J.H., Barker,N., and Clevers,H. (2003). You Wnt some, you lose some: oncogenes in the Wnt signaling pathway. Curr. Opin. Genet. Dev. *13*, 28-33.

van Ooyen,A. and Nusse,R. (1984). Structure and nucleotide sequence of the putative mammary oncogene int-1; proviral insertions leave the protein-encoding domain intact. Cell *39*, 233-240.

Verrijdt,G., Schoenmakers,E., Alen,P., Haelens,A., Peeters,B., Rombauts,W., and Claessens,F. (1999). Androgen specificity of a response unit upstream of the human secretory component gene is mediated by differential receptor binding to an essential androgen response element. Mol. Endocrinol. *13*, 1558-1570.

Virkkunen,P., Hedberg,P., Palvimo,J.J., Birr,E., Porvari,K., Ruokonen,M., Taavitsainen,P., Janne,O.A., and Vihko,P. (1994). Structural comparison of human and rat prostate-specific acid phosphatase genes and their promoters: identification of putative androgen response elements. Biochem. Biophys. Res. Commun. *202*, 49-57.

vom Saal,F.S., Timms,B.G., Montano,M.M., Palanza,P., Thayer,K.A., Nagel,S.C., Dhar,M.D., Ganjam,V.K., Parmigiani,S., and Welshons,W.V. (1997). Prostate enlargement in mice due to fetal exposure to low doses of estradiol or diethylstilbestrol and opposite effects at high doses. Proc. Natl. Acad. Sci. U. S. A. *94*, 2056-2061.

Walterhouse,D.O., Yoon,J.W., and Iannaccone,P.M. (1999). Developmental pathways: Sonic hedgehog-Patched-GLI. Environ. Health Perspect. *107*, 167-171.

Wang,B.E., Shou,J., Ross,S., Koeppen,H., De Sauvage,F.J., and Gao,W.Q. (2003). Inhibition of epithelial ductal branching in the prostate by sonic hedgehog is indirectly mediated by stromal cells. J. Biol. Chem. *278*, 18506-18513.

Wang,J.C., Stromstedt,P.E., O'Brien,R.M., and Granner,D.K. (1996). Hepatic nuclear factor 3 is an accessory factor required for the stimulation of phosphoenolpyruvate carboxykinase gene transcription by glucocorticoids. Mol. Endocrinol. *10*, 794-800.

Wang,J.C., Stromstedt,P.E., Sugiyama,T., and Granner,D.K. (1999). The phosphoenolpyruvate carboxykinase gene glucocorticoid response unit: identification of the functional domains of accessory factors HNF3 beta (hepatic nuclear factor-3 beta) and HNF4 and the necessity of proper alignment of their cognate binding sites. Mol. Endocrinol. *13*, 604-618.

Wang,J.C., Waltner-Law,M., Yamada,K., Osawa,H., Stifani,S., and Granner,D.K. (2000a). Transducin-like enhancer of split proteins, the human homologs of Drosophila groucho, interact with hepatic nuclear factor 3beta. J. Biol. Chem. *275*, 18418-18423.

Wang,Q.T. and Holmgren,R.A. (1999). The subcellular localization and activity of Drosophila cubitus interruptus are regulated at multiple levels. Development *126*, 5097-5106.

Wang,X.D., Shou,J., Wong,P., French,D.M., and Gao,W.Q. (2004). Notch1-expressing cells are indispensable for prostatic branching morphogenesis during development and re-growth following castration and androgen replacement. J. Biol. Chem. *279*, 24733-24744.

Wang,Y., Hayward,S., Cao,M., Thayer,K., and Cunha,G. (2001). Cell differentiation lineage in the prostate. Differentiation *68*, 270-279.

Wang,Y., Hayward,S.W., Donjacour,A.A., Young,P., Jacks,T., Sage,J., Dahiya,R., Cardiff,R.D., Day,M.L., and Cunha,G.R. (2000b). Sex hormone-induced carcinogenesis in Rb-deficient prostate tissue. Cancer Res. *60*, 6008-6017.

Warot,X., Fromental-Ramain,C., Fraulob,V., Chambon,P., and Dolle,P. (1997). Gene dosage-dependent effects of the Hoxa-13 and Hoxd-13 mutations on morphogenesis of the terminal parts of the digestive and urogenital tracts. Development *124*, 4781-4791.

Weaver,M., Batts,L., and Hogan,B.L. (2003). Tissue interactions pattern the mesenchyme of the embryonic mouse lung. Dev. Biol. *258*, 169-184.

Weigel,D. and Jackle,H. (1990). The fork head domain: a novel DNA binding motif of eukaryotic transcription factors? Cell *63* , 455-456.

Weigel,D., Jurgens,G., Kuttner,F., Seifert,E., and Jackle,H. (1989). The homeotic gene fork head encodes a nuclear protein and is expressed in the terminal regions of the Drosophila embryo. Cell *57*, 645-658.

Weinstein,D.C., Altaba,A., Chen,W.S., Hoodless,P., Prezioso,V.R., Jessell,T.M., and Darnell,J.E., Jr. (1994). The winged-helix transcription factor HNF-3 beta is required for notochord development in the mouse embryo. Cell *78*, 575-588.

Wells,J.M. and Melton,D.A. (1999). Vertebrate endoderm development. Annu. Rev. Cell Dev. Biol. *15*, 393-410.

Wieschaus,E. and Riggleman,R. (1987). Autonomous requirements for the segment polarity gene armadillo during Drosophila embryogenesis. Cell *49*, 177-184.

Williams,S.P. and Sigler,P.B. (1998). Atomic structure of progesterone complexed with its receptor. Nature *393*, 392-396.

Wilson,J.D., Griffin,J.E., Leshin,M., and George,F.W. (1981). Role of gonadal hormones in development of the sexual phenotypes. Hum. Genet. *58*, 78-84.

Wilson,J.D. and Lasnitzki,I. (1971). Dihydrotestosterone formation in fetal tissues of the rabbit and rat. Endocrinology *89*, 659-668.

Wong,Y.C., Wang,Y.Z., and Tam,N.N. (1998). The prostate gland and prostate carcinogenesis. Ital. J. Anat. Embryol. *103*, 237-252.

Workman,J.L. and Kingston,R.E. (1998). Alteration of nucleosome structure as a mechanism of transcriptional regulation. Annu. Rev. Biochem. *67*, 545-579.

Wu,S.C., Grindley,J., Winnier,G.E., Hargett,L., and Hogan,B.L. (1998). Mouse Mesenchyme forkhead 2 (Mf2): expression, DNA binding and induction by sonic hedgehog during somitogenesis. Mech. Dev. *70*, 3-13.

Xin,L., Ide,H., Kim,Y., Dubey,P., and Witte,O.N. (2003). In vivo regeneration of murine prostate from dissociated cell populations of postnatal epithelia and urogenital sinus mesenchyme. Proc. Natl. Acad. Sci. U. S. A *100 Suppl 1*, 11896-11903.

Xu,X., Weinstein,M., Li,C., Naski,M., Cohen,R.I., Ornitz,D.M., Leder,P., and Deng,C. (1998). Fibroblast growth factor receptor 2 (FGFR2)-mediated reciprocal regulation loop between FGF8 and FGF10 is essential for limb induction. Development *125*, 753-765.

Xue,Y., Smedts,F., Debruyne,F.M., de la Rosette,J.J., and Schalken,J.A. (1998a). Identification of intermediate cell types by keratin expression in the developing human prostate. Prostate *34*, 292-301.

Xue,Y., Smedts,F., Verhofstad,A., Debruyne,F., de la Rosette,J., and Schalken,J. (1998b). Cell kinetics of prostate exocrine and neuroendocrine epithelium and their differential interrelationship: new perspectives. Prostate Suppl. *8*, 62-73.

Xue,Y., Verhofstad,A., Lange,W., Smedts,F., Debruyne,F., de la Rosette,J., and Schalken,J. (1997). Prostatic neuroendocrine cells have a unique keratin expression

pattern and do not express Bcl-2: cell kinetic features of neuroendocrine cells in the human prostate. Am. J. Pathol. *151* , 1759-1765.

Yamagishi,H., Maeda,J., Hu,T., McAnally,J., Conway,S.J., Kume,T., Meyers,E.N., Yamagishi,C., and Srivastava,D. (2003). Tbx1 is regulated by tissue-specific forkhead proteins through a common Sonic hedgehog-responsive enhancer. Genes Dev. *17*, 269-281.

Yan,G., Fukabori,Y., Nikolaropoulos,S., Wang,F., and McKeehan,W.L. (1992). Heparin-binding keratinocyte growth factor is a candidate stromal-to-epithelial-cell andromedin. Mol. Endocrinol. *6*, 2123-2128.

Yan,Y., Sheppard,P.C., Kasper,S., Lin,L., Hoare,S., Kapoor,A., Dodd,J.G., Duckworth,M.L., and Matusik,R.J. (1997). A large fragment of the probasin promoter targets high levels of transgene expression to the prostate of transgenic mice. The Prostate *32*, 129-139.

Yang,F., Li,X., Sharma,M., Sasaki,C.Y., Longo,D.L., Lim,B., and Sun,Z. (2002). Linking beta-catenin to androgen-signaling pathway. J. Biol. Chem. *277*, 11336-11344.

Yao,T.P., Ku,G., Zhou,N., Scully,R., and Livingston,D.M. (1996). The nuclear hormone receptor coactivator SRC-1 is a specific target of p300. Proc. Natl. Acad. Sci. U. S. A *93*, 10626-10631.

Yayon,A., Klagsbrun,M., Esko,J.D., Leder,P., and Ornitz,D.M. (1991). Cell surface, heparin-like molecules are required for binding of basic fibroblast growth factor to its high affinity receptor. Cell *64*, 841-848.

Yeh,S. and Chang,C. (1996). Cloning and characterization of a specific coactivator, ARA70, for the androgen receptor in human prostate cells. Proc. Natl. Acad. Sci. U. S. A *93*, 5517-5521.

Yoon,J.W., Liu,C.Z., Yang,J.T., Swart,R., Iannaccone,P., and Walterhouse,D. (1998). GLI activates transcription through a herpes simplex viral protein 16-like activation domain. J. Biol. Chem. *273*, 3496-3501.

Yoshinaga,S.K., Peterson,C.L., Herskowitz,I., and Yamamoto,K.R. (1992). Roles of SWI1, SWI2, and SWI3 proteins for transcriptional enhancement by steroid receptors. Science *258*, 1598-1604.

Yu,J., Carroll,T.J., and McMahon,A.P. (2002). Sonic hedgehog regulates proliferation and differentiation of mesenchymal cells in the mouse metanephric kidney. Development *129*, 5301-5312.

Yuan,X., Lu,M.L., Li,T., and Balk,S.P. (2001). SRY interacts with and negatively regulates androgen receptor transcriptional activity. J. Biol. Chem. *276*, 46647-46654.

Zaret,K. (1999). Developmental competence of the gut endoderm: genetic potentiation by GATA and HNF3/fork head proteins. Dev. Biol. *209*, 1-10.

Zaret,K.S. (2002). Regulatory phases of early liver development: paradigms of organogenesis. Nat. Rev. Genet. *3*, 499-512.

Zelivianski,S., Igawa,T., Lim,S., Taylor,R., and Lin,M.F. (2002). Identification and characterization of regulatory elements of the human prostatic acid phosphatase promoter. Oncogene *21*, 3696-3705.

Zhang ZF, Gao,N., Kasper,S., Reid K., Nelson,C., and Matusik,R.J. (2004a). An androgen dependent upstream enhancer is essential for high levels of probasin gene expression. Endocrinology *145*, 134-148.

Zhang ZF, Gao,N., Kasper,S., and Matusik,R.J. (2004b). Ubiquitous transription factors Octamer Factor 1, c-Jun, Nuclear Factor 1, tissue-restricted Hepatocyte Nuclear Factor-3alpha, and Androgen Receptor arre required for prostate-specific probasin gene expression. Manuscript in Preparation.

Zhang ZF, Thomas,T.Z., Kasper,S., and Matusik,R.J. (2000). A small composite probasin promoter confers high levels of prostate-specific gene expression through regulation by androgens and glucocorticoid *in vitro* and *in vivo*. Endocrinology *141*, 4698-4710.

Zhang,M., Magit,D., and Sager,R. (1997). Expression of maspin in prostate cells is regulated by a positive ets element and a negative hormonal responsive element site recognized by androgen receptor. Proc. Natl. Acad. Sci. U. S. A *94*, 5673-5678.

Zhao,H.H., Herrera,R.E., Coronado-Heinsohn,E., Yang,M.C., Ludes-Meyers,J.H., Seybold-Tilson,K.J., Nawaz,Z., Yee,D., Barr,F.G., Diab,S.G., Brown,P.H., Fuqua,S.A., and Osborne,C.K. (2001). Forkhead homologue in rhabdomyosarcoma functions as a bifunctional nuclear receptor-interacting protein with both coactivator and corepressor functions. J. Biol. Chem. *276*, 27907-27912.

Zhou,W., Park,I., Pins,M., Kozlowski,J.M., Jovanovic,B., Zhang,J., Lee,C., and Ilio,K. (2003). Dual regulation of proliferation and growth arrest in prostatic stromal cells by transforming growth factor-beta1. Endocrinology *144*, 4280-4284.

Zhou,Z., Corden,J.L., and Brown,T.R. (1997). Identification and characterization of a novel androgen response element composed of a direct repeat. J. Biol. Chem. *272*, 8227-8235.

Zhou,Z.X., Sar,M., Simental,J.A., Lane,M.V., and Wilson,E.M. (1994). A ligand-dependent bipartite nuclear targeting signal in the human androgen receptor. Requirement for the DNA-binding domain and modulation by NH2-terminal and carboxyl-terminal sequences. J. Biol. Chem. *269*, 13115-13123.